1998

Nonlinear Tracking Control Using a Robust Differential-Algebraic Approach.

Michael Christopher Mickle
Louisiana State University and Agricultural & Mechanical College

NONLINEAR TRACKING CONTROL
USING
A ROBUST DIFFERENTIAL-ALGEBRAIC APPROACH

A Dissertation

Submitted to the Graduate Faculty of the
Louisiana State University and
Agricultural and Mechanical College
in partial fulfillment of the
requirements for the degree of
Doctor of Philosophy

in

The Department of Electrical and Computer Engineering

by
Michael Christopher Mickle
B.S., Lamar University, 1993
M.S., Louisiana State University, 1995
December 1998

UMI Number: 9922101

ACKNOWLEDGMENTS

The author wishes to express appreciation to Professor Jianchao Zhu of the Electrical and Computer Engineering Department at Louisiana State University for his insightful advice and patient help as major professor and Committee Chairman. Also, the author sincerely appreciates the time and assistance of the following committee members: Professor Guoxiang Gu, Professor Morteza Naraghi-Pour, Professor Raymond C. Fabec, Professor Jimmie D. Lawson, and Professor Jerry P. Draayer. Also, the author would like to express his special thanks to Professor Jimmie D. Lawson for making a special effort and joining the committee on short notice, and to Professor Kemin Zhou for inspiring discussions during his graduate study.

The author is very grateful to the Louisiana Board of Regents for their financial support, and to the AFOSR for the unique summer research opportunity they provided and for their support. Additionally, the author is indebted to Professor Gu and the AFOSR for the financial assistance they afforded. Also, the author is grateful to the advice and guidance of Dr. James R. Cloutier, Lt. Colonel Curtis P. Mracek, and Mr. Johnny Evers of Munitions Directorate of AFRL at Eglin AFB.

TABLE OF CONTENTS

LIST OF SYMBOLS

C^k A k times differentiable function with continuous kth derivative
$\mathbb{R}^{n\times n}$ An $n \times n$ matrix of Real numbers
$C^k(J, \mathbb{R}^{n\times n})$ An $n \times n$ matrix of C^k functions on the interval J
$\boldsymbol{A}(t)$ System matrix
$\boldsymbol{B}(t)$ Input matrix
$\boldsymbol{C}(t)$ Output matrix
$\boldsymbol{D}(t)$ Direct Transmission matrix
$y^{(n)}$ The nth derivative
$\boldsymbol{x}(t)$ Linear States (error)
$\boldsymbol{X}(t)$ (Fundamental) Matrix Solution
$\Phi(t, t_0)$ State Transition Matrix
$\boldsymbol{W}(\phi_1,\ldots,\phi_n)$ Wronskian Matrix
$\Delta(\phi_1,\ldots,\phi_n)$ Wronskian (determinant)
$\|\cdot\|$ Norm
$\boldsymbol{Q}_c(t)$ Controllability Matrix
$\delta = \frac{d}{dt}$ differential operator
$\Delta_c(t) = -\boldsymbol{A}(t) + \delta$ vector differential operator for controllability
$\mathrm{M}(t_0, t_f) = \int_{t_0}^{t_f} \phi(t_0, t) B(t) B'(t) \phi'(t_0, t) dt$ Controllability Gramian
$\boldsymbol{Q}_o(t)$ Observability Matrix
$\Delta_o := A'(t) + \delta$ vector differential operator for observability
$\mathrm{N}(t_0, t_f) = \int_{t_0}^{t_f} \phi'(t_0, t) C'(t) C(t) \phi(t_0, t)$ Observability Gramian
$\boldsymbol{A}_c(t) = \mathrm{comp}(\alpha_1(t), \alpha_2(t), \ldots, \alpha_n(t))$ A (time varying) Companion Canonical Matrix
$\mathcal{D}_\alpha\{y\}$ Scalar Polynomial Differential Operator (SPDO)
$\{\lambda_k(t)\}_{k=1}^n$ Series Differential (SD)-Spectrum
$\{\rho_k(t) = \lambda_{1,k}(t)\}_{k=1}^n$ Parallel Differential (PD)-Spectrum
$\boldsymbol{V}(t)$ Canonical Modal Matrix
$\mathcal{D}_{\rho_i} = (\delta + \rho_i)$ Vector Differential Operator Associated with $\boldsymbol{V}(t)$
$\mathbb{C}$ The Complex Numbers
$\mathbb{I}$ A subset of the D-ring of regulated analytic functions
$\boldsymbol{\Gamma}(t)$ Series Spectral Canonical Matrix
$\boldsymbol{\Upsilon}(t)$ Parallel Spectral Canonical Matrix
$\mathbf{diag}\,[\rho_1(t), \rho_2(t), \cdots, \rho_n(t)]$ a diagonal matrix with diagonal elements $\rho_i(t)$
Ω_i ith Subsection of a Wronskian Matrix
$\Delta_i(\lambda_1,\ldots,\lambda_i)$ ith nonlinear characteristic equation associated with $\lambda_k(t)$, $k = 1, 2, \ldots i$
$\boldsymbol{v}_i(t)$ Row PD-eigenvector associated with $\rho_i(t)$
$\boldsymbol{u}_i(t)$ Column PD-eigenvector associated with $\rho_i(t)$
$\underset{t_0,\, t\in I}{\mathrm{em}} (\sigma(t)) = \underset{T\to\infty,\, t_0\ge T_0}{\lim\sup} \frac{1}{T}\int_{t_0}^{t_0+T} \sigma(\tau) \mathrm{d}\tau$ Extended mean of $\sigma(t)$
$\tilde{\boldsymbol{v}}_{ij}$ Algebraic cofactor of v_{ij}
$\mathcal{P}_A = \delta - \boldsymbol{A}(t)$ Vector Polynomial Differential Operator
$\mathcal{P}_A^{-1} = [\delta \boldsymbol{I} - \boldsymbol{A}(t)]^{-1}$ Inverse $\mathcal{P}_A$ operator, Vector Polynomial Integral Operator

$\mathcal{Q}_A = \delta + A^T(t)$ Vector Polynomial Differential Operator
$\mathrm{T}(t)$ Lyapunov Transformation matrix
$z(t)$ Transformed Linear States
$A_p(t)$ MIMO Block Phase Variable canonical form
$A_n(t)$ Nominal System Matrix
$\Delta A_n(t)$ Perturbation in Nominal System Matrix
$\Delta B(t)$ Perturbation in Input Matrix
$\mathbf{K}(t)$ State Feedback Matrix
$\mathcal{L}^p$ The space of all signals with bounded p norm
$\mathcal{L}_e^p = \{u | u_\tau \in \mathcal{L}^p, \forall \tau \geq 0\}$ The extended $\mathcal{L}^p$ space
H An input Output mapping
ξ Nonlinear states
$\overline{\xi}$ Nominal State Trajectory
$x = \xi - \overline{\xi}$ State errors
η Nonlinear output
$\overline{\eta}$ Nominal output
y Linear output
v Nonlinear input
$\overline{v}$ Nonlinear nominal input
u Linear input

ABSTRACT

This dissertation presents the development and application of an inherently robust nonlinear trajectory tracking control design methodology which is based on linearization along a nominal trajectory. The problem of trajectory tracking is reduced to two separate control problems. The first is to compute the nominal control signal that is needed to place a nonlinear system on a desired trajectory. The second problem is one of stabilizing the nominal trajectory. The primary development of this work is the development of practical methods for designing error regulators for Linear Time Varying systems, which allows for the application of trajectory linearization to time varying trajectories for nonlinear systems. This development is based on a new Differential Algebraic Spectral Theory. The problem of robust tracking for nonlinear systems with parametric uncertainty is studied in relation to the Linear Time Varying spectrum. The control method presented herein constitutes a rather general control strategy for nonlinear dynamic systems. Design and simulation case studies for some challenging nonlinear tracking problems are considered. These control problems include: two academic problems, a pitch autopilot design for a skid-to-turn missile, a two link robot controller, a four degree of freedom roll-yaw autopilot, and a complete six degree of freedom Bank-to-turn planar missile autopilot. The simulation results for these designs show significant improvements in performance and robustness compared to other current control strategies.

CHAPTER 1

INTRODUCTION

1.1 - Problem Statement and Background

The problems that will be handled in this work are nonlinear and time-varying (NLTV) dynamic systems with multiple-inputs and multiple-outputs (MIMO). In general we will describe the nth order NLTV MIMO systems using

$$\dot{\boldsymbol{\xi}} = \boldsymbol{f}(t, \boldsymbol{\xi}, \boldsymbol{v})$$

$$\boldsymbol{\eta} = \boldsymbol{h}(t, \boldsymbol{\xi}, \boldsymbol{v})$$

Where $\boldsymbol{\xi} \in \mathbb{R}^n$ is an n vector of states; $\boldsymbol{v} \in \mathbb{R}^m$ is an m vector of external inputs to the process; $\boldsymbol{\eta} \in \mathbb{R}^p$ is a p vector of outputs of the plant which are directly measurable from an external sensor; $\boldsymbol{f}$ is a nonlinear vector function which relates the states, inputs, and time to the state derivatives; and $\boldsymbol{h}$ is a nonlinear vector function which relates the states, inputs, and time to the measurable outputs. Processes described by governing equations of this type are also often called non-autonomuos nonlinear. If $\boldsymbol{f}$ and $\boldsymbol{h}$ are not explicit functions of time then the system is called Nonlinear time-invariant (NLTI) or autonomous nonlinear.

All physical systems are actually nonlinear, time varying, and infinite dimensional. To allow for any design some simplifying assumptions about the model of a system must be made. Often Linear Time Invariant (LTI) models of a process sufficiently capture the behavior of a process to allow for a LTI controller that can achieve the desired controlled

behavior. Finite dimensional linear time invariant controller design is a mature engineering science so where it can achieve the prespecified output performance requirements, it is a very valuable tool. However, over time more demanding systems that can only be poorly handled by LTI controller design methods have arisen and are becoming more common.

Aerospace control is an important branch of the science which contains some of the most demanding nonlinear design problems, *cf.* [11], [17], [27]. The first airplanes did not have the benefit of modern control (including both techniques and technology). Thus early aircraft were designed with inherent stability. That is, the center of lift is designed to be behind the center of gravity to provide pitch stability, and large vertical fins are used to provide stability to yaw.

By allowing the center of lift to move forward, the aircraft is capable of making greater pitch maneuvers which are critical to fighter aircraft in the contest for air superiority. The use of automatic control allowed for aircraft designs which are inherently unstable and capable of more rapid maneuvers while maintaining flight quality characteristics and without causing greater demands on the aircraft operator. The continued desire to increase performance characteristics has led to greater inherent nonlinearity of aerosystems, *viz* [6]. Some examples of current areas of research and technical development that are attempting to realize such performance demands include moving to non-axisymmetric missile bodies and the use of nontraditional effectors in the next generation of super-maneuverable aircraft.

All aircraft exhibit time variance from such exogenous states as altitude, time varying lift coefficients, and changing mass distribution because of fuel loss. Additionally, high performance aircraft change flight conditions rapidly and lead to greater time variance and model imprecision. Rapid maneuvers decrease the reliability of the steady state assumptions on airflow which lead to the imprecision in the aerodynamic models of the

vehicle. These facts add to the increasing need for rigorous nonlinear control design strategies which can handle highly nonlinear and time varying plants.

Traditional axisymmetric missiles use Skid-to-Turn (STT) autopilots which effect a maneuver by pitching or yawing. To improve the maneuvering capabilities, research is being done on developing Bank-to-Turn (BTT) autopilots for non-axisymmetric missile bodies. These preferred orientation control airframes have a primary lift plane which gives the missile greater pitch capability. However, the non-axisymmetric design creates large coupling, especially between sideslip and roll rate and between the roll and yaw control inputs. Additionally, the primary lift plane allows for high angle of attack maneuvers which exhibit greater nonlinearity. Thus, the design of BTT autopilots requires nonlinear controllers that can deal with plants which are highly nonlinear and highly coupled.

There is also a demand for performance improvement in terms of agility and flight envelope expansion for manned aircraft. Greater agility allows a pilot to place and maintain himself in an advantageous position, *i.e.* in a position that threatens his opponent and in which his foe can not threaten him. High agility maneuvers elicit more nonlinear behavior as the aircraft rapidly moves through diverse flight conditions limiting the effectiveness of linear approximations. Flight envelope expansion refers to increasing the range of sideslip and Angle-of-Attack (AOA) at which the aircraft can safely function. The flight envelope is normally limited by air intake for propulsion and high AOA aerodynamic stalls. Envelope expansion is also useful for placing the pilot in an advantageous threat position. However, the nonlinearity of the aircraft becomes more prominent.

There are also changes in the airframe that have beneficial effects for the aircraft but create greater inherent nonlinearity. One consideration is improved stealth. Reasonable stealth improvements are being incorporated into new designs, even for aircraft not designed specifically for stealth missions. These modifications improve the detectability

characteristics of the aircraft but can create undesirable aerodynamic behavior. Tallies aircraft are also being researched. Removing the vertical tail results in lower radar signature, reduced weight and drag, and reduced cost and maintenance. It also reduces stability and creates greater demands on the controller.

Perhaps the greatest new demand on nonlinear airframe control arises from the use of nontraditional effectors. These novel effectors exhibit highly nonlinear response characteristics. These effectors include thrust vectoring, reaction control, pneumatic devices, vortex control, and active flexible structure control. Thrust vectoring creates yaw or pitch moments by mechanically redirecting the thrust from the jet exhaust. Thrust vectoring allows for effective control in the expanded flight envelope, *i.e.* high AOA and large sideslip. Reaction control uses small jets located around the airframe which can creative a reactive force such as is used in spacecraft. Reaction control is not dependent on aerodynamics and is also capable of flight envelope expansion. Pneumatic devices affect the boundary layer of airflow, and can provide moderate roll, pitch, and yaw moments. Passive porosity control equalizes pressure gradients across an airfoil. Wing flexion can also be used to generate control moments. Allowing the wings to be more flexible can reduce the weight of an aircraft, thereby reducing the cost, and allows for deformations that improve performance.

The combined use of these new effectors allow for aircraft behavior far beyond anything presently attainable. Aircraft designs currently being researched incorporate multiple sets of effectors for each axis of rotation. Thus, in addition to the highly nonlinear response of the effectors, there is also the added problem of control allocation. The problem of controller allocation has yet to be adequately addressed and must incorporate several different factors. First, the control problem for the next generation of aircraft is what is typically referred to as the over controlled plant. That is, there are more control inputs than outputs to be controlled. Second, the effectors have different regions of greater effectiveness. Third, there are considerations outside of the control perspective

that influence the selection of which effectors are to be used. One such consideration is stealth, *e.g.* optimizing effector allocation to minimize radar signature. Fourth, all effector allocations must avoid controller saturation which can lead to instability such as susceptibility to pilot induced oscillations. Finally, the design must allow for time varying control allocation. This allocation scheme allows for the aircraft to perform in multiple modes which have been optimized to either minimize fuel consumption, maximize agility, maximize stealth, minimize wear, *et. al.*

These more demanding problems have precluded traditional LTI designs and are the driving force for the development of nonlinear controllers which can provide the higher agility and expanded flight envelope envisioned for the next generation of super-maneuverable aircraft and high reliability missiles. This dissertation presents the application of a new control strategy to the problem of missile autopilot design. These preliminary results indicate much promise in many of these areas of air vehicle control.

1.2 - Overview of Other Current Nonlinear Design Methods

There are many nonlinear design methods that have recently been proposed and some have been shown to be able to meet the stringent performance requirements. Among the most notable are feedback linearization, sliding mode control, neural network control, Lyapunov-Based Design, and dynamic inversion. Each has its individual strengths and weaknesses. However, current demanding designs have relied heavily on Gain Scheduling, which is based on LTI design which has only limited justification.

Obviously, by far the most well studied and developed control strategies are for LTI systems. This fact creates a powerful incentive to try to generalize LTI controllers to nonlinear plants. This is the motivation for gain scheduled (GS) controllers. Effective implementation is contingent upon successfully capturing the plant nonlinearity of the

plant. This method is very popular in industry especially in aerospace control. Some of the numerous examples include [29], [53], [71], [79], and [92]. This design technique has evolved from so called naive gain scheduling into more sophisticated forms but still only has theoretical validation for slowly varying commands. The greatest justification for this method is that it has been used successfully to design a large number of practical controllers. The benefits are obvious. It maintains all the properties of LTI systems during design. This includes not only classical concepts of modality and frequency, but also allows for designs that incorporate optimality and robustness. Thus, this method has been used to generalize H_∞ and μ-synthesis design to nonlinear systems.

There are several limitations associated with gain scheduled design, cf. [91]. All of these arise from the fact that theoretical justification has been provided only for sufficiently slowly varying systems in which the scheduling variable sufficiently covers the nonlinearity of the system. First, there has been no development to show that linear properties of the design such as robustness measures will be carried over into the closed loop nonlinear system. This can translate to decreased performance but certainly means that more conservative designs are used to increase stability margins. This means sacrificing performance. Second, in high performance systems the assumption about slowness of the system is lost. Thus, the only way to justify performance or even stability is by substantial simulation. This leads to the third point. Part of the overall design process involves redesign of individual airframe components. This iterative redesign of the airframe leads to new plant models for which the controller must be redesigned. So, each new model requires a tedious redesign of the controller which includes a thorough simulation justification to validate, and possibly a large number of design iterations to reach performance requirements in the nonlinear system. This iterative design can be exacerbated by using robust designs, such as μ-synthesis, that are already iterative in nature, with no guarantee of translating the robustness into the actual plant.

Feedback Linearization is a nonlinear design methodology that conceptually is based on precise cancellation of nonlinearities, and assigning the desired error dynamics. This is a relatively well explored nonlinear method of control in aerodynamic applications, *cf.* [37], and [6]. Here we will only consider the input-output feedback linearization problem which is more relevant to the output tracking problem under consideration. Perhaps the greatest benefit of using this method is that the error dynamics are assigned a desired LTI structure. Thus, classical concepts of mode and frequency response can be considered for the closed loop system. Additionally, the nominal design provides exponential tracking. In other words, the tracking error decays exponentially.

However, there are numerous limitations to consider. First, the traditional design methodology is in effect non-causal as it assumes the availability of not only the desired output but also $r + 1$ derivatives, where r is the relative degree. This requires a practical method of estimating these functions. Second, the method is limited to autonomous nonlinear systems which are linear in the input, *a.k.a.* affine nonlinear systems. Third, the design is limited to systems in which the internal dynamics are stable. The problem of tracking in non-minimum phase systems can however be handled by output redefinition which can afford approximate trajectory tracking, but does not have a systematic formulation. Even with stable internal dynamics, theoretical justifications can only guarantee that the internal states are bounded. Thus, at the least the performance can become extremely degraded due to internal states, and at worst can depart from the domain of operation. Finally, stability justification of such designs rely on precise nonlinearity cancellation. This fact means that model uncertainties lead to unpredictable behavior. In other words, the robustness of such designs is extremely difficult to analyze or design for.

Another nonlinear control methodology currently being researched is sliding mode control, which also has a strong theoretical foundation. Some applications of sliding mode control to aerospace problems are in [94]-[96], and [57]. Some of the positive

aspects include LTI error dynamics and a robustness to nonlinear parametric perturbations. Sliding mode control assigns a desired LTI sliding manifold which can be achieved in finite time. Thus, modal and bandwidth properties of the error dynamics can be used in the design. In addition, Sliding mode control uses either a discontinuity or a smoothed nonlinear approximation to insure robustness with respect to state and input uncertainties. This robustness is limited only by the bandwidth of the actuators.

Perhaps the most insidious limitation of this method is the high control activity, *i.e.* chattering and rapid switching. While this is the source of the robustness of this design, it limits the applicability. High control activity can lead to actuator saturation, accelerated aging of mechanical systems, or excitation of unmodeled dynamics. All of these can cause a degradation of performance, or even possibly loss of stability. A tradeoff can be made between robustness of performance and control activity by appropriately choosing a region of smooth controller action. Additionally, the tracking problem is limited by controller form and internal dynamics just as feedback linearization. Specifically, general methods are currently available only for tracking autonomous affine nonlinear systems for minimum phase systems.

Lyapunov-Based design is a broad title which covers any method which seeks to applies Lyapunov's second method directly to a particular plant. This method encompasses Lyapunov redesign and backstepping control. One very important benefit of this method is that it allows the designer to directly design for nonlinear robustness. Also, these methods allow for a great variety of nonlinear systems including nonautonomous systems. This broad design class also includes nonminimum phase plants. Perhaps the greatest benefit of this method is its greater flexibility. This flexibility allows for the opportunity of the designer to assign whatever stability properties that are desired and physically feasible for a given nonliear plant, which includes global, uniform, and exponential stability.

On the other hand, this same flexibility requires greater effort and consequently greater design times due to the lack of a fixed design paradigm. Additionally, where a fixed design structure is applied, such as in Backstepping, the flexibility is lost. Also in general, LTI concepts such as modality and frequency response are lost. In the face of perturbations of the nominal model, global properties can be lost. Given a general nonlinear model, the nonlinear error dynamics about a nominal trajectory can be very difficult to express directly. This fact contributes to the difficulty in formulating a trajectory tracking design. Thus, there are currently no general methods for trajectory tracking, and apparently at best very few specific examples. One notable exception is the problem of setpoint tracking for which the method of redefining equilibrium points offers an obvious solution.

Dynamic inversion is another popular nonlinear design methodology with particular applicability to aerospace applications, *viz.* [3], [5], [19], [66], [80], [102], and [119]. Generally, this method separates the airframe into fast dynamics (pitch rate, roll rate, and yaw rate), and slow dynamics (angle of attack, sideslip, and roll angle). The fast states are used to drive the slow states to their desired values, and the effectors are used to drive the fast states to their desired values. For the case when the aircraft is over controlled, Snell [103] has modified the solution by using the fact that the nonlinear input gain is right invertible.

Dynamic inversion is a popular design that appears to be gaining in popularity as a method for aircraft control synthesis. Its greatest benefit to designers is that it explicitly handles the nonlinearity of a plant and allows the nonlinear behavior to be replaced with linear. This fact means that all of the methods of LTI control can be applied to the nonlinear problem, including optimization such as H_∞, μ-synthesis, or Eigenstructure assignment for decoupling.

Dynamic inversion shares a severe limitation with feedback linearization. Any inherent nonlinearity which could improve performance is canceled out. Consider a

hypothetical nonlinear system described by

$$\dot{x} = x - x^3 + u$$

The dynamic inversion control (and also feedback linearization control) that achieves the linear behavior

$$\dot{x} = -x$$

is given by

$$u = -x + x^3$$

This means that dynamic inversion control has canceled out an inherent stabilizing nonlinearity of the plant. This nonlinear cancellation could actually reduce the envelope of stability of a trajectory because canceling useful nonlinearities can lead to actuator saturation for moderate errors.

Nonlinear robustness analysis is important for dynamic inversion design because of imprecise nonlinear cancellation, aerodynamic disturbance forces and unmodeled dynamics arising from model simplifications such as rigidity. However, nonlinear robustness analysis is very difficult and means any attempt at precise nonlinear cancellation must be handled very carefully. Attempts at robust assignment of the desired LTI dynamics may not provide commensurate improvements of the nonlinear system because of the unmodeled nonlinear effects arising from imprecise cancellation.

One very important limitation for all of these nonlinear techniques is that the design procedures assume that the states are directly measurable. Even in the case where such states are directly measurable, the cost for including sensors to measure these states can be considerable if not prohibitive. As is well known, in general nonlinear systems do not have the separability principle that linear systems have. So even for exponentially stable observers and exponentially stable controllers, there is no guarantee of stability for the closed loop system. More restrictive assumptions can be made which do insure the stability of an observer based design.

Each design methodology has unique benefits and detractions which make it more or less applicable to a particular problem. However, the usefulness of true nonlinear designs seems to be somewhat limited. It seems that few nonlinear design methods are actually being used in practice. In cases where LTI controllers are found to be simply incapable of achieving the desired performance, there is considerable incentive to try these relatively new methods. While it is true that capable controllers have been designed by gain scheduling, the design process is made more involved and lengthy and in some cases may not be sufficient. This may be especially true for the next generation of effectors, which exhibit such highly nonlinear behavior that linear designs may not be able to take advantage of them. So, it seems that a true nonlinear design methodology that can retain some useful properties of each nonlinear controller with sufficient theoretical justification might be very useful. The design method presented in this paper shows great promise in realizing this goal by accurately preserving some linearity properties, allowing for rapid single pass redesign, and taking advantage of the nonlinear nature of plant and effectors.

1.3 - Overview of Proposed Control Method

The genesis of most engineering development in nonlinear system theory is indirectly based on the original work of Lyapunov, *The General Problem of the Stability of Motion* [61]. He developed two distinct methods for assessing the stability of a trajectory. The first method, also called the indirect, relies on finding explicit or approximate solutions to the disturbed equations of motion, *i.e.* the error dynamics about a nominal trajectory. He used successive linear approximations to find solutions which converged to solutions of the nonlinear equations. A very famous result of his first method, is the method of linearization. He used his first method to prove that for a large class of systems if the first approximation, the linearization, is stable then the nonlinear equation is stable. The lineairzaiton of a nonlinear system is given by

$$\dot{\boldsymbol{x}} = \boldsymbol{A}(t)\boldsymbol{x} + \boldsymbol{B}(t)\boldsymbol{u} \tag{1.1}$$
$$\boldsymbol{y} = \boldsymbol{C}(t)\boldsymbol{x} + \boldsymbol{D}(t)\boldsymbol{u}$$

where

$$\boldsymbol{A}(t) = \frac{\partial \boldsymbol{f}}{\partial \boldsymbol{\xi}}\Big|_{\bar{\boldsymbol{\xi}},\bar{\boldsymbol{v}}} \qquad \boldsymbol{B}(t) = \frac{\partial \boldsymbol{f}}{\partial \boldsymbol{v}}\Big|_{\bar{\boldsymbol{\xi}},\bar{\boldsymbol{v}}}$$

$$\boldsymbol{C}(t) = \frac{\partial \boldsymbol{h}}{\partial \boldsymbol{\xi}}\Big|_{\bar{\boldsymbol{\xi}},\bar{\boldsymbol{v}}} \qquad \boldsymbol{D}(t) = \frac{\partial \boldsymbol{h}}{\partial \boldsymbol{v}}\Big|_{\bar{\boldsymbol{\xi}},\bar{\boldsymbol{v}}}$$

Lyapunov's original theorem on the linearized system is

Theorem 1.1 *If the system of differential equations of the first approximation is regular, and if all the characteristic numbers are positive, then the undisturbed motion is stable.*

Linearization is the method that is used in the development of the design strategy presented herein.

The second method, also called the direct, relies on what has come to be called Lyapunov functions to justify the stability of a trajectory. This is perhaps the most common method for proving the stability of a trajectory that most current nonlinear control strategies use. Additionally, the second method has now been used to justify the stability of a trajectory of a nonlinear system based on the linearization about the nominal trajectory.

Application of Lyapunov's Theorem 1.1 to control problems has been very fruitful. Although he was originally only interested in stability in the sense of boundedness as applied to the motions of the planets, control scientists have made suitable development to allow for asymptotic stability which is more critical to engineering problems. His development on linearization is the justification for all linear control strategies as applied to nonlinear plants.

For a given constant output of a particular autonomous nonlinear process, a constant nominal input can be derived along with a LTI regulator to maintain the desired output. A natural extension of this method is to generalize this procedure to track a given trajectory. However, as is well known, when the linearization is applied to a time-varying trajectory the resulting linearized error dynamics is itself time-varying. Thus, the linearizaiton can only properly be applied for control synthesis if LTV controllers can be designed to stabilize a given trajectory.

There are two problems that have prevented the application of the linearization technique of design for trajectory tracking controllers. The first is the need for a general method of inversion of nonlinear plants. The inverse plant generates a nominal control that places the plant on the desired trajectory. The second limitation has been general techniques for handling LTV systems. LTV stabilization methods are necessary to stabilize the nominal trajectory. A method for handling LTV system stabilization will be presented and is based on early work by Floquet [21].

In 1879 Floquet published a little known work on linear differential equations with analytic coefficients [21]. He first proposed the extension of factorization to the problem of linear differential equations with complex valued non-constant coefficients. This work has since been extended to LTV dynamic systems, *cf.* [142], and [136]. This research along with the developments in LTV transformations by Silverman [97], and Wolovich [121] has led to practical methods for handling LTV error dynamics.

The first difficulty that has limited the application of linearization to nonlinear trajectory tracking is the need for an effective method of nonlinear system inversion. Several researchers have developed techniques for nonlinear inversion, *cf.*[33]-[35], [77], [85], and [100]. Developing a nominal control for any plant is made more difficult by the fact that a nonlinear inverse of non-minimum phase plants will be unstable. The problem of finding causal stable inverses is a very difficult area of research which is still very

active. However, the work in this field is sufficiently mature to allow for application to many nonlinear control problems.

The intention of this work is to present a design method which uses linearization to achieve the trajectory tracking control of a nonlinear system. This design method first applies feasible nonlinear inversion to design a controller which causes the plant to acquire a desired output trajectory. Second, the method presents a systematic procedure for the design of a feedback controller which realizes a LTV error regulator to make the trajectory exponentially stable. Thus with some mild and reasonable assumptions on the nonlinear plant which will be stated later, the complete controller achieves exponential tracking of any desired output.

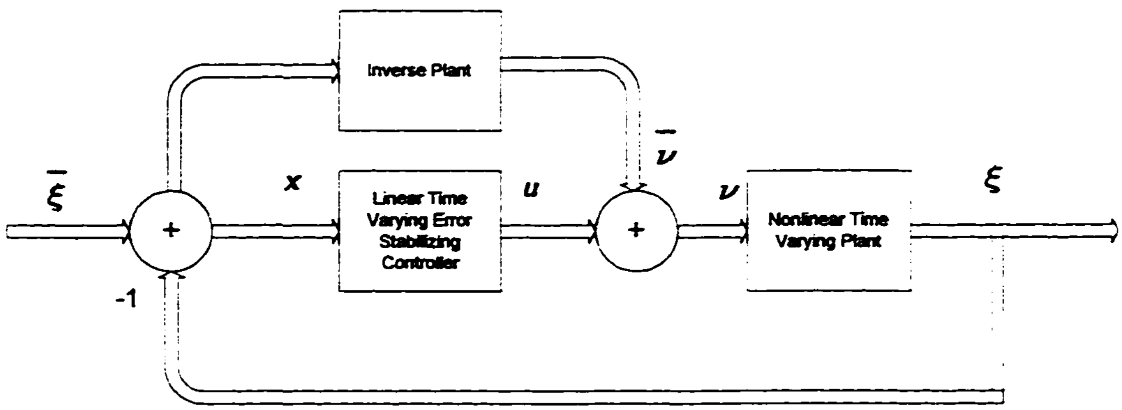

Figure 1.1 Controller Structure

Practical limitations must be pointed out here. First, to gain access to derivatives of the desired output trajectory, the desired output must be filtered. This action leads to bandwidth limitations on the space of output functions which can be tracked. This is a minor limitation as the output can be made arbitrarily close to the desired output. This effect can also be used to achieve desired plant behavior, such as avoiding actuator limits and output rate limits. Second, real systems are modeled with differential equations

which that only approximately represent the true behavior. Thus, any controller must be able to maintain stability and performance in the presence of unmodeled and improperly modeled system behavior.

The problem of robustness with respect to plant uncertainty is a very important consideration for nonlinear designers. Early simulation results on the trajectory linearization control seemed to indicate a large amount of inherent robustness in this control strategy. So this work attempts to investigate and quantify this inherent robustness to allow for the design of sufficient robustness to controller and plant parametric uncertainty in trajectory tracking problems. To this end, new results are presented on the robustness of the control structure to parametric perturbations in terms of the LTV spectrum.

1.4 - Dissertation Organization

Chapter 1: General background information is presented on the nature of the type of systems to be controlled and then some of the control methodologies that have been applied to them. First, the motivation for the control strategy is given. Then, a brief analysis of the benefits and limitations of some of the most common nonlinear control strategies are considered. Finally, an overview of the control strategy of the particular control strategy used is given.

Chapter 2: This chapter presents an overview of LTV differential equations. First fundamental definitions and results such as existence of solutions are shown. In the second section LTV concepts of observability and controllability are given. Next, the background on Differential Algebraic Spectral Theory (DAST) that forms the basis of the LTV tracking error stabilization is given. The development begins by considering scalar differential equations and then extends results to vector differential equations.

Chapter 3: A procedure is presented for the systematic design of a robust nonlinear tracking controller. Methods for PD-eigenstructure assignment are given and then methods are given for generating a pseudoinversion for minimum and nonminimum phase systems based on differential geometric methods.

Chapter 4: This chapter consists of the theoretical basis for the observed inherent robustness of trajectory linearization. First, the perturbation models are defined. Then the robustness theories that derive from these models are presented. The robustness of the Bounded-Input Bounded-State (BIBS), and uniform exponential stability with respect to parametric uncertainty in LTV systems is stated in terms of the PD-spectrum. These results are then extended to the nonlinear robustness question of trajectory tracking. Finally, the question of the unavailability of states is addressed by considering LTV observers. The observer based PD-spectrum assignment tracking of trajectories is shown to be exponentially stable under certain mild conditions.

Chapter 5: The usefulness of the trajectory linearization control strategy is illustrated by applying this procedure to several nonlinear control problems, where simulation results are offered for each. First, two academic problems are studied that illustrate the unusual capabilities of this new method versus other design methods. Second, a straight forward design of a two link robot arm is implemented and simulated. This design procedure can be generalized to similar systems derived from the Lagrange equations of motion. Third, the design of an AOA trajectory tracking controller is presented for a time varying pitch axis missile. This design uses a Radial Basis Function (RBF) neural network to realize the pseudo-inverison of the plant. Next, a controller which can track arbitrary roll angles while regulating sideslip in a four degree of freedom (4DOF) missile model is designed and simulated. Finally, a complete 6DOF missile autopilot is designed and simulated using the trajectory tracking controller for a Bank-To-Turn (BTT) missile. This design is then compared with a feedback linearization controller and a dynamic inversion controller.

Chapter 6: A summary of the main results are presented. Then conclusions are drawn about the effectiveness of this nonlinear control strategy. Finally, insight gained in this work is used to speculate on useful future work.

The main contributions of this dissertation include:

1) developing robustness measures based on PD-spectra

2) combining state-of-the-art NL control techniques to accomplish causal, stable nonlinear pseudo-inversion

3) designing and implementing in simulation LTV stabilizing controllers and observers based on PD-spectral assignment

4) making practical application of LTV transformations to achieve state feedback stabilization and realizing time varying system matrices

5) Applying these techniques to the design of demanding control problems

CHAPTER 2

OVERVIEW OF LTV SYSTEMS

2.1 - Fundamentals of Linear Time Varying System Theory

LTV systems are common in many engineering problems. Discrete time linear systems, signal modulators and demodulators, and linearization of nonlinear plants along trajectories are some very well known origins of LTV systems. The last example is a very important one that is particularly relevant in this work. Unlike LTI systems, general analytic techniques for arriving at solutions to LTV ordinary differential equations do not exist. This fact has limited the development and applicability of LTV techniques for control.

Before presenting the definition of a LTV system we need to consider the nature of a time varying matrix. A matrix $U(t) = [u_{ij}(t)]$ represents two separate mappings. First it represents a mapping from time to a matrix of real numbers which is denoted by $U(\cdot) \in C^k(J, \mathbb{R}^{m\times l})$ where

$$C^k(J, \mathbb{R}^{m\times l}) := \{[a_{ij}] : J \to \mathbb{R}^{m\times l} | \text{ the derivative } a_{ij}^{(p)} \text{ exist on } J \text{ and}$$

$$a_{ij}^{(p)} \text{ is continuous on } J \text{ for } p = 0, 1, \ldots, k\}$$

Second, this matrix at any time t represents a mapping from the real space $\mathbb{R}^l$ to another real space $\mathbb{R}^m$. This meaning of the matrix is a useful mapping in describing differential equations and is written $U(t)$.

An axiomatic development of LTV systems can be found in [105]. However, we shall assume a less formal development more typical of engineering analysis. By a LTV system defined on the interval J we mean a differential equation of the form

$$\begin{aligned}\dot{\boldsymbol{x}}(t) &= \boldsymbol{A}(t)\boldsymbol{x}(t) + \boldsymbol{B}(t)\boldsymbol{u}(t)\\ \boldsymbol{y}(t) &= \boldsymbol{C}(t)\boldsymbol{x}(t) + \boldsymbol{D}(t)\boldsymbol{u}(t)\end{aligned} \tag{2.1}$$

where $\boldsymbol{A}(\,\cdot\,) \in C^{n-2}(J, \mathbb{R}^{n\times n})$ is called the system matrix, $\boldsymbol{B}(\,\cdot\,) \in C^{n-1}(J, \mathbb{R}^{n\times m})$ is called the input matrix, $\boldsymbol{C}(\,\cdot\,) \in C^{n-1}(J, \mathbb{R}^{p\times n})$ is called the output matrix, $\boldsymbol{D}(\,\cdot\,) \in C(J, \mathbb{R}^{p\times m})$ is called the direct feedthrough matrix, $\boldsymbol{x}(t) \in \mathbb{R}^n$ is the vector of n states at time t, $\boldsymbol{u}(t)$ is the vector of m inputs, and $\boldsymbol{y}(t)$ is the vector of p outputs. Note that all matrices are assumed to be bounded even on open intervals. This assumption simplifies analysis and is common in engineering analysis, $cf.$ [14], [48], [82], [109], [122], *et. al.*

Note that as a special case of (2.1) some scalar LTV systems are defined by

$$y^{(n)}(t) + \alpha_1(t)y^{(n-1)}(t) + \ldots + \alpha_n(t)y(t) = \beta_0 u^{(n)}(t) + \ldots \beta_n(t)u(t) \tag{2.2}$$

where $y(t)$ is the output, $r(t)$ is the input and $y^{(i)}(t)$ denotes the ith derivative of $y(t)$ with respect to time. D'Angelo presents a method for a state-space realization of this scalar equation, *viz.* [14] p.22. These scalar systems have state space realizations of the form

$$\begin{aligned}\dot{\boldsymbol{x}}(t) &= \boldsymbol{A}(t)\boldsymbol{x}(t) + \boldsymbol{b}(t)u(t)\\ y(t) &= \boldsymbol{c}\boldsymbol{x}(t) + b_0(t)u(t)\end{aligned} \tag{2.3}$$

where

$$\boldsymbol{A}(t) = \begin{bmatrix} 0 & 1 & 0 & \cdots & 0 \\ 0 & 0 & 1 & \cdots & 0 \\ \vdots & \vdots & \vdots & \ddots & \vdots \\ 0 & 0 & 0 & \cdots & 1 \\ -\alpha_n(t) & -\alpha_{n-1}(t) & -\alpha_{n-2}(t) & \cdots & -\alpha_1(t) \end{bmatrix} \tag{2.3a}$$

$$b(t) = \begin{bmatrix} b_1(t) \\ b_2(t) \\ \vdots \\ b_n(t) \end{bmatrix} \tag{2.3b}$$

$$b_0(t) = \beta_0(t) \tag{2.3c}$$

$$b_i(t) = \beta_i(t) - \sum_{j=0}^{i-1}\sum_{k=0}^{i-j}\binom{n+k-i}{n-1}\alpha_{i-j-k}(t)\frac{d^k b_j(t)}{dt^k} \tag{2.3d}$$

$$c(t) = [1 \quad 0 \quad \cdots \quad 0 \quad 0] \tag{2.3e}$$

Any system matrix of the form of (2.2) is said to be in the companion canonical form. Of particular note, SISO *phase variable* form is a realization as above with a system matrix in companion canonical form and with input matrix such that $b_n(t) \equiv 1$, and $b_i(t) \equiv 0$ $\forall i \neq n$.

We will make some further practical assumptions about the type of plants that will be considered. By relative degree we take the standard definition. The relative degree of a MIMO system is a vector, in which the ith element of the vector is equal to the number of times the ith output must be differentiated to be an explicit function of the inputs. Throughout, we shall only consider LTV systems with relative degree greater than zero, or equivalently that $D(t) \equiv 0$. This assumption simplifies much of the analysis and is reasonable as it is consistent with the high frequency attenuation of physical plants.

The following definitions are useful in the expression of nonhomogenous, also called forced, solutions to (2.2). To allow the development of the non homogenous solution of

$$\dot{x} = A(t)x + h(t) \tag{2.4}$$

we must first consider the homogenous solution of the state equation

$$\dot{x} = A(t)x. \tag{2.5}$$

Definition 2.1 An $n \times n$ matrix $\boldsymbol{X}(t)$ is a matrix solution of (2.5) if each column of $\boldsymbol{X}(t)$ satisfies (2.5).

Definition 2.2 A fundamental matrix solution of (2.5) is an $n \times n$ matrix solution $\boldsymbol{X}(t)$ such that $\det\boldsymbol{X}(t) \neq 0$.

The importance of a fundamental matrix solution of (2.5) is that it consists of n linearly independent solutions for (2.5). Thus, these n independent solutions form a solution basis for (2.5). The fundamental matrix leads to a general solution of (2.5) given by

$$\boldsymbol{x}(t) = \boldsymbol{X}(t)[\boldsymbol{X}^{-1}(\tau)\boldsymbol{x}(\tau) + \int_{\tau}^{t} \boldsymbol{X}^{-1}(s)\boldsymbol{h}(s)ds]$$

which is called the variation of constants formula for (2.5). This formula leads to another useful definition.

Definition 2.3 A state transition matrix of (2.5) is the $n \times n$ matrix

$$\Phi(t, t_0) = \boldsymbol{X}(t)\boldsymbol{X}^{-1}(t_0)$$

The state transition has also been called the matrizant, the principal fundamental matrix, the normalized fundamental matrix, and the characteristic matrix. In [14], it is verified that the state transition matrix has the following properties :

(1) $$\Phi(t, t) = \boldsymbol{I}.$$

(2) $$\Phi(t, \tau) = \Phi(t, t_1)\Phi(t_1, \tau).$$

(3) $$\Phi^{-1}(t, \tau) = \Phi(\tau, t)$$

(4) $$\frac{\partial \Phi(t,\tau)}{\partial t} = A(t)\Phi(t,\tau)$$

(5) $$\frac{\partial \Phi(t,\tau)}{\partial \tau} = -\Phi(t,\tau)A(t)$$

This definition leads to solutions of (2.5) in the form of

$$x(t) = \Phi(t,t_0)x(t_0) + \int_{t_0}^{t} \Phi(t,\tau)h(\tau)d\tau$$

which for quiescent systems, i.e. $x(t_0) = 0$, yields the superposition integral

$$x(t) = \int_{t_0}^{t} \Phi(t,\tau)h(\tau)d\tau.$$

Thus, equation (2.1) is linear with respect to inputs only when the system is quiescent.

Although general solutions do not exist, useful characterizations of the stability of (2.1) can be given in terms of the state transition matrix. The following theorem is from page 3 of [109].

Theorem 2.1 State Transition matrix characterization of stability: *The equilibrium point $x_e = 0$ of (2.5), $t \geq t_0 \geq 0$, is*

1. *stable iff* $\sup_{t \geq t_0} ||\Phi(t,t_0)|| := c(t_0) < \infty$.

2. *asymptotically stable iff* $\lim_{t \to \infty} ||\Phi(t,t_0)|| = 0$.

3. *uniformly stable iff* $\sup_{t_0 \geq 0} c(t_0) = \sup_{t_0 \geq 0} \sup_{t \geq t_0} ||\Phi(t,t_0)|| := c < \infty$

4. *uniformly asymptotically stable and uniformly exponentially stable (u.e.s) iff there exist constants* $k, a > 0$ *such that* $||\Phi(t,t_0)|| \leq k\exp[-a(t-t_0)], \forall t \geq t_0, \forall t_0 \geq 0$.

for any finite initial conditions $x(t_0)$.

The following definitions and results come from [31]. Another important definition for LTV systems is the Wronskian matrix associated with (2.2).

Definition 2.4 The Wronskian matrix is an $n \times n$ matrix

$$W(\phi_1,\ldots,\phi_n) = \begin{bmatrix} \phi_1 & \phi_2 & \cdots & \phi_n \\ \delta\phi_1 & \delta\phi_2 & \cdots & \delta\phi_n \\ \vdots & \vdots & \ddots & \vdots \\ \delta^{n-1}\phi_1 & \delta^{n-1}\phi_2 & \cdots & \delta^{n-1}\phi_n \end{bmatrix}$$

where ϕ_i are solutions of (2.2), and δ is the derivative operator $\delta = \frac{d}{dt}$.

The independence of ϕ_i are characterized by the Wronskian.

Definition 2.5 The Wronskian $\Delta(\phi_1,\ldots,\phi_n)$ is the determinant of the Wronskian matrix $W(\phi_1,\ldots,\phi_n)$.

Lemma 2.1 *If $\phi_1,\ldots,\phi_n$ are $n-1$ times continuously differentiable scalar functions on an interval J, then $\phi_1,\ldots,\phi_n$ are linearly independent on J iff the Wronskian $\Delta(\phi_1,\ldots,\phi_n)$ is nonzero on J.*

There is an important relation between fundamental matrices for vector systems with system matrix in companion canonical form (2.3a) and the Wronskian matrix for scalar systems. The scalar system (2.2) is equivalent to the state space realization of (2.3) with companion canonical system matrix. A fundamental matrix for (2.3) forms a linearly independent Wronskian matrix for (2.2).

Finally and perhaps most importantly, we come to a justification of the existence and uniqueness for a solution of the LTV system. The following existence theorem and its extensions come directly from [122].

Theorem 2.2 *For the linear system represented by (2.5), with $A(t)$ continuous for all $t \in (-\infty, \infty)$, the system has a unique solution $x(t; x(t_0), t_0)$ which is defined for all $t \in (-\infty, \infty)$ and which passes through $x(t_0)$ at t_0.*

The existence and uniqueness of solutions of (2.5) is especially important in this development as we shall be considering state feedback regulation of LTV systems and the closed loop system will be in the form of (2.5). This result has already been well developed for the general systems in the form of (2.1), *viz.* [122]. In the case where the input is continuous, the state vector is continuously differentiable, and the output is continuous. If the input is piecewise continuous, then the state vector is continuous and the output is piecewise continuous, or continuous under our assumption that $D(t) \equiv 0$. Similarly, the assumptions on $A(t)$ in (2.5) can be relaxed so that it is only required to be a regulated function of t, i.e. has a right and left hand limit at each point. This implies that a regulated function is continuous a.e. and thus is integrable. Under this assumption, a unique continuous function $x(t; x(t_0), t_0)$ exists that satisfies (2.5) a.e. Additionally, characterizations of the state solutions can be related to the output according to the assumptions on $C(t)$ and $D(t)$.

2.2 - Definitions of Controllability and Observability

The notions of controllability and observability are more complex for LTV systems than for LTI systems. The following definitions are useful in capturing the many different controllability and observability properties for LTV systems as represented by (2.1). Because concepts of controllability and observability are so complex for LTV systems and definitions vary according to the author and his particular needs, there are many different definitions and consequent theorems. The definitions and theorems stated herein are as used throughout this work and are consistent with many other authors, *cf.* [14], and [99].

The first definition captures the most basic meaning of controllability of a LTV system defined on an infinite interval. A system that is completely controllable on an interval is a system for which a bounded input exists on the interval that takes the system from the initial state to any desired final state.

Definition 2.6 A system is said to be completely (state) controllable on the interval $[t_0,t_f]$, or simply, controllable on $[t_0,t_f]$, if each initial state $x(t_0)$ can be transferred to any final state $x(t_f)$ using some bounded control $u(t)$ over the closed interval $[t_0,t_f]$.

Common practice has come to be to use the term controllable in reference to state-controllability. We shall also use controllability in this fashion. Anywhere controllability is used, it assumed to mean state controllability. Similar definitions for output controllability have been given in the sources but are unnecessary in the current work, *cf.* [14].

Definition 2.7 A plant is said to be totally controllable on $[t_0,t_f]$ if it is completely controllable on every finite subinterval of $[t_0,t_f]$; it is said to be totally controllable at t_0 if for a given t_0 it is completely controllable on every finite interval $[t_0,t_f]$.

Definition 2.8 The controllability matrix is given by

$$Q_c(t) = [B(t), \Delta_c B(t), \cdots, \Delta_c^{n-1} B(t)]$$

where $\Delta_c(t)$ is a Vector Polynomial Differential Operator (VPDO) given by

$$\Delta_c(t) = -A(t) + \delta$$

Theorem 2.3 *The following are equivalent*

(i) (1) *is completely state-controllable on* $[t_0, t_f]$

(ii) $M(t_0, t_f) = \int_{t_0}^{t_f} \phi(t_0, t)B(t)B'(t)\phi'(t_0, t)dt$ *is nonsingular*

(iii) *The rows of* $\phi(t_0, t)B(t)$ *(or, equivalently, the rows of* $W^{-1}(t)B(t)$*, where* $W(t)$ *is a fundamental Wronskian matrix) are linearly independent functions of* t *on some finite subinterval* $[t_1, t_2]$ *of* $[t_0, t_f]$.

$M(t_0, t_f)$ is called the controllability gramian of the LTV system. Because general solutions to LTV systems are typically uncomputable, the controllability gramian is more useful for LTI systems. The controllability matrix for LTV systems in the form of (2.1) offers a convenient method for verifying the controllability properties of a system, without having to find explicit solutions. The following two theorems provide a method for verifying that a given system is either completely, or totally controllable on an interval. Also, uniform complete controllability is a stronger version of total controllability, and is defined after the theorems.

Theorem 2.4 *System (2.1) with* $A(t)$, $B(t)$ *differentiable* $n-2$, $n-1$ *times almost everywhere on* $[t_0, t_f]$ *is completely state controllable on* $[t_0, t_f]$ *if the controllability matrix* $Q_c(t)$ *has rank* n *almost everywhere on some finite subinterval.*

Theorem 2.5 *System (2.1) with* $A(t)$, $B(t)$ *differentiable* $n-2$, $n-1$ *times almost everywhere on* $[t_0, t_f]$ *is totally state-controllable iff the controllability matrix* $Q_c(t)$ *has rank* n *almost everywhere on* $[t_0, t_f]$.

Definition 2.9 The system characterized by Eq. (2.1) is said to be uniformly (completely) controllable on $[t_0, t_f]$ if the controllability matrix $Q_c(t)$ has rank n everywhere on $[t_0, t_f]$.

Clearly, if a linear time-invariant system is controllable in either the complete or total sense, then it is also uniformly controllable.

Uniform complete controllability is a stronger condition than total controllability. This property will be useful in finding transformations to LTV canonical forms. This controllability property has also been called instantaneous controllability. This appellation is appropriate because impulsive functions can be used to achieve any desired state instantaneously for any system which is uniformly controllable.

Observability in LTV systems is more complex than for LTI systems. Roughly speaking, an observable system in the form of (2.1) is one in which internal information about the states can be found from the external signals of the output and input.

Definition 2.10 A system characterized by (2.1) is said to be completely observable on the interval $[t_0, t_f]$ if, for specified t_0 and t_f, the initial state $\boldsymbol{x}(t_0) = \boldsymbol{x}_0$ of the system can be determined from the knowledge of $\boldsymbol{y}(t)$ and $\boldsymbol{u}(t)$ on $[t_0, t_f]$.

Definition 2.11 A system characterized by (2.1) is said to be totally observable on the interval $[t_0, t_f]$ if it is completely observable on every subinterval of $[t_0, t_f]$.

Definition 2.12 The observability matrix $\boldsymbol{Q}_o(t)$ is defined by

$$\boldsymbol{Q}_o(t) := [\boldsymbol{C}'(t) \quad \Delta_o \boldsymbol{C}'(t) \quad \ldots \quad \Delta_o^{n-1} \boldsymbol{C}'(t)]$$

where Δ_o is the VPDO is given by

$$\Delta_o := \boldsymbol{A}'(t) + \delta$$

The observability matrix can be used as the controllability matrix is used to characterize the observability of a LTV system without finding explicit solutions to (2.1).

Theorem 2.6 *The following are equivalent*

(i) *(2.1) is completely observable on* $[t_0, t_f]$

(ii) $N(t_0, t_f) = \int_{t_0}^{t_f} \phi'(t_0, t) C'(t) C(t) \phi(t_0, t) dt$ *is nonsingular*

(iii) *The rows of* $C(t_f)\phi(t_0, t)$ *are linearly independent on* $[t_0, t_f]$.

(iv) *The following adjoint system is completely state-controllable*

$$\dot{x}^*(t) = -A'(t)x^*(t) \pm C'(t)u(t)$$

$$y(t) = \mp B(t)x(t)$$

$N(t_0, t_f)$ is called the observability gramian of the LTV system. Because general solutions to LTV systems do not exist, the observability gramian is more useful for LTI systems. Part (iv) of Theorem 2.6 and Theorem 2.7 use what is commonly called the duality property. The duality property of LTV systems allows one to make statements about the observability of a system by considering the controllability of the adjoint system. Similarly, the controllability of a system can be found by studying the observability of the adjoint system.

Theorem 2.7 *The system characterized by (2.1) is totally observable on* $[t_0, t_f]$ *if and only if the adjoint system is totally state-controllable on* $[t_0, t_f]$.

Theorem 2.8 *The system characterized by (2.1) is totally observable on the interval* $[t_0, t_f]$ *if the columns of* $C(t)\phi(t_0, t)$ *are linearly independent on every subinterval of* $[t_0, t_f]$.

Corollary 2.1 *The system characterized by (2.1) is totally observable on the interval* $[t_0, t_f]$ *if* $N(t_0, t_f)$ *is nonsingular on every subinterval of* $[t_0, t_f]$.

The following two theorems use the observability matrix to characterize the complete or total observability of a LTV system.

Theorem 2.9 *The system characterized by (2.1) with* $A(t)$, $C(t)$ *differentiable* $n-2$, $n-1$ *times almost everywhere on* $[t_0, t_f]$ *is completely observable on* $[t_0, t_f]$ *if the observability matrix* $Q_o(t)$ *has rank* n *almost everywhere on some finite subinterval.*

Theorem 2.10 *The system characterized by (2.1) with* $A(t)$, $C(t)$ *differentiable* $n-2$, $n-1$ *times almost everywhere on* $[t_0, t_f]$ *is totally observable on* $[t_0, t_f]$ *if and only if the observability matrix* $Q_o(t)$ *has rank* n *almost everywhere on* $[t_0, t_f]$.

Definition 2.13 The system characterized by (2.1) is said to be uniformly observable on $[t_0, t_f]$ if the observability matrix $Q_o(t)$ has rank n everywhere on $[t_0, t_f]$.

Uniform complete observability is a stronger observability condition than total observability similar to the relation between total and complete controllability. It amounts to instantaneous observability, *i.e.* with knowledge of the input and output the states can be found instantaneously. Uniform observability will be used to construct transformations of (2.1) to a canonical observability form.

2.3 - Overview of SPDO's

Now we will consider theoretical characterizations of scalar LTV differential equations based on Differential Algebraic Spectral Theory (DAST). This material is adapted from work presented in [128], [129], [130], [136], [137], [142]. Consider a general nth order scalar unforced LTV differential equation represented by

$$y^{(n)} + \alpha_n(t)y^{(n-1)} + \cdots + \alpha_2(t)\dot{y} + \alpha_1(t)y = 0 \tag{2.6}$$

with initial conditions

$$y^{(k)}(t_0) = y_{k0}\,,\, k = 0, 1, \cdots, n-1$$

This equation can be represented using a symbolic operator called a scalar polynomial differential operator (SPDO)

$$\mathcal{D}_\alpha = \delta^n + \alpha_n(t)\delta^{n-1} + \cdots + \alpha_2(t)\delta + \alpha_1(t) \tag{2.7}$$

This system is equivalent to the state space representation of (2.3) with no input and with system matrix in the companion canonical form $A_c(t) = \text{comp}(\alpha_1(t), \alpha_2(t), \ldots, \alpha_n(t))$

$$A_c(t) = \begin{bmatrix} 0 & 1 & 0 & \cdots & 0 \\ \vdots & \ddots & \ddots & \ddots & \vdots \\ 0 & \cdots & 0 & 1 & 0 \\ 0 & \cdots & \cdots & 0 & 1 \\ -\alpha_1(t) & -\alpha_2(t) & \cdots & \cdots & -\alpha_n(t) \end{bmatrix} \tag{2.8}$$

The SPDO representation of (2.6) is $\mathcal{D}_\alpha\{y\} = 0$. Brisson originally introduced the symbolic operator representation of (2.6) in 1808. In 1827, Cauchy used a factorized symbolic operator

$$\mathcal{D}_\alpha = (\delta - \lambda_n)\cdots(\delta - \lambda_2)(\delta - \lambda_1) \tag{2.9}$$

to represent a linear differential equation with $\alpha_i(t) \equiv \alpha_i$. It is well-known that this subclass, which is the class of LTI systems, enjoys an *algebraic* spectral theory that

facilitates analytical solutions, precise stability criteria, frequency domain analysis and synthesis, and (robust) stabilization control design techniques. However, as is also well-known, this (time-invariant) algebraic spectral theory does not carry over, in general, to the time-varying case.

In 1879, Floquet considered a more general factorized symbolic operator

$$\mathcal{D}_\alpha = (\delta - \lambda_n(t))\cdots(\delta - \lambda_2(t))(\delta - \lambda_1(t)). \tag{2.10}$$

for analytic differential equations in the form of (2.6). In general, the order of the $\lambda_i(t)$ is important due to the loss of commutativity from the time invariant to the time variant factorization. Floquet showed that for coefficients with Laurent expansions, there was a factorization which could be expressed in terms of another Laurent expansion. These results have since been extended to LTV dynamic systems where the coefficients $\alpha_i(t)$ are real valued functions of a real variable t. A well known problem for the factorization of LTV dynamic systems is that the $\lambda_i(t)$ exhibit finite time singularities for real valued factorizations. In a revision of [136], necessary and sufficient conditions were established for the existence of a factorization of the SPDO representation (2.7) of a general LTV system. The solution is to allow for complex factorizations even for real valued coefficients $\alpha_i(t)$.

Before presenting this existence result, three key terms need to be defined. The concept of eigenvalues associated with this factorization (2.10) can be generalized to the time varying case with two entities

Series D-spectrum (SD-spectrum) for $\mathcal{D}_\alpha$

$$\{\lambda_k(t)\}_{k=1}^n$$

Parallel D-spectrum (PD-spectrum) for $\mathcal{D}_\alpha$

$$\{\rho_k(t) = \lambda_{1,k}(t)\}_{k=1}^{n}$$

Also, associated with the PD-spectrum $\{\rho_k(t)\}_{k=1}^{n}$ is the *Canonical Modal matrix* $\boldsymbol{V}(t)$ given by

$$\boldsymbol{V}(t) = \begin{bmatrix} 1 & 1 & \cdots & 1 \\ \mathcal{D}_{\rho_1}\{1\} & \mathcal{D}_{\rho_2}\{1\} & \cdots & \mathcal{D}_{\rho_n}\{1\} \\ \mathcal{D}_{\rho_1}^2\{1\} & \mathcal{D}_{\rho_2}^2\{1\} & \cdots & \mathcal{D}_{\rho_n}^2\{1\} \\ \vdots & & \ddots & \vdots \\ \mathcal{D}_{\rho_1}^{n-1}\{1\} & \cdots & \cdots & \mathcal{D}_{\rho_n}^{n-1}\{1\} \end{bmatrix} \tag{2.11}$$

where $\mathcal{D}_{\rho_i} = (\delta + \rho_i)$, $\mathcal{D}_{\rho_i}^k = \mathcal{D}_{\rho_i}\mathcal{D}_{\rho_i}^{k-1}$

$\mathcal{D}_\alpha$ is said to be a well defined SPDO if the coefficients α_i are regulated C^∞ functions of time, *i.e.* that the coefficients have derivatives of any order except at a countable number of finite discontinuities. A PD-spectrum is said to be well defined if it is free of finite time singularities.

With these definitions we can now state the main theorem on existence of a factorization of the form of (2.10) for general LTV systems (2.6).

Theorem 2.11 *Let $\mathcal{D}_\alpha$ be a well defined nth order SPDO with complex valued coefficients. Then the following are equivalent:*

(i) $\mathcal{D}_\alpha\{y\} = 0$ has a fundamental set of solutions $\{y_k\}_{k=1}^{n}$ such that for each $k \leq n$,

$$\boldsymbol{W}_k = \Delta(y_1, \ldots, y_n) \in \mathbb{I}^{\perp}(\mathbb{C})$$

where $\mathbb{I}$ is a subset of the D-ring of regulated analytic functions for which $f(t) = 0$ for some t.

(ii) $\mathcal{D}_\alpha$ has a well-defined PD-spectrum $\{\rho_k(t)\}_{k=1}^{n}$ such that for each $k \leq n$

$$V_k = \det \boldsymbol{V}(\rho_1, \dots \rho_k) \in \mathbb{I}^{\perp}(\mathbb{C})$$

(iii) $\mathcal{D}_\alpha$ has a well defined SD-spectrum $\{\lambda_k(t)\}_{k=1}^{n}$

An nth-order SPDO $\mathcal{D}_\alpha$ with locally integrable coefficients has well-defined SD- and PD-spectrum, where the SD- and PD-eigenvalues are solutions to the SD- and PD-characteristic equations, if and only if $\mathcal{D}_\alpha$ can be factored into 1st-order and irreducible 2nd-order SPDOs with locally integrable coefficients. The SD- and PD-eigenvalues are unique up to the constants of integration.

The Series D-spectrum is so named as there is an obvious realization for (2.6) with an input $u(t)$ as a series of 1st order systems connected as in figure 2.1, where $\lambda_k(t)$ are in general complex valued. Similarly, the Parallel D-spectrum has been so named because (2.6) with complex valued $\rho_k(t)$ can be realized with the parallel conneciton of 1st order systems as in figure 2.2. Because the complex PD-eigenvalues occur in conjugate pairs, each conjugate pair $\rho_{i,i+1}(t) = \sigma_i(t) \pm \omega_i(t)$ can be realized through the algebraically similar realization in figure 2.3. These two spectra merge in the LTI case into the well established eigenvalue spectrum. The system matrix $\boldsymbol{\Gamma}(t)$ for the state space realization with the output of each 1st order subsystem in figure 2.1 as a state variable is called the *Series Spectral canonical form* (*SS canonical form*) associated with the SD-spectrum.

$$\boldsymbol{\Gamma}(t) = \begin{bmatrix} \lambda_1(t) & 1 & 0 & \cdots & 0 \\ 0 & \lambda_2(t) & \ddots & \ddots & \vdots \\ \vdots & \ddots & \ddots & \ddots & 0 \\ \vdots & & \ddots & \ddots & 1 \\ 0 & \cdots & \cdots & 0 & \lambda_n(t) \end{bmatrix} \tag{2.12}$$

and the system matrix $\boldsymbol{\Upsilon}(t)$ for the state space realization with the output of each 1st order subsystem in figure 2.2 taken as a state is called the *Parallel Spectral canonical form* (*PS canonical form*) associated with the PD-spectrum

$$\Upsilon(t) = \text{diag}\left[\rho_1(t), \rho_2(t), \cdots, \rho_n(t)\right] \tag{2.13}$$

where $\text{diag}[\rho_1(t), \rho_2(t), \cdots, \rho_n(t)]$ is a (block) diagonal matrix with elements $[\rho_1(t), \rho_2(t), \cdots, \rho_n(t)]$ on the diagonal from left to right.

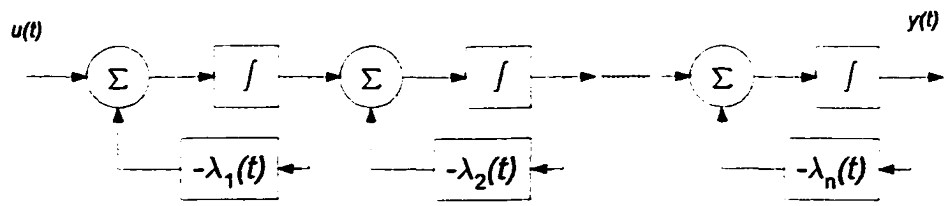

Figure 2.1 Series Realization of SPDO

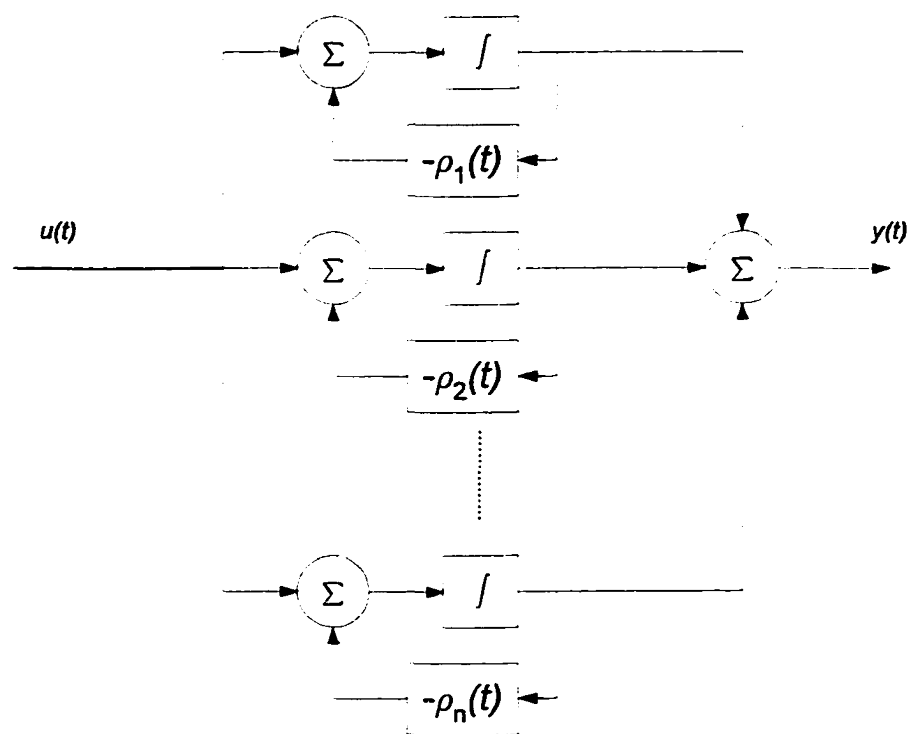

Figure 2.2 Parallel Realization of SPDO

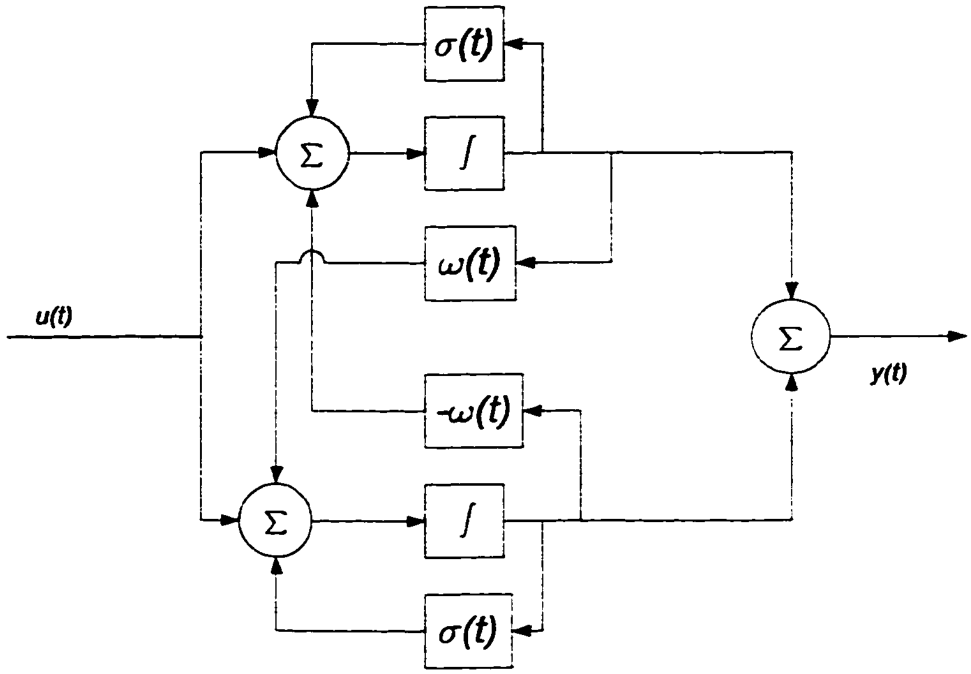

Figure 2.3 Real Coefficient Realization of Complex Conjugate PD-Eigenvalues

The following theorem originally formulated by Floquet, formally details a method for finding a SPDO factorization when a fundamental set solutions of (2.6) is known.

Theorem 2.12 *Let $\mathcal{D}_\alpha$ be an nth order SPDO operator and let $\{y_i(t)\}_{i=1}^{n}$ be any fundamental set of solutions to $\mathcal{D}_\alpha\{y\} = 0$. Let*

$$\Omega_i = \det \begin{bmatrix} y_1 & y_2 & \cdots & y_i \\ \dot{y}_1 & \dot{y}_2 & \cdots & \dot{y}_i \\ \vdots & \vdots & \ddots & \vdots \\ y_1^{(i-1)} & y_2^{(i-1)} & \cdots & y_i^{(i-1)} \end{bmatrix}$$

and

$$\Omega_0 := 1.$$

Then the scalar function $\lambda_i(t)$ in (2.10) can be written as

$$\lambda_i(t) = \delta\left\{\log\frac{\Omega_i(t)}{\Omega_{i-1}(t)}\right\}$$

In particular,

$$\lambda_1(t) = \frac{\dot{y}(t)}{y(t)}$$

satisfies (2.10) for any solution $y(t)$ *to* $\mathcal{D}_\alpha\{y\} = 0$.

A useful consequence which illustrates the relation between a PD-spectrum and a fundamental set is the following corollary from [142].

Corollary 2.2 *Let* $\rho(t)$ *be any function such that* $\lambda_1(t) = \rho(t)$ *satisfies (2.10). Then*

$$y(t) = \exp\int \rho(t)dt$$

satisfies $\mathcal{D}_\alpha\{y\} = 0$.

A few technical results from [142] facilitate finding SD- and PD-eigenvalues for the SPDO (2.7). First, the following Lemma gives a method for realizing an SPDO of order n from one of order $n-1$.

Lemma 2.14 *Let* $\mathcal{D}_\beta$ *be an* $(n-1)$*th order SPDO operator given by*

$$\mathcal{D}_\beta = \delta^{n-1} + \beta_{n-1}\delta^{n-2} + \cdots + \beta_2\delta + \beta_1$$

$$= (\delta - \lambda_{n-1})\cdots(\delta - \lambda_2)(\delta - \lambda_1),$$

and let $\mathcal{D}_\alpha$ *be an nth order SPDO operator related to* $\mathcal{D}_\beta$ *by*

$$\mathcal{D}_\alpha = (\delta - \lambda_n)\mathcal{D}_\beta$$

$$= \delta^n + \alpha_n \delta^{n-1} + \cdots + \alpha_2\delta + \alpha_1.$$

Then the coefficients α_k of $\mathcal{D}_\alpha$ can be obtained from the coefficients β_k of $\mathcal{D}_\beta$ by:

$$\begin{bmatrix} \alpha_1 \\ \alpha_2 \\ \vdots \\ \alpha_{n-1} \\ \alpha_n \end{bmatrix} = \begin{bmatrix} -\lambda_n & 0 & \cdots & \cdots & 0 \\ 1 & -\lambda_n & \ddots & & \vdots \\ 0 & 1 & \ddots & \ddots & \vdots \\ \vdots & \ddots & \ddots & -\lambda_n & 0 \\ 0 & \cdots & 0 & 1 & -\lambda_n \end{bmatrix} \begin{bmatrix} \beta_1 \\ \beta_2 \\ \vdots \\ \beta_{n-1} \\ \beta_n \end{bmatrix} + \begin{bmatrix} \dot{\beta}_1 \\ \dot{\beta}_2 \\ \vdots \\ \dot{\beta}_{n-1} \\ \dot{\beta}_n \end{bmatrix} \tag{2.15}$$

where $\beta_n := 1$.

With this Lemma, we can now define a method to construct an important matrix $P_n \in \mathbb{F}^{n\times n}$ recursively by

$$P_1 = [1],$$

and

$$P_n = \begin{bmatrix} P_{n-1} & 0 \\ \alpha_{n-1} & 1 \end{bmatrix} \tag{2.16}$$

where the kth element $\alpha_{n-1,k}$ in the row vector α_{n-1} is an explicit function of $\lambda_1, \lambda_2, \cdots,$ λ_{n-1} and their appropriate derivatives obtained by repeated applications of (2.15) to

$$\mathcal{D}_{\alpha_k} = (\delta - \lambda_k)(\delta - \lambda_{k-1})\cdots(\delta - \lambda_1)$$

$$= \delta^k + \alpha_{kk}\delta^{k-1} + \cdots + \alpha_{k2}\delta + \alpha_{k1}$$

With these tools, we can now state a general method for solving for the SD-eigenvalues and the PD-eigenvalues. The following Theorem contains the characteristic equations which can be used to solved for an SD-spectrum.

Theorem 2.13 *Let $\mathcal{D}_\alpha$ be an nth order SPDO as in (2.7). Then $\Gamma_\alpha = \{\lambda_i\}_{i=1}^n$ is a SD-spectrum for $\mathcal{D}_\alpha$ if and only if λ_i, $i = 1, 2, \cdots, n$, satisfy simultaneously the set of n nonlinear differential equations $\Delta(\,\cdot\,) = 0$, each of order $n-k$, $k = 1, 2, \cdots, n$, given by*

$$\begin{bmatrix} \Delta_1(\lambda_1) \\ \Delta_2(\lambda_1, \lambda_2) \\ \vdots \\ \Delta_n(\lambda_1, \cdots, \lambda_n) \end{bmatrix} = \boldsymbol{R}^T(\lambda_1, \cdots, \lambda_n) \begin{bmatrix} \alpha_1 \\ \alpha_2 \\ \vdots \\ \alpha_n \\ 1 \end{bmatrix} = \begin{bmatrix} 0 \\ 0 \\ \vdots \\ 0 \end{bmatrix}$$

where $\boldsymbol{R}(\lambda_1, \cdots, \lambda_n) \in F^{n\times(n+1)}$ is the block matrix consisting of the first n columns of the $(n+1)$th order canonical matrix $\boldsymbol{R}_{n+1}(\lambda_1, \cdots, \lambda_n, \lambda) = \boldsymbol{P}_{n+1}^{-1}$ given by (2.16).

Similarly, the PD-spectrum consists of n linearly independent solutions of the characteristic equation $\Delta_1(\lambda_1)$. The independence constraint insures that the PD-spectrum forms a fundamental set for (2.7). However, these are nonlinear equations which can be solved to find PD- and SD-spectrum for the LTV equations. These equations exhibit undesirable behavior such as finite escape times. However, theorem 2.11 guarantees the existence of well behaved complex solutions to these characteristic equations. In effect, the problem of finding fundamental sets which can characterize the solutions of these LTV equations can be translated into the problem of finding solutions to n nonlinear differential equations. For control problems, these techniques do provide a method of synthesizing LTV differential equations from a desired PD-spectrum (or SD-spectrum) which can achieve time varying characteristics unobtainable by LTI methods. And in the context of state feedback control problems, this will allow us to create a time varying state feedback which gives the closed loop plant a desired PD-spectrum.

The Canonical Modal matrix (2.11) mentioned earlier has additional important uses in describing a PD-spectrum. The first importance of the canonical modal matrix, is in characterizing a PD-spectrum. This is brought out in the following Theorem.

Theorem 2.14 *Let $\Upsilon_\alpha = \{\rho_k(t)\}_{k=1}^{n}$ be a set of PD-eigenvalues of an nth order SPDO of $\mathcal{D}_\alpha$. Then Υ_α constitutes a PD-spectrum for $\mathcal{D}_\alpha$ if and only if*

$$\det \boldsymbol{V}(t) \neq 0$$

where $\boldsymbol{V}(t)$ is the Canonical Modal matrix associated with Υ_α.

Another fundamental importance of the Canonical Modal matrix, is that the columns of the Canonical modal matrix are the column PD-eigenvectors $\boldsymbol{v}_i(t)$ of $\boldsymbol{A}_c(t)$ which satisfy

$$\boldsymbol{A}_c(t)\boldsymbol{v}_i(t) - \rho_i(t)\boldsymbol{v}_i(t) = \dot{\boldsymbol{v}}_i(t)$$

and the rows $\boldsymbol{u}_i(t)$ of $\boldsymbol{V}^{-1}(t)$ are the row PD-eigenvectors of $\boldsymbol{A}_c(t)$ which satisfy

$$\boldsymbol{u}_i^{\mathrm{T}}(t)\boldsymbol{A}_c(t) - \rho_i(t)\boldsymbol{u}_i^{\mathrm{T}}(t) = -\dot{\boldsymbol{u}}_i^{\mathrm{T}}$$

Also, the Canonical modal matrix can be used to characterize a Wronskian matrix $\boldsymbol{W}(t)$ for (2.7).

$$\boldsymbol{W}(t) = \boldsymbol{V}(t)\exp\int \Upsilon(t)dt$$

where $\Upsilon(t)$ is the Parallel Spectral canonical form (2.13). Because of the equivalence between the SPDO representation of (2.7) and the state space realization in Phase variable canonical form with companion matrix $\boldsymbol{A}_c(t)$ and the fact that the PD-eigenvalues form a fundamental set of solutions, this Wronskian matrix also forms a fundamental matrix for the state space realization.

The following definition is used in characterizing the exponential stability of LTV systems in terms of the PD-spectra.

Definition 2.14 Let $\sigma : J \to \mathbb{R}$ be a locally integrable function on the interval $J = [T_0, \infty)$. The extended mean of $\sigma(t)$ over J is defined by

$$\underset{t_0,\, t \in I}{\mathrm{em}} \; (\sigma(t)) = \limsup_{T \to \infty,\, t_0 \geq T_0} \frac{1}{T} \int_{t_0}^{t_0+T} \sigma(\tau) \mathrm{d}\tau$$

$$= \lim_{T \to \infty} \left[\sup_{t \geq t_0 + T,\, t_0 \geq T_0} \frac{1}{t - t_0} \int_{t_0}^{t} \sigma(\tau)\, \mathrm{d}\tau \right]$$

With the previous definition, the following Theorem formally treats the problem of characterizing the stability of a LTV differential equation in either the scalar form of (2.6) or the equivalent state space realization in phase variable canonical form in terms of the PD-spectra.

Theorem 2.15 *Let $\mathcal{D}_\alpha$ be a well defined nth order scalar polynomial differential operator*

$$\mathcal{D}_\alpha = \delta^n + \alpha_n(t)\delta^{n-1} + \cdots + \alpha_2(t)\delta + \alpha_1(t)$$

with a well defined PD-spectrum $\{\rho_k(t)\}_{k=1}^{n}$ in $I = [T_0, \infty)$. Let $\boldsymbol{v}_k(t)$ and $\boldsymbol{u}_k^T(t)$ be a column PD-eigenvector and a row PD-eigenvector associated with $\rho_k(t)$ respectively. Then the null solution to the LTV system $\mathcal{D}_\alpha\{y\} = 0$ is uniformly asymptotically stable for all $t_0 \geq T_0$ if and only if

(i) there exists a $0 < c_k < \infty$ such that

$$\mathrm{Re}\left\{ \underset{t \in I}{em} \; (\rho_k(t)) \right\} = -c_k < 0$$

and moreover

(ii) there exist $h_k > 0$ and $0 < d_k < c_k$ such that

$$\left\| \boldsymbol{v}_k(t)\boldsymbol{u}_k^T(t_0) \right\| < h_k \exp d_k(t - t_0)$$

Remark Condition (ii) is automatically satisfied if all PD-eigenvalues are of polynomial order or slower; that is, an integer $m > 0$ exists such that

$$\lim_{t \to \infty} \frac{\rho_k(t)}{t^m} = 0,\ k = 1,\ 2,\ \cdots,\ n$$

A similar sufficient condition to guarantee exponential stability of a LTV system also exists based on the extended mean of SD-eigenvalues.

The last Lemma to be presented in this section provides a method of synthesizing a LTV differential equation in either the phase variable canonical form or as a scalar differential equation (2.6).

Lemma 2.2 *Let $\Upsilon_\alpha = \{\rho_k(t)\}_{k=1}^n$ be a PD-spectrum for $\mathcal{D}_\alpha$ and let $V_{n+1}(\rho_1, \rho_2, \cdots, \rho_n, \rho)$ be the $(n+1) \times (n+1)$ modal canonical form obtained by augmenting with ρ the modal canonical matrix $V_n(\rho_1, \rho_2, \cdots, \rho_n)$ associated with Υ_α as follows:*

$$V_{n+1}(\rho_1, \rho_2, \cdots, \rho_n, \rho) = [\boldsymbol{v}_{ij}]$$

$$= \begin{bmatrix} & & & 1 \\ & V_n(\rho_1, \rho_2, \cdots, \rho_n) & & \rho \\ & & & \mathcal{D}_\rho\{\rho\} \\ & & & \vdots \\ \mathcal{D}_{\rho_1}^{n-1}\{\rho_1\} & \cdots & \mathcal{D}_{\rho_n}^{n-1}\{\rho_n\} & \mathcal{D}_\rho^{n-1}\{\rho\} \end{bmatrix}$$

Then the coefficients $\alpha_k(t)$ of $\mathcal{D}_\alpha$ can be obtained by

$$\alpha_k = \frac{\widetilde{v}_{k,n+1}}{\det V_n(\rho_1, \rho_2, \cdots, \rho_n)},$$

where $\widetilde{v}_{ij}$ denotes the algebraic cofactor of v_{ij}.

Thus given a desired PD-spectrum, the time varying coefficients $\alpha_i(t)$ of the corresponding SPDO (2.7) can be found. This result will be used in the PD-spectrum assignment design presented in the sequel.

2.4 - Extension of PD-Spectra to Multi-input Multi-output systems

The preceding section developed the concepts of PD- and SD-spectra for scalar LTV systems and the equivalent phase variable canonical form. This section will generalize the concepts of PD-spectrum to the LTV MIMO problem as in equation (2.1). To facilitate this, we will first introduce the concept of Vector Polynomial Differential Operators (VPDO) which are useful in dealing with state space realizations.

Let $\mathbb{K}$ be the differential ring of regulated C^∞ functions on $[0, \infty)$. Let $\mathbb{K}^n$ be the n-dimensional differential module of n-vectors $v(t) = \mathrm{col}\,[v_i(t)]$, and $\mathbb{K}^{n\times n}$ be the differential module of $n \times n$ matrices $A(t) = [a_{ij}(t)]$, with entries v_i and a_{ij} from $\mathbb{K}$. The following two n-dimensional, first-order, mutually adjoint vector polynomial differential operators (VPDO)

$$\mathcal{P}_A = \delta - A(t) = \mathcal{Q}_{(-A^{\mathrm{T}})}$$

and

$$\mathcal{Q}_A = \delta + A^{\mathrm{T}}(t) = \mathcal{P}_{(-A^{\mathrm{T}})}$$

play an instrumental role in the development of a differential-algebraic spectral theory for both LTI and LTV systems. For instance, a MV LTV system (2.1) can be represented by

$$\begin{aligned} \mathcal{P}_A \boldsymbol{x} &= \boldsymbol{B}(t)\boldsymbol{u} \\ \boldsymbol{y} &= \boldsymbol{C}(t)\boldsymbol{x} + \boldsymbol{D}(t)\boldsymbol{u} \end{aligned}$$

Moreover, if we define the inverse VPDO $\mathcal{P}_A^{-1} = [\delta \boldsymbol{I} - \boldsymbol{A}(t)]^{-1}$ as the integral operator such that $\mathcal{P}_A^{-1}\mathcal{P}_A = \mathcal{I}$, where $\mathcal{I}$ is the identity operator, then the output $\boldsymbol{y}(t)$ with zero initial conditions can be conveniently represented by

$$\boldsymbol{y}(t) = \left[\boldsymbol{C}(t)[\delta \boldsymbol{I} - \boldsymbol{A}(t)]^{-1}\boldsymbol{B}(t) + \boldsymbol{D}(t)\right]\boldsymbol{u}(t) \tag{2.17}$$

In the sequel, we shall adopt the convention that $\mathcal{P}_A^0 = \mathcal{I}$, the identity operator, and $\mathcal{P}_A^k = \mathcal{P}_A \mathcal{P}_A^{k-1}$. The same applies to $\mathcal{Q}_A$. Although the VPDOs $\mathcal{P}_A$ and $\mathcal{Q}_A$ are defined for n-vectors $\boldsymbol{v} \in \mathbb{K}^n$, we will also use them on matrices $\boldsymbol{M} \in \mathbb{K}^{n \times r}$ in a column wise fashion. For $n = 1$, $\boldsymbol{A}(t)$ becomes a scalar function, say $a(t)$, and the VPDOs $\mathcal{P}_A$ and $\mathcal{Q}_A$ become SPDOs denoted by $\mathcal{P}_a$ and $\mathcal{Q}_a$, respectively. The following definitions characterizes a PD-spectrum for general system matrices.

Definition 2.15 (a) A continuously differentiable scalar function $\rho(t)$ is called a PD-eigenvalue of an n-dimensional VPDO $\mathcal{P}_A$ if there exists a Lyapunov transformation matrix $\boldsymbol{L}(t)$ such that the vector

$$\boldsymbol{p}(t) = \boldsymbol{L}(t)\boldsymbol{p}_0(\rho(t))$$

where

$$\boldsymbol{p}_0(\rho(t)) = \begin{bmatrix} 1 \\ \mathcal{Q}_\rho(1) \\ \vdots \\ \mathcal{Q}_\rho^{n-1}(1) \end{bmatrix}$$

satisfies $\mathcal{P}_{[A-\rho I]}\boldsymbol{p} = 0$, or what is the same

$$\dot{\boldsymbol{p}}(t) = [\boldsymbol{A}(t) - \rho(t)I]\boldsymbol{p}(t) \tag{2.18}$$

The vector $\boldsymbol{p}(t)$ is then called a PD-eigenvector of $\mathcal{P}_A$ associated with $\rho(t)$.

(b) Let $\rho(t)$ be a PD-eigenvalue of $\mathcal{P}_A$. A vector $q(t)$ satisfying $\mathcal{Q}_{[A-\rho I]}q = 0$, or what is the same

$$\dot{\boldsymbol{q}}(t) = -[\boldsymbol{A}(t) - \rho(t)I]^{\mathrm{T}}\boldsymbol{q}(t) \tag{2.19}$$

is called an adjoint PD-eigenvector of $\mathcal{P}_A$ associated with $\rho(t)$.

(c) Let $\boldsymbol{p}(t)$ and $\boldsymbol{q}(t)$ be a PD-eigenvector and an adjoint PD-eigenvector for $\mathcal{P}_A$ associated with a PD-eigenvalue $\rho(t)$. Then $\rho(t)$ is called a PD-eigenvalue of $A(t)$. The vectors $\boldsymbol{p}(t)$ and $\boldsymbol{q}^{\mathrm{T}}(t)$ are called a column PD-eigenvector and a row PD-eigenvector, respectively, of $\boldsymbol{A}(t)$ associated with $\rho(t)$.

The following definition introduces the notions of a differentially distinct set. This notion is subsequently used to define the concept of a PD-spectrum for a MIMO LTV system.

Definition 2.16 Let $\{\rho_i(t)\}_{i=1}^{k}$ be a set of k PD-eigenvalues of $\boldsymbol{A}(t)$. The set is said to be differentially distinct if the associated set of column PD-eigenvectors $\{\boldsymbol{p}_i(t)\}_{i=1}^{k}$ is linearly independent.

Remark. Being in a set, $\rho_i(t)$ are distinct in the sense that $\rho_i(t) \neq \rho_j(t)$. However, they are not necessarily differentially distinct. Consider, for example, the set $\{\rho_i(t)\}_{i=1}^{3} = \{-\frac{1}{2}, \frac{1}{2}, \frac{e^t-1}{2(e^t+1)}\}$ for $\boldsymbol{A} = \mathrm{comp}[1, 0.25, -4]$. The associated column PD-eigenvectors are

$$\boldsymbol{p}_1 = \begin{bmatrix} 1 \\ -\frac{1}{2} \\ \frac{1}{4} \end{bmatrix}, \quad \boldsymbol{p}_2 = \begin{bmatrix} 1 \\ \frac{1}{2} \\ \frac{1}{4} \end{bmatrix}, \quad \boldsymbol{p}_3 = \begin{bmatrix} 1 \\ \frac{e^t-1}{2(e^t+1)} \\ \frac{1}{4} \end{bmatrix}$$

which are clearly linearly dependent.

Definition 2.17 (a) A differentially distinct set of n PD-eigenvalues $\{\rho_i(t)\}_{i=1}^{n}$ for an n-dimensional VPDO $\mathcal{P}_A$ is called a PD-spectrum for $\mathcal{P}_A$, and for the associated $n \times n$ matrix $A(t)$.

(b) A PD-spectrum $\{\rho_i(t)\}_{i=1}^{n}$ for an n-dimensional VPDO $\mathcal{P}_A$ together with a set of associated PD-eigenvectors $\{p_i(t)\}_{i=1}^{n}$ is called a PD-eigenstructure for $\mathcal{P}_A$, and for the associated $n \times n$ matrix $A(t)$.

The following theorem defines a block diagonal matrix that is useful in the synthesis of PD-spectra for MIMO systems.

Theorem 2.16 *Let* $A(t) = diag[A_1(t), A_2(t), \ldots, A_l(t)]$, *where* $A_i \in \mathbb{K}^{n_i \times n_i}$ *are bounded companion matrices. If* $\rho(t)$ *is a PD-eigenvalue of* $A_i(t)$ *for some* $i \leq l$ *with an associated column PD-eigenvector* $p_i(t) \in \mathbb{K}^{n_i}$, *then it is a PD-eigenvalue for* $A(t)$ *with an associated column PD-eigenvector* $p(t)$ *generated from* $p_i(t)$.

With what has been presented we can now state necessary and sufficient conditions for the uniform exponential stability of a MIMO LTV system in terms of the PD-spectrum.

Theorem 2.17 *Let* $\mathcal{P}_A$ *be a VPDO having a PD-spectrum* $\{\rho_k(t)\}_{k=1}^{n}$ *with* $|Re\,\rho_k(t)| < M$, $t \geq 0$, *for some* $M < \infty$. *Let* $p_k(t)$ *and* $q_k^T(t)$ *be a column PD-eigenvector and a row PD-eigenvector associated with* $\rho_k(t)$ *respectively. Then the null solution to the LTV system* $\mathcal{P}_A x = 0$ *is uniformly asymptotically stable for all* $t_0 \geq T_0$ *if and only if for every* $k = 1, 2, \ldots, n$,

(i) *there exists a* $0 < c_k \leq \infty$ *such that* $\underset{t_0,\, t \in I}{\text{em}}\,(\text{Re}\,\rho_k(t)) = -c_k < 0$

(ii) *there exist* $h_k > 0$ *and* $0 < d_k < c_k$ *such that* $\left\| p_k(t) q_k^T(t_0) \right\| < h_k e^{d_k(t-t_0)}$ *for all* $t \geq t_0 \geq T_0$.

Theorem 2.17, given above, gives necessary and sufficient stability criteria in terms of the PD-spectrum of a LTV system. This theorem will allow us to assign LTV dynamics to a closed loop system that maintain u.e.s.. This will permit us to design LTV controllers that can achieve performance beyond the capabilities of LTI controllers while guaranteeing the stability of the closed loop plant.

Remarks

1. Condition (ii) is automatically satisfied if the imaginary parts of all PD-eigenvalues are of polynomial order or slower; that is, an integer $m > 0$ exists such that

$$\lim_{t \to \infty} \frac{\mathrm{Im}\, \rho_k(t)}{t^m} = 0\,, \qquad k = 1,\, 2,\, \cdots,\, n$$

In particular, it holds if $\mathrm{Im}\, \rho_k(t)$ are uniformly bounded.

2. If $\underset{t_0, t \in I}{\mathrm{em}}(\mathrm{Re}\, \rho_k(t)) > 0$ for some $t_0 \geq T_0$, and $1 \leq k \leq n$, then the null solution to $\mathcal{P}_A x = 0$ is unstable. However, if $\underset{t_0, t \in I}{\mathrm{em}}(\mathrm{Re}\, \rho_k(t)) = 0$ for some $t_0 \geq T_0$, and $1 \leq k \leq n$, the null solution may be either stable, asymptotically stable, or unstable, but it cannot be exponentially stable.

CHAPTER 3

TRAJECTORY LINEARIZATION DESIGN

3.1 - Design Method

Lyapunov's original work *The General Problem of The Stability of Motion* is arguably the most fundamental work in the analysis and synthesis of feedback control of nonlinear systems for modern control engineers. His results were first published in 1892, and since then have been used in the proof of stability of almost all nonlinear controllers. Any control strategy which relies on linear approximation, either implicitly or explicitly make use of his results. Modern control strategies such as variable structure control and backstepping make explicit use of his techniques in the proof of the stability of the closed loop controlled system.

Originally, his work was motivated by the question of what effect perturbations in the orbit of the planets would have. In planetary mechanics, disturbances to the fixed elliptical orbits occur in two kinds. The first are periodic disturbances arising from the effect of the planets on each other. The second kind is the effect of slow changes in the elliptical patterns of orbit also called secular inequalities. Would the secular inequalities build up over time and cause the pattern of planetary orbits to take on a new configuration. To put this in a context more appropriate to control engineers, when perturbed would the path of a planet return asymptotically to its original orbit, or would it

diverge from the original path and assume a new trajectory. Lyapunov and earlier researchers such as Laplace and Lagrange wanted to know if slow changes in the ellipse parameters of the solar system could lead to the destruction of the solar system. This is a question of the stability of motion. Is a given trajectory stable in the face of disturbances? To this end he considered two methods.

The second method, or the direct, relies on generalized energy functions that could be used to characterize the behavior of nonlinear systems. These generalized energy functions have come to be called Lyapunov functions and were generalized from mechanical system concepts. A point in a system of minimum potential energy is an equilibrium point for a mechanical system, and the stability of an equilibrium can be determined by looking at the time derivative of the potential. The origins of this method began with Toricelli's principle. Lagrange, Dirichlet, and Liouville were instrumental in the development of this method which was later refined, generalized, and rigorously developed by Lyapunov.

The first method of Lyapunov is also called the indirect. The first method is the method of determining the stability by examining the solutions to the disturbed equations of motion. Lyapunov introduced a characteristic number concept of exponential growth or decay of solutions of differential equations whose negative value has since come to be called the Lyapunov exponent. When the Lyapunov exponents of all solutions to a differential equation can be shown to be negative, the system is asymptotically stable.

One important result that Lyapunov was able to prove by the indirect method, was that for a large class of systems if the first approximation is stable then so is the nonlinear system. His technique for finding solutions was to use successive linear approximations. The first approximation is what is now commonly termed the linearization. Linearization forms a powerful tool for the analysis of nonlinear systems, and for the synthesis of exponentially stabilizing nonlinear controllers.

Linearization does more than justify the stability of a trajectory. It also gives qualitative information in that the linearization gives characteristic modes of decay or growth, *i.e.* spectral information, which locally characterizes the behavior of the nonlinear system. In the context of stability of motion, the local stability of a trajectory of a nonlinear system can be characterized by the stability property of a linearization about the nominal trajectory. Most commonly for autonomous nonlinear systems, linearization is used about a constant trajectory which results in LTI error dynamics. Linearization of NLTV systems about any trajectory or of NLTI systems about a time-varying trajectory results in LTV error dynamics. General explicit solutions for LTV systems do not exist and thus linearization has been limited as a method of characterizing the stability of a trajectory. However, constant trajectories for NLTI systems result in LTI linearization for which explicit solutions with well defined modal behavior can be found and used to characterize the local nonlinear behavior. So, linearization has proved useful in formulating local LTI controllers for constant trajectories. A technique called Gain Scheduling has been used as an *ad hoc* method to extend these results to time varying trajectories.

The design method presented in this dissertation was developed in the context of true trajectory linearization. The problem of controlling a nonlinear plant is broken into two parts. The first part consists of finding a feedforward control signal that causes the plant to obtain a desired nominal trajectory. This design amounts to the problem of nonlinear inversion. This method will be applied to both minimum and nonminimum phase plants. The existence of nonminimum phase plants means that stable inversion generalizations will be needed to avoid unbounded nominal controls. This generalization of the inversion problem is called pseudoinversion.

Lyapunov's original question was whether a trajectory is stable. For his needs bounded stability was sufficient to show the stability of the structure of the solar system. In control, the problem is one of finding an input that asymptotically stabilizes the

trajectory. However, assuming the existence of a nominal control, Lyapunov's techniques can be very useful in formulating feedback stabilizing controls. The second part of the design relies on linearization to formulate a state feedback that exponentially stabilizes the desired trajectory. PD-spectral design methods are used to design a state feedback control law that exponentially stabilizes the nominal trajectory. Thus the complete controller generates a control input that will achieve exponential tracking of a given output trajectory.

The design procedure will now be outlined. We assume that there is a nonlinear plant described by the following differential equation.

$$\begin{aligned} \dot{\boldsymbol{\xi}}(t) &= \boldsymbol{f}(\boldsymbol{\xi}(t), \boldsymbol{v}(t)) \\ \boldsymbol{\eta}(t) &= \boldsymbol{h}(\boldsymbol{\xi}(t), \boldsymbol{v}(t)) \end{aligned} \tag{3.1}$$

where $\boldsymbol{\xi}$ are the n states that describe the system. There are m inputs $\boldsymbol{v}(t)$, and p outputs $\boldsymbol{\eta}(t)$. Now, the design objective is to track a desired output $\overline{\boldsymbol{\eta}}(t)$. Suppose there exists a nominal state trajectory $\overline{\boldsymbol{\xi}}(t)$ and a nominal control $\overline{\boldsymbol{v}}(t)$ that satisfy

$$\begin{aligned} \dot{\overline{\boldsymbol{\xi}}}(t) &= \boldsymbol{f}(\overline{\boldsymbol{\xi}}(t), \overline{\boldsymbol{v}}(t)) \\ \overline{\boldsymbol{\eta}}(t) &= \boldsymbol{h}(\overline{\boldsymbol{\xi}}(t), \overline{\boldsymbol{v}}(t)) \end{aligned}$$

That is, the nominal control places the system on the desired trajectory. In section 3.3 we will present methods that can be used to compute the nominal control $\overline{\boldsymbol{v}}(t)$.

Now, state feedback is required to stabilize the trajectory. The error about the nominal trajectory is given by

$$\begin{aligned} \boldsymbol{e}(t) &= \boldsymbol{\xi}(t) - \overline{\boldsymbol{\xi}}(t) \\ \boldsymbol{y}(t) &= \boldsymbol{\eta}(t) - \overline{\boldsymbol{\eta}}(t) \end{aligned}$$

and the tracking error control input by

$$\boldsymbol{u}(t) = \boldsymbol{v}(t) - \overline{\boldsymbol{v}}(t)$$

The linearized tracking error dynamics are given by

$$\dot{\boldsymbol{x}} = \boldsymbol{A}(t)\boldsymbol{x} + \boldsymbol{B}(t)\boldsymbol{u} \qquad (3.2)$$
$$\boldsymbol{y} = \boldsymbol{C}(t)\boldsymbol{x} + \boldsymbol{D}(t)\boldsymbol{u}$$

where

$$\boldsymbol{A}(t) = \frac{\partial \boldsymbol{f}}{\partial \boldsymbol{\xi}}\Big|_{\overline{\boldsymbol{\xi}},\overline{\boldsymbol{v}}} \qquad \boldsymbol{B}(t) = \frac{\partial \boldsymbol{f}}{\partial \boldsymbol{v}}\Big|_{\overline{\boldsymbol{\xi}},\overline{\boldsymbol{v}}}$$

$$\boldsymbol{C}(t) = \frac{\partial \boldsymbol{h}}{\partial \boldsymbol{\xi}}\Big|_{\overline{\boldsymbol{\xi}},\overline{\boldsymbol{v}}} \qquad \boldsymbol{D}(t) = \frac{\partial \boldsymbol{h}}{\partial \boldsymbol{v}}\Big|_{\overline{\boldsymbol{\xi}},\overline{\boldsymbol{v}}}$$

In section 3.2 we will present methods that assign uniform exponentially stable linearized error dynamics using a PD-spectral assignment procedure. The robustness of PD-eigenstructure assignment will be considered in Chapter 4.

Trajectory Linearization Design Procedure for Trajectory Tracking

1. Find a controller that generates an input $\overline{\boldsymbol{v}}(t)$ that places the system on the desired trajectory. This is the problem of inversion of the nonlinear input-output mapping. Due to the causality constraint, stable and causal inverses do not exist for physical systems. Thus pseudo-inverses that use stable and causal approximations to the exact inverse must be used.

2. Assume the plant is on the nominal trajectory and the state errors are available. Design a PD-spectrum assignment controller that generates a control $\boldsymbol{u}(t) = \mathrm{K}(t)\boldsymbol{x}(t)$ that stabilizes the nominal trajectory and achieves the required robustness.

3. If the states are not available, then an exponential observer is required. The observer states can then be used for the feedback. For LTV systems the principle of separability is valid, and an observer based controller can be used to achieve exponential stability of a nonlinear system under some mild conditions.

4. The complete control that achieves the trajectory tracking objective is $\boldsymbol{v}(t) = \overline{\boldsymbol{v}}(t) + \boldsymbol{u}(t)$.

The complete nonlinear controller is shown schematically in figure 3.1. The inverse plant or pseudo-inverse generates a nominal control to achieve the nominal trajectory. The LTV error stabilizing controller uses feedback to cause the nonlinear plant to remain on the nominal trajectory.

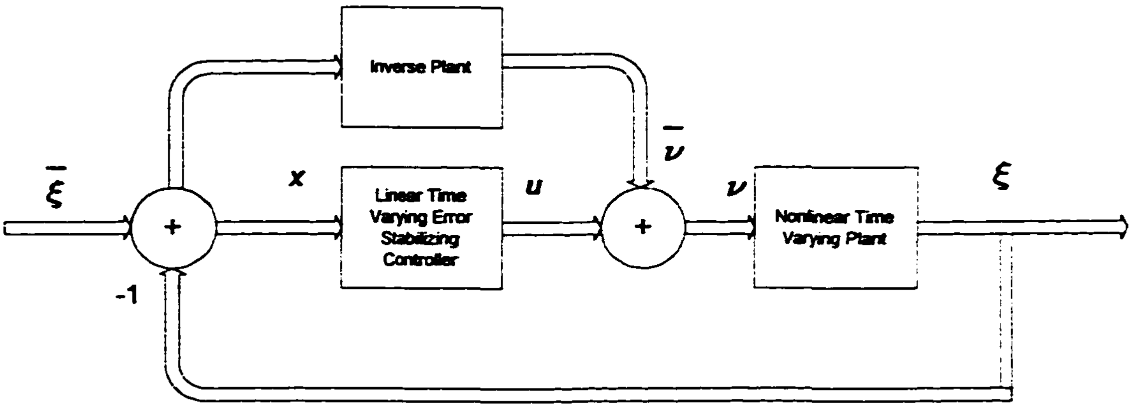

Figure 3.1 Controller Structure

3.2 - PD-Spectral Assignment Design

A formal development of the LTV technique for assignment of exponentially stable error dynamics to achieve trajectory tracking will be presented in this section. Certain assumptions about the linearized plant are necessary to insure the existence of a feedback controller that stabilizes the plant.

Assumption 3.1 We will consider general LTV systems described by

$$\dot{\boldsymbol{x}} = \boldsymbol{A}(t)\boldsymbol{x} + \boldsymbol{B}(t)\boldsymbol{u}, \ \forall t > t_0 \tag{3.3}$$

$$y = C(t)x$$

Where, $x(t)$ is an n vector of states; $u(t)$ is an m vector of inputs; $y(t)$ is a p vector of outputs; $A(\cdot) \in C^{n-2}(J, \mathbb{R}^{n\times n})$ is a $n \times n$ system matrix; $B(\cdot) \in C^{n-1}(J, \mathbb{R}^{n\times m})$ is a $n \times m$ input matrix; $C(\cdot) \in C(J, \mathbb{R}^{p\times n})$ is a $p \times n$ output matrix. Also, $A^{(q)}(t)$ $B^{(r)}(t)$ are bounded for $0 \leq q \leq n-1$, and $0 \leq r \leq n-1$ and $C(t)$ is a matrix of bounded functions. Also, we will assume that system (3.3) is uniformly complete controllable with a lexicographically fixed basis of the controllability matrix, *i.e.* the columns of the controllability matrix that are linearly independent are fixed in time, and that $B(t)$ is of rank m $\forall t$.

All, of these assumptions are reasonable for engineered systems. Specifically, complete controllability is an important consideration when designing a system because for any system without this property no controller will be able to effect the stability or performance of the uncontrollable portion of the plant in the face of uncertainties and disturbances. It is also unlikely that engineering systems will lose controllability on sets of finite measure for the operational range of the system. Thus, uniform controllability is a reasonable assumption. Also, the designer is unlikely to design for a system that uses an actuator to primarily effect one output variable for a period of time, and then is used to realize another desired output variable for another period of time. Thus the lexicographic basis is reasonable. However, generalizations can be made for systems in which such control activity is required or desired.

Recall, that a LTV system is uniformly (state) controllable if the controllability matrix given by

$$Q_c(t) = [B(t), \Delta_c B(t), \cdots, \Delta_c^{n-1} B(t)]$$

where $\Delta_c(t)$ is a VPDO given by

$$\Delta_c(t) = -A(t) + \delta$$

is of rank n for all t in which the system is defined. A lexicographically fixed basis of the controllability matrix means that there exist n fixed columns of $Q_c(t)$ that are linearly independent for all t.

The concept of similarity transformations is well known for LTI systems. A similarity transform preserves the eigenvalues, spectral and stability properties, and system properties such as controllability and observability. This concept can be generalized to a time varying state transformation by the Lyapunov transform.

Definition 3.1 Consider a linear transformation

$$z(t) = \mathbf{T}(t)x(t)$$

where $\mathbf{T}(t)$ is a $n \times n$ differentiable matrix function of time. This matrix transformation is called a Lyapunov transformation if

1) $\mathbf{T}(t)$ and $\dot{\mathbf{T}}(t)$ are matrices of continuous and bounded functions for all $t > t_0$

2) $\epsilon < |\det\mathbf{T}(t)|$ for some $\epsilon > 0$, and for all $t > t_0$

A Lyapunov transformation $\mathbf{T}(t)$ effects a coordinate transformation on a system matrix. Given one state space description (4.0), the state space description with the redefinition $z(t) = \mathbf{T}(t)x(t)$ is given by

$$\dot{z} = A_{\mathrm{T}}(t)z + B_{\mathrm{T}}(t)u, \ \forall t > t_0 \tag{3.4}$$

$$y = C_{\mathrm{T}}(t)$$

where

$$A_{\mathrm{T}}(t) = [\mathbf{T}(t)A(t) + \dot{\mathbf{T}}(t)]\mathbf{T}^{-1}(t) \tag{3.5}$$

$$B_{\mathrm{T}}(t) = \mathbf{T}(t)B(t)$$

$$C_{\mathrm{T}}(t) = C(t)\mathbf{T}^{-1}(t)$$

Note that a Lyapunov transformation reduces to a similarity transformation for constant matrices.

The following definition is useful in discussing two systems for which a Lyapunov transformation exists.

Definition 3.2 The system characterized by (3.3) and denoted by $[A(t), B(t), C(t)]$ is algebraically equivalent to the system characterized by (3.4), and denoted by $[A_{\mathrm{T}}(t), B_{\mathrm{T}}(t), C_{\mathrm{T}}(t)]$, if they are related by a Lyapunov transformation.

The Lyapunov transformation is important in that it preserves the most important properties of a system. The first property is the input-output property. That is

$$y(t) = C(t)\Phi(t, t_0)x(t_0) + \int_{t_0}^{t} C(t)\Phi(t, \tau)B(\tau)u(\tau)d\tau$$

$$= C_{\mathrm{T}}(t)\Phi_{\mathrm{T}}(t, t_0)z(t_0) + \int_{t_0}^{t} C_{\mathrm{T}}(t)\Phi_{\mathrm{T}}(t, \tau)B_{\mathrm{T}}(t)u(\tau)d\tau$$

where $z(t_0) = \mathbf{T}(t_0)x(t_0)$. The second property is that a Lyapunov transformation preserves the internal (state) stability of the system. This fact is shown in the following theorem.

Theorem 3.1 *Suppose the* $n \times n$ *matrix* $\mathbf{T}(t)$ *is a Lyapunov transformation. Then the linear state equation* $\dot{x} = A(t)x$ *is uniformly stable (respectively, uniformly exponentially stable) if and only if the state equation*

$$\dot{z}(t) = [\mathbf{T}(t)A(t) + \dot{\mathbf{T}}(t)]\mathbf{T}^{-1}(t)z(t)$$

is uniformly stable (respectively, uniformly exponentially stable).

With this important concept of Lyapunov transformation, we now show that for any uniformly controllable LTV system of the form (3.3) there exists an algebraically equivalent Canonical realization. This transformation is the so called Silverman-Wolovich transformation. The existence of such a transformation and the form of the Multi-Variable Phase Variable Canonical form are given in the following theorem.

Theorem 3.2 (Silverman-Wolovich): *A Lyapunov transformation* $\mathrm{T}(t)$ *for (3.3) exists such that the realization* $\boldsymbol{z}(t) = \mathrm{T}(t)\boldsymbol{x}(t)$ *is in the Multi-Variable Phase Variable Canonical form if (3.3) satisfies Assumption 3.1, i.e. the smoothness conditions and uniform controllability.*

The Multi-Variable Phase Variable Canonical form is given by

$$\dot{\boldsymbol{z}} = (\dot{\mathrm{T}}(t) + \mathrm{T}(t)\boldsymbol{A}(t))\mathrm{T}^{-1}(t)\boldsymbol{z} + \mathrm{T}(t)\boldsymbol{B}(t)\boldsymbol{u}, \ \forall t > t_0 \tag{3.6}$$

$$\dot{\boldsymbol{z}} = \boldsymbol{A}_p(t)\boldsymbol{z} + \boldsymbol{B}_p(t)\boldsymbol{u}, \ \forall t > t_0$$

$$\boldsymbol{y}(t) = \boldsymbol{C}(t)\mathrm{T}^{-1}(t)\boldsymbol{z}(t)$$

$$\boldsymbol{A}_p(t) = \begin{bmatrix} \boldsymbol{A}_{11}(t) & \boldsymbol{A}_{12}(t) & \cdots & \boldsymbol{A}_{1l}(t) \\ \boldsymbol{A}_{21}(t) & \boldsymbol{A}_{22}(t) & \cdots & \boldsymbol{A}_{2l}(t) \\ \vdots & \vdots & \ddots & \vdots \\ \boldsymbol{A}_{l1}(t) & \boldsymbol{A}_{l2}(t) & \cdots & \boldsymbol{A}_{ll}(t) \end{bmatrix}$$

$$\boldsymbol{B}_p(t) = \begin{bmatrix} 0 & 0 & 0 & \cdots & 0 \\ \vdots & \vdots & \vdots & & \vdots \\ 0 & 0 & 0 & \cdots & 0 \\ 1 & b_{12}(t) & b_{13}(t) & \cdots & b_{1m}(t) \\ 0 & 0 & 0 & \cdots & 0 \\ \vdots & \vdots & \vdots & & \vdots \\ 0 & 0 & 0 & \cdots & 0 \\ 0 & 1 & b_{23}(t) & \cdots & b_{2m}(t) \\ 0 & 0 & 0 & \cdots & 0 \\ \vdots & \vdots & \vdots & & \vdots \\ 0 & 0 & 0 & \cdots & 1 \end{bmatrix}$$

where

$$A_{ii}(t) = \begin{bmatrix} 0 & 1 & 0 & \cdots & 0 \\ 0 & 0 & 1 & \cdots & 0 \\ \vdots & \vdots & \vdots & \ddots & \vdots \\ 0 & 0 & 0 & \cdots & 1 \\ \alpha_{i,d_{i-1}+1} & \alpha_{i,d_{i-1}+2} & \alpha_{i,d_{i-1}+3} & \cdots & \alpha_{i,d_i} \end{bmatrix}$$

$$A_{ik}(t) = \begin{bmatrix} 0 & 0 & 0 & \cdots & 0 \\ 0 & 0 & 0 & \cdots & 0 \\ \vdots & \vdots & \vdots & \ddots & \vdots \\ 0 & 0 & 0 & \cdots & 0 \\ \alpha_{i,d_{k-1}+1} & \alpha_{i,d_{k-1}+2} & \alpha_{i,d_{k-1}+3} & \cdots & \alpha_{i,d_k} \end{bmatrix}$$

The proof of this is given for SISO systems in Silverman [97], and the proof for MIMO systems is given in Wolovich [121]. Additionally, the proofs are constructive in nature and provide a method for finding a Lyapunov Transformation which will realize the phase variable canonical form. This means that any LTV system that satisfies Assumption 3.1 can be transformed to the MVPV canonical form.

We now define another useful canonical form. The following canonical form is useful in synthesizing a closed-loop feedback system that realizes a desired MIMO PD-spectrum. This system can be realized from the MVPV form by canceling out the sub-blocks which are not on the main diagonal and assigning to each diagonal block a TV companion matrix that realizes the d_i desired PD-eigenvalues. The algebraic equivalence of this realization will provide a method for uniform exponential stabilization of LTV systems. The Block Decoupled Phase Variable Canonical form is given by

$$\dot{z} = A_d(t)z + B_p(t)u, \ \forall t > t_0 \tag{4.1}$$

$$y(t) = C_T(t)z(t)$$

$$A_d(t) = \begin{bmatrix} A_{11}(t) & A_{12}(t) & \cdots & A_{1l}(t) \\ A_{21}(t) & A_{22}(t) & \cdots & A_{2l}(t) \\ \vdots & \vdots & \ddots & \vdots \\ A_{l1}(t) & A_{l2}(t) & \cdots & A_{ll}(t) \end{bmatrix}$$

$$A_{ii}(t) = \begin{bmatrix} 0 & 1 & 0 & \cdots & 0 \\ 0 & 0 & 1 & \cdots & 0 \\ \vdots & \vdots & \vdots & \ddots & \vdots \\ 0 & 0 & 0 & \cdots & 1 \\ \beta_{i,d_{i-1}+1} & \beta_{i,d_{i-1}+2} & \beta_{i,d_{i-1}+3} & \cdots & \beta_{i,d_i} \end{bmatrix}$$

$$A_{ik}(t) = \begin{bmatrix} 0 & 0 & 0 & \cdots & 0 \\ 0 & 0 & 0 & \cdots & 0 \\ \vdots & \vdots & \vdots & \ddots & \vdots \\ 0 & 0 & 0 & \cdots & 0 \\ 0 & 0 & 0 & \cdots & 0 \end{bmatrix}$$

$$B_p(t) = \begin{bmatrix} 0 & 0 & 0 & \cdots & 0 \\ \vdots & \vdots & \vdots & & \vdots \\ 0 & 0 & 0 & \cdots & 0 \\ 1 & b_{12}(t) & b_{13}(t) & \cdots & b_{1m}(t) \\ 0 & 0 & 0 & \cdots & 0 \\ \vdots & \vdots & \vdots & & \vdots \\ 0 & 0 & 0 & \cdots & 0 \\ 0 & 1 & b_{23}(t) & \cdots & b_{2m}(t) \\ 0 & 0 & 0 & \cdots & 0 \\ \vdots & \vdots & \vdots & & \vdots \\ 0 & 0 & 0 & \cdots & 1 \end{bmatrix}$$

and $C_T(t)$ is an unprespecified output matrix. This canonical form is useful as it represents the closed loop structure of a physical system with the state feedback for a Decoupled MIMO system with a desired PD-spectrum.

The following theorem formally states the method for assigning a desired PD-Spectrum to a LTV system which satisfies Assumption 3.1.

Theorem 3.3 (LTV PD-spectral assignment): *Let* $\{\rho_{ij}(t)\}_{i=1,j=1}^{n_i,m}$ *be a desired PD-spectrum and let* $\{\beta_{ij}(t)\}_{i=1,j=1}^{n_i,m}$ *be the synthesis coefficients for this PD-spectrum. For a LTV system that satisfies Assumption 3.1, there exists a state feedback* $\boldsymbol{u}(t) = \mathbf{K}(t)\boldsymbol{x}(t)$ *that can exponentially stabilize the system by assigning a closed loop system matrix that*

is algebraically equivalent to a Block Decoupled Multi-Variable Canonical system as in equation 4.1 with the desired pd-spectrum.

Proof: First by Theorem 3.2 there exists a Lyapunov transformation $\mathrm{T}(t)$ that will give an algebraically equivalent realization that is in Multi-Variable Phase-Variable canonical form. Now, define the state feedback in terms of the new states

$$u_m(t) = \sum_{i=1}^{n} - \alpha_{m,i}(t) z_i(t) + \sum_{j=1}^{\sigma_m} \beta_{m,j} z_{(d_m - \sigma_m + j)}$$

$$u_k(t) = \sum_{i=1}^{n} - \alpha_{k,i}(t) z_i(t) + \sum_{j=1}^{\sigma_k} \beta_{k,j}(t) z_{(d_k - \sigma_k + j)} -$$

$$- \sum_{l=1}^{m-k} b_{(k,m-k+l+1)}(t) u_{(m-k+l+1)}(t)$$

$$\boldsymbol{u}(t) = \mathbf{K}_z(t)\boldsymbol{z}(t)$$

where σ_m is the mth lexicographic index and $d_m = \sum_{k=1}^{m} \sigma_m$ are the indices used in forming the lexicographic basis of the controllability matrix, and $\beta_{k,j}(t)$ are the synthesis coefficients for the kth companion block of an exponentially stable PD-Spectrum. This system matrix realizes the desired PD-spectrum for MIMO systems, and is thus exponentially stable. A Lyapunov transformation preserves the stability of the original system, and thus (3.3) is exponentially stabilized by

$$\boldsymbol{u}(t) = \mathbf{K}_z(t)\mathbf{T}(t)\boldsymbol{x}(t)$$

$$\boldsymbol{u}(t) = \mathbf{K}(t)\boldsymbol{x}(t) \qquad \square$$

The above theorem formally states a method for assigning a PD-spectrum. Theorem 3.1 gives a state feedback $\mathbf{K}(t)$ that yields a closed loop system which is algebraically equivalent to the Block Decoupled Multi-variable Canonical form 3.1 with a desired PD-spectrum. By appropriately assigning the desired spectrum the LTV system can be exponentially stabilized. However, perfect cancellation is impractical and it is thus important to study the robustness of this closed loop system, which will be discussed in Chapter 4.

PD-Spectrum Assignment Procedure.

1. Transform the MIMO LTV system into Multi-Variable Phase Variable (MVPV) canonical form by a state coordinate transformation $\mathbf{T}(t)\boldsymbol{x}(t) = \boldsymbol{z}(t)$.

2. For each block companion matrix $\boldsymbol{A}_{ii}(t)$ in the MVPV matrix $\boldsymbol{A}(t)$, choose the desired PD-eigenvalues and synthesize the coefficients of the SPDO associated with $\boldsymbol{A}_{ii}(t)$. Then design the state feedback control law $\boldsymbol{v}(t) = \mathbf{K}_z(t)\boldsymbol{z}(t)$ to obtain the desired closed-loop dynamics in the MVPV coordinates.

3. The actual control law $\boldsymbol{u}(t) = \mathbf{K}(t)\boldsymbol{x}(t)$ is given by $\mathbf{K}(t) = \mathbf{K}_z(t)\mathbf{T}(t)$.

Remarks.

1. For BIBO stability, exponential stability must be achieved by assigning negative extended mean to all the PD-eigenvalues. To this end, it suffices to keep $\mathrm{Re}\{\rho_k(t)\} \leq -\epsilon < 0$ for some prescribed $\epsilon > 0$.

2. No identical PD-eigenvalues should be assigned within any companion block $A_{ii}(t)$. For block size larger than 2×2, ensure that all PD-eigenvalues are differentially distinct.

3. If a pair of complex conjugate PD-eigenvalues $\rho_{i,j}(t) = \sigma(t) + j\omega(t)$ is assigned, keep $\omega(t)$ from vanishing.

4. The PD-eigenvalues should be continuously differentiable $n - 1$ times.

5. Assign a PD-spectrum that achieves the required robustness. In effect, this amounts to assigning PD-eigenvalues sufficiently far left as will be justified in Chapter 4. Some tradeoff may be necessary to avoid exciting unmodeled modes, i.e. avoiding singular perturbations.

6. To assure that the time variance of the PD-eigenvectors does not decrease the stability radius of the trajectory, move the PD-eigenvalues slowly to limit the growth bound on the PD-eigenvectors as used in the PD-spectral stability theorem. Moving slowly involves keeping the derivatives of the PD-eigenvalues small. This keeps the canonical modal matrix close to the constant value, which is one easy way to limit the growth bound on the PD-eigenvalues. This is not a limit on the inherent time variance of the system or trajectory to be followed which using this method is theoretically unlimited.

3.3 - Techniques For Nonlinear Pseudoinversion

The problem of system inversion has been widely studied and is an often considered method for the problem of trajectory realization, obtaining a desired trajectory. Additionally, inversion is an implicit part of design in many popular nonlinear trajectory tracking controllers such as feedback linearization. Explicit methods for system inversion have been developed for large classes of SISO and MIMO nonlinear systems. However, these general methods do not seem to consider two very important points. First, these methods assume the availability of derivatives of the desired output that may not actually available. That is to say the methods actually invert the plant from $\overline{\eta}^{(r)} \rightarrow u$ for some $r > 0$, and not from $\overline{\eta} \rightarrow u$. Unless the reference signal actually generates these signals directly, causality will require some sort of approximation to

obtain this value in real time. Second, these methods do not consider the stability of the inverse.

Now, we will present a general method for pseudo-inversion of a large class of nonlinear systems which can be used to synthesize a controller which will generate a nominal control that places the system on the nominal trajectory. This method is named pseudo-inversion as it results in a stable inverse system even for non-minimum phase systems. First, we will consider SISO systems, and then a method will be provided for generalizing to MIMO systems.

Consider the SISO, affine, autonomous nonlinear systems

$$\begin{aligned} \dot{\xi} &= f(\xi) + g(\xi)v \\ \eta &= h(\xi) + d(\xi)v \end{aligned} \tag{3.7}$$

as a special case of 3.1, where $f(\xi)$, $g(\xi)$, and $h(\xi)$ are smooth vector fields, *i.e.* they have continuous partial derivatives of any required order. The *Lie derivative* of a scalar function $h(\boldsymbol{x})$ with respect to a vector field $f(\boldsymbol{x})$ is defined by:

$$L_f h(\xi) = \frac{\partial h(\xi)}{\partial \xi} \cdot f(\xi)$$

Let Ω be a region in $\mathbb{R}^n$ containing the origin. The system (3.7) is said to have a *well-defined relative order* $r = 0$ *in* Ω if $d(\boldsymbol{x}) \neq 0 \; \forall \boldsymbol{x} \in \Omega$. Suppose that $\forall \boldsymbol{x} \in \Omega$,

$$\eta^{(k)} = L_f^k h(\xi) + L_g L_f^{k-1} h(\xi) v, \quad L_g L_f^{k-1} h(\xi) \equiv 0, \quad k = 1, 2, \ldots, r-1$$

$$\eta^{(r)} = L_f^r h(\xi) + L_g L_f^{r-1} h(\xi) v, \quad L_g L_f^{r-1} h(\xi) \neq 0$$

where $L_f^0 h = h$, $L_f^k h = L_f L_f^{k-1} h$. Then (3.7) is said to have a *well-defined relative order* $r > 0$ *in* Ω.

The notion of zerodynamics can be extended to nonlinear systems with a well defined relative order r as follows. Let $\boldsymbol{z} = [\zeta_1 \,|\, \zeta_2]^{\mathrm{T}}$, where

$$\zeta_1 = \begin{bmatrix} z_1 \\ z_2 \\ \vdots \\ z_r \end{bmatrix} = \begin{bmatrix} \eta \\ \dot{\eta} \\ \vdots \\ \eta^{(r-1)} \end{bmatrix} \tag{3.8}$$

$$\zeta_2 = \begin{bmatrix} z_{r+1} \\ \vdots \\ z_n \end{bmatrix}$$

Then it is possible to find a (nonlinear) state coordinate transformation $\boldsymbol{z} = \boldsymbol{\Phi}(\boldsymbol{x})$, where $\boldsymbol{\Phi}(\,\cdot\,)$ is a smooth invertible function (a diffeomorphism), such that

$$\dot{\boldsymbol{z}} = \frac{\partial \boldsymbol{\Phi}}{\partial \xi}\dot{\xi} = \begin{bmatrix} \dot{\zeta}_1 \\ \hline \dot{\zeta}_2 \end{bmatrix} \tag{3.9}$$

$$\eta = \boldsymbol{z}_1$$

where

$$\dot{\zeta}_1 = \begin{bmatrix} \dot{z}_1 \\ \dot{z}_2 \\ \vdots \\ \dot{z}_{r-1} \\ \dot{z}_r \end{bmatrix} = \begin{bmatrix} z_2 \\ z_3 \\ \vdots \\ z_r \\ L_f^r h(\boldsymbol{\Phi}^{-1}(\boldsymbol{z})) \end{bmatrix} + \begin{bmatrix} 0 \\ 0 \\ \vdots \\ 0 \\ L_g L_f^{r-1} h(\boldsymbol{\Phi}^{-1}(\boldsymbol{z})) \end{bmatrix} v \tag{3.9a}$$

and

$$\dot{\zeta}_2 = \begin{bmatrix} \dot{z}_{r+1} \\ \vdots \\ \dot{z}_n \end{bmatrix} = \boldsymbol{\Psi}(\boldsymbol{z}) = \boldsymbol{\Psi}(\zeta_1, \zeta_2) \tag{3.9b}$$

Equation (3.9) is called the ***normal form*** for the NL system (3.7). Equation (3.9a) is in NL phase variable canonical form. Equation (3.9b) defines an $m = n - r$ dimensional submanifold wherein the state evolution can be rendered unobservable in the closed-loop system by letting

$$v = \frac{-L_f^r h(\boldsymbol{x})}{L_g L_f^{r-1} h(\boldsymbol{x})} + \frac{1}{L_g L_f^{r-1} h(\boldsymbol{x})}\overline{\eta}^{(r)} \tag{3.10}$$

The state feedback control law (3.10) renders the I/O mapping $v \rightarrow \overline{\eta}^{(r)}$ of the closed-loop system linear as a chain of r integrators, and (3.9a) is termed "internal dynamics" for the closed-loop system. In particular,

$$\dot{\zeta}_2 = \Psi(0, \zeta_2) \tag{3.11}$$

is defined to be the *zerodynamics* of the NL system (3.7). Thus, (3.7) is said to be (exponentially) minimum phase if its zerodynamics (3.11) is (exponentially) asymptotically stable.

For a SISO, affine, autonomous nonlinear system (3.7) with a well-defined relative order $r > 0$ in a region Ω, define

$$\mu(\xi) = \frac{1}{L_g L_f^{r-1} h(\xi)}$$

Then the inverse I/O mapping from the nominal $\overline{\eta}^{(r)} \rightarrow \overline{u}$ is given by (3.10) with $\nu = \overline{\eta}^{(r)}$

$$\begin{aligned} \overline{v} &= -\mu(\overline{\xi}) L_f^r h(\overline{\xi}) + \mu(\overline{\xi})\overline{\eta}^{(r)} \\ &= \psi(\overline{\xi}) + \mu(\overline{\xi})\overline{\eta}^{(r)} \end{aligned} \tag{3.12}$$

The governing equation for the nominal state variables is obtained by substituting (3.12) into (3.7):

$$\begin{aligned} \dot{\overline{x}} &= f(\overline{\xi}) + g(\overline{\xi})\left[\psi(\overline{\xi}) + \mu(\overline{\xi})\overline{\eta}^{(r)}\right] \\ &= \left[f(\overline{\xi}) - \mu(\overline{\xi}) L_f^r h(\overline{\xi}) g(\overline{\xi})\right] + \left[\mu(\overline{\xi}) g(\overline{\xi})\right]\overline{\eta}^{(r)} \\ &= \phi(\overline{\xi}) + \gamma(\overline{\xi})\overline{\eta}^{(r)} \end{aligned} \tag{3.13}$$

In order for the inverse system defined by (3.12) and (3.13) to be (small signal, finite gain) BIBO stable, the origin $\xi = 0$ must be (locally) exponentially stable, or at least uniformly asymptotically stable. The dynamics of the nominal inverse system (3.12) and (3.13) consists of a chain of r integrators and the zerodynamics of (3.7); see Figure 3.2. Thus, even if the latter is stable, (3.13) still needs to be stabilized. This can be accomplished by approximating $\overline{\eta}^{(r)}$ with $\hat{\eta}^{(r)} = \hat{\eta}^{(r)}(\xi, \overline{\eta})$.

First, suppose that the zerodynamics of (3.7) is uniformly asymptotically stable. Let

$$\begin{aligned}\widehat{\eta}^{(r)}(\xi,\overline{\eta}) &= -\sum_{k=1}^{r} a_k z_k + a_1\overline{\eta} \\ &= -\sum_{k=1}^{r} a_k L_f^{k-1} h(\xi) + a_1\overline{\eta}\end{aligned} \tag{3.14}$$

This results in the following stable pseudo-inverse of (3.7) from $\overline{\eta} \rightarrow \widehat{v}$

$$\dot{\xi} = \left[f(\xi) - \mu(\xi)\sum_{k=0}^{r} a_{k+1} L_f^k h(\xi) g(\xi) \right] + a_1 \mu(\xi) g(\xi) \overline{\eta} \tag{3.15}$$

$$\widehat{u} = -\mu(\xi)\sum_{k=0}^{r} a_{k+1} L_f^k h(\xi) + a_1 \mu(\xi) \overline{\eta} \tag{3.16}$$

where $\sum_{k=0}^{r} a_{k+1}\lambda^k$ with $a_{r+1} = 1$ is a Hurwitz polynomial to be designed; see Figure 3. 3(a). Note that the coefficients a_k need not be constant, and time-varying dynamics may provide performance improvement or real-time design tradeoffs that are not attainable by LTI designs.

If the zerodynamics of the nonlinear plant (3.7) is not uniformly asymptotically stable, design

$$\widehat{\eta}^{(r)}(\xi,\overline{\eta}) = = k_1(\xi) - \sum_{k=1}^{r} a_k L_f^{k-1} h(\xi) + k_2(\overline{\eta}) \tag{3.17}$$

where $k_1(\xi)$ is to stabilize the unstable modes of the inverse system corresponding to the unstable zerodynamics of (3.7), and $k_2(\overline{\eta})$ is to equalize the "DC gain" of the corresponding pseudo-identity. This results in the closed-loop inverse system shown in Figure 3.3(b),

$$\dot{\xi} = \left\{ f(\xi) + \mu(\xi) \left[k(\xi) - \sum_{k=0}^{r} a_{k+1} L_f^k h(\xi) \right] g(\xi) \right\} + \mu(\xi) g(\xi) k_2(\overline{\eta}) \tag{3.18}$$

$$\widehat{u} = \mu(\xi) \left[k(\xi) - \sum_{k=0}^{r} a_{k+1} L_f^k h(\xi) \right] + \mu(\xi) k_2(\overline{\eta}) \tag{3.19}$$

It is noted that in both cases the inverse system is stabilized by state feedback. Since state feedback does not alter the zerodynamics, the zeros dynamics of the inverse system, which is the (pole) dynamics of the plant. Therefore, the pseudo-inverse is guaranteed to cancel out the dynamics of the plant. If the plant zerodynamics is uniformly asymptotically stable, then it will be canceled by the control law (3.14). The resulting pseudo-identity will consist of the poles defined by $\sum_{k=0}^{r} a_{k+1}\lambda^k$ (or PD-eigenvalues if a time-varying SPDO $\sum_{k=0}^{r} a_{k+1}(t)\delta^k$ is used). Otherwise, the pseudo-identity will include the unstable plant zerodynamics, and the dynamics of the inverse system under the control law (3.17). In other words, the pseudo-identity will be nonminimum phase.

Since the goal of the stabilization of the inverse system is to achieve small signal BIBO stability, it is imperative to design for exponential stability, or at least uniform asymptotic stability. It is not necessary to achieve global stability, as long as the domain of stability encompasses the operating envelope. The performance goal of the design is to minimize the error $\|\widehat{u} - \overline{u}\| \simeq \mu(\xi)\left\|\widehat{\eta}^{(r)} - \overline{\eta}^{(r)}\right\|$ in a suitable norm within the operating envelope and bandwidth.

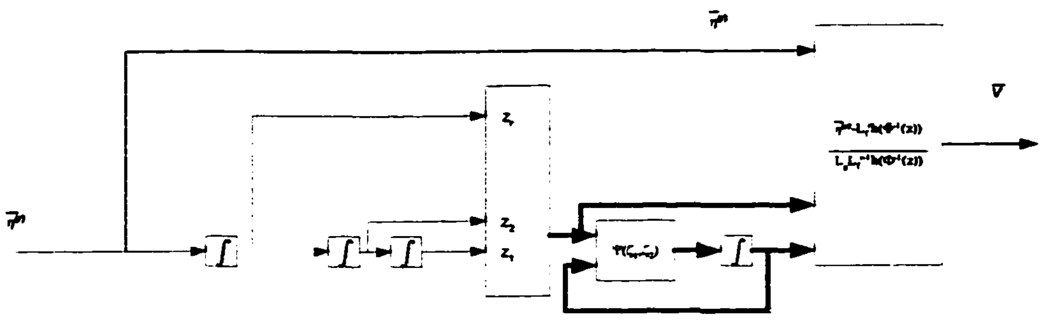

Figure 3.2 Nominal inverse $\overline{\eta}^{(r)} \rightarrow \overline{u}$

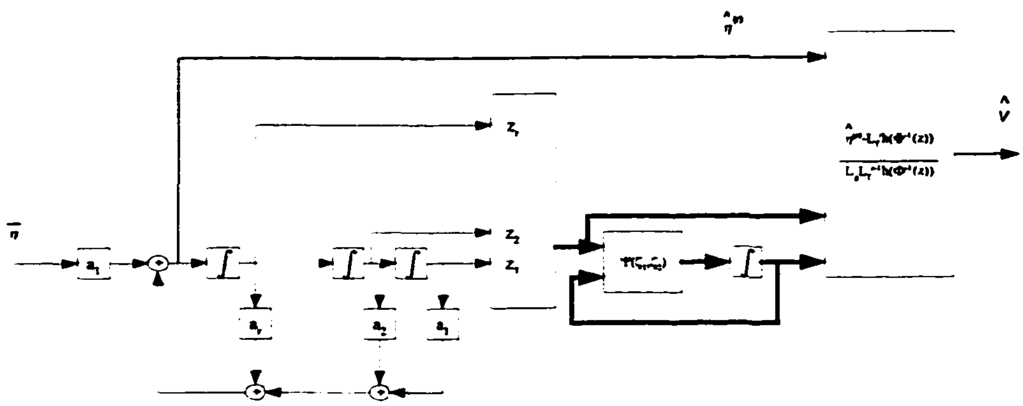

(a) Minimum phase plant
Figure 3.3 Stable pseudo-inverse $\overline{\eta} \rightarrow \overline{u}$

(figure continued)

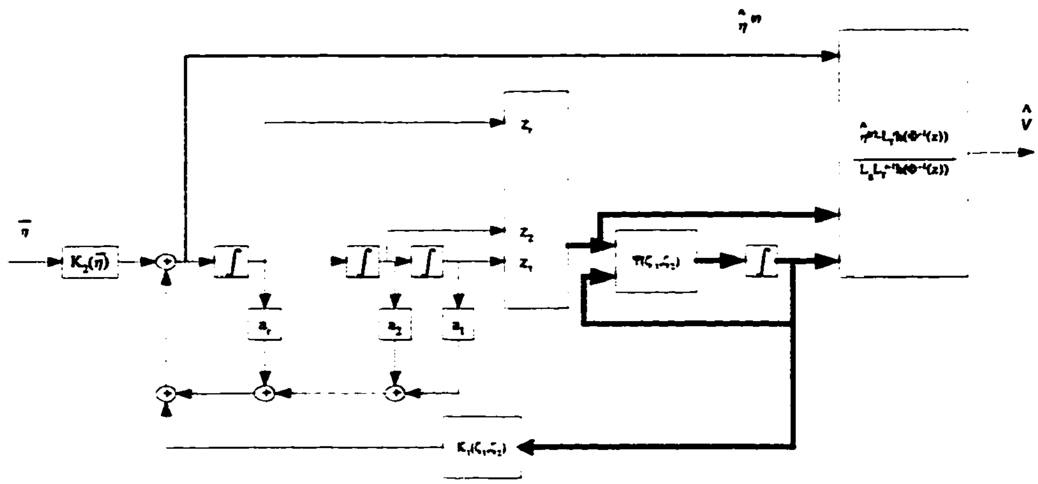

(b) Nonminimum phase plant

CHAPTER 4

ROBUSTNESS OF PD-SPECTRUM ASSIGNMENT

The preceding chapter presents a method for design of a nonlinear trajectory tracking controller. The design relies on Lyapunov's first method to achieve this goal. The error dynamics are assigned desired exponentially stable time varying modes. Exponential stability provides powerful inherent robustness. However, additional insight is desired concerning the placement of PD-eigenvalues that can achieve robust performance. This insight is useful in the design of the nonlinear trajectory tracking controller. A design engineer can use this information to determine the location of PD-eigenvalues that will keep the output trajectories sufficiently close to the desired trajectory for the range of expected parametric uncertainty in the plant.

In this chapter the robustness of PD-spectrum assignment is first developed for LTV systems. Toward this end, Section 4.1 details the specific perturbation model. This model includes uncertainty in the system and in the input matrix. Section 4.2 gives the norm bound on the uncertainty for which a given PD-spectrum is bounded input bounded state (internally) stable, and exponentially stable.

Next, the robust stability criteria are extended to nonlinear systems in Section 4.3. First, the overall control structure is shown to achieve exponential tracking in the nominal case. Next, the norm bound on the uncertainty of the plant is shown for a given PD-spectrum when the nominal control does not change for a given nonlinear perturbation.

The nonlinear robustness theorem guarantees that if the nominal control realizes the desired trajectory for the perturbed system and the perturbations are less than a certain bound then the trajectory is exponentially stable. A nonlinear perturbation in the nominal plant that falls within a certain bound limit and causes a change in the required nominal control will result in a trajectory which will remain in a ball about the nominal trajectory. This property will be captured in the concept of a uniformly ultimately bounded solution.

Section 4.4 addresses the problem of trajectory tracking control when the states are not available for feedback in formulating the control law. This problem is addressed by using LTV observers. First, the seperability property is established for LTV systems, which allows for independent design of controller and observer. Then conditions are given for which the observer based trajectory linearization design method will achieve asymptotic tracking of a desired output trajectory for a nonlinear plant.

4.1 - Robustness Models

Due to imprecision in the plant model and controller implementation, it is necessary to consider the robustness of the trajectory linearization design as well as any control design method. To this end it is necessary to construct a robustness model which predicts the effect of such imprecisions. The robustness model of the closed loop plant includes time varying perturbations in the plant system and input matrices, and in the controller. Let $\Delta \mathcal{A}_p(t)$ represent the uncertainty in the model of the plant system matrix, and $\Delta \mathcal{B}(t)$ represent the uncertainty in the model of the plant input matrix. Perturbations in the state feedback that assigns the desired PD-Spectrum are denoted by $\Delta \mathbf{K}(t)$. The perturbation in the controller arises due to numerical imprecision in the physical realization of the controller, and due to simplifying assumptions in the controller design which reduce the

difficulty in finding $\mathbf{K}(t)$. Now, if we add these perturbations into the nominal system model, then the perturbed system is given by.

$$\dot{x}(t) = (A_p(t) + \Delta A_p(t))x(t) +$$
$$+ (B_p(t) + \Delta B_p(t))\{[\mathbf{K}(t) + \Delta\mathbf{K}(t)][x(t) + w_n(t)] + w_d(t)\} \tag{4.2}$$

where $w_n(t)$ represents error in the state measurement and $w_d(t)$ is a general disturbance. The only assumption on these two signals $w_n(t)$ and $w_d(t)$ is that they are bounded in some suitable norm. The perturbed system and input matrices are assumed to satisfy Assumption 3.1. This implies that the controllability of the system remains unchanged and the perturbations are sufficiently smooth and bounded. The perturbation model (4.6) is shown in figure 4.1.

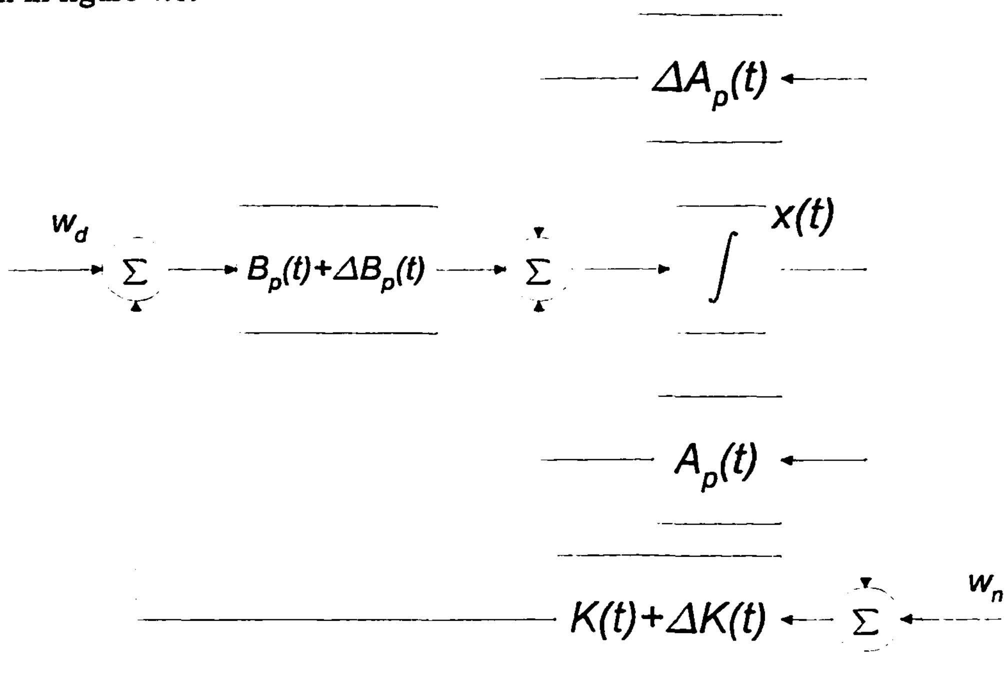

Figure 4.1 LTV Robustness Model

We can rewrite the terms in the perturbation model (4.6) in the form of the following equation

$$\dot{x}(t) = [A_p(t) + B_p(t)\mathbf{K}(t)]x(t) +$$

$$+ [\Delta A_p(t) + \Delta B_p(t)\mathbf{K}(t) + \Delta B_p(t)\Delta\mathbf{K}(t) + B_p(t)\Delta\mathbf{K}(t)][x(t) + w_n(t)] +$$

$$+ [B_p(t) + \Delta B_p(t)]w_d(t) + [B_p(t)\mathbf{K}(t) - \Delta A_p(t)]w_n(t)$$

where the disturbance terms and matrix perturbations are bounded and thus the disturbance terms can be captured into two new bounded disturbance terms $u_1(t)$ and $u_2(t)$ where

$$u_1(t) = [B_p(t) + \Delta B_p(t)]w_d(t) + [B_p(t)\mathbf{K}(t) - \Delta A_p(t)]w_n(t)$$

$$u_2(t) = w_n(t)$$

We can also group all of the uncertainty terms into a single uncertainty term by defining

$$\Delta A_d(t) = \Delta A_p(t) + \Delta B_p(t)\mathbf{K}(t) + \Delta B_p(t)\Delta\mathbf{K}(t) + B_p(t)\Delta\mathbf{K}(t)$$

Recall the fact that the desired closed loop matrix $A_d(t)$ is given by

$$A_d(t) = A_p(t) + B_p(t)\mathbf{K}(t)$$

We can now write the perturbation model in the following form.

$$\dot{x}(t) = A_d(t)x(t) + \Delta A_d(t)[x(t) + u_2(t)] + u_1(t) \tag{4.3}$$

The perturbation model (4.3) represents a system as shown in figure 4.2, or the equivalent representation of figure 4.3. The perturbation model shown in figure 4.2 represents a system in Block Decoupled MVPV canonical form. For LTV systems that satisfy Assumption 3.1, we can assume the nominal system is in the form of figure 4.2 because any realization of the system is algebraicly equivalent to the Block Decoupled MVPV canonical form. Figure 4.3 is an equivalent representation. This form clarifies the mappings used in the Small Gain theorem. The nominal system is the mapping H_1, and the perturbation is analyzed as a feedback mapping H_2, which puts the system in a form conveniently formulated for the Small Gain theorem.

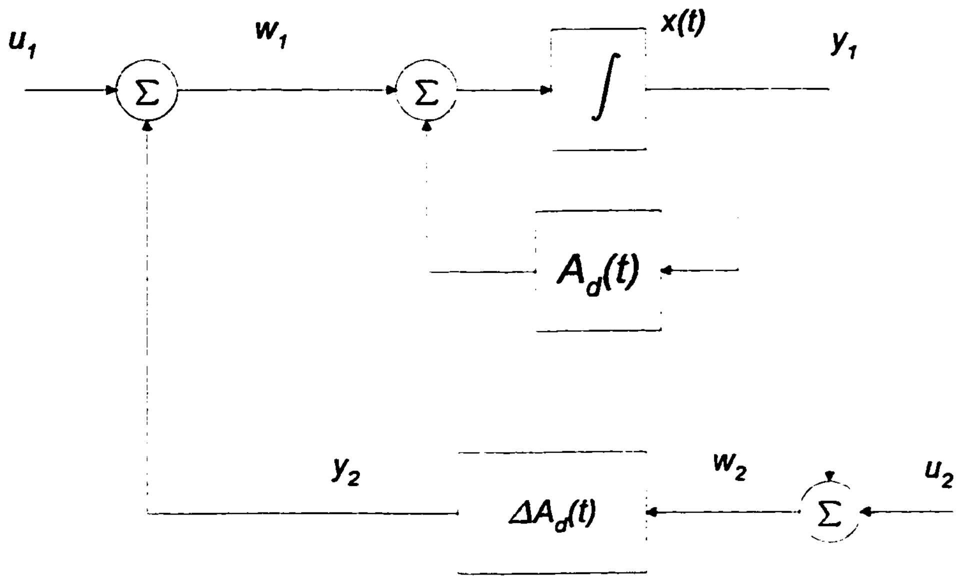

Figure 4.2 Perturbation Model

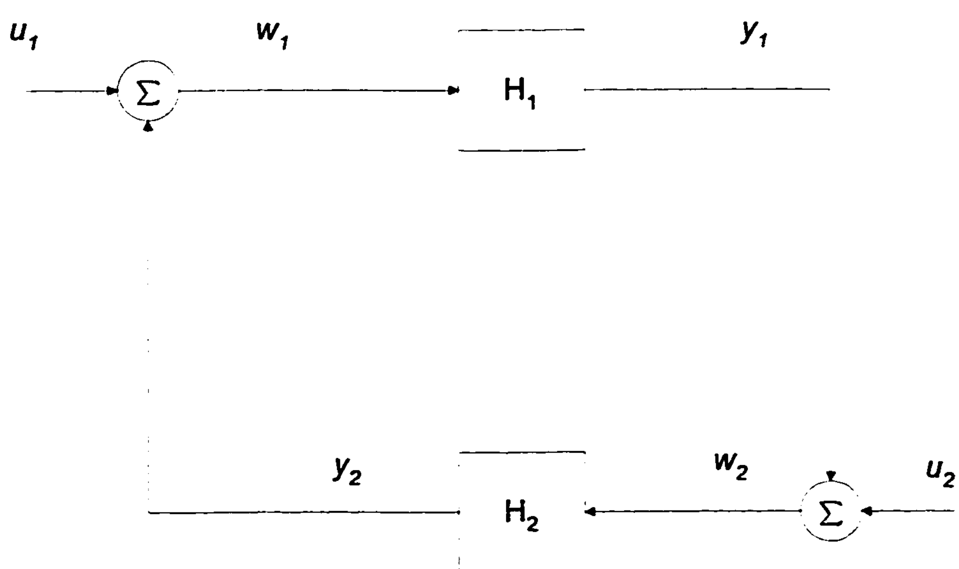

Figure 4.3 Equivalent Perturbation Model

4.2 - Robustness Analysis of LTV Systems

In this section we consider the problem of the robustness of PD-eigenstructure assignment. The importance of this analysis for nonlinear control will be made clearer in the next section. Before this analysis can begin, we must give some fundamental definitions and consider two theorems which we will use to justify this robustness. The first is the Small Gain theorem which will be used to establish Bounded Input Bounded Output (BIBO) stability of the perturbed model. The second is the Gronwall-Bellman Lemma which will be used to guarantee the exponential stability of the perturbed system.

Some of the terminology in the Small Gain theorem needs to be defined here before stating the theorem. Two definitions are necessary to understand the formulation of the theorem. The first definition is the concept of extended $\mathcal{L}^p$ spaces. The space C of continuous functions on an interval J forms a normed vector space $\mathcal{L}^p$ with a finite norm where the $\mathcal{L}^p$ norm of a function $w(\,\cdot\,) \in C(J, \mathbb{R})$ is defined by

$$\|w(\,\cdot\,)\|_p = \left(\int_J |w(\tau)|^p d\tau\right)^{\frac{1}{p}}$$

and

$$\|w(\,\cdot\,)\|_p = \left(\int_J |w(\tau)|^p d\tau\right)^{\frac{1}{p}}$$

$$\|w(\,\cdot\,)\|_\infty = \sup_{t \in J} |w(t)|$$

However, for control problems it is often necessary to deal with signals that are bounded in $\mathcal{L}^p$ norm on every finite interval, but may be unbounded over an infinite time interval. Thus, the following definition is needed to cope with these signals.

Definition 4.1 $\mathcal{L}_e^p$ is called the extended $\mathcal{L}^p$ space where

$$\mathcal{L}_e^p = \{u | u_\tau \in \mathcal{L}^p, \forall \tau \geq 0\}$$

and u_τ is a truncation of u, defined by

$$u_\tau = \begin{cases} u(t), & 0 \leq t \leq \tau \\ 0, & \tau < t \end{cases}$$

The next definition clarifies the concept of $\mathcal{L}$-stable mappings.

Definition 4.2 A mapping $H : \mathcal{L}_e^p \rightarrow \mathcal{L}_e^q$ is $\mathcal{L}$-stable if there exist finite nonnegative constants γ and β such that

$$\|(Hu)_\tau(\cdot)\|_q \leq \gamma \|u_\tau(\cdot)\|_p + \beta$$

for all $u \in \mathcal{L}_e^p$ and $\tau \in [0,\infty)$.

This definition of an $\mathcal{L}$-stable mapping allows us to consider some terminology which relates the input to output. γ is called the gain of the mapping H. It is a gain in the sense that the $\mathcal{L}_e^q$ norm of the output is less than γ times the $\mathcal{L}_e^p$ norm of the input. Thus the output will not be amplified by more than the game γ. Similarly, β is called the bias of the mapping H. The reason why β is called the bias is also obvious. β represents a constant bound on any transients in the mapping. The bias is a convenient method for accounting for the initial conditions on mappings which are represented by differential equations.

These definitions form the conceptual analysis tools for the Small Gain theorem. This theorem is used to characterize the input-output behavior of two systems interconnected in the feedback form of figure 4.4. What this theorem says is that the feedback connection of two $\mathcal{L}_p$ stable systems is stable if the product of the two system gains is less than one. This theorem is often used in justifying BIBO stability and the robustness of a system to parametric perturbations.

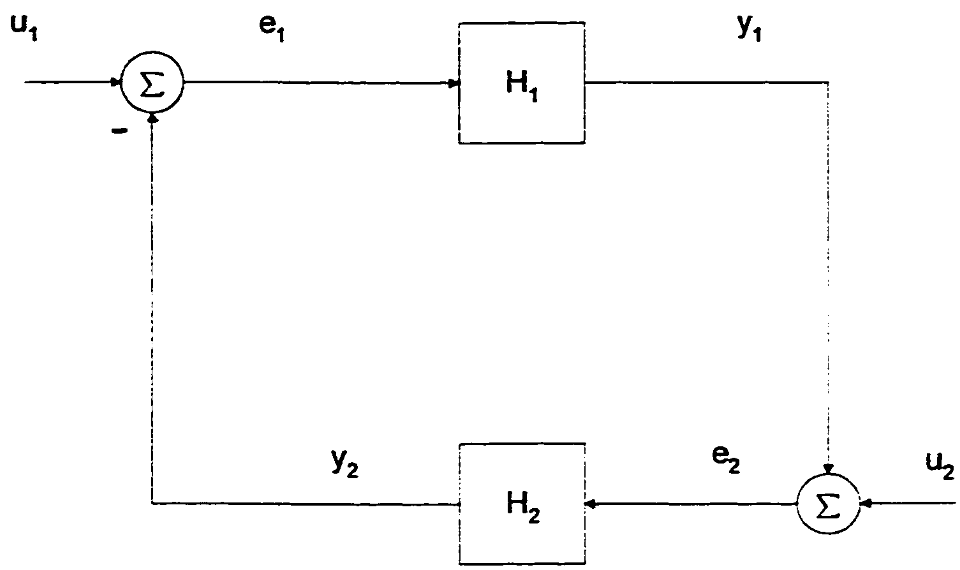

Figure 4.4 Feedback Connection in Small Gain Theorem

Theorem 4.1 (Small Gain Theorem): *Assume feedback systems of the form in figure 4.4, with two subsystems $H_1 : \mathcal{L}_e^p \rightarrow \mathcal{L}_e^q$ and $H_2 : \mathcal{L}_e^q \rightarrow \mathcal{L}_e^p$. Both systems are $\mathcal{L}$-stable with finite gains γ_1 and γ_2 and associated biases β_1 and β_2. Further, assume that for every pair of inputs $u_1 \in \mathcal{L}_e^p$ and $u_2 \in \mathcal{L}_e^q$ there exist unique outputs $e_1 \in \mathcal{L}_e^p$ and $e_2 \in \mathcal{L}_e^q$. Then if*

$$\gamma_1\gamma_2 < 1$$

then for all $u_1 \in \mathcal{L}_e^p$ and $u_2 \in \mathcal{L}_e^q$

$$\|e_{1\tau}(\,\cdot\,)\| \leq \frac{1}{1-\gamma_1\gamma_2}(\|u_{1\tau}(\,\cdot\,)\| + \gamma_2\|u_{2\tau}(\,\cdot\,)\| + \beta_2 + \gamma_2\beta_1)$$

$$\|e_{2\tau}(\,\cdot\,)\| \leq \frac{1}{1-\gamma_1\gamma_2}(\|u_{2\tau}(\,\cdot\,)\| + \gamma_1\|u_{1\tau}(\,\cdot\,)\| + \beta_1 + \gamma_1\beta_2)$$

for all $\tau \in [0,\infty)$. If $u_1 \in \mathcal{L}^p$ and $u_2 \in \mathcal{L}^q$, then e_1, $y_2 \in \mathcal{L}^p$, and e_2, $y_1 \in \mathcal{L}^q$ and the norms of e_1 and e_2 are bounded by the right-hand side above with non truncated functions.

The Small Gain theorem given above applies to SISO systems directly. By extension, using the definitions of $\mathcal{L}^p$ norm for vector functions of time, the Small Gain theorem applies to MIMO systems as well.

By norm of a vector $x \in \mathbb{R}^n$ we shall intend the standard l^p norm. The p norm of a vector $x \in \mathbb{R}^n$ is given by

$$\|x\|_p = \left(\sum_{i=1}^{n} |x|^p\right)^{\frac{1}{p}}, \; 1 \le p < \infty$$

and

$$\|x\|_\infty = \max_i |x_i|$$

A continuous vector function of time $w(\,\cdot\,) \in C(J, \mathbb{R}^n)$ at time t is just a vector of real numbers given by $w(t)$. This will allow us to extend the definition of $\mathcal{L}^p$ norms to the vector case. We shall do this by defining the $\mathcal{L}^p$ norm of a vector function $w(\,\cdot\,) \in C(J, \mathbb{R}^n)$ by

$$\|w(\,\cdot\,)\|_p = \left(\int_J \|w(\tau)\|_p^p d\tau\right)^{\frac{1}{p}}, \; 1 \le p < \infty$$

and

$$\|w(\,\cdot\,)\|_\infty = \sup_{t \in J} \|w(t)\|_\infty$$

Thus, a time varying vector function $w(\,\cdot\,)$ is first reduced to a scalar function of time by taking a l^p norm of $w(t)$ at time t. Then the $\mathcal{L}^p$ norm of this scalar function of time can be taken, which is a real number.

The induced l^p norm of a linear mapping U from $\mathbb{R}^m$ to $\mathbb{R}^n$ is defined as

$$\|U\|_p := \sup_{x \neq 0} \frac{\|U(t)x\|_p}{\|x\|_p}$$

which for $p = 1, 2,$ and ∞ is given by

$$\|U\|_1 = \max_j \sum_{i=1}^{m} |u_{ij}|$$

$$\|U\|_2 = \left(\lambda_{\max}\{U^{\mathrm{T}}U\}\right)^{\frac{1}{2}}$$

$$\|U\|_\infty = \max_i \sum_{j=1}^{n} |u_{ij}|$$

The induced $\mathcal{L}^p$ norms for a linear mapping $U(\,\cdot\,)$ from $C(J,\mathbb{R}^m)$ to $C(J,\mathbb{R}^n)$ is given by

$$\|U(\,\cdot\,)\|_1 = \sup_{t\in J} \max_j \sum_{i=1}^{m} |u_{ij}(t)|$$

$$\|U(\,\cdot\,)\|_2 = \sup_{t\in J} \left(\lambda_{\max}\{U^{\mathrm{T}}(t)U(t)\}\right)^{\frac{1}{2}}$$

$$\|U(\,\cdot\,)\|_\infty = \sup_{t\in J} \max_i \sum_{j=1}^{n} |u_{ij}(t)|$$

for $p = 1, 2,$ and ∞.

The following lemma offered by Bellman is a generalization of the lemma originally offered by Gronwall. It is sometimes simply called the Bellman Lemma. It is a generalization in that the Bellman inequality allows for time varying coefficients and Gronwall Lemma assume constant coefficients. It is a useful theorem in finding an upper bound on a continuous function for which explicit solutions are not available. It will be used to establish the exponential stability of the perturbed system.

Lemma 4.1 (Gronwall-Bellman Inequality): *Let* $\lambda : [a,b] \mapsto \mathbb{R}$ *be continuous and* $\mu : [a,b] \mapsto \mathbb{R}$ *be continuous and nonnegative. If a continuous function* $y : [a,b] \mapsto \mathbb{R}$ *satisfies*

$$y(t) \le \lambda(t) + \int_a^t \mu(s)y(s)ds$$

for $a \leq t \leq b$, then on the same interval

$$y(t) \leq \lambda(t) + \int_a^t \lambda(s)\mu(s)\exp^{\int_s^t \mu(\tau)d\tau} ds$$

In particular if $\lambda(t) \equiv \lambda$ is a constant, then

$$y(t) \leq \lambda \exp^{\int_a^t \mu(\tau)d\tau}$$

If, in addition, $\mu(t) \equiv \mu \geq 0$ is a constant, then

$$y(t) \leq \lambda \exp^{\mu(t-a)}$$

Several more theorems need to be stated. These theorems will be used in stating the norm bounds on the LTV pertubation matrices in terms of the PD-spectrum for which the perturbed plant is still stable. Where the following theorems are well known or the results are obvious, no proof will be given. As has been stated before, a scalar LTV system of the form

$$y^{(n)} + a_1(t)y^{(n-1)} + a_2(t)y^{(n-2)} + \cdots + a_n(t)y(t) = 0 \tag{4.4}$$

with initial conditions

$$y^{(n-1)}(0) = y_{n-1,0},\ y^{(n-2)}(0) = y_{n-2,0},\ \ldots, y(0) = y_0$$

is equivalent to a state space realization of the form

$$\dot{x} = \mathbf{A}_c(t)x \tag{4.5}$$

with companion matrix

$$\boldsymbol{A}_c = \begin{bmatrix} 0 & 1 & 0 & \cdots & 0 \\ 0 & 0 & 1 & \cdots & 0 \\ \vdots & \vdots & \vdots & \ddots & \vdots \\ 0 & 0 & 0 & \cdots & 1 \\ -a_n(t) & -a_{n-1}(t) & -a_{n-2}(t) & \cdots & -a_1(t) \end{bmatrix}$$

and initial conditions

$$\begin{bmatrix} x_1(0) \\ x_2(0) \\ \vdots \\ x_n(0) \end{bmatrix} = \begin{bmatrix} y_0 \\ y_{10} \\ \vdots \\ y_{n0} \end{bmatrix}$$

and

$$y(t) = x_1(t)$$

This equivalence provides a useful relation between the Wronskian matrix of (4.4) and the fundamental matrix of systems with a system matrix in companion canonical form (4.5). The concept of the following lemma is a rather standard result in LTV systems and the proof straightforward.

Lemma 4.2 *For LTV state space systems in companion canonical form (4.5), a fundamental matrix of solutions $W(t)$ is a wronskian matrix for the equivalent scalar system (4.4).*

In terms of the PD-eigenvalues $\{\rho_k\}_{k=1}^{n}$of (4.4), a fundamental set of solutions is given by $\{y_k = \exp^{\int \rho_k(t)dt}\}_{k=1}^{n}$. A fundamental matrix of solutions of (4.5) is given by

$$\mathbf{W}_1(t) = V(\rho_1, \rho_2, \ldots, \rho_n)\mathbf{D} \tag{4.6}$$

with

$$V(\rho_1, \rho_2, \ldots, \rho_n) = \begin{bmatrix} 1 & 1 & \ldots & 1 \\ \mathcal{D}_{\rho_1}\{1\} & \mathcal{D}_{\rho_2}\{1\} & \ldots & \mathcal{D}_{\rho_n}\{1\} \\ \mathcal{D}^2_{\rho_1}\{1\} & \mathcal{D}^2_{\rho_2}\{1\} & \ldots & \mathcal{D}^2_{\rho_n}\{1\} \\ \vdots & \vdots & \ddots & \vdots \\ \mathcal{D}^{n-1}_{\rho_1}\{1\} & \mathcal{D}^{n-1}_{\rho_2}\{1\} & \ldots & \mathcal{D}^{n-1}_{\rho_n}\{1\} \end{bmatrix}$$

and

$$\mathbf{D} = \mathrm{diag}[y_1, y_2, \ldots, y_n]$$

We can now use this fundamental matrix $\mathbf{W}_1(t)$ to establish a bound on the growth of the state transition matrix.

Theorem 4.2 *If a scalar LTV system described by (4.5) has PD-eigenvalues s.t* $\mathrm{Re}\{\rho_k(t)\} < -a\,\forall t, \forall k,$ *for some* $a > 0$ *and a set of PD-eigenvectors that satisfy* $\|\boldsymbol{v}_k(t)\boldsymbol{u}_k^{\mathrm{T}}(t_0)\| \leq h\exp^{d(t-t_0)}$, *then for any wronskian W of the LTV system*

$$\|W(t)W^{-1}(t_0)\|_\infty \leq h\exp^{(d-a)(t-t_0)}$$

where

$$h = \sum_{k=1}^{n} h_k$$

and h_k is the magnitude bound on the kth pd-eigenvector, and d is the pd-eigenvector growth bound.

Proof: Let $W_1(t)$ be the fundamental matrix from Lemma 4.2. i.e.

$$W_1(t) = V(\rho_1, \rho_2, \ldots, \rho_n)\mathrm{D}$$

Since $W(t)$ is also a fundamental matrix for (4.5), and any fundamental matrix differs from another by an invertible constant matrix so

$$\begin{aligned}
\|\boldsymbol{W}(t)\boldsymbol{W}^{-1}(t_0)\| &= \|\boldsymbol{W}_1(t)\boldsymbol{C}\boldsymbol{C}^{-1}\boldsymbol{W}_1^{-1}(t_0)\| \\
&= \|\boldsymbol{W}_1(t)\boldsymbol{W}_1^{-1}(t_0)\| \\
&= \|\boldsymbol{V}(t)\mathbf{D}(t, T_0)\mathbf{D}^{-1}(t_0, T_0)\boldsymbol{U}(t_0)\| \\
&= \|\boldsymbol{V}(t)\mathbf{D}(t, t_0)\boldsymbol{U}(t_0)\| \\
&= \|\sum_{k=1}^{m} \boldsymbol{v}_k(t)\exp^{\int_{t_0}^{t}\rho_k(\tau)d\tau}\boldsymbol{u}_k^{\mathrm{T}}(t_0)\| \\
&\leq \sum_{k=1}^{m} \|\boldsymbol{v}_k(t)\exp^{\int_{t_0}^{t}\rho_k(\tau)d\tau}\boldsymbol{u}_k(t_0)\|
\end{aligned}$$

Using the assumption on the PD-eigenvalues yields

$$\|\boldsymbol{W}(t)\boldsymbol{W}^{-1}(t_0)\| \leq \sum_{k=1}^{m} \|\boldsymbol{v}_k(t)\exp^{\int_{t_0}^{t} -ad\tau}\boldsymbol{u}_k(t_0)\|$$

which by the assumption on the eigenvectors

$$\begin{aligned}\|\boldsymbol{W}(t)\boldsymbol{W}^{-1}(t_0)\| &\leq \sum_{k=1_k}^{m} h_k\exp^{\int_{t_0}^{t}(d-a)d\tau} \\ &= \sum_{k=1_k}^{m} h_k\exp^{(d-a)(t-t_0)}\end{aligned}$$

So for any Wronskian matrix $\boldsymbol{W}$

$$\|\boldsymbol{W}(t)\boldsymbol{W}^{-1}(t_0)\|_\infty \leq h\exp^{(d-a)(t-t_0)}$$ □

Recall that the state transition matrix can be given in terms of a fundamental matrix. Specifically,

$$\Phi(t,\tau) = \boldsymbol{W}(t)\boldsymbol{W}^{-1}(\tau).$$

Now, the fundamental matrix properties of SISO systems for systems with companion canonical system matrices can be expanded to MIMO system with system matrices in Decoupled Multivariable Phase Variable canonical form (4.1). The following lemma is a formal extension of the fundamental matrix of each individual companion system matrix to the complete MIMO system matrix. This is possible because each block is in effect completely decoupled from each other block.

Lemma 4.3 *The matrix $\boldsymbol{W}$, where*

$$\boldsymbol{W} = \text{diag}(W_1, W_2, \ldots, W_m)$$

is a fundamental matrix for $\dot{\boldsymbol{x}} = \boldsymbol{A}_d\boldsymbol{x}$, W_i is a Wronskian matrix for the partitioned subsystem $\dot{\boldsymbol{x}}_i = \boldsymbol{A}_i\boldsymbol{x}_i$, and $\boldsymbol{A}_i$ are the diagonal matrices of the Block Decoupled Phase Variable Canonical system matrix of 4.1.

The proof of this is straightforward and has been omitted. Now, we come to a fundamental robustness theory for PD-spectrum assignment. The robustness of a LTV system assumed to be in the decoupled Multivariable Phase Variable Canonical form is given in terms of the right bounds on the PD-eigenvalues, and the growth bounds on the PD-eigenvectors. The PD-eigenvalues are assumed to be assigned to be bounded on the right by $-a$, and the growth bounds on the PD-eigenvectors must be such that

$$\|\boldsymbol{v}_k(t)\boldsymbol{u}_k^{\mathrm{T}}(t_0)\| < h_k \exp^{d_k(t-t_0)} \; \forall t \geq t_0 \geq T_0$$

in order to satisfy the PD-spectral stability criteria.

Theorem 4.3 (PD-eigenvalue robust stability theorem): *The LTV system of figure 4.2 is bounded input bounded state stable if the nominal system is u.e.s and has PD-eigenvalues whose real parts are less than* $-a$ *with PD-eigenvectors s.t.* $\|\boldsymbol{v}_k(t)\boldsymbol{u}_k^T(t_0)\| < h_k \exp^{d_k(t-t_0)}$ *and the perturbation matrix* $H_2 = \Delta \boldsymbol{A}_d(t)$ *satisfies* $\|H_2 \boldsymbol{w}_2(\,\cdot\,)\|_\infty < \gamma_2 \|\boldsymbol{w}_2(\,\cdot\,)\|_\infty + \beta = \frac{a-d}{h}\|\boldsymbol{w}_2(\,\cdot\,)\|_\infty + \beta$.

Proof: Let $\boldsymbol{\Phi}$ be the state transition matrix for the nominal closed loop system, then

$$\begin{aligned}
\|\mathrm{H}_1 \boldsymbol{w}_1(\,\cdot\,)\|_\infty &= \|\boldsymbol{\Phi}(t,t_0)\boldsymbol{x}(t_0) + \int_{t_0}^{t} \boldsymbol{\Phi}(t,\tau)\boldsymbol{w}_1(\tau)d\tau\|_\infty \\
&\leq \|\int_{t_0}^{t} \boldsymbol{W}(t)\boldsymbol{W}^{-1}(\tau)\boldsymbol{w}_1(\tau)d\tau\|_\infty + \|\Phi(t,t_0)\boldsymbol{x}(t_0)\|_\infty \\
&\leq \int_{t_0}^{t} \|\boldsymbol{W}(t)\boldsymbol{W}^{-1}(\tau)\boldsymbol{w}_1(\tau)\|_\infty d\tau + \beta \\
&\leq \int_{t_0}^{t} \|\boldsymbol{W}(t)\boldsymbol{W}^{-1}(\tau)\|_\infty \|\boldsymbol{w}_1(\,\cdot\,)\|_\infty d\tau + \beta \\
&= \int_{t_0}^{t} \|\boldsymbol{W}(t)\boldsymbol{W}^{-1}(\tau)\|_\infty d\tau \|\boldsymbol{w}_1(\,\cdot\,)\|_\infty + \beta \\
&\leq \int_{t_0}^{t} (\max_{1 \leq i \leq m} \|\boldsymbol{W}_i(t)\boldsymbol{W}_i^{-1}(\tau)\|_\infty) d\tau \|\boldsymbol{w}_1(\,\cdot\,)\|_\infty + \beta
\end{aligned}$$

Corollary 1 gives

$$\begin{aligned}\|\mathrm{H}_1 \boldsymbol{w}_1(\,\cdot\,)\|_\infty &\le \int_{t_0}^{t} h\exp^{(d-a)(t-\tau)} d\tau \|\boldsymbol{w}_1(\,\cdot\,)\|_\infty + \beta \\ &= \frac{h}{a-d}(1-\exp^{(d-a)(t-\tau)})\|\boldsymbol{w}_1(\,\cdot\,)\|_\infty + \beta \\ &\le \frac{h}{a-d}\|\boldsymbol{w}_1(\,\cdot\,)\|_\infty + \beta \\ &= \gamma_1\|\boldsymbol{w}_1(\,\cdot\,)\|_\infty + \beta\end{aligned}$$

Thus with the assumption that $\gamma_2 < \frac{a-d}{h}$, $\gamma_1\gamma_2 < 1$, it then follows from the Small Gain theorem that if $u_1, u_2 \in \mathcal{L}^\infty$, then $\boldsymbol{w}_1, \boldsymbol{w}_2, \boldsymbol{y}_1, \boldsymbol{y}_2 \in \mathcal{L}^\infty$. Note that $\boldsymbol{y}_1, \boldsymbol{y}_2$ are the states. Thus, if the inputs are bounded, then all of the states are bounded for the norm bounded perturbations. □

Theorem 4.3 gives bounds on the perturbations in the system matrices to guarantee BIBS stability on the perturbed system of figure 4.2. It also considers the effect of the disturbances on the perturbed system. Now it is necessary to establish the exponential stability of the perturbed system. Corollary 4.1, presented below, gives the norm bounds on the total perturbation matrix $\Delta\boldsymbol{A}_d(t)$ for which the total system remains exponentially stable. The disturbance terms $\boldsymbol{w}_1(t)$ and $\boldsymbol{w}_2(t)$ do not effect the exponential stability of the perturbed system and so are dropped in this analysis. The next lemma is a purely technical requirement of the following Corollary 4.1.

Lemma 4.4 $\frac{k_1}{a}\exp^{-\frac{1}{2}at_1} \ge t_1 k_1 \exp^{-at_1}\ \forall t_1 \ge 0,\ k_1 \ge 0,\ a > 0$

Proof: Let

$$f(t_1) := 5\frac{k_1}{a}\exp^{-\frac{1}{2}at_1} - t_1 k_1 \exp^{-at_1}$$

so, $f(0) = 5\frac{k_1}{a}$, and $f(\infty) = 0$. Taking the derivative gives

$$f'(t_1) = \exp^{-at_1}(\,-k_1 + at_1k_1 - \frac{5k_1}{2}\exp^{\frac{1}{2}at_1})$$

now define, $g(t_1) := -k_1 + at_1k_1 - \frac{5k_1}{2}\exp^{\frac{1}{2}at_1}$ so, $g(0) = -k_1 - \frac{5k_1}{2}$, and $g(\infty) = -\infty$. Taking the derivative of $g(t)$ gives

$$g'(t_1) = ak_1 - \frac{5k_1}{4}a\exp^{\frac{1}{2}at_1} < 0 \, \forall t_1$$

so, $g(t_1)$ is a strictly decrescent function on $[0, \infty)$. This means that $g(t_1) \leq g(0)$ on $[0, \infty)$ or equivalently $g(t_1)$ is strictly negative. This means that $f'(t_1) \leq 0$ which means $f(t_1)$ is a decrescent function and thus $f(t_1) \geq 0$ on $[0, \infty)$ or equivalently

$$5\frac{k_1}{a}\exp^{-\frac{1}{2}at_1} \geq t_1k_1\exp^{-at_1} \, \forall t_1 \geq 0, \, k_1 \geq 0, \, a > 0 \qquad \square$$

Corollary 4.1 *The perturbed LTV system of figure 4.2 is uniformly exponentially stable provided that*

(a) the nominal system has PD-eigenvalues whose real parts are uniformly less than $-a$

(b) the PD-eigenvectors are s.t. $\|\boldsymbol{v}_k(t)\boldsymbol{u}_k^T(t_0)\| < h_k\exp^{d_k(t-t_0)}$ *and* $a > d$

(c) the perturbation matrix $H_2 = \Delta\boldsymbol{A}_d(t)$ *satisfies* $\|H_2\boldsymbol{w}_2(\cdot)\|_\infty < \gamma_2\|\boldsymbol{w}_2(\cdot)\|_\infty = \frac{a-d}{h}\|\boldsymbol{w}_2(\cdot)\|_\infty$.

Proof: The perturbed closed loop LTV system (4.3) with no driving disturbances is given by

$$\dot{\boldsymbol{x}} = \boldsymbol{A}_d\boldsymbol{x} + \Delta\boldsymbol{A}_d\boldsymbol{x}$$

Theorem 4.3 guarantees the boundedness of the states for the perturbed system so the following equation can be realized with a bounded input and then the equation can be described by

$$\dot{\boldsymbol{x}} = \boldsymbol{A}_d x + \mathbf{I}_n\boldsymbol{u}_d$$

the solution is then given by

$$\boldsymbol{x}(t) = \Phi_{A_d}(t, t_0)\boldsymbol{x}(t_0) + \int_{t_0}^{t} \Phi_{A_d}(t, \tau)\mathbf{I}_n \boldsymbol{u}_d(\tau) d\tau$$

Thus,

$$\begin{aligned}
\|\boldsymbol{x}(t)\| &= \|\Phi_{A_d}(t, t_0)x(t_0) + \int_{t_0}^{t} \Phi_{A_d}(t, \tau)\mathbf{I}_n \boldsymbol{u}_d(\tau) d\tau\| \\
&= \|\Phi_{A_d}(t, t_0)\boldsymbol{x}(t_0) + \int_{t_0}^{t} \Phi_{A_d}(t, \tau)\Delta \boldsymbol{A}_d(\tau)\boldsymbol{x}(\tau) d\tau\| \\
&\leq \|\Phi_{A_d}(t, t_0)\boldsymbol{x}(t_0)\| + \int_{t_0}^{t} \|\Phi_{A_d}(t, \tau)\Delta \boldsymbol{A}_d(\tau)\boldsymbol{x}(\tau)\| d\tau \\
&\leq \|\Phi_{A_d}(t, t_0)\|\|\boldsymbol{x}(t_0)\| + \int_{t_0}^{t} \|\Phi_{A_d}(t, \tau)\|\|\Delta \boldsymbol{A}_d(\tau)\|\|\boldsymbol{x}(\tau)\| d\tau \\
&\leq \|\Phi_{A_d}(t, t_0)\|\|\boldsymbol{x}(t_0)\| + \|\Delta \boldsymbol{A}_d(\,\cdot\,)\|_\infty \int_{t_0}^{t} \|\Phi_{A_d}(t, \tau)\|\|\boldsymbol{x}(\tau)\| d\tau
\end{aligned}$$

Now, by Lemma 4.2 and by assumption about the perturbation matrix

$$\begin{aligned}
&\|\boldsymbol{x}(t)\| \leq h\exp^{(d-a)(t-t_0)}\|\boldsymbol{x}(t_0)\| + \|\Delta A_d(\,\cdot\,)\|_\infty \int_{t_0}^{t} h\exp^{(d-a)(t-\tau)}\|\boldsymbol{x}(\tau)\| d\tau \\
&< h\exp^{(d-a)(t-t_0)}\|\boldsymbol{x}(t_0)\| + \frac{a-d}{h}\int_{t_0}^{t} h\exp^{(d-a)(t-\tau)}\|\boldsymbol{x}(\tau)\| d\tau
\end{aligned}$$

It then follows from the Gronwall-Bellman inequality that

$$\begin{aligned}
\|\boldsymbol{x}(t)\| &< h\exp^{(d-a)(t-t_0)}\|\boldsymbol{x}(t_0)\| + \\
&+ \frac{a-d}{h}\int_{t_0}^{t} h\exp^{(d-a)(\tau-t_0)}\|\boldsymbol{x}(t_0)\| h\exp^{(d-a)(t-\tau)}\exp^{\int_\tau^t (a-d)h\exp^{(d-a)(t-s)}ds} d\tau \\
&= \|\boldsymbol{x}(t_0)\|\left\{ h\exp^{(d-a)(t-t_0)} + (a-d)h\exp^{(d-a)(t-t_0)}\int_{t_0}^{t} \exp^{1-\exp^{(t-\tau)(d-a)}} d\tau \right\}
\end{aligned}$$

Using

$$1 - \exp^{(t-\tau)(d-a)} < 1 \,\forall \tau < t$$

and $\exp^1 = e$ gives,

$$\begin{aligned}\|x(t)\| &< \|x(t_0)\|\left\{h\exp^{(d-a)(t-t_0)} + he(a-d)\exp^{(d-a)(t-t_0)}\int_{t_0}^{t} d\tau\right\} \\ &= \|x(t_0)\|\left\{h\exp^{(d-a)(t-t_0)} + he(a-d)\exp^{(d-a)(t-t_0)}(t-t_0)\right\}\end{aligned}$$

Now using Lemma 4.4 gives

$$\begin{aligned}\|x(t)\| &< \left(h\exp^{(d-a)(t-t_0)} + 5he\exp^{\frac{1}{2}(d-a)(t-t_0)}\right)\|x(t_0)\| \\ &= \left(h\exp^{\frac{1}{2}(d-a)(t-t_0)} + 5he\right)\exp^{\frac{1}{2}(d-a)(t-t_0)}\|x(t_0)\| \\ &\leq (h+5he)\exp^{\frac{1}{2}(d-a)(t-t_0)}\|x(t_0)\|\end{aligned}$$

Thus,

$$\|x(t)\| < (h+5he)\exp^{\frac{1}{2}(d-a)(t-t_0)}\|x(t_0)\| \qquad \square$$

4.3 - Extension to Robustness of Nonlinear Tracking

The importance of the exponential stability of LTV systems in the analysis and design of nonlinear tracking controllers will be illustrated and used in this section. The idea behind this technique is Lyapunov's first method. If a control signal can be generated to place a given nonlinear system on a desired trajectory, then a controller that exponentially stabilizes the linearized tracking error dynamics governed by a LTV system will locally exponentially stabilize the nominal trajectory. The ability to use a linear controller can be very important as finding the defining nonlinear error dynamics from a given nonlinear system can be prohibitively difficult, but finding the linear error dynamics is rather straightforward.

Assumption 4.1 We will assume that the nonlinear system to be designed for is of the form

$$\dot{\xi} = f(t, \xi, v) \tag{4.7}$$

$$\xi(t_0) = \xi_0$$

$$\eta = h(t, \xi)$$

Where $\xi \in \mathbb{R}^n, \eta \in \mathbb{R}^p$, $v \in \mathbb{R}^m$, $f \in C^{n-1}$ and $h \in C^{n-1}$and $t \geq t_0$. Also, we will assume that for a given nominal state trajectory $\bar{\xi}$, there is a nominal input $\bar{v}$ that places (4.7) on the desired trajectory. The nominal trajectory satisfies

$$\dot{\bar{\xi}} = f(t, \bar{\xi}, \bar{v})$$

Additionally, we shall assume that the time varying matrices of partial derivatives of $f(t, \xi, v)$ evaluated at the nominal states and nominal controls

$$A(t) = \frac{\partial f}{\partial \xi}(t, \bar{\xi}, \bar{v}), \; B(t) = \frac{\partial f}{\partial v}(t, \bar{\xi}, \bar{v})$$

satisfy Assumption 3.1 on the time varying system and input matrices.

The LTV matrices above are the system and input matrices of the linearized error dynamics. Thus, these assumptions will allow us to extend the results on LTV systems to nonlinear trajectory stabilization. Also, the assumptions about the existence of a nominal control amount to an assumption of invertibility of the nonlinear system. This assumption will be loosened to allow for pseudo-inversion of systems for which no true inversion is possible, and the robustness of the method will be used to account for the error in the nominal control. These topics will be explored further in the next chapter.

Theorem 4.4, given below, is a standard result in nonlinear texts, *cf.* [48]. It states that the equilibrium of a nonlinear system is exponentially stable iff the linearized equation at that equilibrium is exponentially stable and the Jacobian of the defining nonlinear function satisfies a Lipschitz condition.

Theorem 4.4 *Let $x = 0$ be an equilibrium point for the nonlinear system*

$$\dot{\xi} = f(t, \xi)$$

where $f : [0, \infty) \times D \rightarrow \mathbb{R}^n$ *is continuously differentiable w.r.t* ξ, $D = \{\xi \in \mathbb{R}^n \mid \|\xi\|_2 < r\}$, *and the Jacobian matrix* $[\frac{\partial f}{\partial \xi}(t, \xi)]$ *is bounded and Lipschitz on D, uniformly in t. Let*

$$A(t) = \frac{\partial f}{\partial \xi}(t, \xi)\Big|_{\xi=0}$$

Then, the origin is an exponentially stable equilibrium point for the nonlinear system if it is an exponentially stable equilibrium point for the linear system

$$\dot{x} = A(t)x$$

It is often stated that Theorem 4.4 can be extended to the question of stability of a given time varying trajectory. However, proof is seldom given. Thus the following theorem is a formal statement of this oft asserted fact. This theorem states that a time varying trajectory of a nonautonomous nonlinear system is locally exponentially stable if and only if the jacobian is bounded, Lipschitz in a ball about the trajectory and the linearized error dynamics along the trajectory satisfy the PD-spectral stability requirements under the given assumptions. It is important to note that time varying trajectories result in LTV linearized error dynamics even for autonomous nonlinear systems.

Theorem 4.5 *The system characterized by (4.7) is exponentially stable about a nominal trajectory provided that*

(a) the Jacobian of $f(\cdot, \cdot, \cdot)$ *is continuously differentiable w.r.t.* ξ *and is uniformly Lipschitz along the nominal trajectory*

(b) all of the PD-eigenvalues of the linearization have negative extended mean

(c) the growth bound on the PD-eigenvectors do not exceed the magnitude of the smallest extended mean.

Proof: First define the state error as

$$e = \xi - \overline{\xi}$$

which gives the error dynamics

$$\begin{aligned} \dot{e} &= \dot{\xi} - \dot{\overline{\xi}} \\ &= f(t, \xi, v) - f(t, \overline{\xi}, \overline{v}) \\ &:= g(t, e, v_e) \end{aligned}$$

with

$$v_e = v - \overline{v}$$

Note that the equilibrium for the LTV error dynamics is,

$$e = 0, v_e = 0$$

Which is equivalent to

$$\xi = \overline{\xi}, v = \overline{v}$$

so that 0 is an equilibrium of the nonlinear error dynamics which is shown by

$$\begin{aligned} g(t, 0, 0) &= f(t, \overline{\xi}, \overline{v}) - f(t, \overline{\xi}, \overline{v}) \\ &= 0 \end{aligned}$$

Now, the linearized error dynamics are realized by

$$\dot{x} = A(t)x$$

where

$$A(t) = \frac{\partial g}{\partial e}\Big|_{e=0}$$

$$= (\frac{\partial f(t,\xi,v)}{\partial e} + \frac{\partial f(t,\bar{\xi},\ \bar{v}\ )}{\partial e})\Big|_{e=0}$$

however $f(t,\bar{\xi},\ \bar{v}\ )$ is independent of e, so

$$A(t) = (\frac{\partial f(t,\xi,v)}{\partial e})\Big|_{e=0}$$

$$= (\frac{\partial f(t,\xi,v)}{\partial \xi}\frac{\partial \xi}{\partial e})\Big|_{e=0}$$

$$= (\frac{\partial f(t,\xi,v)}{\partial \xi})\Big|_{\xi=\bar{\xi}}$$

Thus $\frac{\partial f}{\partial \xi}$ is Lipschitz along $\bar{\xi}$ iff $\frac{\partial g}{\partial e}$ is Lipschitz in a neighborhood about $e = 0$. Thus, by Theorem 4.4 the nominal trajectory is exponentially stable iff the Jacobian of $g(\ \cdot\ ,\cdot\ ,\cdot\ )$ at $e = 0$ is a uniformly exponentially stable system matrix for the LTV error dynamics. But the linearized error dynamics are exponentially stable iff the system matrix of the linearized error dynamics satisfies the PD-spectral stability criteria. Thus, the nominal trajectory is exponentially stable iff the PD-spectrum satisfies the PD-spectral stability criteria. □

We will now consider the robustness of the PD-spectral assignment tracking control design. Theorem 4.6, given below, provides a robustness guaranty for a nonlinear perturbation of the plant model which vanishes at the nominal trajectory. We shall consider nonlinear systems described by

$$\dot{\xi} = f(t,\xi,v) = f_n(t,\xi,v) + \Delta f_n(t,\xi,v) \tag{4.8}$$

where $f_n(t,\xi,v)$ is the nonlinear plant for which the nominal control and time varying PD-spectral error controller are designed and $\Delta f_n(t,\xi,v)$ represents a nonlinear time varying perturbation in the nominal plant. For the nominal trajectory $\bar{\xi}$ of a nonlinear

system with nominal control $\bar{v}$, a vanishing perturbation $\Delta f_n(t, \xi, v)$ is a perturbation such that

$$\Delta f_n(t, \bar{\xi}, \bar{v}) = 0$$

This type of perturbation is useful in modeling a nonlinear system $f(t, \xi, v)$ as a nominal model $f_n(t, \xi, v)$ for which the design process is significantly simpler plus a perturbation term $\Delta f_n(t, \xi, v)$ which represents the approximation error arising from the simplifying assumptions. Theorem 4.6, below, guarantees that the controller designed under the simplifying assumptions will still achieve exponential stability as long as the linearization of the perturbation falls within the given norm bound.

Theorem 4.6 *Given the existence of a desired trajectory* $\bar{\xi}$ *with nominal control* $\bar{v}$ *for the perturbed nonlinear system given by*

$$\dot{\xi} = f(t, \xi, v) = f_n(t, \xi, v) + \Delta f_n(t, \xi, v)$$

that satisfies Assumption 4.1., there is a state error feedback $\mathbf{K}_z(t)$ *that achieves exponential stability for any perturbation* $\Delta f_n(t, \xi, v)$ *provided that*

(a) the linearization satisfies

$$\|T(t)\{\Delta A_n(t)T^{-1}(t) + \Delta B_n(t)K_z(t) + \Delta B_n(t)\Delta K_z(t)\}\|_\infty < \frac{a-d}{h}$$

(b) the closed loop PD-spectrum is chosen s.t. the real part of all PD-eigenvalues are less than $-a$

(c) the PD-eigenvectors of the closed loop system are chosen s.t. $\sum_{k=1}^{n} h_k < h$ *where* h_k *are the magnitude bounds on the assigned PD-eigenvectors,* d *is the maximum growth bound on the PD-eigenvectors*

(d) $f(t, \xi) : [0, \infty) \times D \to R^n$ *is continuously differentiable w.r.t.* ξ $D = \{\xi \in R^n : \|\xi - \bar{\xi}\|_2 < r\}$

(e) the Jacobian matrix $[\partial f/\partial\xi]$ is bounded and Lipshcitz on D, uniformly in t

where, $\mathbf{T}(t)$ *is the Lyapunov transformation that realizes the algebraically equivalent Multi-variable Phase-variable canonical form for the linear portion of the nominal system,* $\Delta \boldsymbol{A}_n(t)$ *is the linearized perturbation in the system matrix,* $\Delta \boldsymbol{B}_n(t)$ *is the linearized perturbation in the input matrix, and* $\Delta \mathbf{K}_z(t)$ *is the error in the linear state feedback.*

Proof: First, by assumption there is a nominal control for the unperturbed nonlinear system that achieves the desired trajectory $\bar{\xi}$ for the perturbed nonlinear system since

$$\begin{aligned}\dot{\bar{\xi}} &= \boldsymbol{f}(t,\bar{\xi},\bar{\boldsymbol{v}}) \\ &= \boldsymbol{f}_n(t,\bar{\xi},\bar{\boldsymbol{v}}) + \Delta\boldsymbol{f}_n(t,\bar{\xi},\bar{\boldsymbol{v}}) \\ &= \boldsymbol{f}_n(t,\bar{\xi},\bar{\boldsymbol{v}})\end{aligned}$$

Thus the nonlinear system can be linearized about the nominal trajectory and gives

$$\boldsymbol{A}(t) = \frac{\partial \boldsymbol{f}}{\partial \xi}(t,\xi)\big|_{\bar{\xi},\bar{\boldsymbol{v}}}$$

which by the linearity of differentiation is equivalent to

$$\begin{aligned}\boldsymbol{A}(t) &= \frac{\partial \boldsymbol{f}_n}{\partial \xi}(t,\xi)\big|_{\bar{\xi},\bar{\boldsymbol{v}}} + \frac{\partial(\Delta \boldsymbol{f}_n)}{\partial \xi}(t,\xi)\big|_{\bar{\xi},\bar{\boldsymbol{v}}} \\ &= \boldsymbol{A}_n(t) + \Delta\boldsymbol{A}_n(t)\end{aligned}$$

Similarly,

$$\boldsymbol{B}(t) = \boldsymbol{B}_n(t) + \Delta\boldsymbol{B}_n(t)$$

Thus the linearization about the origin is given by

$$\dot{\boldsymbol{x}} = \boldsymbol{A}(t)\boldsymbol{x} = \{\boldsymbol{A}_n(t) + \Delta\boldsymbol{A}_n(t)\}\boldsymbol{x} + \{\boldsymbol{B}_n(t) + \Delta\boldsymbol{B}_n(t)\}\boldsymbol{u}(t)$$

The transformation $\mathbf{T}(t)$ that puts the unperturbed system in the algebraically equivalent Multi-Variable Phase Variable Canonical form renders the perturbed system into the form

$$\begin{aligned}\dot{z} = &\left\{(\dot{\mathrm{T}}(t) + \mathrm{T}(t)\boldsymbol{A}_n(t))\mathrm{T}^{-1}(t) + \mathrm{T}(t)\Delta\boldsymbol{A}_n(t)\mathrm{T}^{-1}(t)\right\}\boldsymbol{z} + \\ &+ \mathrm{T}(t)\{\boldsymbol{B}(t) + \Delta\boldsymbol{B}_n(t)\}\boldsymbol{u}(t)\end{aligned}$$

Theorem 3.3 guarantees the existence of a feedback matrix $\boldsymbol{K}_z(t)$ that achieves the desired PD-spectrum. Now allowing for uncertainty in the state feedback matrix the perturbed closed loop equation is

$$\begin{aligned}\dot{z} = &\left\{(\dot{\mathrm{T}}(t) + \mathrm{T}(t)\boldsymbol{A}_n(t))\mathrm{T}^{-1}(t) + \mathrm{T}(t)\Delta\boldsymbol{A}_n(t)\mathrm{T}^{-1}(t)\right\}\boldsymbol{z} + \\ &+ \mathrm{T}(t)\{\boldsymbol{B}(t) + \Delta\boldsymbol{B}_n(t)\}\{\boldsymbol{K}_z(t) + \Delta\boldsymbol{K}_z(t)\}\boldsymbol{z}\end{aligned}$$

Rewriting this equation in terms of the Block Decoupled Phase Variable Canonical Form that realizes the desired PD-spectrum gives

$$\dot{z} = \left\{\boldsymbol{A}_d(t) + \mathrm{T}(t)[\Delta\boldsymbol{A}_n(t)\mathrm{T}^{-1}(t) + \Delta\boldsymbol{B}_n(t)\boldsymbol{K}_z(t) + \Delta\boldsymbol{B}_n(t)\Delta\boldsymbol{K}_z(t)]\right\}\boldsymbol{z}$$

Corollary 4.1 guarantees that the above system is uniformly exponentially stable if

$$\left\|\mathrm{T}(t)\left\{\Delta\boldsymbol{A}_n(t)\mathrm{T}^{-1}(t) + \Delta\boldsymbol{B}_n(t)\boldsymbol{K}_z(t) + \Delta\boldsymbol{B}_n(t)\Delta\boldsymbol{K}_z(t)\right\}\right\|_\infty < \frac{a-d}{h}$$

By the Lyapunov stability Theorem 3.1, the linearized system is uniformly exponentially stabilized iff the transformed system is u.e.s. Finally, the nominal trajectory $\bar{\xi}$ of the nonlinear system is locally uniformly exponentially stable if and only if the linearized system about the nominal trajectory is u.e.s. □

Without explicit proof being sought, the results obtained so far and especially Theorem 4.6 provide considerable heuristic insight into tracking control of nonlinear systems using the proposed design technique. Generally, the deeper into the left half complex plane that the PD-eigenvalues are placed consistent with the time varying nature being such that the associated PD-eigenvectors are kept relatively small, then the more robust the system will be with respect to parametric uncertainty, and the greater the tolerance to the approximate nature of the nominal control.

Robustness results for this type of nonlinear perturbation will be presented formally in Theorem 4.9. However, first we must introduce the concept of uniformly ultimately bounded and two useful theorems.

Definition 4.3 The solutions of $\dot{\xi} = f(t, \xi)$ are said to be uniformly ultimately bounded if there exist positive constants b, and c, and for every $\alpha \in (0, c)$ there is a positive constant $T = T(\alpha)$ such that

$$\|\xi(t_0)\| < \alpha \Rightarrow \|\xi(t)\| \leq b, \ \forall t > t_0 + T$$

The tracking error about a nominal trajectory $\overline{\xi}$ is said to be uniformly ultimately bounded if there exist constants b, and c, and for every $\alpha \in (0, c)$ there is a positive constant $T = T(\alpha)$ such that

$$\|\xi(t_0) - \overline{\xi}(t_0)\| < \alpha \Rightarrow \|\xi(t) - \overline{\xi}(t)\| \leq b, \ \forall t > t_0 + T$$

Where b is called the ultimate bound

When the tracking error is uniformly ultimately bounded it is stable in the sense that if the system is ever sufficiently close to the nominal trajectory then it will never leave the vicinity of the nominal trajectory. This definition is a very useful one in characterizing the ability of a closed loop control system to track a given desired trajectory. If a controller can be designed to keep a system within b of the desired trajectory, then this is a quantitative assurance of the precision of the trajectory tracking controller.

The following Theorems 4.7-4.8 are adapted from [48] and will be instrumental in showing the uniform ultimate boundedness of the tracking error about a nominal trajectory for a non-vanishing nonlinear time varying perturbation. Theorem 4.7 is useful in guaranteeing the existence of the inequalities 4.9a-c which will be necessary for the other theorems.

Theorem 4.7 *Let $\bar{\xi}$ be an equilibrium point for the nonlinear system*

$$\dot{\xi} = f(t, \xi)$$

where $f : [0, \infty) \times D \rightarrow \mathbb{R}^n$ *is continuously differentiable,* $D = \{\xi \in \mathbb{R}^n | \|\xi(t) - \bar{\xi}(t)\| < r\}$, *and the Jacobian matrix* $[\frac{\partial f}{\partial \xi}]$ *is bounded on* D, *uniformly in* t. *Let* k, γ, *and* r_0 *be positive constants with* $r_0 < \frac{r}{k}$. *Let* $D_0 = \{\xi \in \mathbb{R}^n | \|\xi(t) - \bar{\xi}(t)\| < r_0\}$. *Assume that the trajectories of the system satisfy*

$$\|\xi(t) - \bar{\xi}(t)\| \leq k\|\xi(t_0) - \bar{\xi}(t_0)\| \exp^{-\gamma(t-t_0)}, \ \forall\xi(t_0) \in D_0, \ \forall t > t_0 \geq 0$$

Then there is a function $V : [0, \infty) \times D_0 \rightarrow \mathbb{R}$ *that satisfies the inequalities*

$$c_1\|\xi(t) - \bar{\xi}(t)\|^2 \leq V(t, \xi) \leq c_2\|\xi(t) - \bar{\xi}(t)\|^2 \tag{4.9a}$$

$$\frac{\partial V}{\partial \xi} + \frac{\partial V}{\partial \xi} f(t, \xi) \leq -c_3\|\xi(t) - \bar{\xi}(t)\|^2 \tag{4.9b}$$

$$\left\|\frac{\partial V}{\partial \xi}\right\| \leq c_4\|\xi(t) - \bar{\xi}(t)\| \tag{4.9c}$$

for some positive constants c_1, c_2, c_3, *and* c_4.

Theorem 4.8, given below, gives sufficient conditions on the norm bound of a non-vanishing perturbation of a nonlinear system to maintain the stability of an equilibrium in the sense that the states are uniformly ultimately bounded about the origin. The perturbed nonlinear system is defined to be

$$\dot{\xi} = f(t, \xi) + g(t, \xi)$$

where $f(t, \xi)$ is defined as the nominal nonlinear system and $f(t, 0) = 0$, and $g(t, \xi)$ is a non-vanishing nonlinear time varying perturbation to the nonlinear system. The perturbation is said to be non-vanishing if we can not specifically say

$$g(t, 0) = 0$$

That is to say a non-vanishing perturbation is any perturbation that can not be *a priori* specified as a vanishing perturbation.

Theorem 4.8 *Let $\bar{\xi}$ be an exponentially stable equilibrium point of the nominal system. Let $V(t,\xi,\bar{\xi})$ be a Lyapunov function of the nominal system that satisfies 4.9a-4.9c in $[0,\infty)\times D$, where $D=\{\xi\in\mathbb{R}^n | \|\xi-\bar{\xi}\|<r\}$. Suppose the perturbation term $g(t,\xi,\bar{\xi})$ satisfies*

$$\|g(t,\xi,\bar{\xi})\|\le\delta<\frac{c_3}{c_4}\sqrt{\frac{c_1}{c_2}}\theta r.$$

$\forall\ t\ge 0$, $\forall\ \xi\in D$, *and some positive constant* $\theta<1$. *Then, for all* $\|\xi(t_0)-\bar{\xi}(t_0)\|<\sqrt{\frac{c_1}{c_2}}r$, *the solution* $\xi(t)$ *of the perturbed system satisfies*

$$\|\xi(t)-\bar{\xi}(t)\|\le k\exp^{-\gamma(t-t_0)}\|\xi(t_0)-\bar{\xi}(t_0)\|,\ \forall t_0\le t<t_1$$

and

$$\|\xi(t)\|\le b,\ \forall t\ge t_1$$

for some finite time t_1, *where*

$$k=\sqrt{\frac{c_2}{c_1}},\ \gamma=\frac{(1-\theta)c_3}{2c_2},\ b=\frac{c_4}{c_3}\sqrt{\frac{c_2}{c_1}}\frac{\delta}{\theta}$$

We can now use these theorems to present the robustness results for our nonlinear control technique with non-vanishing perturbations. We shall consider nonlinear systems in the form of

$$\dot{\xi}=f_n(t,\xi,v)+\Delta f_n(t,\xi,v)$$

Where $f_n(t,\xi,v)$ is the nominal nonlinear system and satisfies Assumption 4.1. The nonlinear time varying perturbation $\Delta f_n(t,\xi,v)$ is non-vanishing. This more general perturbation model permits more versatility. First, in the case of where precise inversion is not possible and some method of pseudo-inversion must be used to obtain the nominal

control then the nominal system can be defined as inverse of the pseudo-inverse. Thus, the nonlinear perturbation can hold the difference between the inverse of the pseudo-inverse and the original model of the system. Additionally, the nonlinear perturbation term can represent an unmatched uncertainty in the model of the plant.

Theorem 4.9 *Given the existence of a desired trajectory $\bar{\xi}$ with nominal control $\bar{v}$ and that the nominal system satisfies Assumption 4.1 then the perturbed plant given by*

$$\dot{\xi} = f(t, \xi, v) = f_n(t, \xi, v) + \Delta f_n(t, \xi, v)$$

has an error bounded by

$$\|\xi(t) - \bar{\xi}(t)\| \leq k\exp^{-\gamma(t-t_0)}\|\xi(t_0) - \bar{\xi}(t_0)\|, \ \forall t_0 \leq t < t_1$$

and

$$\|\xi(t) - \bar{\xi}(t)\| \leq b, \ \forall t \geq t_1$$

for some finite t_1 for any perturbation that satisfies

$$\|\Delta f_n(t, \xi, v) - \Delta f_n(t, \bar{\xi}, \bar{v})\| = \frac{c_3}{c_4}\sqrt{\frac{c_1}{c_2}}\theta r$$

for all $t \geq 0$, all $\xi \in D = \{\xi \in \mathbb{R}^n \mid \|\xi(t) - \bar{\xi}(t)\| < r\}$

where, c_i are the constants in inequalities 4.9a-c, θ is the ratio from theorem 4.8, and r is the radius from Theorem 4.8.

Proof: By assumption there is a nominal control $\bar{v}$ that places the nominal plant on the desired nominal trajectory $\bar{\xi}$. Thus we can consider the error dynamics about the nominal trajectory with **0** as the equilibrium point. Let e be the error states then

$$\dot{e} = g_n(t, e, v_e) + \Delta g_n(t, e, v_e)$$

where $g_n(t, e, v_e)$ is the nominal error dynamics and is given by

$$g_n(t, e, v_e) = f_n(t, \xi, v) - f_n(t, \bar{\xi}, \bar{v})$$

and $\Delta g_n(t, e, v_e)$ is the perturbation in the error dynamics and is given by

$$\Delta g_n(t, e, v_e) = \Delta f_n(t, \xi, v) - \Delta f_n(t, \bar{\xi}, \bar{v})$$

Linearizing the nominal system about the nominal trajectory gives

$$\dot{x} = A(t)x + B(t)u$$

Using Assumption 4.1, namely the conditions on the linearized plant, and Theorem 3.3, there exists a feedback matrix $\mathbf{K}(t)$ which achieves a closed loop system that is algebraically equivalent to a Block Decoupled Multi-variable Phase Variable Canonical system matrix that attains the desired PD-spectrum. Thus the closed loop Linearized error system is u.e.s and is given by

$$\dot{x} = [A(t) + B(t)\mathbf{K}(t)]x$$

By Theorem 4.4, the nonlinear error dynamics for the nominal system are uniformly exponentially stable because the linearized error dynamics for the nominal system are uniformly exponentially stable. By Theorem 4.7 there is a Lyapunov function $V(t, e)$ for the nominal error dynamics that satisfies inequalities 4.9a-c, where the domain $D_0 = \{e \in \mathbb{R}^n \mid \|e\| < r_0\}$ is dependent on the choice of magnitude bound k, and decay rate γ of the decaying exponential error from an initial error $e(t_0)$.

So by Theorem 4.8 if

$$\|\Delta g_n(t, e, v_e)\| = \frac{c_3}{c_4}\sqrt{\frac{c_1}{c_2}}\theta r$$

for all $t \geq 0$, all $e \in D = \{e \in \mathbb{R}^n \mid \|e\| < r\}$ then

$$\|e(t)\| \leq k\exp^{-\gamma(t-t_0)}\|e(t_0)\|, \ \forall t_0 \leq t < t_1$$

and

$$\|e(t)\| \leq b, \, \forall t \geq t_1$$

for some finite t_1. □

Theorem 4.9 says that for sufficiently small perturbations in the nominal nonlinear plant and for trajectories that begin sufficiently close to the desired trajectory, the trajectories will remain close to the desired trajectory. The uniform ultimate bound on the error is k. However for exponentially stable systems such as this one, the error bound exponentially decreases with time and ultimately falls within the ball B_b in some finite amount of time. Finding quantitative values for these bounds is of limited utility, but can provide useful insight into the depth of the PD-eigenvalues required to achieve a desired tracking precision specification.

4.4 - Linear Time Varying Observers

Thus far we have only considered the case where the states are available to achieve stability by assigning a desired PD-spectrum for a LTV system as in 4.3. A system for which the states are completely available can be represented by 4.3 if $C(t) \equiv I_n$, and $D(t) \equiv 0_{n\times m}$, where I_n is the $n \times n$ identity matrix, and $0_{n\times m}$ is the $n \times m$ matrix of 0's. In this section we shall consider the more general case where the states are not available, that is we will consider the case with a general time varying output matrix $C(t)$. That is to say we will consider general LTV systems in the form of

$$\dot{x} = A(t)x + B(t)u \tag{4.10}$$

$$y(t) = C(t)x$$

where the time varying matrices in the system 4.10 satisfy Assumption 3.1. Additionally, the system represented by 4.10 is assumed to be uniformly completely observable with a lexicographically fixed basis. We shall show that for LTV systems in the form of 4.10 that satisfy all of the above assumptions, there is a dynamic output

feedback control law that achieves uniform exponential stability which can be derived from an independently designed LTV observer and an independently designed PD-spectrum assignment. Like LTI observer based design, if the initial coniditions on the observer match the initial conditions on the plant, then the output response is indistinquishable from the state feedback design. Unlike LTI designs the closed loop PD-eigenvalues are not the PD-eigenvalues of the observer and controller.

Theorem 4.10, given below, is an analog to the Silveram-Wolovich theorem. It guarantees the existence of a Lyapunov transformation that can transform a Lexicographically fixed uniformly completely control LTV system to a canonical form. Luenberger [60] offered a complete investigation of canonical forms for LTI systems, Wolovich [121] presented a canonical form for uniformly controllable LTV systems, and the following theorem by Nguyen [70] presents a method for constructing a canonical form for lexicographically fixed uniformly observable LTV systems.

Theorem 4.10 *For a LTV system in the form of 4.10 that satisfies the assumptions from above, there is a Lyapunov transformation P_I that transforms the system to the Observer Canonical Form of the following*

$$A_o = \begin{bmatrix} A_{11} & A_{12} & \cdots & A_{1p} \\ A_{21} & A_{22} & \cdots & A_{2p} \\ \vdots & \vdots & \ddots & \vdots \\ A_{p1} & A_{p2} & \cdots & A_{pp} \end{bmatrix}$$

where

$$A_{ii}(t) = \begin{bmatrix} \alpha_{ii,1}(t) & 1 & 0 & \cdots & 0 & 0 \\ \alpha_{ii,2}(t) & 0 & 1 & \cdots & 0 & 0 \\ \vdots & \vdots & \vdots & \ddots & \vdots & \vdots \\ \alpha_{ii,n_i-1}(t) & 0 & 0 & \cdots & 0 & 1 \\ \alpha_{ii,n_i}(t) & 0 & 0 & \cdots & 0 & 0 \end{bmatrix} \in \mathbb{R}^{n_i \times n_i}$$

for $i = 1, 2, \ldots, p$

$$A_{ij}(t) = \begin{bmatrix} \alpha_{ij,1}(t) & 0 & 0 & \cdots & 0 & 0 \\ \alpha_{ij,2}(t) & 0 & 0 & \cdots & 0 & 0 \\ \vdots & \vdots & \vdots & \ddots & \vdots & \vdots \\ \alpha_{ij,n_i-1}(t) & 0 & 0 & \cdots & 0 & 0 \\ \alpha_{ij,n_i}(t) & 0 & 0 & \cdots & 0 & 0 \end{bmatrix} \in \mathbb{R}^{n_i \times n_j}$$

for $i \neq j$; $i, j = 1, 2, \ldots, p$, *and*

$$C_0(t) = \begin{bmatrix} 1 & 0 & \ldots & 0 & 0 & 0 & \ldots & 0 & & 0 & 0 & \ldots & 0 \\ \mathrm{x}(t) & \mathrm{x}(t) & \ldots & \mathrm{x}(t) & 1 & 0 & \ldots & 0 & & 0 & 0 & \ldots & 0 \\ \mathrm{x}(t) & \mathrm{x}(t) & \ldots & \mathrm{x}(t) & \mathrm{x}(t) & \mathrm{x}(t) & \ldots & \mathrm{x}(t) & & 0 & 0 & \ldots & 0 \\ \vdots & \vdots & & \vdots & \vdots & \vdots & & \vdots & \cdots & \vdots & \vdots & & \vdots \\ \mathrm{x}(t) & \mathrm{x}(t) & \ldots & \mathrm{x}(t) & \mathrm{x}(t) & \mathrm{x}(t) & \ldots & \mathrm{x}(t) & & 0 & 0 & \ldots & 0 \\ \mathrm{x}(t) & \mathrm{x}(t) & \ldots & \mathrm{x}(t) & \mathrm{x}(t) & \mathrm{x}(t) & \ldots & \mathrm{x}(t) & & 1 & 0 & \ldots & 0 \end{bmatrix}$$
$$= [\, C_{01}(t) \quad C_{02}(t) \quad \ldots \quad C_{0p}(t) \,]$$

$\mathrm{x}(t)$ *is an unspecified time varying parameter*

n_i *is the observability index of the ith subsystem*

and

$$C_{0i}(t) \in \mathbb{R}^{p \times n_i}$$

Note that the Observer Canonical form is the dual of the Multivariable Phase Variable form. This allows for a observer feedback $L(t)$ that achieves any desired PD-spectrum of the closed loop observer system matrix $A_o(t) + L(t)C(t)$. The PD-eigenvectors are reversed so that the column PD-eigenvectors become row PD-eigenvectors and vice versa.

The controller-observer separability property of LTI systems extends to LTV systems. This fact is easy to establish and is proven in Lemma 4.5.

Lemma 4.5 (Separability of LTV Systems): *A LTV system in the form of 4.10 that satisfies Assumption 3.1 and also is uniformly completely observable with fixed lexicographic basis can be exponentially stabilized by separately designing a uniformly exponentially stable observer and a uniformly exponentially stable state feedback.*

Proof: First, by assumption the system satisfies the conditions of Theorem 3.3 which means there exists a state feedback $\mathrm{K}(t)$ that uniformly exponentially stabilizes the closed loop system, *i.e.* the closed loop system given by

$$\dot{\boldsymbol{x}} = [\boldsymbol{A}(t) + \boldsymbol{B}(t)\mathbf{K}(t)]\boldsymbol{x}$$

is u.e.s. Now, we assume that the states are not available. So we propose to use a LTV observer with observer states $\boldsymbol{x}_o$. So the closed loop equation is given by

$$\dot{\boldsymbol{x}} = \boldsymbol{A}(t)x + \boldsymbol{B}(t)\mathbf{K}(t)\boldsymbol{x}_o$$

The observer equation is chosen as

$$\dot{\boldsymbol{x}}_o = \boldsymbol{A}(t)\boldsymbol{x}_o + \boldsymbol{B}(t)\mathbf{K}(t)\boldsymbol{x}_o + \boldsymbol{L}(t)(\boldsymbol{y}_o - \boldsymbol{y})$$

$$\boldsymbol{y} = \boldsymbol{C}(t)\boldsymbol{x}_o$$

where $\{\boldsymbol{A}(t) + \boldsymbol{L}(t)\boldsymbol{C}(t)\}$ is designed to be exponentially stable by PD-spectrum assignment, by the duality of the observability and controllability. Now, we define the observer error as $\boldsymbol{\epsilon} = \boldsymbol{x}_o - \boldsymbol{x}$ and subtract the controller equation from the observer equation to get the observer error dynamics

$$\dot{\boldsymbol{\epsilon}} = \dot{\boldsymbol{x}}_o - \dot{\boldsymbol{x}} = \{\boldsymbol{A}(t) + \boldsymbol{L}(t)\boldsymbol{C}(t)\}(\boldsymbol{x}_o - \boldsymbol{x})$$

Then, the augmented closed loop controller-observer system is given by

$$\begin{bmatrix} \dot{\boldsymbol{x}} \\ \dot{\boldsymbol{\epsilon}} \end{bmatrix} = \begin{bmatrix} \boldsymbol{A}(t) + \boldsymbol{B}(t)\mathbf{K}(t) & \boldsymbol{B}(t)\mathbf{K}(t) \\ 0 & \boldsymbol{A}(t) + \boldsymbol{L}(t)\boldsymbol{C}(t) \end{bmatrix} \begin{bmatrix} \boldsymbol{x} \\ \boldsymbol{\epsilon} \end{bmatrix}$$

Using the uniform exponential stability of the observer gives

$$\|\epsilon(t)\|_\infty \leq h_1 \exp^{-a_1(t-t_0)} \|\epsilon(t_0)\|_\infty$$

$$\boldsymbol{x}(t) = \Phi_{\mathrm{K}}(t, t_0)\boldsymbol{x}(t_0) + \int_{t_0}^{t} \Phi_{\mathrm{K}}(t, \tau)\boldsymbol{B}(\tau)\mathbf{K}(\tau)\epsilon(\tau)d\tau$$

where $\Phi_{\mathrm{K}}(t, t_0)$ is the state transition matrix of the closed system matrix

$A(t)+B(t)\mathbf{K}(t)$. So the norm of the states at time t is

$$\begin{aligned}\|x(t)\|_\infty &= \|\Phi_K(t,t_0)x(t_0)\|_\infty + \|\int_{t_0}^{t}\Phi_K(t,\tau)B(\tau)\mathbf{K}(\tau)\epsilon(\tau)d\tau\|_\infty \\ &\le \|\Phi_K(t,t_0)\|_\infty\|x(t_0)\|_\infty + \int_{t_0}^{t}\|\Phi_K(t,\tau)B(\tau)\mathbf{K}(\tau)\epsilon(\tau)\|_\infty d\tau \\ &\le h_2\exp^{-a_2(t-t_0)}\|x(t_0)\|_\infty \\ &+ h_1h_2\|B(\cdot)\|_\infty\|\mathbf{K}(\cdot)\|_\infty\|\epsilon(t_0)\|_\infty\int_{t_0}^{t}\exp^{-a_2(t-\tau)-a_1(\tau-t_0)}d\tau\end{aligned}$$

for $a_2 \neq a_1$

$$\begin{aligned}\|x(t)\|_\infty &\le h_2\exp^{-a_2(t-t_0)}\|x(t_0)\|_\infty \\ &+ h_1h_2\|B(\cdot)\|_\infty\|\mathbf{K}(\cdot)\|_\infty\|\epsilon(t_0)\|_\infty\frac{\exp^{a_1t_0}+\exp^{a_2t_0}}{a_2-a_1}\exp^{-a_mt}\end{aligned}$$

where $a_m = \min(a_1,a_2)$

for $a_2 = a_1$

$$\begin{aligned}\|x(t)\|_\infty &\le h_2\exp^{-a_2(t-t_0)}\|x(t_0)\|_\infty \\ &+ h_1h_2\|B(\cdot)\|_\infty\|\mathbf{K}(\cdot)\|_\infty\|\epsilon(t_0)\|_\infty(t-t_0)\exp^{-a_1(t-t_0)} \\ &\le h_2\exp^{-a_2(t-t_0)}\|x(t_0)\|_\infty \\ &+ h_1h_2\|B(\cdot)\|_\infty\|\mathbf{K}(\cdot)\|_\infty\|\epsilon(t_0)\|_\infty\exp^{-a_s(t-t_0)}\end{aligned}$$

where a_s is chosen such that $(t-t_0)\exp^{-a_1t} \le \exp^{-a_s(t-t_0)}\,\forall t \ge t_0$

Thus with $a_t = \min(a_m, a_s)$,

$$\begin{aligned}\left\|\begin{bmatrix} x \\ \epsilon \end{bmatrix}\right\|_\infty &\le \left\|\begin{bmatrix} k_{11} & k_{12} \\ k_{21} & k_{22}\end{bmatrix}\exp^{-a_t(t-t_0)}\begin{bmatrix} x(t_0) \\ \epsilon(t_0)\end{bmatrix}\right\|_\infty \\ &\le K\exp^{-a_t(t-t_0)}\left\|\begin{bmatrix} x(t_0) \\ \epsilon(t_0)\end{bmatrix}\right\|_\infty\end{aligned}$$ □

Lemma 4.5 gives us a technique for designing an output feedback controller that exponentially stabilizes a LTV plant which satisfies certain assumptions. Similar to LTI observer based design, the separability property allows us to design an independent observer with a desired u.e.s PD-spectrum and an independent state feedback controller

that assigns any desired u.e.s. PD-spectrum. The only effect of the observer is to cause a degradation in the performance which results from the transient error in the observer states. If the initial states of the plant is fully know, then the obeserver becomes transparent. In other words, the performance of the output feedback controller is identical to the state feedback controller.

We now wish to use this technique to design a trajectory tracking controller for nonlinear systems. Before we can prove the stability of an observer based trajectory tracking controller, we need to present a Lemma which will be used in the proof. Lemma 4.6 below presents general stability results for vanishing nonlinear perturbations that fall below a norm bounded threshold in a certain domain about the nominal trajectory.

Lemma 4.6 *Let $\overline{\xi}$ be an exponentially stable equilibrium point of the nominal system. Let $V(t,\xi,\overline{\xi})$ be a Lyapunov function of the nominal system that satisfies the inequalities 4.9a-c in $[0,\infty)\times D$. Suppose the perturbation term $g(t,\xi,\overline{\xi})$ satisfies*

$$\|g(t,\xi,\overline{\xi})\| \leq \frac{c_3}{c_4}\|\xi-\overline{\xi}\|,\ \forall t\geq 0,\ \forall\xi\in D$$

Then $\overline{\xi}$ is an exponentially stable equilibrium of the perturbed system.

Lemma 4.6 will allow us to establish the exponential stability of the output feedback observer based controller. Once again we assume the existence of a nominal control that achieves the desired trajectory. Theorem 4.11 below gives the conditions for stability of the observer based controller.

Theorem 4.11 *A nonlinear system that satisfies Assumption 4.1 and with a linearization along all permissible trajectories that is uniformly completely observable, can exponentially track any output trajectory $\overline{\eta}$ for which a nominal control exists if*

$$\|\Delta g(t,e) < \frac{c_3}{c_4}\|e\|,\ \forall t\geq 0,\ \forall e\in D$$

on the domain D, where the domain D is as defined in Theorem 4.7.

Proof: The nonlinear error dynamics about a desired trajectory are given by

$$\dot{e} = f(t, \xi, v) - f(t, \overline{\xi}, \overline{v}) = g(t, e, u)$$

$$\eta_e = h(t, \xi) - \overline{\eta}$$

The linearized error dynamics are given by

$$\dot{x} = A(t)x + B(t)u$$

$$y(t) = C(t)x(t)$$

By assumption the linearized error dynamics are u.c.c. so by Theorem 3.3 there is a state feedback control $\mathbf{K}(t)$ that stabilizes the LTV error dynamics. Using the observer states in the feedback term in the nonlinear tracking error dynamics gives

$$\dot{e} = f(t, \xi, v) - f(t, \overline{\xi}, \overline{v}) = g(t, e, \mathbf{K}(t)x_o)$$

and the nominal LTV error observer is given by

$$\begin{aligned} \dot{x}_o &= A(t)x_o + B(t)\mathbf{K}(t)x_o + L(t)(y_o - y) \\ &= F(t)x_o + L(t)y \\ y_o &= C(t)x_o \end{aligned}$$

where since the Linearized error dynamics are u.c.o. $L(t)$ can be chosen such that $A(t) + L(t)C(t)$ is u.e.s, and the observer as actually physically implemented is

$$\dot{x}_o = A(t)x_o + B(t)\mathbf{K}(t)x_o + L(t)(y_o - \eta_e)$$

which can be written as a perturbation from the nominal case

$$\dot{x}_o = F(t)x_o + L(t)y + \Delta g(t, e)$$

where the disturbance term from the ideal case is

$$\Delta g(t, e) = L(t)\{C(t)e - h(t, \xi) + h(t, \overline{\xi})\}$$

This is a vanishing disturbance as

$$\begin{aligned} \Delta g(t, 0) &= L(t)\{C(t)0 - h(t, \overline{\xi}) + h(t, \overline{\xi})\} \\ &= 0 \end{aligned}$$

Linearizing the augmented nominal nonlinear error dynamics about **0** gives

$$\begin{bmatrix} \dot{x} \\ \dot{x}_o \end{bmatrix} = \begin{bmatrix} A(t) & B(t)\mathrm{K}(t) \\ L(t)C(t) & A(t) + B(t)\mathrm{K}(t) + L(t)C(t) \end{bmatrix} \begin{bmatrix} x \\ x_o \end{bmatrix}$$

Which is the LTV observer-controller of Theorem 4.10. Thus the linearized system for the nominal system is u.e.s. and by Theorem 4.4 the nonlinear error dynamics are locally u.e.s. Applying Theorem 4.7 there is a domain D about the nominal trajectory and a Lyapunov function $V(t,e)$ on $[0,\infty) \times D$ that satisfies the inequalities 4.9a-c. Finally, by Theorem 4.10 the perturbed nonlinear error dynamics are exponentially stable, or equivalently the closed loop system tracks the desired trajectory, if the error begins in D and

$$\|\Delta g(t,e) < \frac{c_3}{c_4}\|e\|, \forall t \geq 0, \forall e \in D \qquad \square$$

Theorem 4.11 presents proof of the stability of a trajectory tracking controller following the method outlined in this dissertation based on output feedback. The complete controller is shown in figure 4.5. The inverse plant is used to achieve the nominal control $\hat{v}$ that achieves the nominal trajectory, and the LTV observer with error stabilizing controller stabilizes the nominal trajectory.

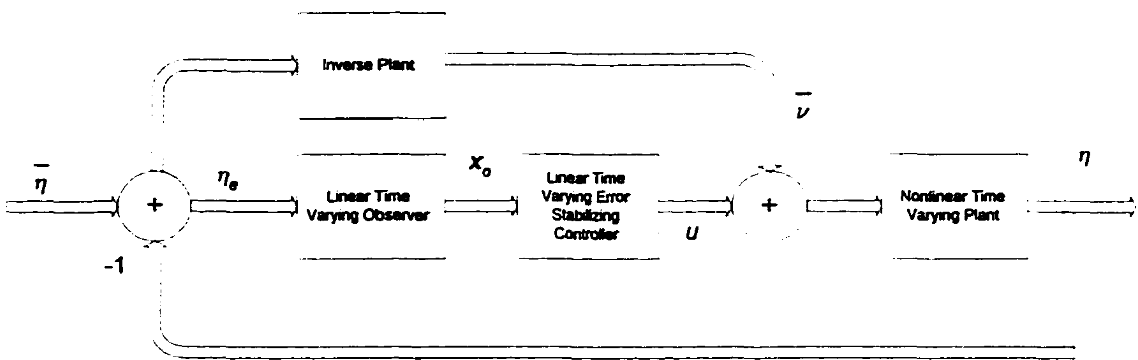

Figure 4.5 Observer Based Trajectory Tracking control

CHAPTER 5

NONLINEAR DESIGN EXAMPLES

In this chapter, we will look at some specific design examples that use the method of nonlinear trajectory tracking control by trajectory linearization. The first section includes two academic examples that will help clarify the specifics of actually designing a complete controller. This method will be compared with similar designs based on LTI methods. The second section is a design example for a two link robot arm manipulator. This design will be used to illustrate some of the robustness of the method. The design used here can be generalized to an n link robot arm in a straightforward manner, and thus the design method can be used as a general method for robot arm controller design. The third design example is an autopilot design for a pitch-axis missile. This design uses a Radial Basis Function (RBF) neural network to implement the nominal control. The nominal control is a static pseudo-inverse that can be trained in real time to handle changes in the nominal control. This design example illustrates the robustness of the trajectory tracking controller to vanishing perturbations. The fourth section details the design for a four degree of freedom (4DOF) roll-yaw Bank-To-Turn (BTT) missile autopilot. The fifth section extends the 4DOF design to the complete nonlinear 6DOF BTT missile autopilot. The PD-spectral method is compared with two other popular autopilot designs with comparable feedback gains. This comparison indicates that trajectory linearization has potential robustness benefits as compared to current design strategies.

5.1 - Academic Design Examples

In this section we will consider two particular design problems. First we will consider a highly nonminimum phase LTI plant. This problem illustrates the complete design procedure and uses time-variance to achieve performance that can not be realized by any LTI controller. The second problem is a challenging nonminimum phase nonlinear tracking control example used by Khalil [48] to demonstrate the evolution of gain scheduling techniques. The performance of the trajectory linearization controller will be compared to the most recent gain scheduled controller technique as of 1995.

The first problem is to design an output feedback controller for a stable, but highly nonminimum phase LTI plant. The control objective is to track step commands while simultaneously reducing the settling time and keeping undershoot from becoming too large. The system is described by the transfer function

$$H(s) = \frac{-s+1}{s^2+5s+6}$$

The zero at $s = 1$ means the plant has a nonminimum phase response. The natural undershoot is 68.45% with a 1% settling time of 3.386 seconds.

The first step to designing the controller is to find a stable and causal inverse for the plant. The true inverse of the plant is

$$H^{-1}(s) = \frac{s^2+5s+6}{-s+1}$$

This realization has a pole at $s = 1$, and is improper. Therefore it is clearly neither stable nor causal. In constructing a pseudo-inverse, we need to make the transfer function $H^{-1}(s)$ proper, and we can do this by adding another LHP pole. We also need to adjust the other pole so as to make it stable. One pseudo-inverse can be constructed by moving the unstable pole to the symmetric location in the LHP. One such pseudo-inverse is given by

$$H_1^{\dagger}(s) = \frac{10(s^2+5s+6)}{(s+1)(s+10)}$$

We can analyze the performance of this pseudo-inverse by considering the cascade system in terms of the corresponding pseudo-identity.

$$H^{\dagger}H(s) = \frac{10(-s+1)}{(s+1)(s+10)} \tag{5.1}$$

The pseudo-Identity is a functional mapping that approximates the Identity function. In the frequency domain, the ideal identity should have a Gain of 0db and a phase lag of 0°. The frequency response of the pseudo-indentity is shown in figure 5.1

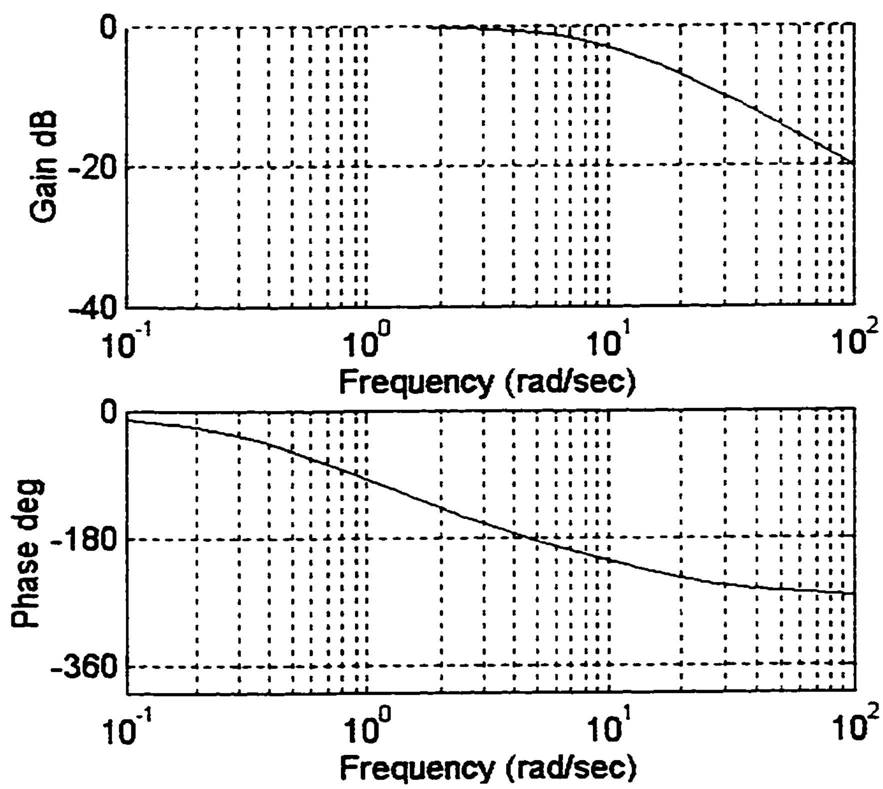

Figure 5.1 Frequency Response of Pseudo-Identity (5.1)

The pseudo-identity (5.1) has decent gain and phase. However, the slow mode $s+1$ slows the time performance of the system. Thus a modification is made that takes

advantage of the nature of the signals to be tracked. We choose the pseudo-inverse

$$H^{\dagger}(s) = \frac{20(s^2 + 5s + 6)}{s^2 + 12s + 20}$$

with pseudo-identity

$$H^{\dagger}H(s) = \frac{20(-s + 1)}{s^2 + 12s + 20} \tag{5.2}$$

The frequency response of this pseudo-identity is given in figure 5.2.

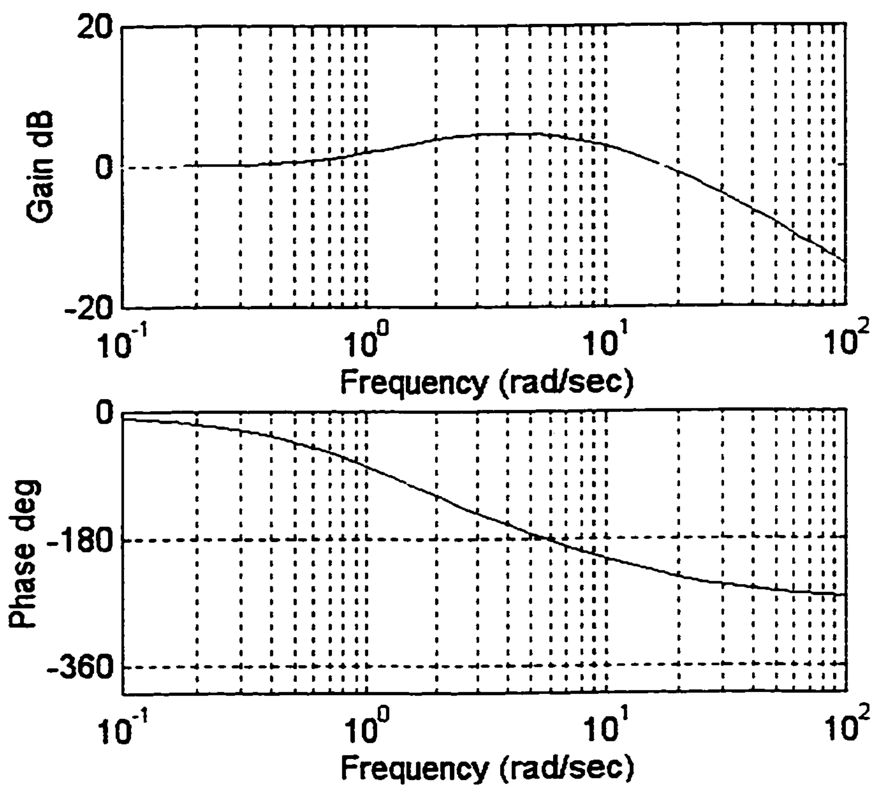

Figure 5.2 Frequency Response of Pseudo-Identity (5.2)

Figure 5.2 indicates a slight magnitude gain centered at 3 rad/s. A tradeoff has been made to achieve better time performance for steps and allowing gain distortion at the relatively higher frequency. In applications where the frequency characteristic of the

signals to be tracked change with time, a time varying pseudo-inverse can be used to achieve better performance.

With the latter pseudo-inverse (5.2) to compute the nominal control, we can now proceed to the design of the output feedback error regulator. The first step to the feedback design is to find a state error observer. The error dynamics of a LTI system are defined by the original LTI dynamics. Thus we need a state space realization of the transfer function. We can choose the Controller canonical form because this is equivalent to the phase variable canonical form for LTI systems and will facilitate the development of LTV state feedback. The state space realization for the error dynamics is given by

$$\dot{\boldsymbol{x}} = \begin{bmatrix} 0 & 1 \\ -6 & -5 \end{bmatrix} \boldsymbol{x} + \begin{bmatrix} 0 \\ 1 \end{bmatrix} u$$

$$y = \begin{bmatrix} 1 & -1 \end{bmatrix} \boldsymbol{x}$$

Using the separation principle we can design the state error feedback based on the availability of the original states. The PD-spectrum to be assigned is chosen as a pair of complex conjugate PD-eigenvalues $\rho_{1,2} = (-3 \pm j)s(t)$. These poles represent fixed damping with a time varying magnitude or natural frequency and satisfy the PD-spectral stability criteria for $s(t) > 0$ and of any polynomial order. By choosing the scaling term $s(t)$ appropriately the exponential decay rate of the error dynamics can be slowed or increased as needed. The phase variable system matrix associated with this pd-spectrum is

$$A(t) = \begin{bmatrix} 0 & 1 \\ -10s^2(t) & -6s(t) + \frac{\dot{s}(t)}{s(t)} \end{bmatrix}$$

The state feedback that achieves the desired PD-spectrum is easily shown to be

$$\begin{aligned} u(t) &= (6 - 10s^2(t))x_1 + (5 - 6s(t) + \frac{\dot{s}(t)}{s(t)})x_2 \\ &= \mathbf{K}(t)\boldsymbol{x} \end{aligned}$$

With this feedback we can now replace the actual states with observer states x_o. We will use a traditional full order Luenberger observer. The observer is realized with

$$\dot{x}_o = Ax + bu + Lc(y_o - y)$$

$$y_o = cx$$

with the observer poles chosen as $-12, -13$ so that

$$L = \begin{bmatrix} -14.166 \\ -5.833 \end{bmatrix}$$

The controller outlined above was designed, simulated and compared to similar LTI controllers. The time varying scaling factor as simulated was realized from the system shown in figure 5.3

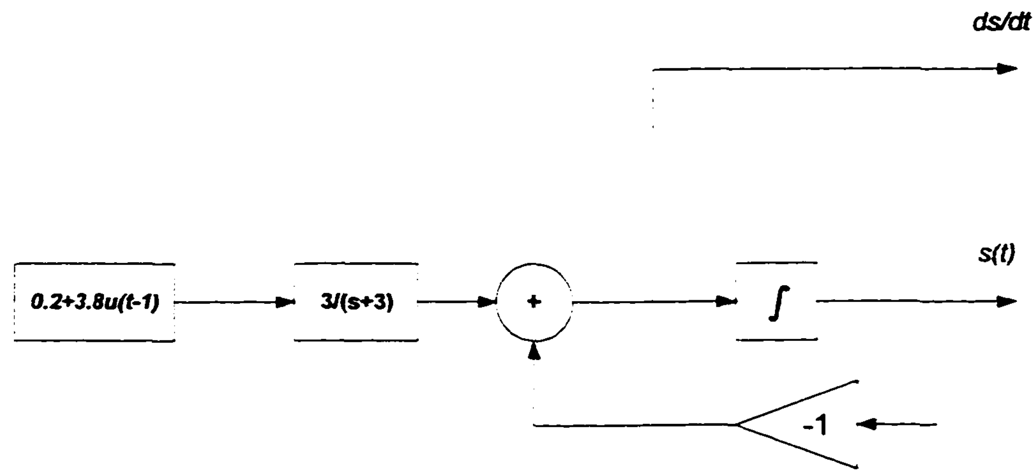

Figure 5.3 Physical Realization of $s(t)$

This physical realization of $s(t)$ does three important things. First, it generates $\dot{s}(t)$ which is necessary to realize the desired PD-spectrum. Second, the first transfer function helps to smoothen $s(t)$ which in turn smoothens the output response of the nonminimum phase system. Finally, $s(t)$ begins at a low value to minimize undershoot, and then slowly becomes larger to decrease the settling time.

Figures 5.4-5.7 compare the results of the trajectory linearization controller with time varying PD-spectrum to 3 different LTI schemes. Figure 5.4 shows the open loop behavior of the system to a step command with a constant gain of 6. The settling time is 2.96 seconds, with an undershoot of 116.7%. In order to achieve a settling time of about 1.25 seconds, an LTI controller with poles at $-12 \pm 4j$ is designed and has an output response as shown in Figure 5.5. The LTI controller achieves a settling time of 1.26 seconds at the cost of an undershoot which exceeds 416%. Figure 5.6 shows the closed loop response with the time varying feedback with the poles controlled by the scaling factor $s(t)$ as designed above. The settling time for this LTV design is 1.28 seconds with an undershoot of 98.4%. Figure 5.7 shows the closed loop behavior for a switched LTI controller. The poles are switched from the lowest value of the time varying PD-eigenvalues to the highest at time $t = 1.6$. The undershoot is 267% with a settling time of 1.16 seconds. Additionally, this output has an undesirable abrupt downturn that occurs because of the coefficient switching. The LTV design easily achieves behavior beyond the capability of similar LTI designs.

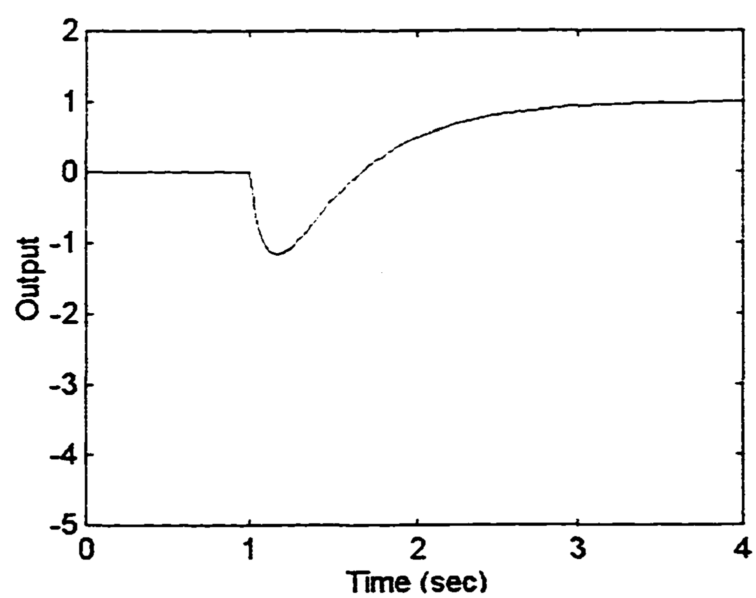

Figure 5.4 Open Loop Step Response

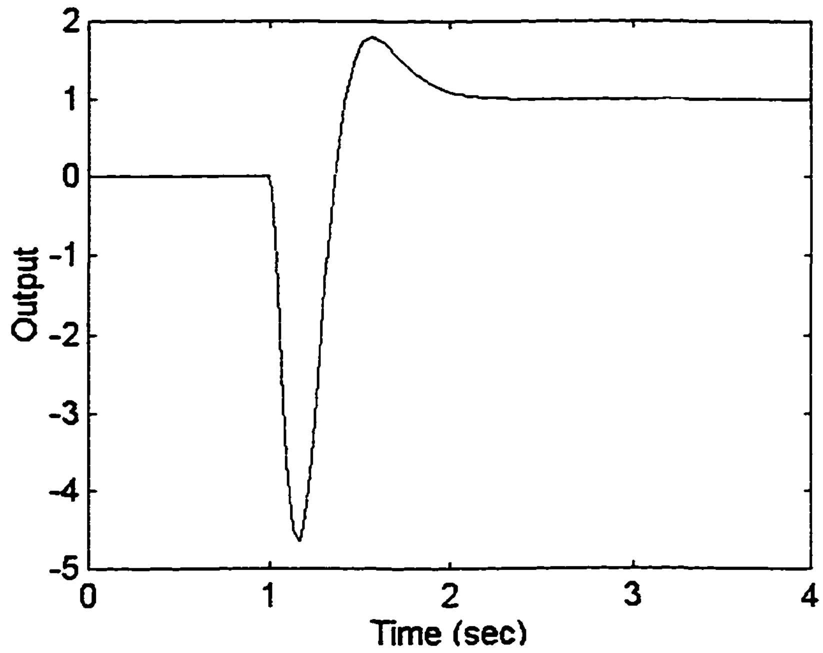

Figure 5.5 Fixed LTI Feedback Design

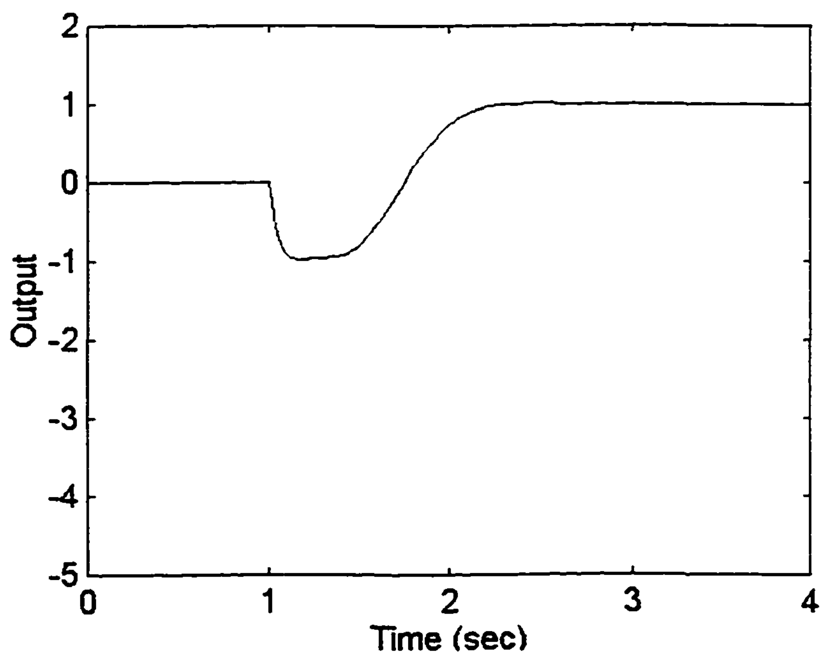

Figure 5.6 Time Varying Trajectory Linearizaiton Design

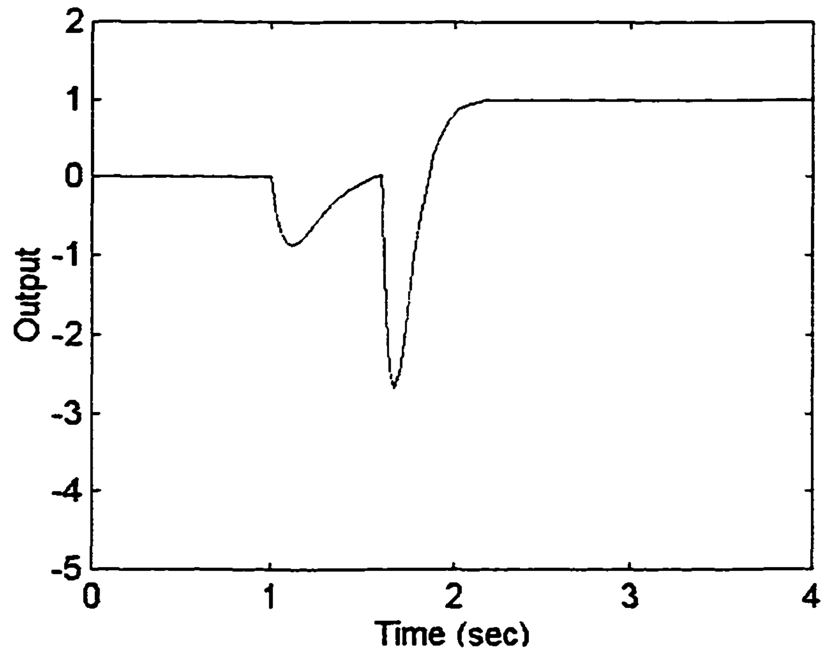

Figure 5.7 Switched LTI Feedback

Now, we will design a trajectory tracking controller for an academic nonlinear problem considered by Khalil as design example 11.6 on pg. 506-509 of [48]. He first used this problem as a test case to compare the results achieved by traditional gain scheduling with results achieved by more sophisticated modern gain scheduling designs. His comparison used an observer based feedback design. We will compare our results with his, with all designs attempting to assign equivalent desired fixed poles.

The nonlinear plant is described by the state space equation

$$\begin{aligned} \dot{\xi}_1 &= \tan(\xi_1) + \xi_2, \qquad |\xi_1| < \frac{\pi}{2} \\ \dot{\xi}_2 &= \xi_1 + v \\ \eta &= \xi_2 \end{aligned}$$

Where ξ, v, and η are respectively the states, input and output. By taking the first derivative with respect to time of the output

$$\dot{\eta} = \dot{\xi}_2 = \xi_1 + v$$

it is seen that the relative order is 1, $r = 1$, $\forall \xi_1, \xi_2$. A global diffeomorphism $\Phi(\boldsymbol{\xi})$ exists that can place the system in the normal form. This diffeomorphism is given by

$$\begin{bmatrix} \Psi_1 \\ \Psi_2 \end{bmatrix} = \Phi(\boldsymbol{\xi}) = \begin{bmatrix} 0 & 1 \\ 1 & 0 \end{bmatrix} \begin{bmatrix} \xi_1 \\ \xi_2 \end{bmatrix} = \begin{bmatrix} \xi_2 \\ \xi_1 \end{bmatrix}.$$

The normal form is

$$\begin{aligned} \dot{\Psi}_1 &= \Psi_2 + v \\ \dot{\Psi}_2 &= \tan(\Psi_2) + \Psi_1 = w(\Psi_1, \Psi_2) \\ \eta &= \zeta_1 \end{aligned}$$

The internal dynamics of the system are then given by

$$\dot{\xi}_1 = \tan(\xi_1) + \xi_2$$

and the zero-dynamics are

$$\dot{\xi}_1 = \tan(\xi_1)$$

Linearization at $\xi_1 = 0$ yields

$$\dot{\xi}_1 = \xi_1$$

Thus the zero-dynamics are unstable, and consequently the system is non-minimum phase. This means inversion based methods such as standard feedback linearization are not directly applicable. Nonetheless, the nominal inverse can be derived by considering the output equation

$$\dot{\eta} = \dot{\xi}_2 = \xi_1 + v$$

The nominal inverse from $\dot{\overline{\eta}} \to \overline{v}$ is

$$\overline{v} = -\xi_1 + \dot{\overline{\eta}}$$

At this point some explanation is necessary. The nominal control used here is a hybrid feedback feedforward inverse. In general, where the inverse is a function of the states,

simulation indicates that better robustness to nonlinear perturbations is achieved by using as much feedforward information as possible. In this instance the terms are rather straightforward and marginally superior performance can be achieved using a feedback of ξ_1. Similar results were achieved using a purely feedforward design. The rth derivative of the output are always supplied in feedforward.

The limitation of controllers such as feedback linearization is that nothing is done to handle the unstable internal dynamics of the closed loop plant. Trajectory linearization control can handle such plants by providing a time varying state feedback that stabilizes the system about the nominal trajectory. So, the next step is to find a nominal state $\bar{\xi}_1$ that corresponds to a stable state trajectory. The closed loop system is to be relatively slow, and is intended to track steps and slow ramps. These design requirements allow for a practical approximation to the nominal states. The nominal states are given by

$$\bar{\xi}_2 = \bar{\eta}$$

$$\bar{\xi}_1 = -\arctan(\bar{\eta})$$

where the last nominal state is derived from the assumption that the nominal states are approximately static, so

$$\tan(\xi_1) + \xi_2 \simeq 0$$

The final stage of creating an inversion involves implementing the derivative of the output. Traditional methods of inverting a plant assume the existence of r derivatives of the output. Since such derivatives do not exist in general, they must be approximated. The following equations describe the low pass filter which approximates the desired output and makes the derivative available.

$$\dot{\widehat{\eta}} + k\widehat{\eta} = k\bar{\eta}$$

The derivative of this filtered output is directly available from filter implementation. The pseudo-inversion from the desired output to the nominal input is then given by

$$\overline{\eta} \to \widehat{v} : \widehat{v} = -\xi_1 + k(\overline{\eta} - \widehat{\eta}) \tag{5.1}$$

The low pass filter $\frac{k}{s+k}$ is a convenient method for generating an output whose derivative is available. However, it can simultaneously perform another important function. The LTV PD-spectral assignment requires smooth command trajectories to assure the smoothness of the linearized error matrices. While these smoothness assumptions can be relaxed to include a finite number of jump discontinuities such as a step command would produce, it is beneficial to filter commanded trajectories to assure that they are smooth. Thus the LTV state feedback is more likely to accurately model the true error dynamics. Thus choosing k appropriately will lead to better system performance.

The next step in the design is developing a LTV state feedback that stabilizes the nominal trajectory $\overline{\eta}(t)$. The linearized error dynamics are given by

$$A(t) = \frac{\partial f}{\partial \xi}\bigg|_{\overline{\xi},\overline{v}}$$

$$B(t) = \frac{\partial f}{\partial v}\bigg|_{\overline{\xi},\overline{v}}$$

$$C(t) = \frac{\partial h}{\partial \xi}\bigg|_{\overline{\xi},\overline{v}}$$

$$D(t) = \frac{\partial h}{\partial v}\bigg|_{\overline{\xi},\overline{v}}$$

where

$$A(t) = \begin{bmatrix} \sec^2[\overline{\xi}_1(t)] & 1 \\ 1 & 0 \end{bmatrix} \quad B(t) = \begin{bmatrix} 0 \\ 1 \end{bmatrix}$$
$$C(t) = [0 \quad 1] \qquad D(t) = [0]$$

The controllability matrix $Q_c(t)$ is

$$
\begin{aligned}
Q_c(t) &= \left[B(t) \,|\, \dot{B}(t) - A(t)B(t)\right] \\
&= \begin{bmatrix} 0 & -1 \\ 1 & 0 \end{bmatrix}
\end{aligned}
$$

This matrix is of rank 2 for all t, so the linearized error dynamics are u.c.c.

This is a Scalar LTV system that satisfies the assumptions, so there is a Silverman transformation that effects a change of coordinates to the phase variable canonical form. The transformation is and its inverse are

$$
\mathbf{T}(t) = \begin{bmatrix} 1 & 0 \\ \sec^2(\overline{\xi}_1(t)) & 1 \end{bmatrix}
$$

$$
\begin{aligned}
L(t) &= \mathbf{T}^{-1}(t) \\
&= \begin{bmatrix} 1 & 0 \\ -\sec^2(\overline{\xi}_1(t)) & 1 \end{bmatrix}
\end{aligned}
$$

The linearized tracking error dynamics in the new state space are

$$
\begin{aligned}
A_p(t) &= \mathbf{T}(t)\left[A(t)\mathbf{T}^{-1}(t) + \dot{\mathbf{T}}(t)\right] \\
&= \begin{bmatrix} 0 & 1 \\ 1 + 2\sec^2(\overline{\xi}_1(t))[\tan^2(\overline{\xi}_1(t)) + \tan(\overline{\xi}_1(t))\overline{\xi}_2(t)] & \sec^2(\overline{\xi}_1(t)) \end{bmatrix}
\end{aligned}
$$

$$
\begin{aligned}
B_p(t) &= \mathbf{T}(t)B(t) \\
&= \begin{bmatrix} 0 \\ 1 \end{bmatrix}
\end{aligned}
$$

$$
\begin{aligned}
C_p(t) &= C(t)\mathbf{T}^{-1}(t) \\
&= \begin{bmatrix} -\sec^2(\overline{\xi}_1(t)) & 1 \end{bmatrix}
\end{aligned}
$$

The next step is to assign the desired PD-spectrum. The SPDO associated with $A_p(t)$ is given by

$$
\begin{aligned}
\mathcal{D}_\alpha &= \delta^2 - \sec^2(\overline{\xi}_1(t))\delta - 1 - 2\sec^2(\overline{\xi}_1(t))[\tan^2(\overline{\xi}_1(t)) + \tan(\overline{\xi}_1(t))\overline{\xi}_2(t)] \\
&= \delta^2 + \alpha_2(t)\delta + \alpha_1(t)
\end{aligned}
$$

The desired closed loop tracking error dynamics are described by the SPDO

$$\mathcal{D}_{\beta} = \delta^2 + \beta_2(t)\delta + \beta_1(t)$$

where $\beta_1(t)$ and $\beta_2(t)$ are synthesized from the desired PD-spectrum by

$$\begin{aligned}\beta_1(t) &= \rho_1(t)\rho_2(t) + \frac{\rho_1(t)\dot{\rho}_2(t) - \dot{\rho}_1(t)\rho_2(t)}{\rho_2(t) - \rho_1(t)} \\ \beta_2(t) &= -\rho_1(t) - \rho_2(t) + \frac{\dot{\rho}_2(t) - \dot{\rho}_1(t)}{\rho_2(t) - \rho_1(t)}\end{aligned}$$

Then the state feedback tracking error dynamics stabilizing control law in the phase-variable coordinates is given by

$$u = \mathbf{K}_{\mathrm{p}}(t)\boldsymbol{z} = [\,\alpha_1(t) - \beta_1(t) \quad \alpha_2(t) - \beta_2(t)\,]\boldsymbol{z}$$

and the control law in the given coordinates is

$$\begin{aligned} u = \mathbf{K}(t)\boldsymbol{x} &= [\,\alpha_1(t) - \beta_1(t) \quad \alpha_2(t) - \beta_2(t)\,]\mathbf{T}(t)\boldsymbol{x} \\ &= [\,\alpha_1(t) - \beta_1(t) + \sec^2(\overline{\xi}_1(t))[\alpha_2(t) - \beta_2(t)] \quad \alpha_2(t) - \beta_2(t)\,]\boldsymbol{x}\end{aligned} \tag{5.2}$$

Like most inherently nonlinear design methods, PD-spectral assignment control relies on state feedback. However, this problem assumes only output information, and thus some sort is observer is required. Nonlinear observer design is not a very mature area. To overcome this limitation, we introduced a unique nonlinear observer. We define the nonlinear observer

$$\dot{\xi}_{o1} = \tan(\xi_{o1}) + \xi_{o2} + h_1(\eta_o, \dot{\eta}_o, \eta, \dot{\eta}, u)$$

$$\dot{\xi}_{o2} = \xi_{o1} + u + h_2(\eta_o, \dot{\eta}_o, \eta, \dot{\eta}, u)$$

now define the observer errors as

$$\epsilon_1 := \xi_{o1} - \xi_1$$

$$\epsilon_2 := \xi_{o2} - \xi_2$$

The observer error dynamics are

$$\dot{\epsilon}_1 = \tan(\xi_{o1}) + \xi_{o2} - \tan(\xi_1) - \xi_2 + h_1(\eta_o, \dot{\eta}_o, \eta, \dot{\eta}, u)$$

$$\dot{\epsilon}_2 = \xi_{o1} - \xi_2 + h_2(\eta_o, \dot{\eta}_o, \eta, \dot{\eta}, u)$$

Now the observer error feedback is limited to measurements of its own states and the outputs of the nonlinear plant. The internal state of the nonlinear plant can be found with an approximation of the derivative of the output by

$$\xi_1 = \dot{\eta} - u$$

So if we choose the observer error feedback as

$$h_1 = -\tan(\xi_{o1}) + \tan(\dot{\eta} - u) - 31(\xi_{o2} - \xi_2)$$

$$h_2 = -11(\xi_{o2} - \xi_2)$$

The observer error dynamics are

$$\dot{\epsilon} = \begin{bmatrix} 0 & -30 \\ 1 & -11 \end{bmatrix} \epsilon$$

which are exponentially stable.

The overall control law can now be pieced together as

$$v = \hat{v} + \mathbf{K}(t)(\boldsymbol{\xi}_o - \overline{\boldsymbol{\xi}})$$

where $\hat{v}$ is given by (5.1), $\mathbf{K}(t)$ is given by (5.2), $\boldsymbol{\xi}_o$ are the observer states, and $\overline{\boldsymbol{\xi}}$ are the nominal states.

In Khalil's example 11.6 on pp. 506-509 three separate controllers are designed to handle this particular nonlinear system. These three designs include a LTI design, a

classical gain scheduled design and a sophisticated modern gain scheduled design. These linear designs use an observer to measure the states and an integrator to generate the nominal control for nonzero commands. All three designs attempt to place the desired closed loop poles at $-1, -\frac{1}{2} \pm j\frac{\sqrt{3}}{2}$. To make the comparison fair the PD-eigenvalues of the PD-spectral controller are assigned constant values $\rho_{1,2} = -\frac{1}{2} \pm j\frac{\sqrt{3}}{2}$. The other three LTI controllers rely on an integrator to achieve a step trajectory and thus the closed loop plant has an extra pole at -1.

When the commanded output is a constant α. The linearized plant is given by

$$A(\alpha) = \begin{bmatrix} 1+\alpha^2 & 1 \\ 1 & 0 \end{bmatrix}, \; B(\alpha) = \begin{bmatrix} 0 \\ 1 \end{bmatrix}, \; C(\alpha) = [0 \quad 1]$$

The integrator is defined as a third state. The fixed LTI controller based on linearization at the origin yields the state feedback matrix and observer input matrix respectively as

$$K = [\,-7 \quad -3 \quad 1\,], \; H = \begin{bmatrix} -14 \\ -4 \end{bmatrix}$$

The traditional gain scheduled state feedback and observer input matrix respectively are

$$K(\alpha) = [\,-(1+\alpha^2)(3+\alpha^2) - 3 - \tfrac{1}{1+\alpha^2} \quad -3-\alpha^2 \quad \tfrac{1}{1+\alpha^2}\,]$$

$$H(\alpha) = \begin{bmatrix} -10 - (4+\alpha^2)(1+\alpha^2) \\ -(4+\alpha^2) \end{bmatrix}$$

The sophisticated gain scheduling controller relies on moving the integrator from the input to the controller to the output of the controller to improve performance. Dividing $K(\alpha)$ into two matrices, with $K_1(\alpha)$ the feedback gain of the observed error and $K_2(\alpha)$ the integral error feedback this controller is realized by

$$\dot{\phi} = [A(\alpha) + B(\alpha)K_1(\alpha) + H(\alpha)C(\alpha)]\phi + B(\alpha)K_2(\alpha)e - H(\alpha)\theta$$

$$\dot{\gamma} = K_1(\alpha)\phi + K_2(\alpha)e$$

$$v = \gamma$$

$$\epsilon\dot{\zeta} = -\zeta + \eta$$

$$\theta = \frac{1}{\epsilon}(-\zeta + \eta)$$

with ϵ chosen sufficiently small to give a good approximation of $\dot{\eta}$.

A comparison of the performance of these four designs are shown in the following figures. Figure 5.8 shows that the fixed LTI controller has unacceptable behavior. Even at the commanded step to 0.4 the transient exhibits a fast undesirable oscillation. When the step command is 0.6 the plant output diverges. This behavior is not particularly surprising, owing to the poor modeling achieved when the states depart far from the origin. Figure 5.9 shows the stair step tracking performance of the traditional gain scheduled design. This design does not loose stability for the commanded trajectory, but clearly illustrates the need for improved performance. It also highlights the potential performance problems that can exist when relying on gain scheduling. Figure 5.10 shows the stairstep tracking performance of the modern gain scheduled design. The performance deteriorates only slightly as the output diverges far from the origin, but is substantially superior to traditional gain scheduling.

The next figures 5.11-5.14 compare trajectory linearization and the modern gain scheduled design. The performance when tracking small steps and slowly moving trajectories as illustrated in figures 5.11 and 5.12 are very comparable. It is to be noted that the PD-spectral design exhibits consistent performance for each step command. In contrast, the gain scheduled design exhibits slightly deteriorating performance as the command magnitude increases.

Figures 5.13 and 5.14 show significant performance improvements for the trajectory linearization method in tracking trajectories that move quickly relative to the speed of the plant. Commonly, the advice concerning commanded trajectories for gain scheduled control is to use slow ramps, or stair step commands to achieve relatively large

trajectories. The intention behind using such commands is to insure that the frozen-time frozen-state assumptions on GS are satisfied so that stability is maintained and better performance can be achieved. Theoretical justifications have been given for GS designs in which the time variance is sufficiently "slow". Thus, if the trajectory is sufficiently slow, then the linearization about the nominal trajectory will satisfy the conditions which guarantee the stability of the closed loop design. The trajectory linearization and PD-spectral assignment method does not require this limitation on the speed of the trajectories to be tracked, and the performance achieved for rapidly varying trajectories tends to illustrate this.

The performance comparison of these four systems is meaningful because the desired closed loop poles are identical. The simulations seem to indicate that trajectory linearization does provide potential performance improvements over the state of the art as of 1995 gain scheduling design.

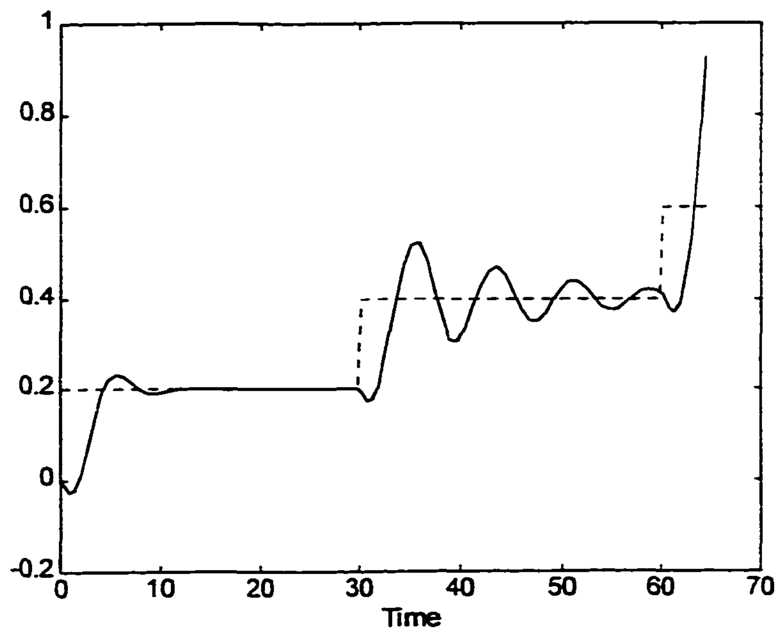

Figure 5.8 LTI Stair Step Tracking

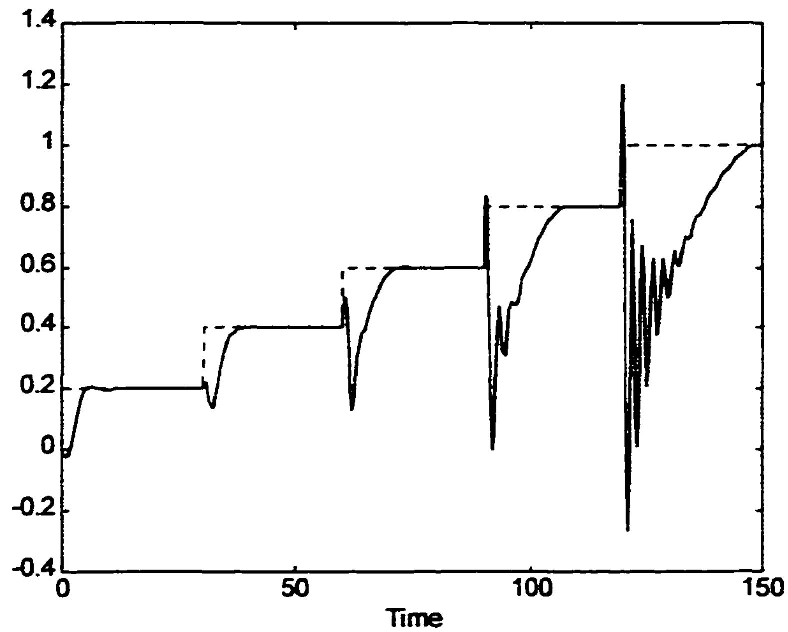

Figure 5.9 Traditional Gain Scheduled Design

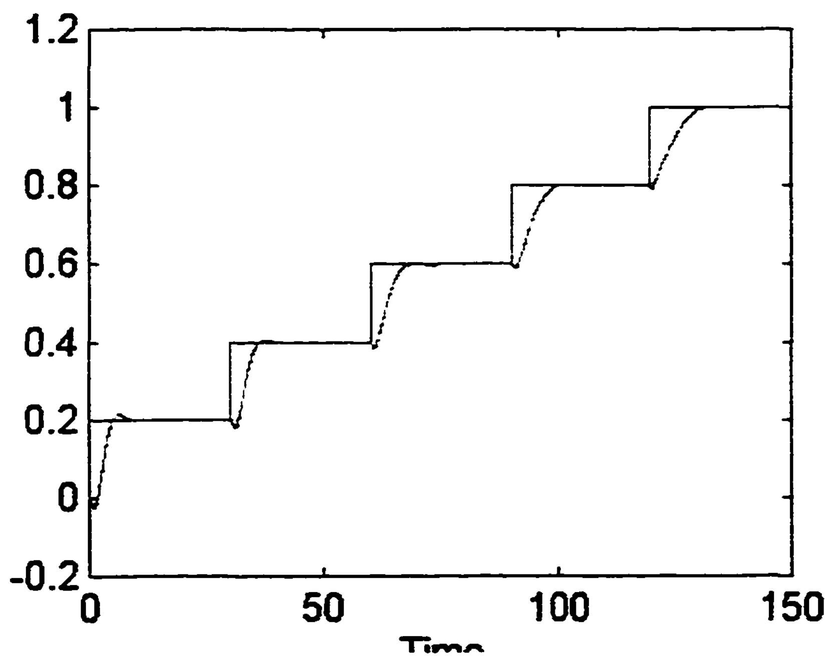

Figure 5.10 Modern Gain Scheduled Design

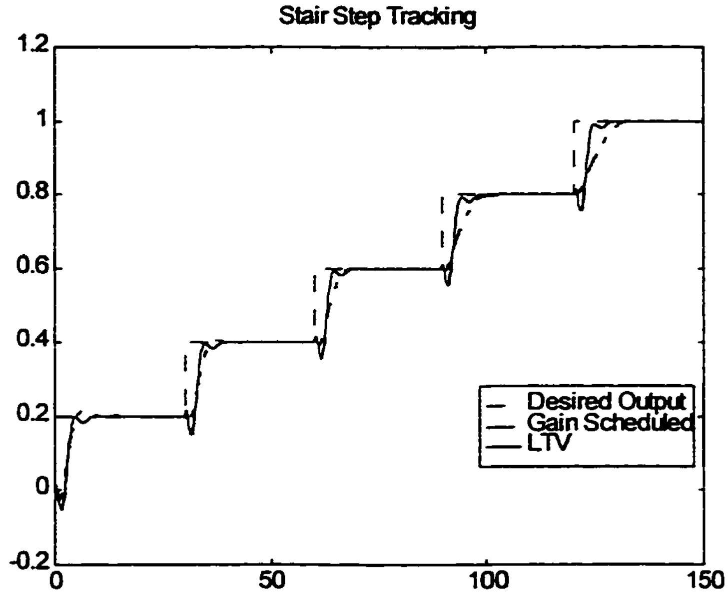

(a) Output trajectories

Figure 5.11 Stair step tracking

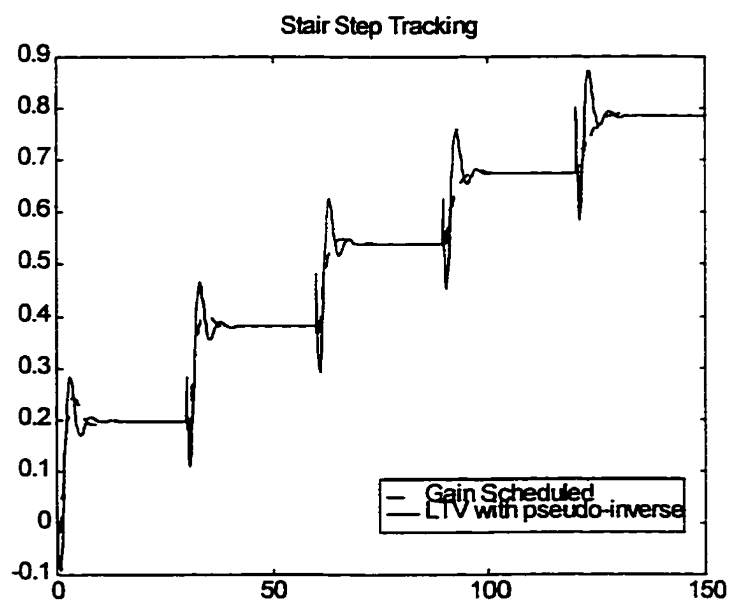

(b) Control functions

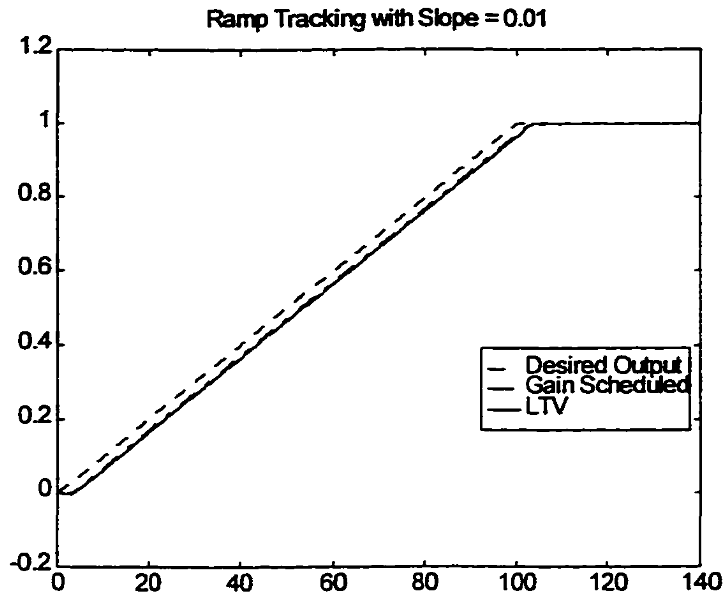

(a) Output trajectories

Figure 5.12 Slow ramp tracking (slope = 0.01)

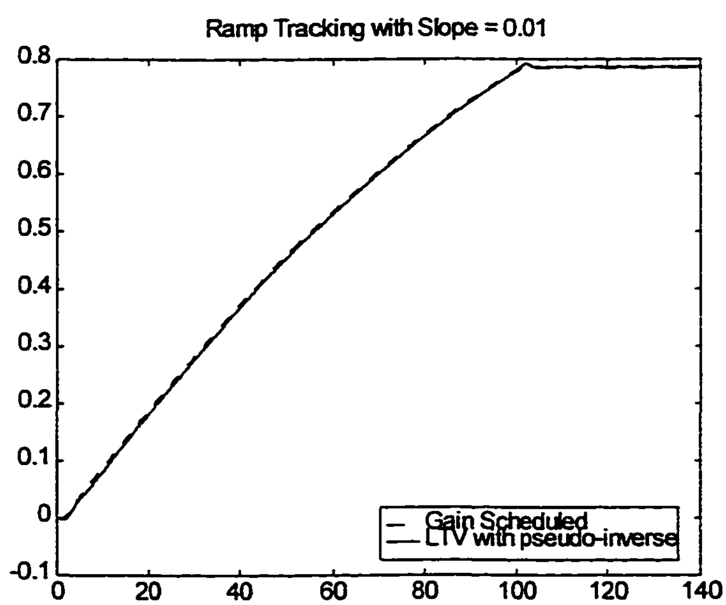

(b) Control functions

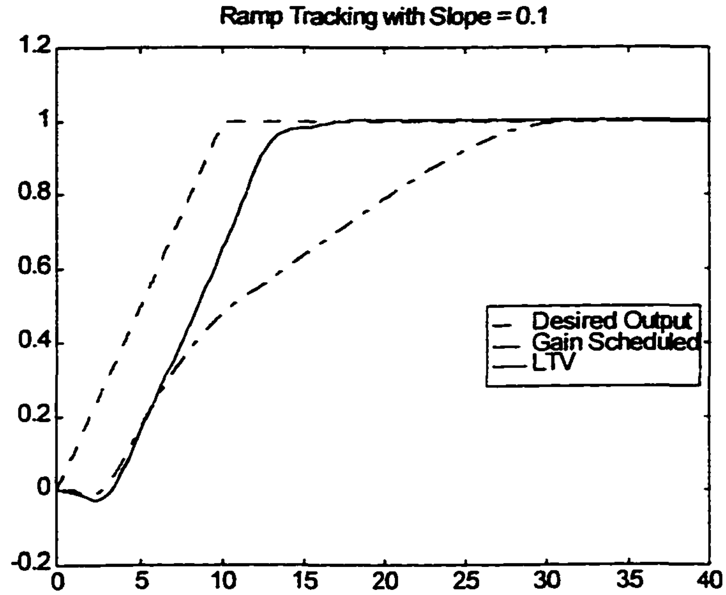

(a) Output trajectories

Figure 5.13 Fast ramp tracking (slope = 0.1)

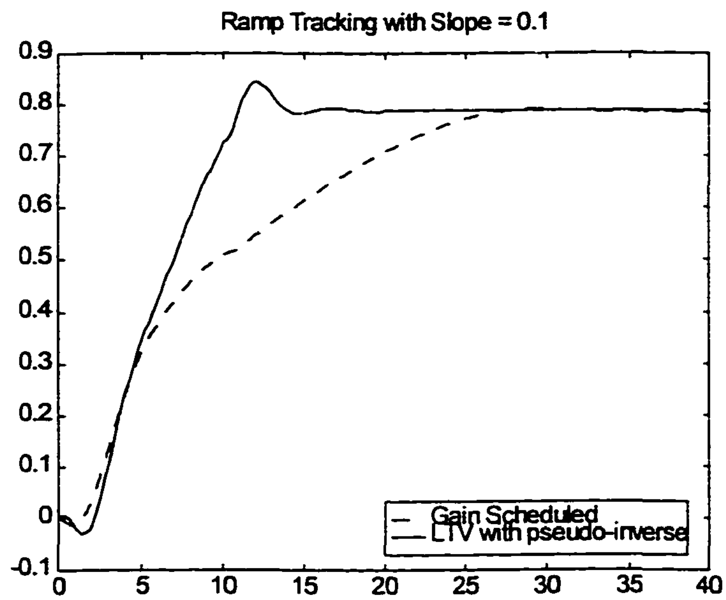

(b) Control functions

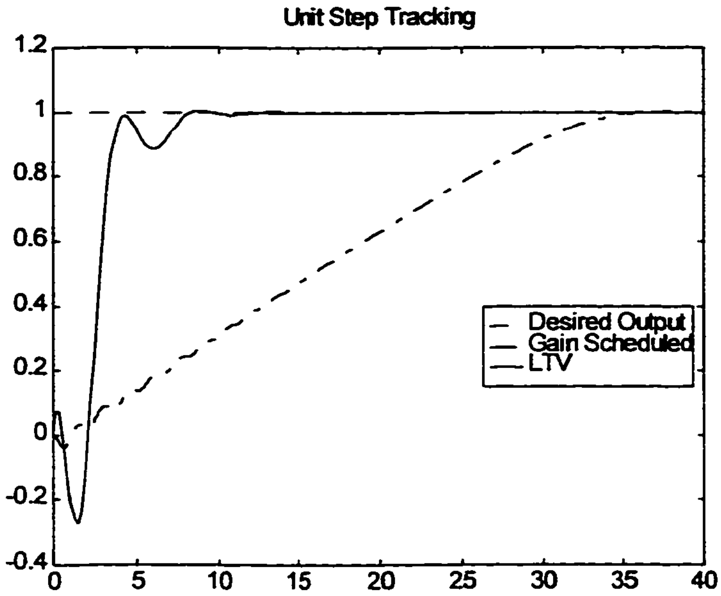

(a) Output trajectories

Figure 5.14 Unit step tracking

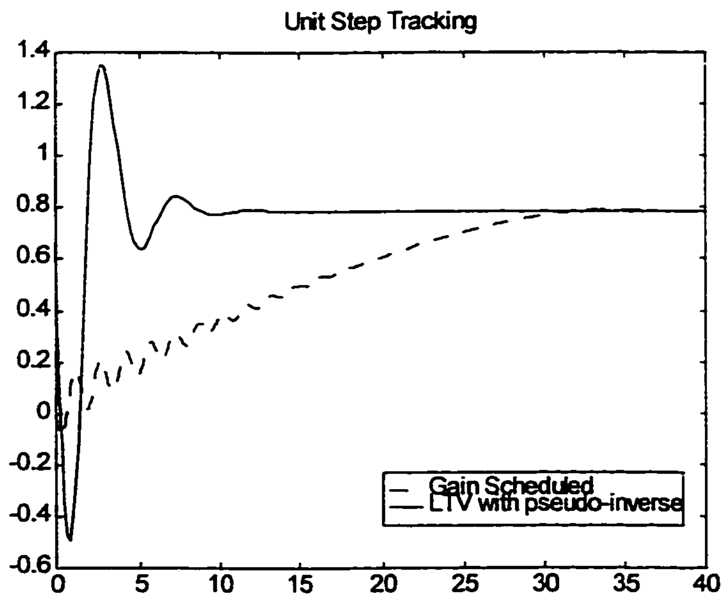

(b) Control functions

Now, we will make explicit use of time varying properties to improve the time performance of the output in the unit step simulation. The undershoot in figure 5.13 (a) is found to be 28% which is excessive. We will now modify the control structure to reduce the undershoot while maintaining the settling time. Conceptually, a nonminimum phase plant adds a term proportional to the derivative of the output but opposite in sign. Thus if the time response is fast, the undershoot will be larger but the settling time will be smaller. Thus to reduce undershoot, the magnitude of the real part of the PD-eigenvalues of the error regulator and the nominal control will be made initially small and then increased to decrease settling time.

The error regulator PD-eigenvalues are placed at

$$\rho_{1,2} = (-\frac{1}{2} \pm j\frac{\sqrt{3}}{2})s(t)$$

for the closed loop system which is stable for $s(t) > 0$, if $s(t)$ is of polynomial order. The time varying term $s(t)$ is a scaling factor which moves the PD-eigenvalues along a line of constant damping ratio deeper into the left half plane thereby increasing the decay rate. This scaling factor will be used to make the plant slightly sluggish at first which will reduce the undershoot, and then increase the scaling factor to decrease the settling time.

The nominal control is generated by a single pole Time Varying Bandwidth Filter which is designed and coordinated with the error regulator to effect the undershoot reduction. The filter is constructed as in figure 5.15. This filter is similar to the LTI filter contracted before, but has a time varying feedback which corresponds to a PD-eigenvalue in a single pole system. The time varying feedforward gain maintains the DC-gain of the filter. The PD-eigenvalue is chosen as

$$\rho(t) = 1s_1(t),$$

which is stable for any $s_1(t) > 0$.

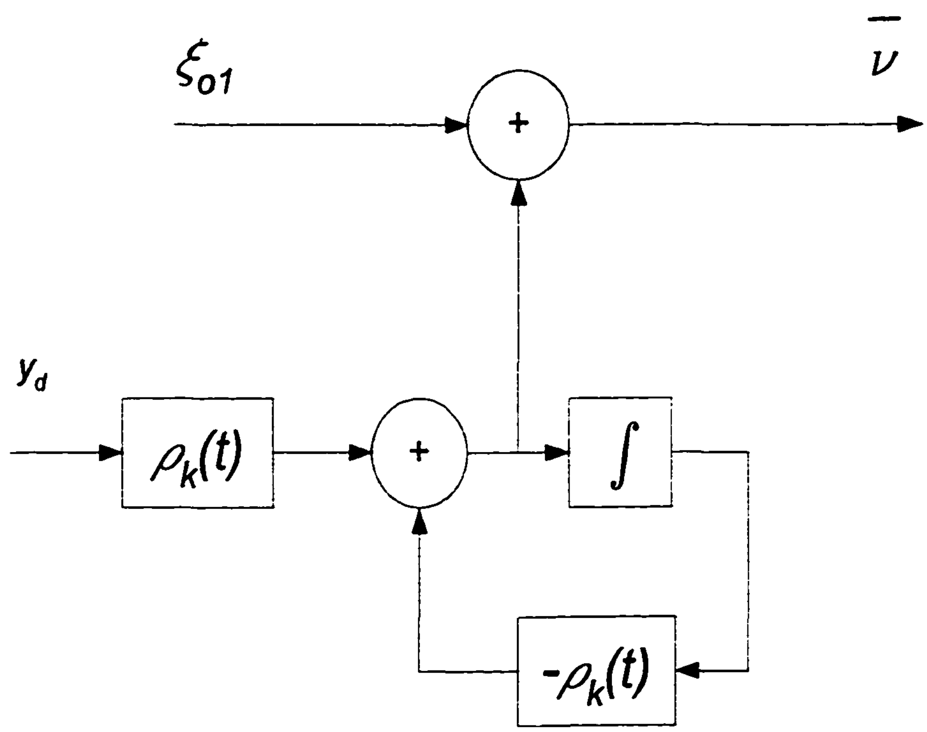

Figure 5.15 Time Varying Bandwidth Filter

Figures 5.16 (a)-(d) show the performance of the system using these time varying PD-eigenvalues. Figure 5.16 (a) shows the output as a function of time using a control law that realizes the time varying PD-spectrum for the error regulator, and the nominal control. The undershoot has been reduced from 28% in figure 5.13 (a) to about 7.15%, while the 1% settling time has been reduced from 8 seconds in figure 5.13 (a) to 5.54 seconds. Increasing the depth of the pole locations in a gain scheduled LTI controller would increase the undershoot by necessity as the output is effected by a term proportional to the derivative of the output, and as the time response becomes faster the undershoot would be increased. The LTV controller allows the system to behave slowly initially and thereby reducing the undershoot. Then the closed loop system is sped up and the nonminimum phase behavior of the system is buried in the rapid rise of the output near the end of the transition.

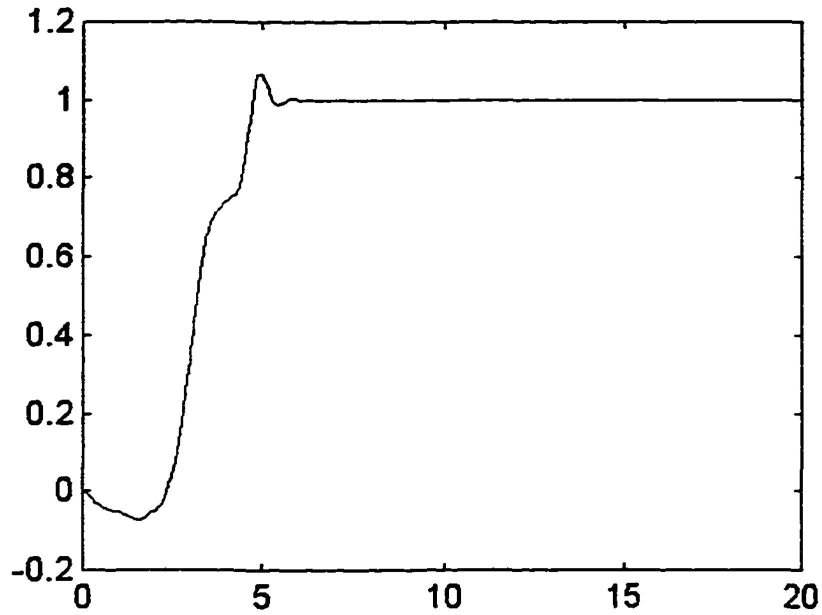

(a) Output

Figure 5.16 Unit Step Tracking Using Time Variance

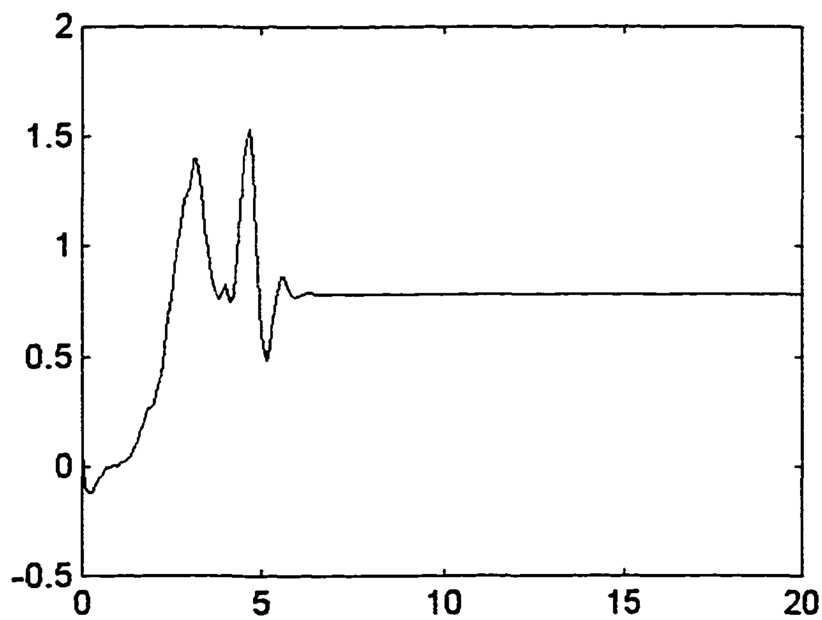

(b) Control Function

(figure continued)

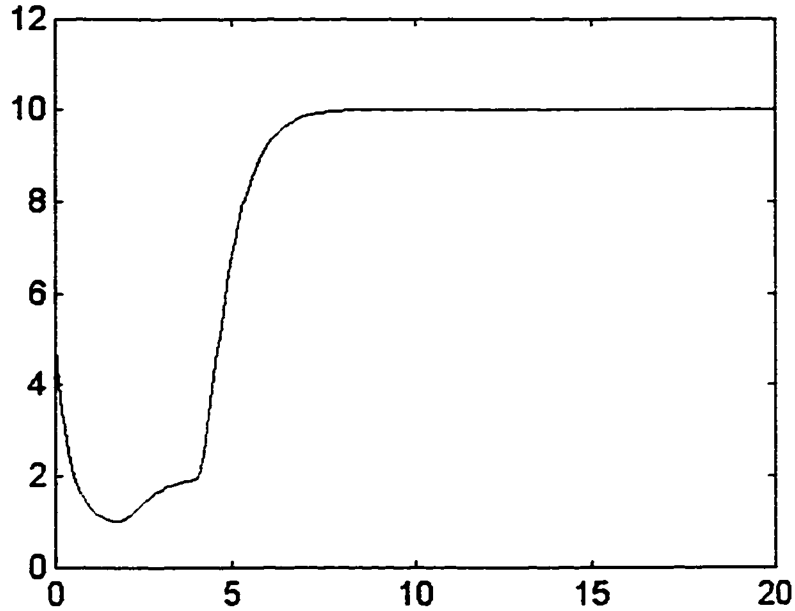

(c) Feedback Scaling Function $s(t)$

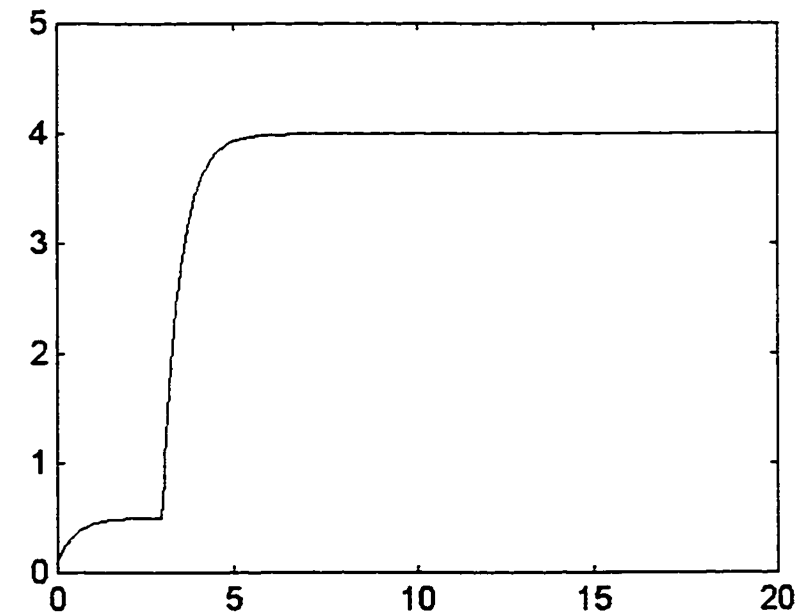

(d) Nominal Control Scaling Function $s_1(t)$

5.2 - Two Link Robot Arm

In this section we will apply trajectory linearization to the problem of controlling a two link robot arm. The control objective is to cause the flexion angles q_1 and q_2 to follow the command profile. This problem lends itself naturally to the trajectory linearization method because the dynamics of the system are solved for using Lagrange's Equations of motion. The nonlinear equation is naturally in phase variable canonical form. And thus no transformation is required to find the time varying feedback that stabilizes the error dynamics. Also, the desired outputs along with appropriate derivatives define the nominal state trajectories. Additionally, the method for finding the nominal control is very straightforward. Finally, the techniques for this problem can be readily generalized to a n link robot arm, or to a large class of similar robot arm designs.

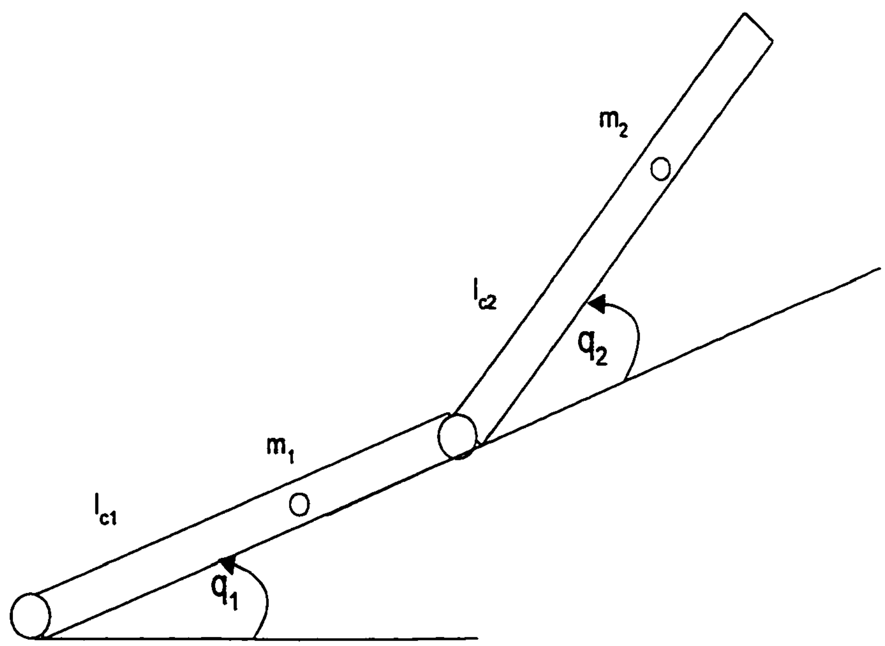

Figure 5.17 Two Link Robot Arm

First we must derive the nonlinear equations describing the motion of the arm using Lagrange's equations of motion. Consider the system depicted in figure 5.17. The total kinetic energy of the system is the sum of the translational and rotational energy of each link and is given by

$$T = \text{translational energy} + \text{rotational energy}$$

$$T = \frac{1}{2}m_1 v_{c1} + \frac{1}{2}m_2 v_{c2} + \frac{1}{2}I_1\omega_1^2 + \frac{1}{2}I_2\omega_2^2$$

The positions of the center of mass of the two links are

$$x_{c1} = l_{c1}\cos q_1$$

$$y_{c1} = l_{c1}\sin q_1$$

$$x_{c2} = l_1\cos q_1 + l_{c2}\cos(q_1 + q_2)$$

$$y_{c2} = l_1\sin q_1 + l_{c2}\sin(q_1 + q_2)$$

The translational velocity can be represented as functions of the flexion in each joint. For example

$$\dot{x}_{c1} = \frac{\partial f(q)}{\partial q_1}\dot{q}_1 + \frac{\partial f(q)}{\partial q_2}\dot{q}_2$$

In general, a velocity V in Cartesian coordinates can be related to the joint rotations by

$$V = J_v\dot{\boldsymbol{q}}$$

where J_V is the Jacobian of V. The translational kinetic energy can thus be represented by

$$T_T = \frac{1}{2}\dot{\boldsymbol{q}}\{m_1 J_{v_{c1}}^{\mathrm{T}} J_{v_{c1}} + m_2 J_{v_{c2}}^{\mathrm{T}} J_{v_{c2}}\}\dot{\boldsymbol{q}}$$

The rotational kinetic energy is

$$T_r = \frac{1}{2}I_1\omega_1^2 + \frac{1}{2}I_2\omega_2^2$$

$$= \frac{1}{2}I_1\dot{q}_1^2 + \frac{1}{2}I_2\dot{q}_1^2 + I_2\dot{q}_1\dot{q}_2 + \frac{1}{2}I_2\dot{q}_2^2$$

The potential energy is

$$\mathrm{V} = m_1 g l_{c1}\sin q_1 + m_2 g(l_1\sin(q_1) + l_{c2}\sin(q_1+q_2))$$

The nonlinear differential equations which describe this system can now be found from Lagrange's equation of motion

$$\frac{d}{dt}\left(\frac{\partial \mathrm{L}}{\partial \dot{q}_i}\right) - \frac{\partial \mathrm{L}}{\partial q_i} = Q_i'$$

where, $\mathrm{L} = \mathrm{T} - \mathrm{V}$ and Q_i' is a generalized force derived from a driving torque in each link joint. The equations of motion are

$$\boldsymbol{H}(\boldsymbol{q})\ddot{\boldsymbol{q}} + \boldsymbol{C}(\boldsymbol{q},\dot{\boldsymbol{q}})\dot{\boldsymbol{q}} + \boldsymbol{g}(\boldsymbol{q}) = \boldsymbol{\tau}$$

$$\begin{bmatrix} H_{11} & H_{12} \\ H_{21} & H_{22} \end{bmatrix}\begin{bmatrix} \ddot{q}_1 \\ \ddot{q}_2 \end{bmatrix} + \begin{bmatrix} -h\dot{q}_2 & -h\dot{q}_1 - h\dot{q}_2 \\ h\dot{q}_1 & 0 \end{bmatrix}\begin{bmatrix} \dot{q}_1 \\ \dot{q}_2 \end{bmatrix} + \begin{bmatrix} g_1 \\ g_2 \end{bmatrix} = \begin{bmatrix} \tau_1 \\ \tau_2 \end{bmatrix}$$

with $\boldsymbol{\tau}$ being the joint inputs, and

$$H_{11} = m_1 l_{c1}^2 + I_1 + m_2\{l_1^2 + l_{c2}^2 + 2l_1 l_{c2}\cos q_2\} + I_2$$

$$H_{22} = m_2 l_{c2}^2 + I_2$$

$$H_{12} = H_{21} = m_2 l_1 l_{c2}\cos q_2 + m_2 l_{c2}^2 + I_2$$

$$h = m_2 l_1 l_{c2}\sin q_2$$

$$g_1 = m_1 l_{c1} g\cos q_1 + m_2 g\{l_{c2}\cos(q_1+q_2) + l_1\cos q_1\}$$

$$g_2 = m_2 l_{c2} g\cos(q_1+q_2)$$

Now we will consider the design of the trajectory linearization controller. The first step in the design is to develop a pseudo-inverse that generates the nominal torque inputs. In order to generate an inverse $\boldsymbol{q} \rightarrow \boldsymbol{\tau}$ derivatives up to the second order of the two desired joint angles are required. As such information is not assumed to be available, an

estimate is necessary. Two filters are used to give a bandwidth limited approximation of the command. The filter is of the form

$$\hat{y}_i = \frac{a_{i1} y_i}{s^3 + a_{i3}s^2 + a_{i2}s + a_{i1}}$$

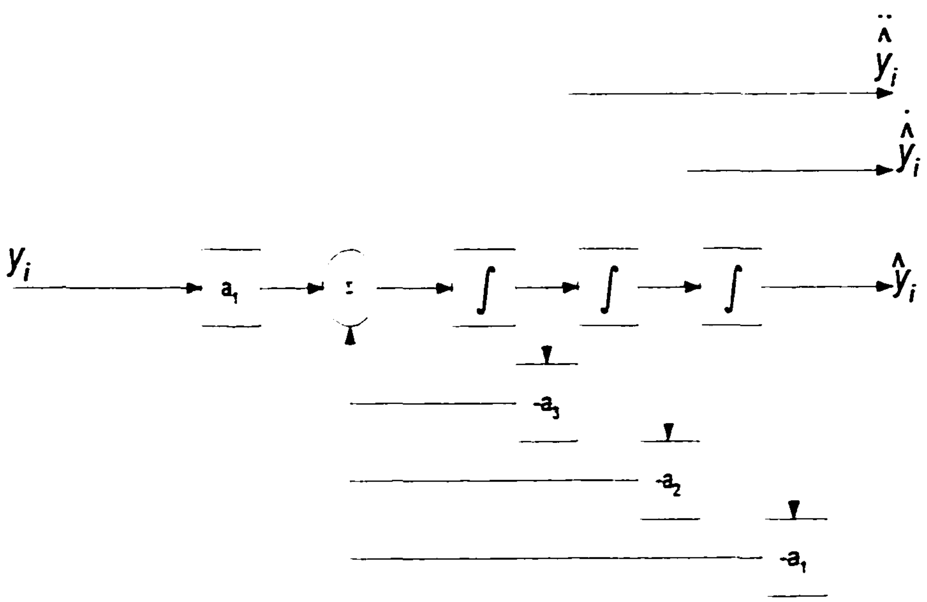

Figure 5.18 Filter Approximation of The Command

with the filter constants a_{ij} chosen to stabilize the filter and fast enough to track signals that fall within the performance requirements. The filtered output and the first two derivatives can be generated from a realization in the form of figure 5.18. The nominal control now can be easily found by

$$H(\bar{q})\ddot{\bar{q}} + C(\bar{q}, \dot{\bar{q}})\dot{\bar{q}} + g(\bar{q}) = \bar{\tau}$$

With the nominal inputs solved for, a trajectory stabilizing controller is now needed. The invertibility of $H(q)$ is a physical property of the system so we rewrite the defining nonlinear equation as

$$\ddot{\boldsymbol{q}} + \boldsymbol{H}^{-1}(\boldsymbol{q})\boldsymbol{C}(\boldsymbol{q},\dot{\boldsymbol{q}})\dot{\boldsymbol{q}} + \boldsymbol{H}^{-1}(\boldsymbol{q})g(\boldsymbol{q}) = \boldsymbol{H}^{-1}(\boldsymbol{q})\boldsymbol{\tau}$$

Defining the nonlinear states to be $[\xi_1 \quad \xi_2 \quad \xi_3 \quad \xi_4]^{\mathrm{T}} = [q_1 \quad \dot{q}_1 \quad q_2 \quad \dot{q}_2]^{\mathrm{T}}$, the nominal states are then given by $[\overline{\xi}_1 \quad \overline{\xi}_2 \quad \overline{\xi}_3 \quad \overline{\xi}_4]^{\mathrm{T}} = [\overline{q}_1 \quad \dot{\overline{q}}_1 \quad \overline{q}_2 \quad \dot{\overline{q}}_2]^{\mathrm{T}}$ and the state space equation is given by

$$\dot{\xi} = f(\xi,\tau)$$

$$\dot{\xi}_1 = \xi_2$$

$$\dot{\xi}_2 = f_2(\xi) + g_2(\xi)\tau$$

$$\dot{\xi}_3 = \xi_4$$

$$\dot{\xi}_4 = f_4(\xi) + g_4(\xi)\tau$$

Linearizing this nonlinear system about the nominal trajectory gives is

$$\dot{\boldsymbol{x}} = \boldsymbol{A}(t)\boldsymbol{x} + \boldsymbol{B}(t)\boldsymbol{u}$$

$$\boldsymbol{y}(t) = \begin{bmatrix} 1 & 0 & 0 & 0 \\ 0 & 0 & 1 & 0 \end{bmatrix} \boldsymbol{x}$$

where

$$\boldsymbol{A}(t) = \frac{\partial \boldsymbol{f}}{\partial \boldsymbol{\xi}}(\xi,\tau)\Big|_{\overline{\xi},\overline{\tau}}$$

which was found to be

$$\boldsymbol{A}(t) = \begin{bmatrix} 0 & 1 & 0 & 0 \\ a_{21}(t) & a_{22}(t) & a_{23}(t) & a_{24}(t) \\ 0 & 0 & 0 & 1 \\ a_{41}(t) & a_{42}(t) & a_{43}(t) & a_{44}(t) \end{bmatrix}$$

and

$$\boldsymbol{B}(t) = \frac{\partial \boldsymbol{f}}{\partial \boldsymbol{\tau}}(\xi,\tau)\Big|_{\overline{\xi},\overline{\tau}}$$

which was found to be

$$\boldsymbol{B}(t) = \begin{bmatrix} 0 & 0 \\ b_{21}(t) & b_{22}(t) \\ 0 & 0 \\ b_{41}(t) & b_{42}(t) \end{bmatrix}$$

The system matrix is in companion canonical form. Additionally, there exists a time varying input transformation matrix $\boldsymbol{M}(t)$ such that

$$\boldsymbol{B}(t)\boldsymbol{M}(t) = \begin{bmatrix} 0 & 0 \\ 1 & 0 \\ 0 & 0 \\ 0 & 1 \end{bmatrix}$$

This input transformation matrix exists and is invertible because the two nonzero rows of $\boldsymbol{B}(t)$ are a linearization of $\boldsymbol{H}^{-1}(q)$ about the nominal trajectory. Redefining the input

$$\boldsymbol{v}(t) = \boldsymbol{M}^{-1}(t)\boldsymbol{u}(t)$$

gives a system in phase variable canonical form.

Now a state feedback that assigns a desired PD-spectrum to the linearized error dynamics is needed. Note that the PD-eigenvalues of the SPDO

$$\delta^2 + \beta_{11}(t)\delta + \beta_{12}(t)$$

and the PD-eigenvalues of

$$\delta^2 + \beta_{21}(t)\delta + \beta_{22}(t)$$

are also PD-eigenvalues of the multi-block system

$$\dot{\boldsymbol{x}}(t) = \begin{bmatrix} 0 & 1 & 0 & 0 \\ \beta_{11}(t) & \beta_{12}(t) & 0 & 0 \\ 0 & 0 & 0 & 1 \\ 0 & 0 & \beta_{21}(t) & \beta_{22}(t) \end{bmatrix} \boldsymbol{x}(t)$$

Using the PD-synthesis equations, two pairs of PD-eigenvalues $\rho_{i1,2}$ for $i = 1, 2$ which satisfy the PD-spectral stability criteria can be synthesize by the time varying coefficients

$$\beta_{i1} = \frac{\rho_{i1}\dot{\rho}_{i2} - \rho_{i1}\rho_{i2}^2 + \rho_{i2}\dot{\rho}_{i1} + \rho_{i2}\rho_{i1}^2}{\rho_{i1} - \rho_{i2}}$$

$$\beta_{i2} = \frac{\dot{\rho}_{i1} + \rho_{i1}^2 - \dot{\rho}_{i2} - \rho_{i2}^2}{\rho_{i2} - \rho_{i1}}$$

So a time varying feedback

$$\boldsymbol{v}(t) = \mathbf{K}(t)\boldsymbol{x}(t)$$

$$\boldsymbol{v}(t) = \begin{bmatrix} 0 & 1 & 0 & 0 \\ \beta_{11}(t) - a_{21}(t) & \beta_{12}(t) - a_{22}(t) & -a_{23}(t) & -a_{24}(t) \\ 0 & 0 & 0 & 1 \\ -a_{41}(t) & -a_{42}(t) & \beta_{21}(t) - a_{43}(t) & \beta_{22}(t) - a_{44}(t) \end{bmatrix} \boldsymbol{x}(t)$$

yields linearized error dynamics that have the desired PD-eigenvalues and are of the form

$$\dot{\boldsymbol{x}}(t) = \begin{bmatrix} 0 & 1 & 0 & 0 \\ \beta_{11}(t) & \beta_{12}(t) & 0 & 0 \\ 0 & 0 & 0 & 1 \\ 0 & 0 & \beta_{21}(t) & \beta_{22}(t) \end{bmatrix} \boldsymbol{x}(t)$$

Thus, the control law that achieves the exponential regulation about the nominal trajectory is

$$\boldsymbol{u}(t) = \boldsymbol{M}(t)\mathbf{K}(t)\boldsymbol{x}(t)$$

The complete control law is given by

$$\tau = \boldsymbol{H}(\overline{\boldsymbol{q}})\ddot{\overline{\boldsymbol{q}}} + \boldsymbol{C}(\overline{\boldsymbol{q}}, \dot{\overline{\boldsymbol{q}}})\dot{\overline{\boldsymbol{q}}} + \boldsymbol{g}(\overline{\boldsymbol{q}}) + \boldsymbol{M}(t)\mathbf{K}(t)\boldsymbol{x}(t)$$

This controller was applied to the nonlinear robot arm. Each joint was assigned two PD-eigenvalues of $\rho_{i1} = -10$, $\rho_{i2} = -11$. Figure 5.19 shows the commanded joint angle profile. In the simulations, an initial error of 1° was set into the first joint. The output errors are shown in figure 5.20. As predicted, the errors decay exponentially. Thus, the controller provides exponential tracking for the nominal system.

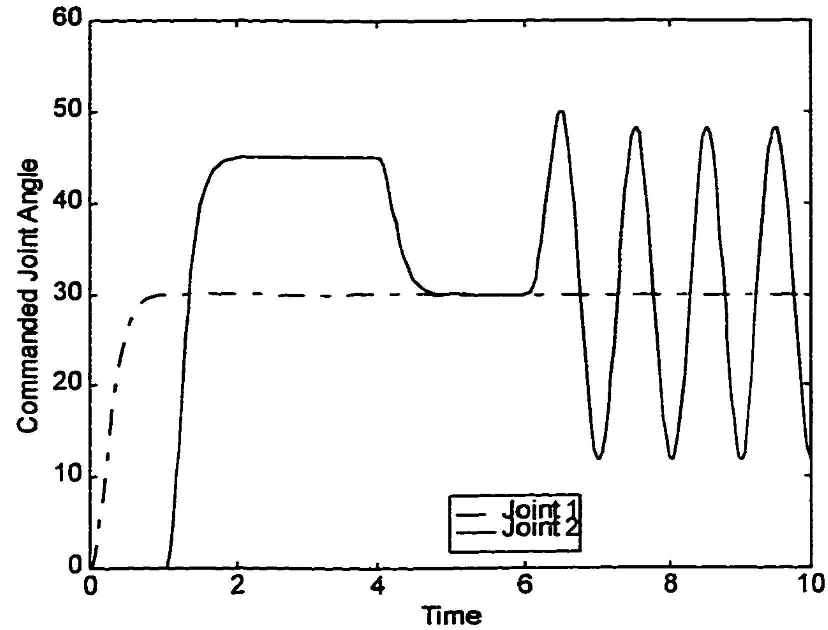

Figure 5.19 Commanded Joint angles

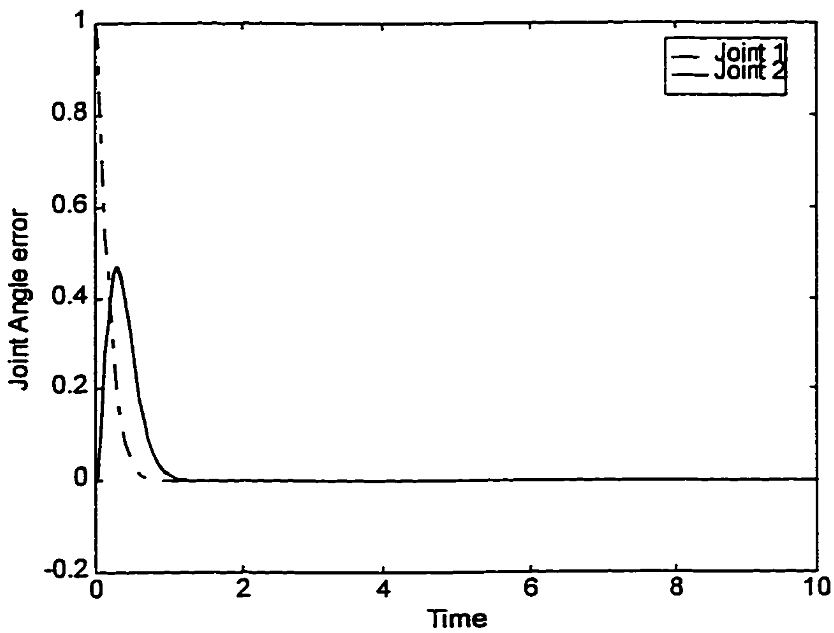

Figure 5.20 Joint Angle Errors

Many more simulations could be produced giving similar results to the above two. For the nominal plant, the system will exponentially track any command within the bandwidth limitations of the command filter. Thus further simulations are not very informative. However, other problems where the nonlinear system is not known precisely are very interesting.

The first problem that we will handle is flexibility. In this problem, the second link in the robot arm is flexible. The flexibility is modeled with

$$\boldsymbol{F} = \boldsymbol{H}^{-1}\{-\boldsymbol{C}(\boldsymbol{q}, \dot{\boldsymbol{q}})\dot{\boldsymbol{q}} - \boldsymbol{g}(\boldsymbol{q}) + \boldsymbol{\tau}\}$$

$$\begin{aligned} \dot{z}_1 &= z_2 \\ \dot{z}_2 &= -\omega_n^2 z_1 - 2\zeta\omega_n z_2 + [\, b_5\cos(q_2) \quad b_4\,]\boldsymbol{F} \end{aligned}$$

where z_1 is the angle of tip deflection, $\omega_n = 10$, $\zeta = 0.2$, and $b_5 = b_4 = -.05$. The rest of the system is modeled as before, except that the angles that the sensors actually measure are $q_{1m} = q_1$, and $q_{2m} = q_2 + z_1$.

We will use the same controller as before, except now we will use the time-variance to damp the vibration of the second link when precise placement is required. The PD-spectrum for the first link is now chosen as

$$\rho_{q_1 1,2} = (\,-5\sqrt{2} \pm 5\sqrt{2}\cdot i)s_1(t)$$

$$\rho_{q_2 1,2} = (\,-10 \pm 4\cdot i)s_2(t)$$

where $s_i(t)$ are the time varying scaling factors of the ith link, and the PD-spectrum is u.e.s for any $s_i(t) > 0$ of polynomial order. The scaling factors are simply increased when precise link placement is required. In the simulation the scaling factors will be increased between 2 and 6 seconds to achieve higher precision during this time. Increased precision is necessary when doing a specific function such as picking up an object, but is unnecessary when the arm is moving between jobs. The scaling factor can be reduced between precision work so as to limit the wear on the actuators.

Figures 5.21 (a)-(c) show the simulation results for the flexible second link robot arm. Figure 5.21 (a) shows the scaling factors. The second scaling factor is increased to try to dampen out the vibration between 2 and 6 seconds. It is kept at 1 when the vibration is tolerable so as to reduce the wear on the actuators from reducing the vibrations. Figure 5.21 (b) shows the desired link angles and the total output link angle. The total link angle includes the link angle and the tip deflection due to bending. Figure 5.21 (c) shows the error in the output link tip angles. The initial errors verify the asymptotic stabilization of initial errors. Increasing the scaling factor has the desired effect of reducing the tip angle error. In effect the controller has damped the inherent vibration of the second link during the required period of time.

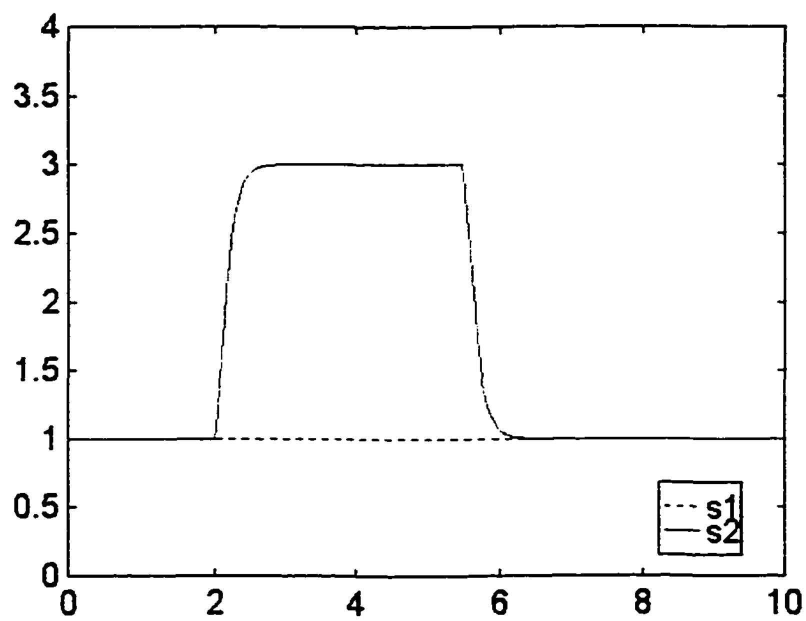

(a) Scaling Factors
Figure 5.21 Flexible Second Link with Time Varying Control

(figure continued)

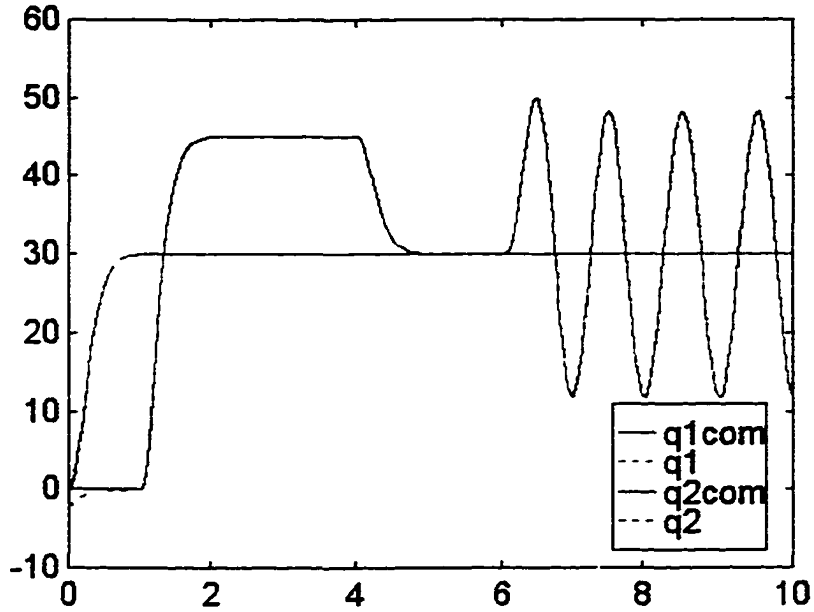

(b) Commanded and Output Total Link Angles

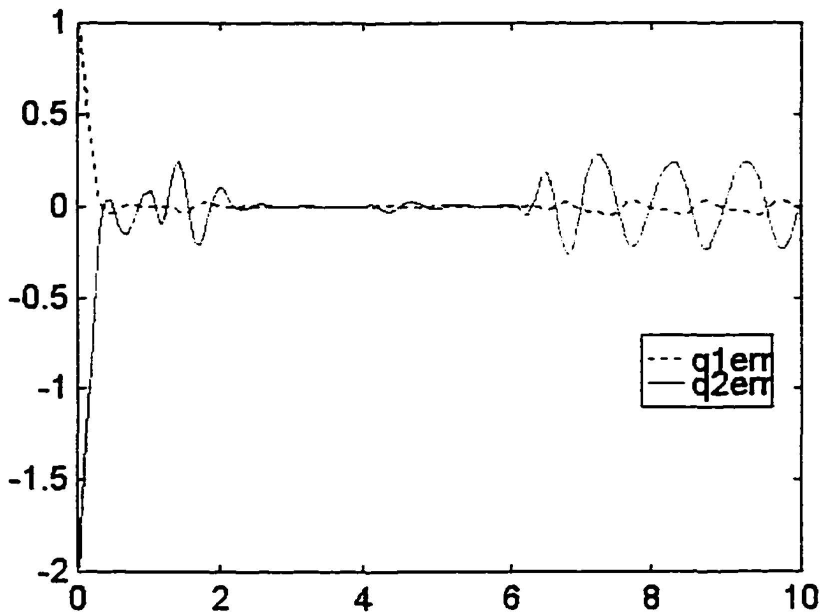

(c) Errors in Total Link Angles

A second problem involves generating a controller that can robustly track a desired trajectory after the arm picks up a poorly known mass. We will assume that the object can be approximated by a point mass m_3 where $0.15 < m_3 < 0.65$. We derive the describing equations for the true nonlinear system for the true mass $m_3 = .65$. Now, the design is similar to the design before where we use the nominal mass $\widehat{m}_3 = 0.4$. The nominal control is generated as before. Finally, we end up with the linearized error dynamics as before.

One of the limitations of the state feedback design is that nonvanishing perturbations lead to changes in the equilibrium of the error dynamics. This move in the equilibrium will cause a bounded disturbance in the trajectory tracking problem. Thus, we augment the error dynamics with integral of the errors to compensate for the change in equilibrium and track static commands exponentially. This leads to the augmented linear error states given by

$$[z_1 \quad z_2 \quad z_3 \quad z_4 \quad z_5 \quad z_6] = [\textstyle\int x_1 \quad x_1 \quad x_2 \quad \int x_3 \quad x_3 \quad x_4]$$

and the corresponding LTV error dynamics

$$\dot{z} = \begin{bmatrix} 1 & 0 & 0 & 0 & 0 & 0 \\ 0 & 1 & 0 & 0 & 0 & 0 \\ 0 & a_{21}(t) & a_{22}(t) & 0 & a_{23}(t) & a_{24}(t) \\ 0 & 0 & 0 & 1 & 0 & 0 \\ 0 & 0 & 0 & 0 & 1 & 0 \\ 0 & a_{41}(t) & a_{42}(t) & 0 & a_{43}(t) & a_{44}(t) \end{bmatrix} z + \begin{bmatrix} 0 & 0 \\ 0 & 0 \\ 1 & 0 \\ 0 & 0 \\ 0 & 0 \\ 0 & 1 \end{bmatrix} v$$

Now, we must choose two sets of three PD-eigenvalues to stabilize this LTV system. For the two third order systems we choose three different PD-eigenvalues with fixed damping. The fact that these poles have only one degree of freedom simplifies the assignment procedure and choosing different constant values assures that they are differentially distinct. A third order SPDO can be synthesized from three PD-eigenvalues with fixed damping by

$$\beta_{i1} = \rho_{i1}\rho_{i2}\rho_{i3}\omega_i(t)$$

$$\beta_{i2} = -\rho_{i1}\rho_{i2}\omega_i^2(t) - \rho_{i1}\omega_i^3(t)\dot{\omega}_i(t) - \rho_{i1}\rho_{i3}\omega_i^2(t) - \dot{\omega}_i(t)\rho_{i2} -$$

$$-\rho_{i2}\rho_{i3}\omega_i^2(t) - 3\frac{\dot{\omega}_i^2(t)}{\omega_i^3(t)} + \frac{\ddot{\omega}_i(t)}{\omega_i(t)} - \dot{\omega}_i(t)\rho_{i3}$$

$$\beta_{i3} = \omega_i(t)\rho_{i1} + \omega_i(t)\rho_{i2} + \omega_i(t)\rho_{i3} + 3\frac{\dot{\omega}_i(t)}{\omega_i^2(t)}$$

with

$$\mathrm{Re}\{\rho_{ij}\} < 0, \text{ and } \omega_i(t) > 0 \, \forall t$$

The linear state feedback is then given by

$$K(t) = \begin{bmatrix} \beta_{11} & \beta_{12} - a_{21} & \beta_{13} - a_{22} & 0 & -a_{23} & -a_{24} \\ 0 & -a_{41} & -a_{42} & \beta_{21} & \beta_{22} - a_{43} & \beta_{23} - a_{44} \end{bmatrix}$$

Figures 5.22-25 show the trajectory tracking performance of the robot arm when it picks up a poorly known mass. In both simulations, the arm picks up a mass $m_3 = 0.65$ at time $t = 2.0$ seconds. The design assumes that the mass is actually $\widehat{m}_3 = 0.4$ and uses the augmented error dynamics. Figure 5.22 shows the desired joint angles. Figure 5.23 shows the joint angle errors for the given commanded trajectories. First, a clear transient exists at two seconds when the arm adjusts to a mass which is heavier than expected. Further, the tracking performance shows reasonable transients during a large step command and the controller does achieve exponential tracking. The integral terms may lead to phase lag and deteriorated tracking performance of time varying trajectories. Figures 5.24 and 5.25 attempt to address this concern by commanding rapidly varying trajectories. This simulation indicates that the controller is capable of achieving adequate precision for time varying trajectories.

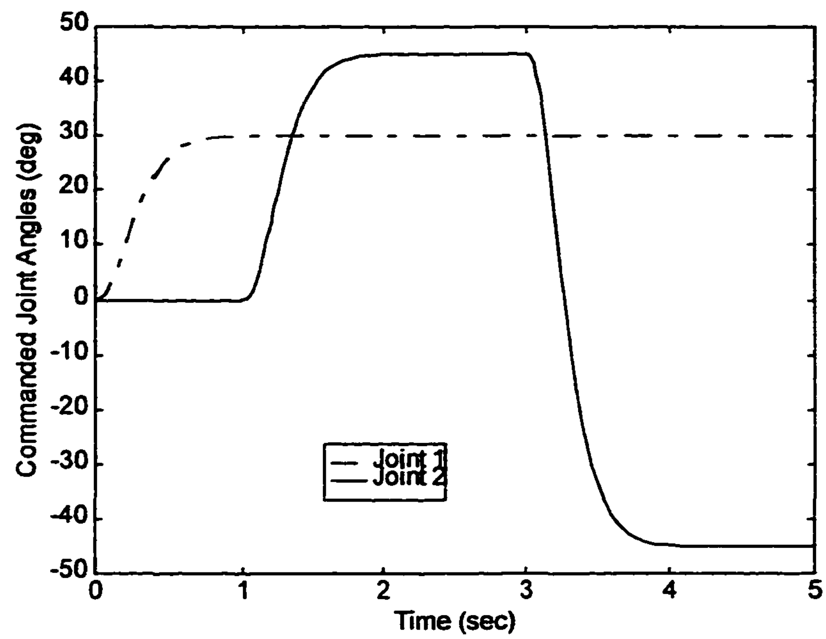

Figure 5.22 Step Commands For Robot Arm with Uncertain Mass

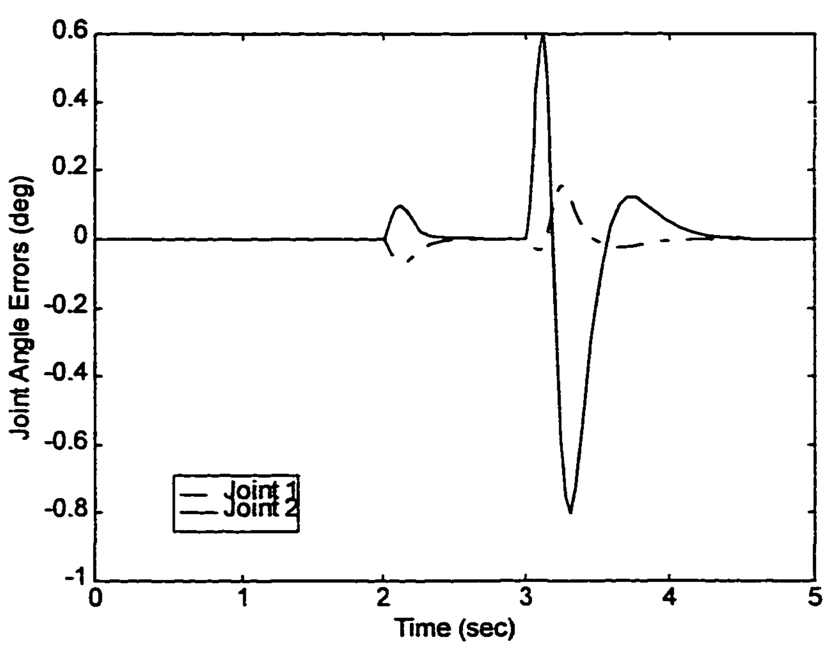

Figure 5.23 Joint Angle Errors with Uncertain Mass

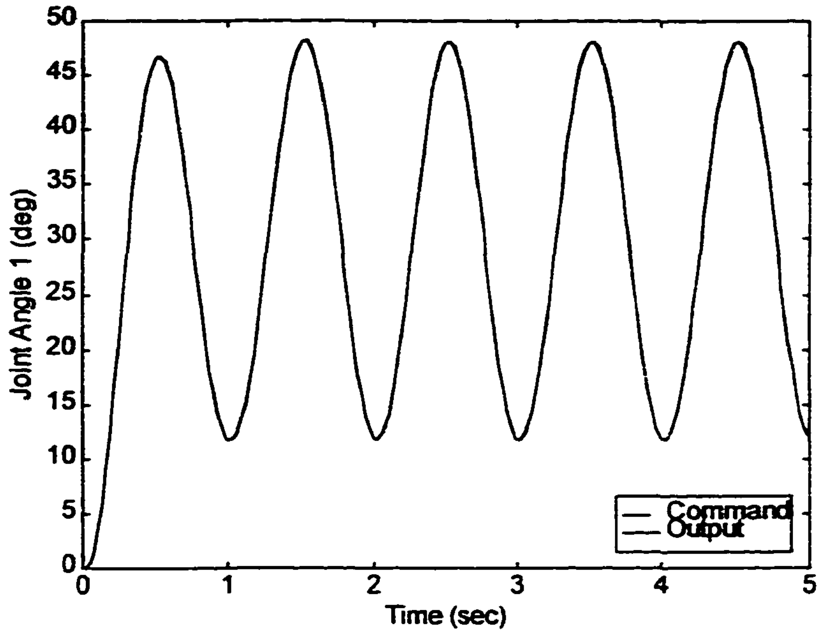

Figure 5.24 Joint 1 Performance with Uncertain Mass

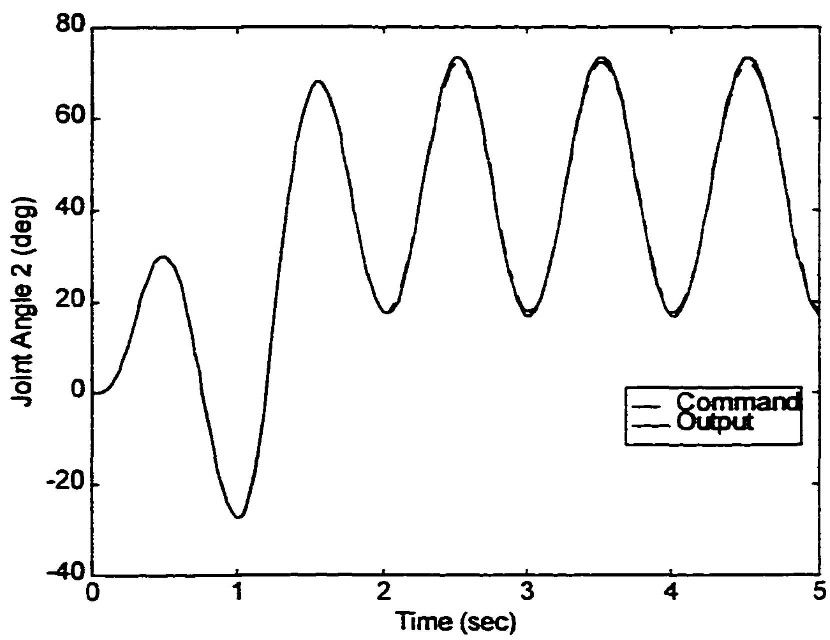

Figure 5.25 Joint 2 Performance with Uncertain Mass

5.3 - Pitch Axis Missile Autopilot

This section presents a trajectory linearization design for a pitch axis missile model [65], [133], and [63]. The contents of these publications are presented here in an abbreviated form.

A missile controller consists of a guidance system and an autopilot. The guidance portion consists of a seeker, a filter, and the guidance law. The seeker provides observed information about the target. The filter uses this information to estimate the relative translation of the target. The guidance law, uses this information to generate a trajectory to cause interception. We will consider the autopilot design. Specifically, we will design a controller which will use deflections of the tail fins to assure stability of the plant and to track the desired trajectory.

The motivation for this research is the inherent nonlinearity and time variance of many control problems. This statement is especially true of modern high performance missile autopilot design, *cf.* [27] and [11], where there are large inherent nonlinearities as well as many exogenous states which lead to a considerable time dependence, *e.g.* changing center of mass, altitude, and velocity. As such, the currently well developed LTI control theory is of limited utility. Though attempts to generalize these techniques to handle NLTV problems using robust gain scheduled methods such as μ-synthesis have met with some success, this approach suffers from some inherent limitations which often leads to failure. For instance, a necessity of such designs is that the scheduling parameters must be chosen such that they vary relatively slowly and "cover" the nonlinearity, c.f. [91]. This is not always possible or desirable. Consequently robust LTI designs do not appear to handle the nonlinear robustness very well. For example, in high angle of attack (AOA) missile autopilots it is necessary to select the AOA as a scheduled parameter so as to "cover" the nonlinearity, but this limits the autopilots ability to handle

rapid maneuvers. Thus it is desirable to have a systematic methodology that can handle nonlinearity, time variance as well as rapid trajectory commands.

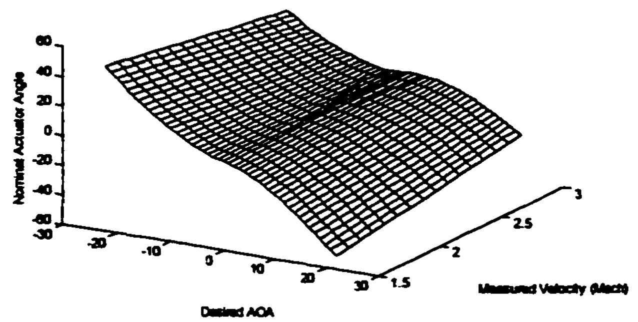

Figure 5.26. Tail Fin Look Up Table

The particular nonlinear pitch axis missile model is defined by the following nonlinear state equation.

$$\begin{aligned} \dot{\alpha}(t) &= K_\alpha M(t) C_n[\alpha(t), \delta(t), M(t)] \cos(\alpha(t)) + q(t) \\ \dot{q}(t) &= K_q M^2(t) C_m[\alpha(t), \delta(t), M(t)] + K_q q_m M^2(t) q(t) \\ \eta_z(t) &= K_z M^2(t) C_n[\alpha(t),\ \delta(t),\ M(t)] \end{aligned} \qquad (5.3)$$

where $\alpha(t)$ is the AOA, $q(t)$ is the pitch rate, $\eta(t)$ is the normal acceleration, and C_n, C_m are aerodynamic coefficients given by

$$\begin{aligned} C_n[\alpha, \delta, M] &= a_n \alpha^3 + b_n \alpha|\alpha| + c_n(2 - M/3)\alpha + d_n \delta \\ C_m[\alpha, \delta, M] &= a_m \alpha^3 + b_m \alpha|\alpha| + \\ &\quad + c_m(-7 + 8M/3)\alpha + q_m q + d_m \delta \end{aligned} \qquad (5.4)$$

The tail-fin actuator dynamics are described by

$$\begin{aligned} \frac{\mathrm{d}}{\mathrm{d}t} \begin{bmatrix} \delta(t) \\ \dot{\delta}(t) \end{bmatrix} &= \qquad (5.5) \\ &= \begin{bmatrix} 0 & 1 \\ -\omega_a^2 & -2\zeta\omega_a \end{bmatrix} \begin{bmatrix} \delta(t) \\ \dot{\delta}(t) \end{bmatrix} + \begin{bmatrix} 0 \\ \omega_a^2 \end{bmatrix} \delta_c(t) \end{aligned}$$

The values of the various constant parameters in the dynamic equations (5.3)-(5.5), with $q_m = 0$, can be found in [114]-[71] where this missile model has been used as a

benchmark for nonlinear gain-scheduling design techniques. Here we set $q_m = -0.1333/K_q$ to make the missile model more realistic and the design slightly more challenging. To simplify the design, the actuator is assumed to be "fast" enough so that it can be ignored in the control model.

Now tracking the nominal trajectory can be achieved by generating the nominal input $\bar{u}(t)$ and exponentially stabilizing the LTV error dynamics. The former requirement is in fact the problem of nonlinear dynamic inversion, which is itself a very difficult problem. The plant inversion can be implemented using a radial basis function neural network which will not be dealt with in detail here, *cf.* [127]. However, for faster simulation and due to the relative simplicity of the given nonlinear map, the inversion is handled by a two dimensional look up table in these simulations. The nominal tail fin deflection was found by using the Matlab function *trim* to solve for the steady state actuator angle that will generate the desired angle of attack for any given mach. The data was stored and then used to generate a two dimensional look up table with measured velocity and desired angle of attack as the two inputs. A plot of the two dimensional figure is shown in figure 5.26. A similar procedure can be used to generate data which then can be used to train a neural network implementation. Additionally, the commanded trajectory is defined in terms of AOA and the derivative of AOA. However, these terms are mapped to AOA and pitch rate which are the given states by the nonlinear equations describing the pitch axis motion.

Linearizing the nonlinear pitch model about the nominal trajectory leads to an equation of the form

$$\begin{aligned} \dot{x} &= A(t)x + B(t)v \\ y &= C(t)x + D(t)v \end{aligned} \tag{5.6}$$

where

$$A(t) = \frac{\partial f}{\partial \xi}\bigg|_{\bar{\xi},\bar{\delta}} = \begin{bmatrix} a_{11}(t) & 1 \\ a_{21}(t) & a_{22}(t) \end{bmatrix} \tag{5.7}$$

with

$$
\begin{aligned}
a_{11}(t) = K_\alpha M(t)[(3a_n\bar{\xi}_1^{\,2}(t) + 2b_n|\bar{\xi}_1(t)| + \\
+ c_n(2 - M(t)/3))\cos(\bar{\xi}_1(t)) - \\
- (a_n\bar{\xi}_1^{\,3}(t) + b_n|\bar{\xi}_1(t)|\bar{\xi}_1(t) + \\
+ c_n(2 - M(t)/3)\bar{\xi}_1(t) + d_n\bar{\delta})\sin(\bar{\xi}_1(t))]
\end{aligned}
$$

$$
\begin{aligned}
a_{21}(t) = K_q M^2(t)[3a_m\bar{\xi}_1^{\,2}(t) + \\
+ 2b_m|\bar{\xi}_1(t)| + c_m(-7 + 8M(t)/3)]
\end{aligned}
$$

$$a_{22}(t) = K_q q_m M^2(t)$$

$$B(t) = \frac{\partial f}{\partial \delta}\Big|_{\bar{\xi},\bar{\delta}} = \begin{bmatrix} b_1(t) \\ b_2(t) \end{bmatrix} = \begin{bmatrix} K_\alpha M(t) d_n \cos(\bar{\xi}_1(t)) \\ K_q d_m M^2(t) \end{bmatrix}$$

Now, the linearized error dynamics are transformed to phase-variable canonical form via a Lyapunov transformation given in Silverman [97]. Define the new coordinates as

$$z = T(t)x$$

where

$$T(t) = \begin{bmatrix} \frac{-b_2(t)}{l(t)} & \frac{b_1(t)}{l(t)} \\ \frac{b_1(t)a_{21}(t) - b_2(t)a_{11}(t)}{l(t)} + \mathrm{D}\left(\frac{-b_2(t)}{l(t)}\right) & \frac{b_1(t)a_{22}(t) - b_2(t)}{l(t)} + \mathrm{D}\left(\frac{b_1(t)}{l(t)}\right) \end{bmatrix}$$

and

$$
\begin{aligned}
l(t) = a_{21}(t)b_1^2(t) + b_1(t)a_{22}(t)b_2(t) - b_1(t)\dot{b}_2(t) - \\
- b_2(t)a_{11}(t)b_1(t) - b_2^2(t) + b_2(t)\dot{b}_1(t)
\end{aligned}
$$

In the new coordinates the open loop state equation is defined by

$$\dot{z} = \begin{bmatrix} 0 & 1 \\ -a_{z1}(t) & -a_{z2}(t) \end{bmatrix} z + \begin{bmatrix} 0 \\ 1 \end{bmatrix} v$$

where $a_{z1}(t)$ and $a_{z2}(t)$ are functions of the nominal trajectory and the time-varying parameters and their higher derivatives. Due to the space limitation, these expressions are omitted here.

Let the desired closed loop equation be

$$\dot{z} = \begin{bmatrix} 0 & 1 \\ -\eta_1(t) & -\eta_2(t) \end{bmatrix}$$

To synthesize the desired closed loop PD-spectrum, first it is necessary to choose two time varying PD-eigenvalues that satisfy the stability criterion of section 2. Next, the coefficients η_k(t) are solved for based on the desired PD-spectrum. For a 2nd-order LTV system with complex conjugate PD-eigenvalues of the form

$$\rho_{1,2}(t) = \sigma(t) \pm j\omega(t)$$

the synthesis formulas are

$$\eta_1(t) = \frac{\sigma(t)\dot{\omega}(t)}{\omega(t)} + \sigma^2(t) - \dot{\sigma}(t) + \omega^2(t)$$

$$\eta_2(t) = -\frac{\dot{\omega}(t)}{\omega(t)} + 2\sigma(t) \tag{5.8}$$

Further if we choose

$$\rho_{1,2}(t) = -(2\zeta \pm j\sqrt{1-\zeta^2})\omega_n(t)$$

where $0 < \zeta < 1$ is a constant damping factor, and $\omega_n(t) > 0$ is the time-varying natural frequency, then

$$\eta_1(t) = \omega_n^2(t)$$

$$\eta_2(t) = +2\zeta\omega_n(t) - \frac{\dot{\omega}_n(t)}{\omega_n(t)} \tag{5.9}$$

The closed loop coefficients are then formed by choosing a feedback

$$v(t) = k_1(t)z_1(t) + k_2(t)z_2(t)$$

where

$$\begin{aligned} k_1(t) &= -\eta_1(t) + a_{z1}(t) \\ k_2(t) &= -\eta_2(t) + a_{z2}(t) \end{aligned} \tag{5.10}$$

Using a 133 MHz Pentium it only took 10.8 seconds to solve for the 2nd-order Silverman transformation and the time varying coefficients in the new coordinates. Though not included in this paper, it is also of note that the transformation to phase-variable canonical form for direct implementation of the complete actuator-plant model, which is of 4th-order, was also computed. Using Maple on a 200 MHz Pentium Pro, it took 1528.6 seconds to find the transformation. This is a one time computation that need not be repeated for changes in plant parameters. Although the resulting expressions contain hundreds of terms involving the exogenous parameters and nominal trajectories and their higher derivatives, it is precise and should allow for a more intelligent way of choosing simplifying assumptions about the plant and commanded trajectory and ending up with a well chosen and tractable controller design.

This AOA trajectory tracking controller was implemented and verified on MATLAB. The simulated missile model is described by the nonlinear equations given above and includes actuator dynamics, time varying velocity, and also actuator rate command limiter of 500 deg/sec. The synthesis equations of (5.10) are used in the following simulations with $\zeta = 0.7$. The simulations include step command tracking, a transition from step to sine wave tracking with a change in natural frequency command, a comparison to a constant natural frequency, and concludes with a test of the robustness of the design. Except where otherwise noted, the original command trajectories have been filtered by a 2nd-order transfer function given by

$$G(s) = \frac{100}{s^2 + 18s + 100}$$

This insures sufficiently smooth commands to avoid actuator rate saturation. For more information concerning a command shaping filter which allows less smooth trajectories see [127], [65].

Figure 5.27 demonstrates the validity of the design. The filtered step command alternates between the maximum design AOA amplitude $\pm 20°$. The 95% settling time is about 0.51 seconds. This figure shows the controller design to provide excellent tracking, comparable to other nonlinear design methods.

Figures 5.28-33 demonstrate some of the practical flexibility of PD-spectrum assignment control. Figure 5.28 shows the trajectory to be followed. The initial four seconds consists of tracking the relatively demanding filtered step command, followed by four seconds of the more tractable sine command. Figure 5.29 assumes some foreknowledge in the nature of the commanded trajectories, and shows an abrupt increase from an approximate PD-Assignment of $\omega_n(t) = 15$ to $\omega_n(t) = 25$. This is offered as a simple example of the controller's ability to safely transition from one bandwidth to another. Figure 5.30 shows the actuator deflection. Figure 5.31 shows the more important commanded actuator deflection rate. The high rates in the first four seconds demonstrate why the filtered step command is more demanding, and why the bandwidth can be increased during the final four seconds. Figure 5.32 shows the exogenous source of time variance in the nonlinear plant, *i.e.* the velocity profile. This figure shows that the missile is in ballistic mode, where the velocity drops from the initial Mach 3 to Mach 2.1 in 8 seconds. Finally, figure 5.33 shows the endogenous source of time variance, the time-varying coefficients $a_{z1}(t)$ and $a_{z2}(t)$ of the transformed linearized error dynamics.

Finally, the inherent robustness of the design was tested and the results are displayed in Figure 5.34 which shows acceptable sinusoidal tracking performance in the face of static aerodynamic coefficient perturbations of $\pm 50\%$. Although, robustness has not been sufficiently studied to give useful measures and design optimizations, it does seem that this methodology has a large degree of inherent robustness.

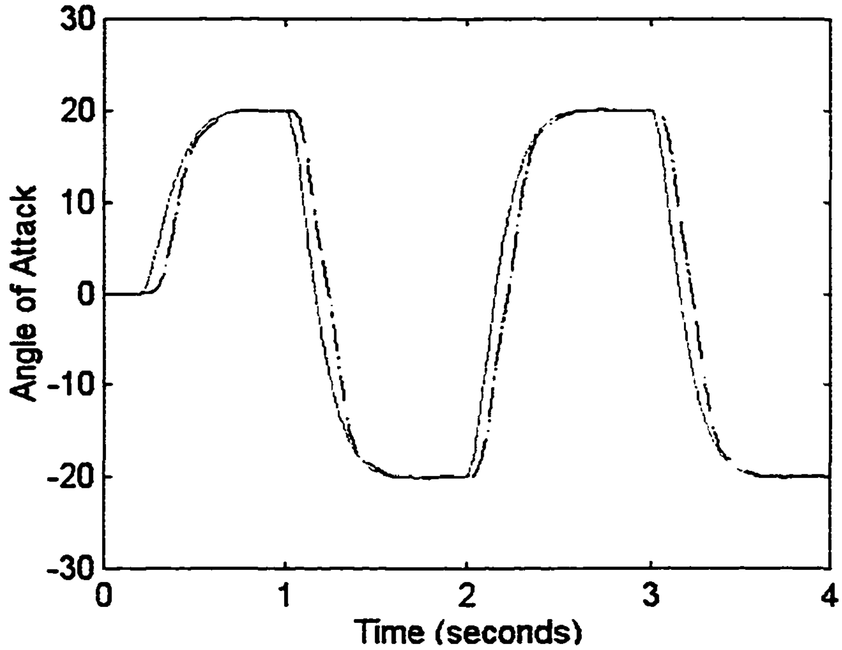

Figure 5.27 Smoothed Step Trajectory Tracking

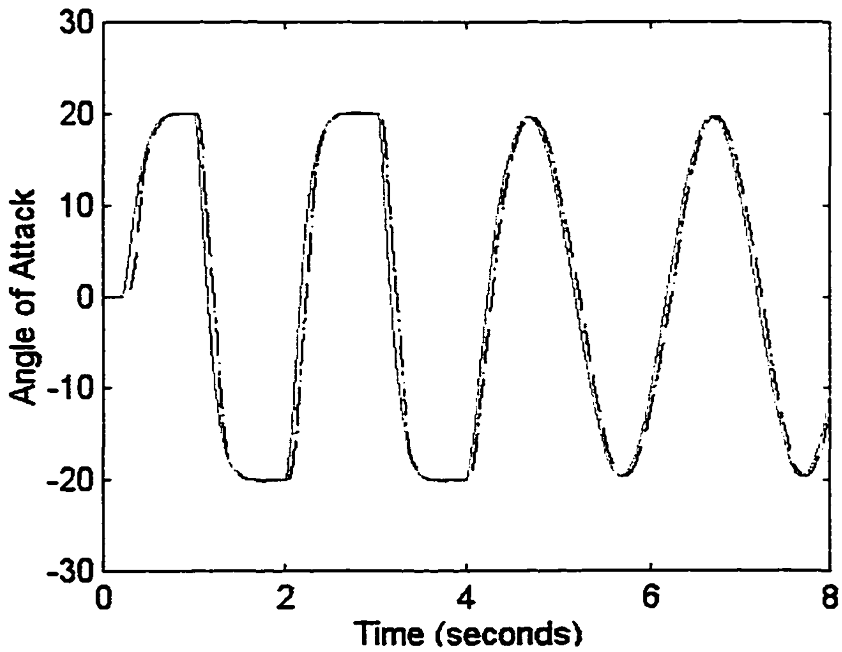

Figure 5.28 Smoothed Step to Sine Trajectory Tracking

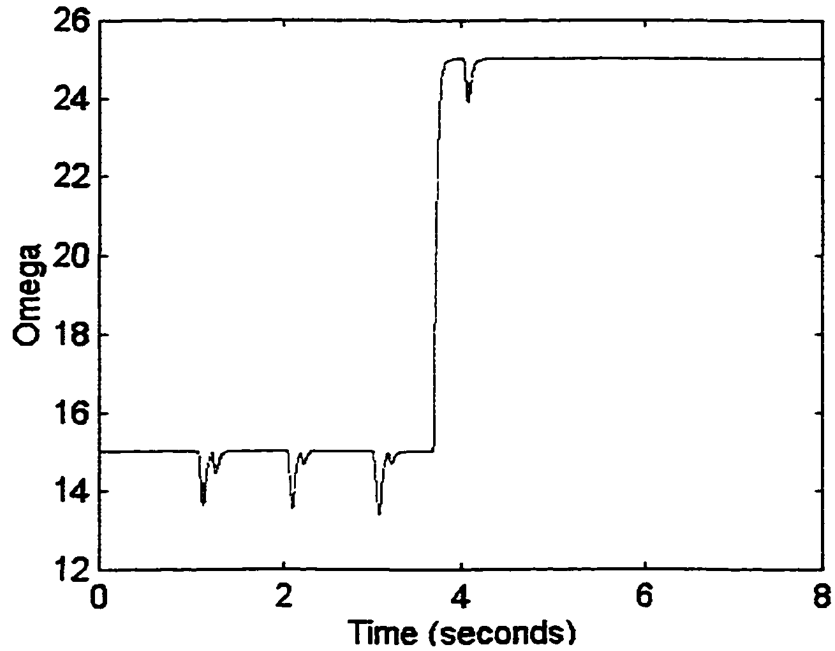

Figure 5.29 Time Varying Controller Bandwidth

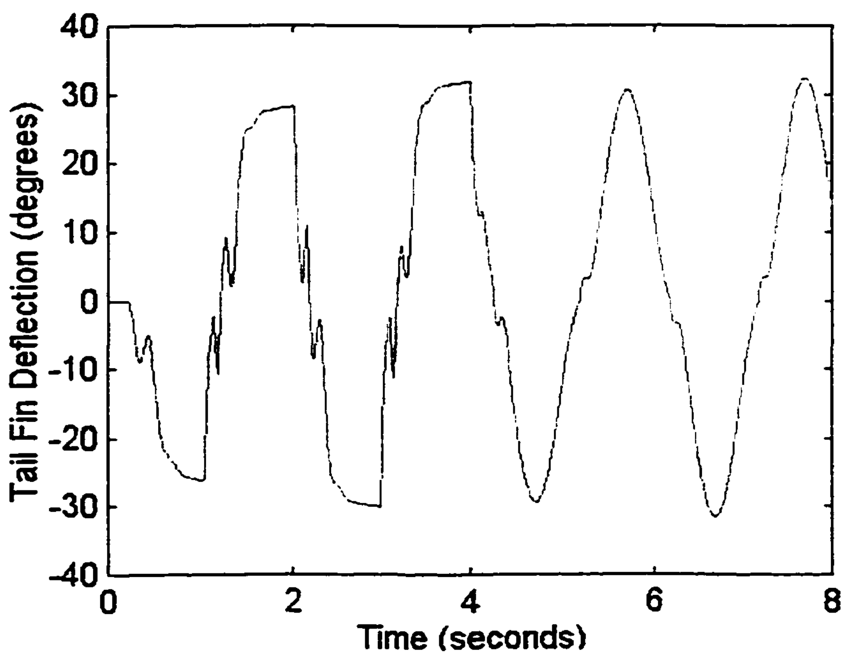

Figure 5.30 Commanded Actuator Deflection

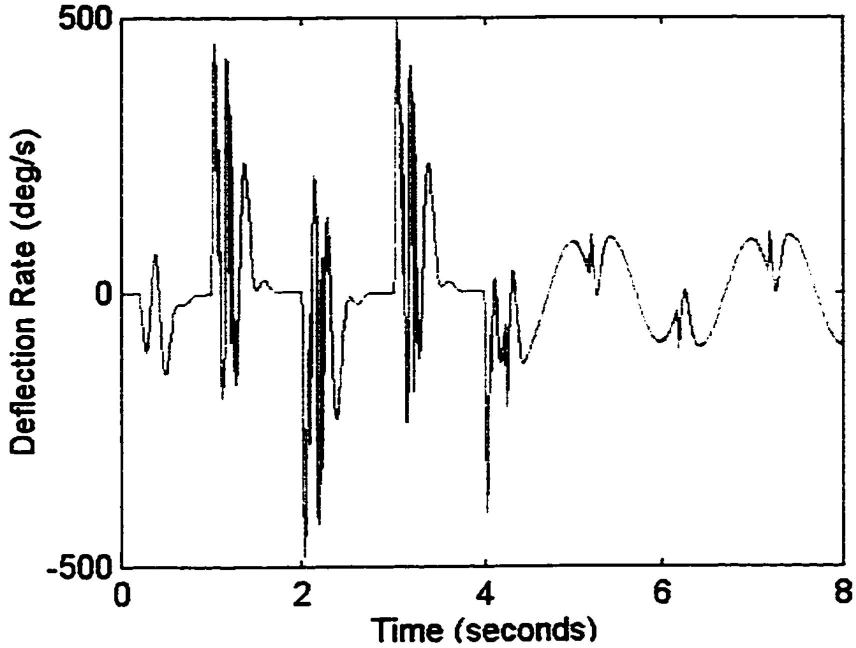

Figure 5.31 Commanded Actuator Deflection Rate

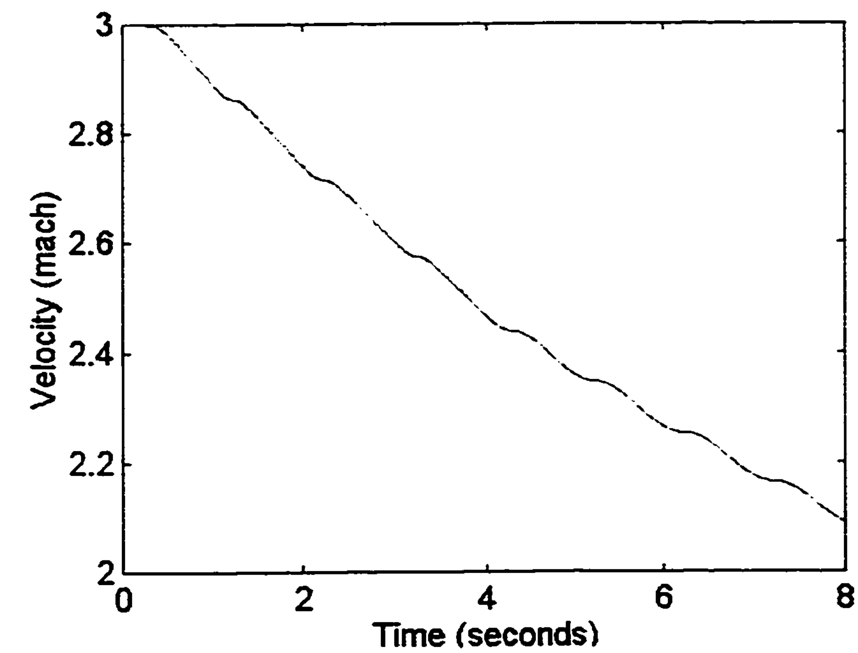

Figure 5.32 Mach Profile

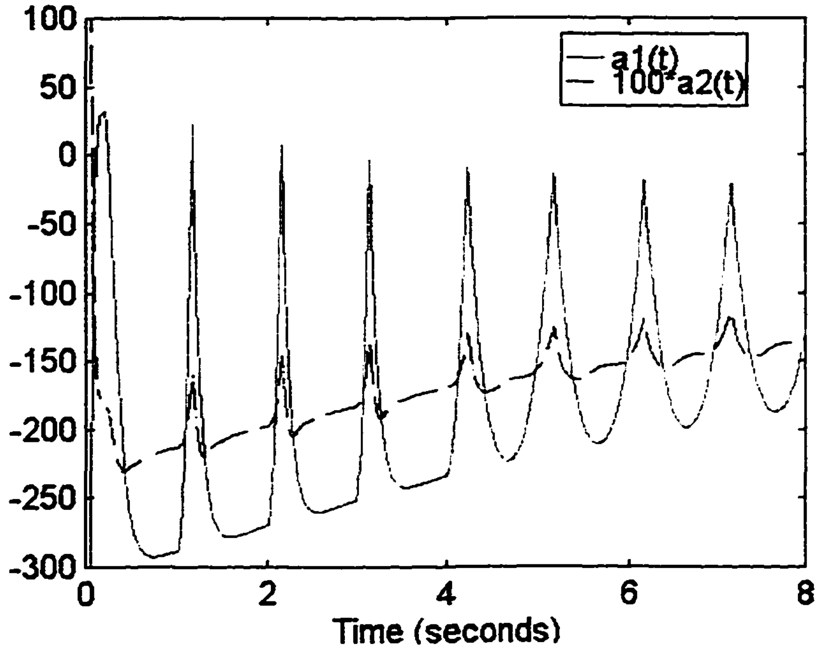

Figure 5.33 Time Varying System Coefficients

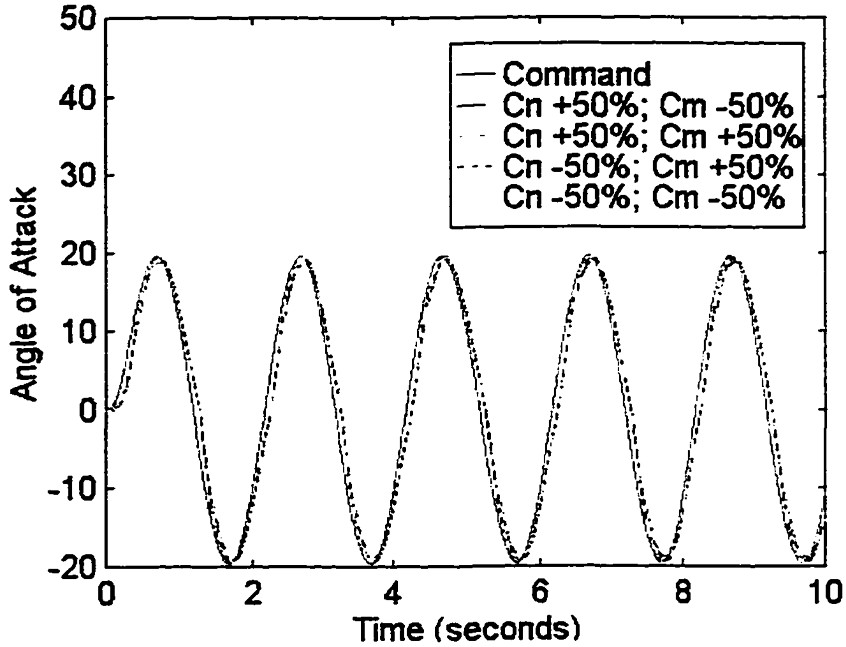

Figure 5.34 Robustness Study

5.4 - 4 DOF Roll-Yaw Missile Autopilot

This section presents the trajectory linearization design of a roll-yaw autopilot for a non-axisymmetric missile model to robustly decouple roll tracking from yaw regulation. The model of section 5.3 is a partial model of a typical skid-to-turn (STT) type missile. Such missiles are axisymmetric with tail fins arranged in a cruciform pattern. The term skid to turn arises because of the way in which a controller effects a turn. The autopilot commands a fin deflection in the direction to which the turn is to be made. This deflection then causes the tail to move in the opposite direction. As the airstream strikes the side of the missile it causes an acceleration in the direction commanded. Thus, maneuvers are achieved by commanding sideslips and angle of attack while keeping the roll to zero.

The push for greater performance has led to interest in Bank-To-Turn missiles. This type of missile has a lifting surface which allows more acceleration in the primary maneuver plane and as such is often called a Preferred Orientation Control (POC) airframe. This type of missile has greater maneuver capabilities but exhibits greater aerodynamic coupling complicating the design.

The roll-yaw airframe is a uniformly completely controllable MIMO nonlinear time-varying system. Thus, this section is an extension of the previous results on SISO designs for the pitch autopilot. Several innovations have been developed. First, methods for finding the Silverman-Wolovich (SW) transformation [97], [121] have been implemented in Maple, a symbolic mathematics programming language. Second, PD-spectral stability criteria for MIMO LTV systems [129] are used here to stabilize the tracking error dynamics. Third, a simple but effective method for nonlinear inversion is used to obtain the nominal control input and is applicable to similar problems.

The BTT missile model used here is obtained by nulling out the pitch terms from the equations of motion for the EMRAAT airframe in Appendix B [86]. Thus the states are

pitch terms involves setting the pitch rate $q(t)$, pitch angle $\theta(t)$, and the angle-of-attack $\alpha(t)$ all to zero. Thus the states of the reduced 4DOF nonlinear missile model are yaw rate $r(t)$, sideslip angle $\beta(t)$, roll rate $p(t)$, and the roll angle $\Phi(t)$ which, at zero pitch angle, is the integral of roll rate. The control inputs are the rudder angle $\delta_r(t)$ and aileron angle $\delta_p(t)$. All system parameters and aerodynamic coefficients can be found in Appendix B, *cf.* [86]. All state variables are assumed on-line measurable and thus no observer is required. The design objective is to cause the roll angle $\Phi(t)$ to track a given desired output profile, while simultaneously regulating the sideslip angle $\beta(t)$. The sideslip angle must be maintained below 5° at all times to insure air breathing propulsive efficiency and to make certain that the simplifying assumptions on the dynamic model remain valid. Additionally, the sideslip angle must be strongly decoupled from the roll rate, because of the large inherent coupling. Thus subsequently $\beta(t)$ and $\Phi(t)$ will be defined as the outputs.

$$\dot{\Phi} = p \tag{5.3}$$

$$\begin{aligned}
\dot{p} = {} & [(-I_{xy}I_{xz}I_{zz} - I_{xz}^2 I_{yz} + I_{xy}^2 I_{yz} + I_{xy}I_{xz}I_{yy})p^2 + \\
& + (-I_{yy}I_{yz}I_{zz} + I_{xy}I_{xz}I_{zz} + I_{yz}^3 + I_{xz}^2 I_{yz})r^2 + \\
& + (I_{xy}I_{zz}^2 + I_{xz}I_{yz}I_{zz} - I_{xy}I_{yy}I_{zz} - I_{xx}I_{xy}I_{zz} + \\
& + 2I_{xy}I_{yz}^2 + I_{xz}I_{yy}I_{yz} - I_{xx}I_{xz}I_{yz})pr + \\
& + QSd(C_{l_p}(I_{yy}I_{zz} - I_{yz}^2) + C_{n_p}(I_{xy}I_{yz} + I_{xz}I_{yy}))p + \\
& + QSd(C_{l_r}(I_{yy}I_{zz} - I_{yz}^2) + C_{n_r}(I_{xy}I_{yz} + I_{xz}I_{yy}))r + \\
& + QSd(C_{l_r}(I_{yy}I_{zz} - I_{yz}^2) + C_{n_r}(I_{xy}I_{yz} + I_{xz}I_{yy}))r + \\
& + QSd(C_{l_{\delta_p}}(I_{yy}I_{zz} - I_{yz}^2) + C_{n_{\delta_p}}(I_{xy}I_{yz} + I_{xz}I_{yy}))\delta_p + \\
& + QSd(C_{l_{\delta_r}}(I_{yy}I_{zz} - I_{yz}^2) + C_{n_{\delta_r}}(I_{xy}I_{yz} + I_{xz}I_{yy}))\delta_r] \\
& (I_{xx}I_{yy}I_{zz} - I_{xy}^2 I_{zz} - I_{xx}I_{yz}^2 - 2I_{xy}I_{xz}I_{yz} - I_{xz}^2 I_{yy})^{-1}
\end{aligned} \tag{5.4}$$

$$\begin{aligned}
\dot{\beta} = {} & -r + \frac{gQS}{WV}(C_{Y_\beta}\beta + C_{Y_p}p + C_{Y_r}r + C_{Y_{\delta_p}}\delta_p + C_{Y_{\delta_r}}\delta_r)\cos(\beta) \\
& + \frac{g}{V}\sin(\phi)\cos(\beta)
\end{aligned} \tag{5.5}$$

$$\begin{aligned}\dot{r} = [&(-I_{xx}I_{xz}I_{yz} + I_{xx}I_{xy}I_{yy} - I_{xy}^3 - I_{xz}^2 I_{xy})p^2 + \\ &+ (-I_{xy}I_{yz}^2 - I_{xz}I_{yy}I_{yz} + I_{xx}I_{xz}I_{yz} + I_{xy}I_{xz}^2)r^2 + \\ &+ (I_{xx}I_{yz}I_{zz} + I_{xy}I_{xz}I_{zz} + I_{xx}I_{yy}I_{yz} - 2I_{xy}^2 I_{yz} - \\ &- I_{yz}I_{xx}^2 - I_{xy}I_{xz}I_{yy} - I_{xx}I_{xy}I_{xz})pr + \\ &+ QSd(C_{l_p}(I_{xy}I_{yz} - I_{xz}I_{yy}) + C_{n_p}(I_{xx}I_{yy} - I_{xy}^2))p + \\ &+ QSd(C_{l_r}(I_{xy}I_{yz} + I_{xz}I_{yy}) + C_{n_r}(I_{xx}I_{yy} - I_{xy}^2))r + \\ &+ QSd(C_{l_\beta}(I_{xy}I_{yz} + I_{xz}I_{yy}) + C_{n_\beta}(I_{xx}I_{yy} - I_{xy}^2))\beta + \\ &+ QSd(C_{l_{\delta_p}}(I_{xy}I_{yz} + I_{xz}I_{yy}) + C_{n_{\delta_p}}(I_{xx}I_{yy} - I_{xy}^2))\delta_p + \\ &+ QSd(C_{l_{\delta_r}}(I_{xy}I_{yz} + I_{xz}I_{yy}) + C_{n_{\delta_r}}(I_{xx}I_{yy} - I_{xy}^2))\delta_r] \\ &(I_{xx}I_{yy}I_{zz} - I_{xy}^2 I_{zz} - I_{xx}I_{yz}^2 - 2I_{xy}I_{xz}I_{yz} - I_{xz}^2 I_{yy})^{-1}\end{aligned} \tag{5.6}$$

Let the system states and inputs be chosen as

$$\xi(t) = \begin{bmatrix} \xi_1(t) \\ \xi_2(t) \\ \xi_3(t) \\ \xi_4(t) \end{bmatrix} = \begin{bmatrix} \Phi(t) \\ p(t) \\ \beta(t) \\ r(t) \end{bmatrix}$$

$$\delta(t) = \begin{bmatrix} \delta_p(t) \\ \delta_r(t) \end{bmatrix}$$

additionally, let the outputs be defined as

$$\eta(t) = \begin{bmatrix} h_1(\xi) \\ h_2(\xi) \end{bmatrix} = \begin{bmatrix} \xi_1(t) \\ \xi_3(t) \end{bmatrix}$$

Then the nonlinear state equation can be written as

$$\dot{\xi} = f(\xi, \delta) = \begin{bmatrix} f_\Phi(\xi_1, \xi_2, \xi_3, \xi_4) \\ f_p(\xi_1, \xi_2, \xi_3, \xi_4) \\ f_\beta(\xi_1, \xi_2, \xi_3, \xi_4) \\ f_r(\xi_1, \xi_2, \xi_3, \xi_4) \end{bmatrix} + \begin{bmatrix} g_\Phi(\xi_1, \xi_2, \xi_3, \xi_4, \delta_p, \delta_r) \\ g_p(\xi_1, \xi_2, \xi_3, \xi_4, \delta_p, \delta_r) \\ g_\beta(\xi_1, \xi_2, \xi_3, \xi_4, \delta_p, \delta_r) \\ g_r(\xi_1, \xi_2, \xi_3, \xi_4, \delta_p, \delta_r) \end{bmatrix}$$

For this design, one simplifying assumption is used to obtain the nonlinear inverse input-output mapping. The direct control input to sideslip is assumed to be negligible, that is

$$g_\beta(\xi_1, \xi_2, \xi_3, \xi_4, \delta_r, \delta_p) \equiv 0,$$

which amounts to ignoring a fast zero in the yaw channel. Then the vector relative degree relative to the outputs $\eta(t)$ is $[2 \quad 2]$. Therefore, taking the second derivative of each output with respect to time gives

$$\ddot{\eta}_1 = L_f^2 h_1(\xi) + L_{g_p} L_f h_1(\xi)\delta_p + L_{g_r} L_f h_1(\xi)\delta_r$$
$$\ddot{\eta}_2 = L_f^2 h_2(\xi) + L_{g_p} L_f h_2(\xi)\delta_p + L_{g_r} L_f h_2(\xi)\delta_r$$

The nominal input $\overline{\delta}$ can now be computed from a given nominal output $\overline{\eta}$

$$\begin{bmatrix} \overline{\delta}_p \\ \overline{\delta}_r \end{bmatrix} = \begin{bmatrix} L_{g_p} L_f h_1(\overline{\xi}) & L_{g_r} L_f h_1(\overline{\xi}) \\ L_{g_p} L_f h_2(\overline{\xi}) & L_{g_r} L_f h_2(\overline{\xi}) \end{bmatrix}^{-1} \begin{bmatrix} \ddot{\overline{\eta}}_1(t) - L_f^2 h_1(\overline{\xi}) \\ \ddot{\overline{\eta}}_2(t) - L_f^2 h_2(\overline{\xi}) \end{bmatrix}$$

where the inverse matrix exists owing to the well defined vector relative degree.

To implement the plant inverse it requires the nominal output and nominal output derivative information. To gain access to these values we create a command shaping filter which approximates the desired output command $\overline{\eta}_i(t)$ and its first two derivatives with a filtered command $\widehat{\eta}_i(t)$. The LTI command shaping filter is described by

$$\widehat{\eta}_i(s) = \frac{a_4}{s^4 + a_1 s^3 + a_2 s^2 + a_3 s + a_4} \overline{\eta}_i(s)$$

where a_i are chosen to make the filter stable, to achieve the desired tracking bandwidth, to give continuous derivatives up to the second order, and to avoid commands which would place the actuators into saturation.

Now, the commanded trajectory must be exponentially stabilized by assigning a stable PD-spectrum to the linearized tracking error dynamics. For a nominal trajectory $\overline{\xi}$ satisfying

$$\dot{\overline{\xi}}(t) = f(\overline{\xi}(t), \overline{\delta}(t))$$

define the tracking errors by

$$x(t) = \xi(t) - \overline{\xi}(t)$$

and the tracking error control input by

$$u(t) = \delta(t) - \overline{\delta}(t)$$

Then the linearized tracking error dynamics are given by

$$\dot{x} = A(t)x + B(t)u$$

$$y = C(t)x + D(t)u$$

For the EMRAAT airframe at an altitude of 30,000 ft. and Mach 2.0

$$A(t) = \frac{\partial f}{\partial \xi}\Big|_{\overline{\xi},\overline{\delta}} = \begin{bmatrix} 0 & 1 & 0 & 0 \\ a_{21}(t) & a_{22}(t) & a_{23}(t) & a_{24}(t) \\ a_{31}(t) & -0.00001806 & -0.36853 & -0.9996 \\ a_{41}(t) & a_{42}(t) & a_{43}(t) & a_{44}(t) \end{bmatrix}$$

$$B(t) = \frac{\partial f}{\partial \delta}\Big|_{\overline{\xi},\overline{u}} = \begin{bmatrix} 0 & 0 \\ -1243 & -1017 \\ -0.0002473 & 0.001979 \\ 17.52 & -75.99 \end{bmatrix}$$

$$C(t) = \begin{bmatrix} 1 & 0 & 0 & 0 \\ 0 & 0 & 1 & 0 \end{bmatrix}$$

$$D(t) = 0$$

where due to space limitations the expressions for some of the $a_{ij}(t)$ are omitted, which can be easily found using Maple by taking the Jacobean of the nonlinear equations of motion and replacing the states with the nominal states. Note, the input matrix is constant because the missile is modeled at a fixed altitude and velocity, and because all of the desired trajectories consist of 0° of sideslip.

These linearized equations of motion must be transformed to the MIMO Phase Variable canonical form using the Silverman-Wolovich transoformation so that PD-spectral assignment can be used. The transformation and subsequent realization may have a large number of terms. Thus, it may be necessary to make practical assumptions

to simplify the problem. These assumptions could include neglecting relatively small coefficients and high order derivatives. In this case, neglecting b_{31} and b_{32} was a useful and reasonable simplification which will be validated subsequently by simulation results. The S-W transformation with lexicographic indices $n_1 = 2$, $n_2 = 2$ was found using Maple, and then implemented in MATLAB. The Lyapunov transformation is given by

$$T(t) = \begin{bmatrix} -\frac{3799}{5650022} & 0 & \frac{21187500}{2353234163} & 0 \\ t_{21}(t) & -\frac{3799}{5650022} & -\frac{31230375}{9412936652} & -\frac{25425}{2825011} \\ -\frac{125}{807146} & 0 & -\frac{11187500}{1008528927} & 0 \\ t_{41}(t) & -\frac{125}{807146} & \frac{16490375}{4034115708} & \frac{4475}{403573} \end{bmatrix}$$

where the expressions for the time-varying elements $t_{21}(t)$ and $t_{41}(t)$ are omitted due to space limitation. The resulting realization is in the 2×2 MVPV canonical form:

$$A_p(t) = \left[\begin{array}{cccc} 0 & 1 & 0 & 0 \\ -\alpha_{21}(t) & -\alpha_{22}(t) & -\alpha_{23}(t) & -\alpha_{24}(t) \\ \hline 0 & 0 & 0 & 1 \\ -\alpha_{41}(t) & -\alpha_{42}(t) & -\alpha_{43}(t) & -\alpha_{44}(t) \end{array}\right]$$

$$B_p(t) = \begin{bmatrix} 0 & 0 \\ 1 & 0 \\ 0 & 0 \\ 0 & 1 \end{bmatrix}$$

Then design the state feedback control gain

$$K_p(t) = \left[\begin{array}{cccc} \alpha_{21}(t)-\beta_{21}(t) & \alpha_{22}(t)-\beta_{22}(t) & \alpha_{23}(t) & \alpha_{23}(t) \\ \hline \alpha_{41}(t) & \alpha_{42}(t) & \alpha_{43}(t)-\beta_{43}(t) & \alpha_{44}(t)-\beta_{44}(t) \end{array}\right]$$

obtain the desired closed-loop dynamics in the MVPV coordinates

$$A_p(t) + B_p(t)K_p(t) = \left[\begin{array}{cc:cc} 0 & 1 & 0 & 0 \\ -\beta_{11}(t) & -\beta_{12}(t) & 0 & 0 \\ \hline 0 & 0 & 0 & 1 \\ 0 & 0 & -\beta_{21}(t) & -\beta_{22}(t) \end{array}\right]$$

where $\beta_{ij}(t)$ are synthesized from the (real) PD-spectral canonical form

$$A_s(t) = \left[\begin{array}{cc|cc} \sigma_1(t) & \omega_1(t) & 0 & 0 \\ -\omega_1(t) & \sigma_1(t) & 0 & 0 \\ \hline 0 & 0 & \sigma_2(t) & \omega_2(t) \\ 0 & 0 & -\omega_2(t) & \sigma_2(t) \end{array}\right]$$

with the desired closed-loop PD-eigenvalues $\rho_{i1,i2}(t) = -(2\zeta \pm j\sqrt{1-\zeta^2})\omega_{ni}(t)$, where $\omega_{ni}(t)$ is called the instantaneous natural frequency of the ith pair of PD-eigenvalues. The synthesis equations are given by

$$\beta_{i1}(t) = \omega_{n_i}^2(t)$$

$$\beta_{i2}(t) = 2\zeta\omega_{n_i}(t) - \frac{\dot{\omega}_{n_i}(t)}{\omega_{n_i}(t)}$$

It is noted that, while the roll and yaw channels appear to be decoupled in the transformed coordinates, the actual roll-yaw channels are still coupled by the inverse coordinate transformation. However, as will be shown in the next section, the decoupling performance accomplished by the present controller without any attempt at minimizing the roll-yaw coupling has already performed comparable to some optimal LTI eigenstructure assignment decoupling controllers applied to LTI plants. Further improvement on decoupling can be accomplished using the LTV PD-eigenstructure assignment *cf.* [129], which is currently being implemented.

The roll-yaw autopilot was implemented and tested using MATLAB/SIMULINK All simulations use the nonlinear equations of motion found in [86] with the pitch terms set to zero. The first simulation validates the design for the nominal plant model (3.1) without any perturbations but with actuator dynamics given by $\frac{1}{\tau s+1}$. For this simulation, $\omega_{n1,2}$ are set to a constant value 20 with $\zeta_{1,2} = 0.8$. The results for tracking a smoothed step command of 180° roll are shown in figures 5.35-38. Filtering of step commands is essential to assure that the commanded trajectory as applied to the autopilot is achievable within the allowable roll rate of 500°/second. Figure 5.35 shows the commanded roll

angle profile. Figure 5.36 shows the errors between the outputs of interest and the filtered commands, which are the roll angle and the sideslip angle. These errors are in the order of .1 degrees. Figure 5.37 compares the nominal actuator deflections $\overline{\delta}_p$ and $\overline{\delta}_r$ with the total actuator deflections δ_p and δ_r, respectively. The difference is in the order of .1 degrees, which shows the effectiveness of the simple nonlinear plant inverse.

The second simulation is intended to test the inherent robustness of the designed autopilot and the effects of using time-varying PD-eigenvalues. This simulation includes actuator dynamics of $\frac{1}{\tau s+1}$, and perturbations in C_{lp}, C_{np}, C_{lr}, C_{nr}, and $C_{Y\beta}$ by $\pm 50\%$. The control objective is to track a smoothed square wave that alternates between 180° and 0°, and switches every second. Figure 5.39 shows the natural frequencies of each PD-eigenvalue pair as a function of time with $\zeta_{1,2} = 0.8$. The PD-spectral synthesis of the LTV error dynamics safely schedules this commanded feedback control law. This simple spectrum is chosen to illuminate the changes in the closed loop behavior with respect to the PD-spectrum of the error dynamics. Figure 5.40 shows the roll angle tracking performance in six different perturbation cases, where C_{lp} and C_{np} are simultaneously perturbed; C_{lr} C_{nr} are also simultaneously perturbed, and $C_{Y\beta}$ is perturbed by itself. These seven trajectories include the commanded profile and the output when the five aerodynamic coefficients are perturbed by $\pm 50\%$. The worst case is for -50% C_{lp}, C_{np}. However, when ω_{n1} is switched to 20 this trajectory is made comparable to the others. Figure 5.41 shows the output of sideslip angle for the six different perturbation cases. Design constraints require that the sideslip angle remain below 5°, which is achieved for each case. These simulations show the improvement in performance as ω_n is switched from 5 to 20. Figures 5.42 and 5.43 respectively show the commanded actuator rates for δ_p and δ_r, which show that they are well below the allowable rate limit of 500°/second.

These simulation figures show that improved tracking performance is gained at the cost of increased actuator activities. Although the actuator rates are still within the design

specifications, the increased actuator activity at higher ω_n requires more control energy and tend to excite unmodeled structural modes. The time-varying spectrum allow for real-time tradeoff between tracking accuracy and energy consumption, and between robustness to regular perturbations (parametric uncertainty) and singular perturbations (parasitic dynamics).

Due to space limitation, no detailed comparisons with other nonlinear controllers will be made here. However, it is useful to briefly compare the results here with feedback linearization (FL) and sliding mode control (SMC), both of which are described in [101]. The nominal performance here is comparable to both of those designs. However, FL does not have the inherent robustness properties of this method and is especially unsuited to handling the unmodeled dynamics of the actuators. Additionally, SMC relies on controller discontinuity to achieve robust performance even with the unmodeled actuator dynamics; but exhibits tremendous actuator activity.

The third simulation is intended to study the inherent decoupling capability of the designed autopilot. Figure 5.44 displays the closed loop response to an initial deviation of 1° of sideslip. The results can be compared with those found in similar problems, *cf.* [116]. This simulation demonstrates the potential decoupling capability of time-varying control techniques.

The simulation results show that the proposed control design method based on nonlinear inversion with PD-spectrum assignment tracking error stabilization has the potential to be applied to nonlinear missile autopilots and general MIMO controllers. The controller structure exhibits considerable inherent robustness and decoupling capability without high actuator activity, providing a useful framework for dealing with truly NLTV problems. The time-varying closed-loop PD-spectrum allow real-time adjustment of bandwidth, thereby achieving in flight tradeoffs between performance, energy consumption, robustness and other operation concerns.

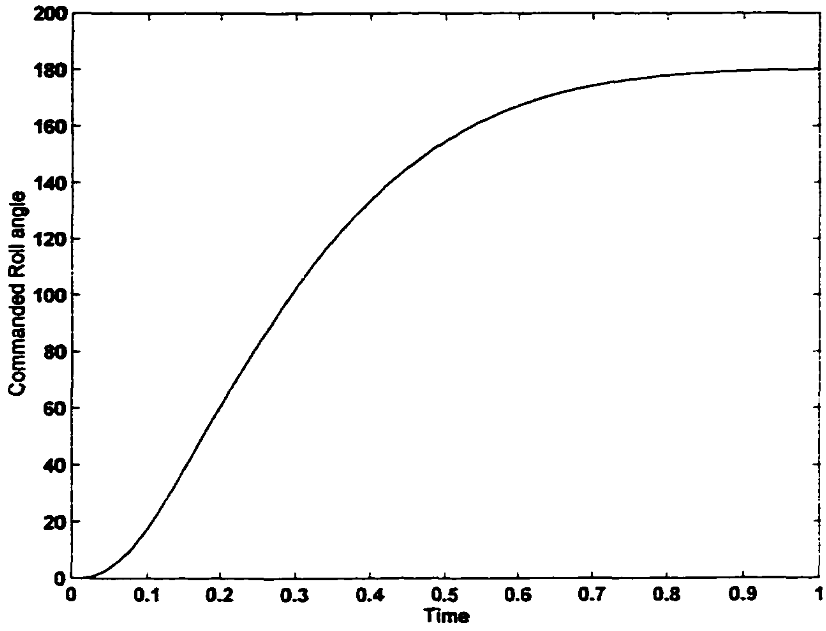

Figure 5.35. Desired Roll Angle Trajectory

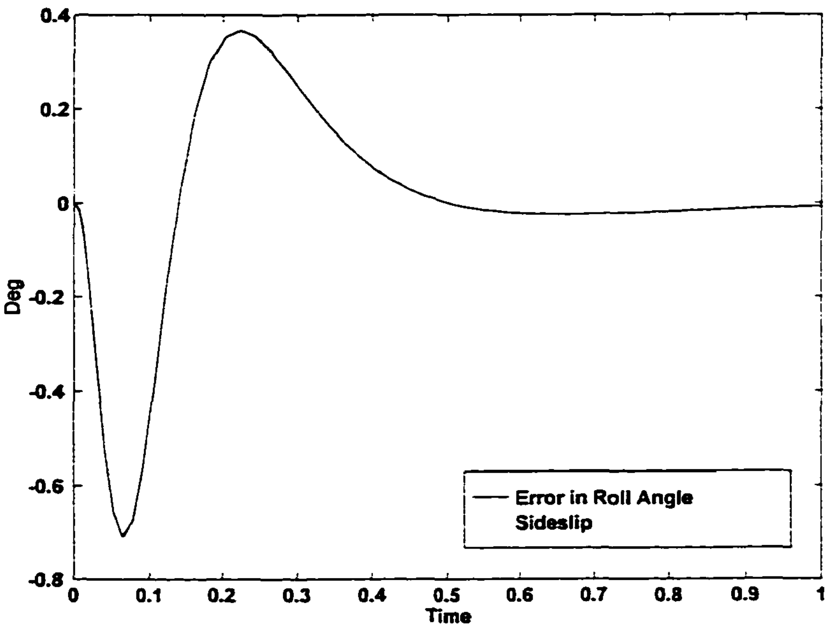

Figure 5.36 Tracking Errors

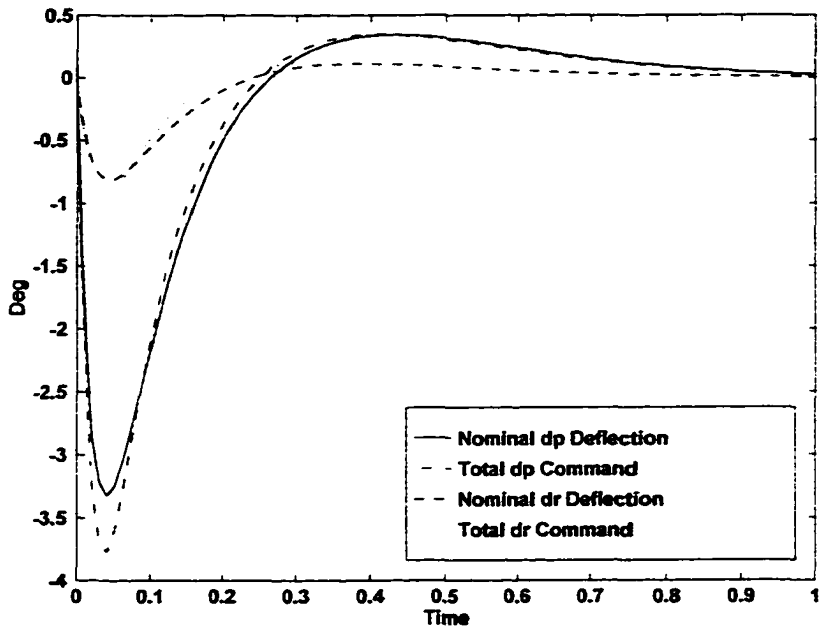

Figure 5.37 Behavior of δ_p

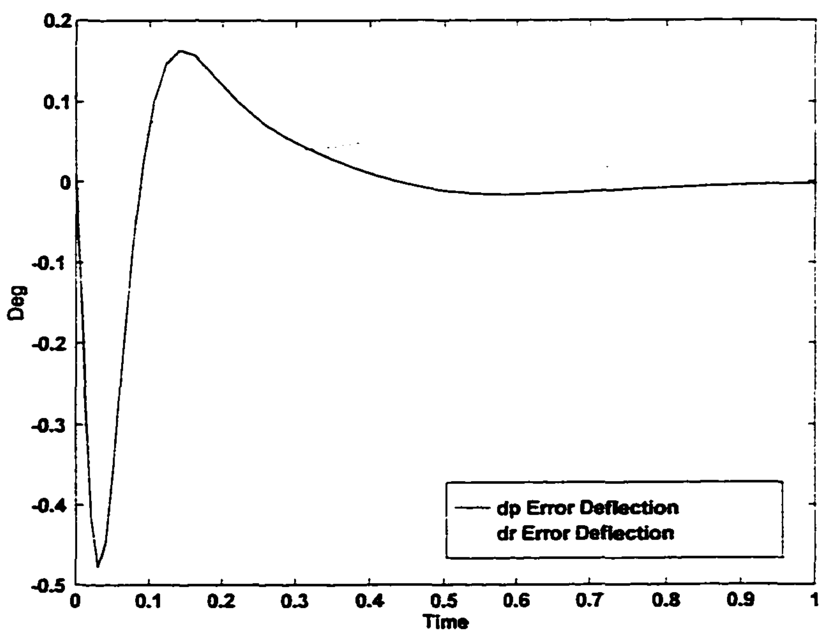

Figure 5.38 Behavior of δ_r

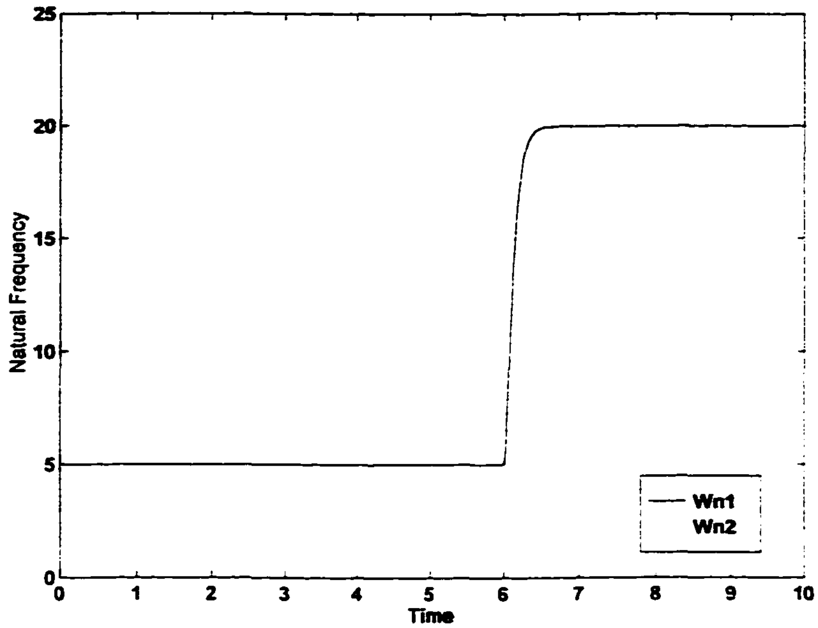

Figure 5.39 Natural Frequency for the PD-Spectrum

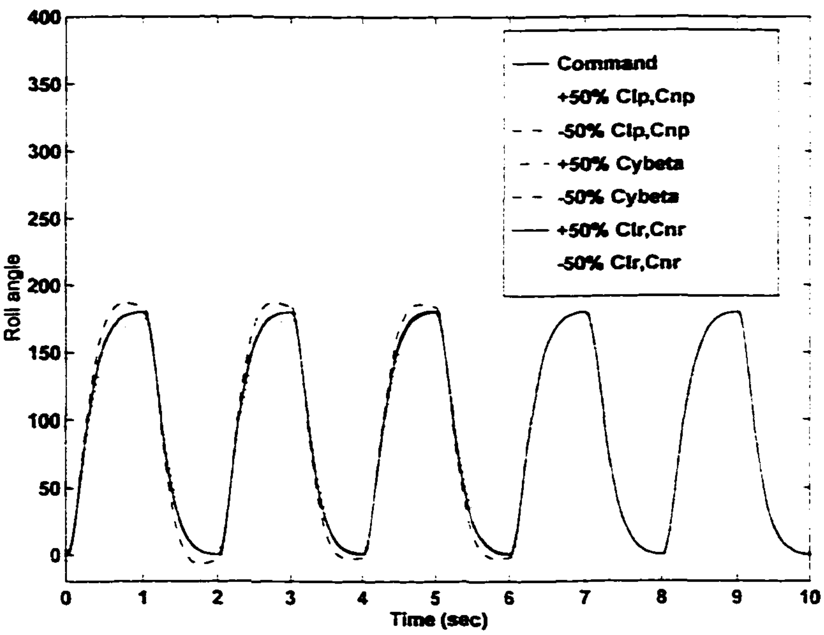

Figure 5.40 Robustness Test for Roll Angle Tracking

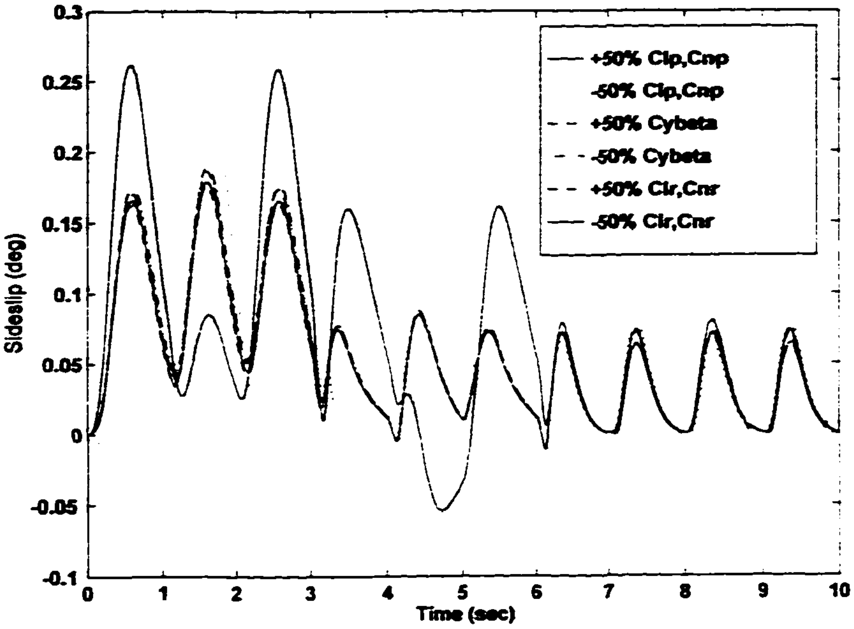

Figure 5.41 Robustness Test for Sideslip Angle

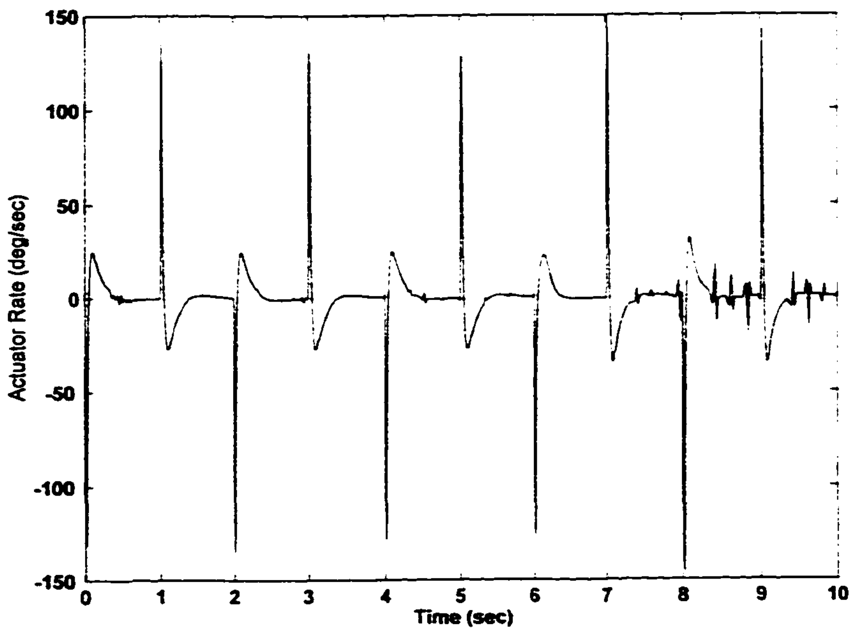

Figure 5.42 Commanded Actuator Rate for δ_p

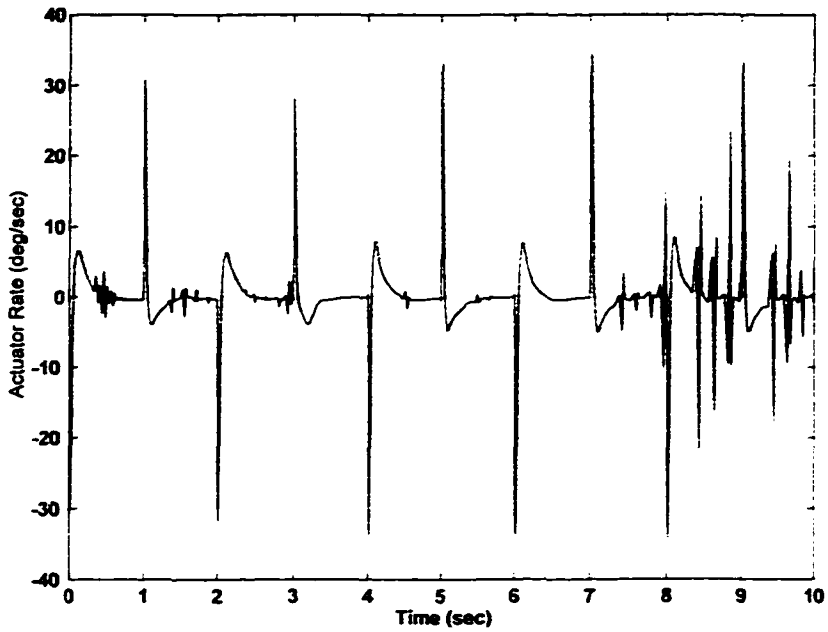

Figure 5.43 Commanded Actuator Rate for δ_r

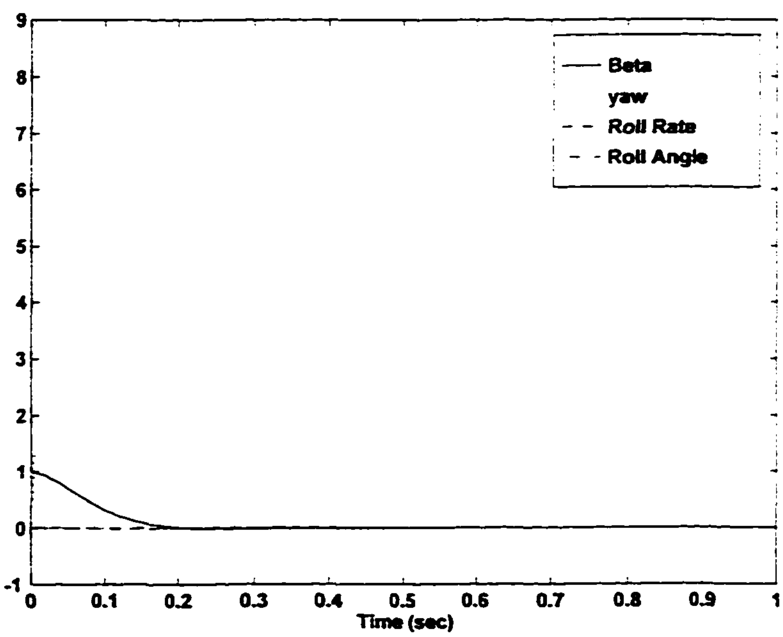

Figure 5.44 State Response to Initial Conditions on Sideslip

5.5 - Bank-To-Turn Roll-Yaw-Pitch Autopilot Design

This section extends the design of a trajectory tracking controller for the 4DOF roll-yaw EMRAAT missile autopilot presented in the preceding section to the 6DOF roll-yaw-pitch autopilot. After some introductory information, the design method is meticulously detailed. The simulation results compare the inherent robustness of the trajectory linearization method with two other nonlinear design methods which have been applied to similar problems.

The full EMRAAT missile model of appendix B will be the plant to be controlled. Due to limitations on the effectors, the ability to simultaneously pitch and roll is limited. As a practical method to avoid actuator deflection or rate saturation, the autopilot will be designed to realize two basic maneuvers. The first type of maneuver is to roll to a desired bank angle. This type of maneuver will be used to rotate the missile so that the target is in the primary lift plane. The second type of maneuver is a simple pitch. The autopilot will track a desired angle of attack to place the missile on a target trajectory. Autopilots that track such maneuvers are called Planar Bank-To-Turn (PBTT). In the sequel, the autopilot wili be designed specifically to handle PBTT maneuvers. However, the trajectory linearization controller will track any command trajectory that falls in the performance capabilities of the missile and within the actuator limits. This means that this autopilot can realize the hybrid problem of skidding for small maneuvers, tracking BTT maneuvers within the given limits, or tracking PBTT maneuvers. The use of BTT maneuvers must be selected very careful, as maneuvers beyond the limit of the actuators will cause saturation and can lead to loss of stability. This is an inherent limitation of the plant.

The three measured outputs of the plant are chosen to be AOA α, bank angle Φ, and sideslip angle β. The objectives of the PBTT autopilot is to robustly track bank angle

changes, and AOA commands. The autopilot must also maintain the following during a bank angle maneuver

1) Sideslip angle less than 5°

2) Rapid and precise command following for bank angle commands not exceeding 180°

3) Control Surface deflections less than 45°

4) Actuator rates less than 500°/sec

5) Roll rate not to exceed 500°/sec

6) Asymptotically stable lateral and longitudinal dynamics.

During pitch maneuvers the autopilot must maintain

1) Sideslip angle less than 5°

2) Rapid and precise command following of angle-of-attack commands up to 20°

3) Control surface deflections less than 45°

4) Actuator rates less than 500°/sec

5) Stable lateral dynamics

The sideslip must remain below 5° at all times because the EMRAAT uses an air breathing propulsion which could be choked by greater sideslip angles, additionally this insures the validity of certain simplifying assumptions on the nonlinear model. Precise and rapid tracking is an obvious requirement as well as stability. The roll rate limit is to keep from exciting unmodeled dynamics, and the other limitations are inherent in the hardware.

We will now state the structure of the nonlinear EMRAAT missile model. A more complete description including the numerical values are contained in appendix B. The states ξ are respectively angle of attack (AOA) α, pitch rate q, bank angle Φ, roll rate p, sideslip β, and yaw rate r. The inputs δ are the three virtual fin deflections δ_q, δ_p, and δ_r. The state space description of the plant is given by

$$\begin{bmatrix} \dot{\alpha} \\ \dot{q} \\ \dot{\Phi} \\ \dot{p} \\ \dot{\beta} \\ \dot{r} \end{bmatrix} = \begin{bmatrix} f_\alpha(\xi,\delta) \\ f_q(\xi,\delta) \\ f_\Phi(\xi,\delta) \\ f_p(\xi,\delta) \\ f_\beta(\xi,\delta) \\ f_r(\xi,\delta) \end{bmatrix} = f_a(\xi,\delta)$$

where

$$f_\alpha(x,\delta) = q - a_3 + k_{11}a_2 + k_{12}a_1$$

$$f_q(x,\delta) = k_{21}p^2 + k_{22}q^2 + k_{23}r^2 + k_{24}pq + k_{25}pr + k_{26}qr + k_{27}p + k_{28}q +$$

$$+ k_{29}r + k_{2a}a_3 + k_{2b}a_2 + k_{2c}a_1 + k_{2d}\alpha + k_{2e}\beta + k_{2f}\delta_p + k_{2g}\delta_q + k_{2h}\delta_r$$

$$f_\Phi(x,\delta) = p + \dot{\psi}\sin\theta = p + (q\sin\phi + r\sin\phi)\tan\theta$$

$$f_p(x,\delta) = k_{41}p^2 + k_{42}q^2 + k_{43}r^2 + k_{44}pq + k_{45}pr + k_{46}qr + k_{47}p + k_{48}q +$$

$$+ k_{49}r + k_{4a}a_3 + k_{4b}a_2 + k_{4c}a_1 + k_{4d}\alpha + k_{4e}\beta + k_{4f}\delta_p + k_{4g}\delta_q + k_{4h}\delta_r$$

$$f_\beta(x,\delta) = p\sin\alpha - r\cos\alpha + (k_{51}\beta + k_{52}p + k_{53}r + k_{54}\delta_p + k_{55}\delta_r)\cos\beta +$$

$$+ k_{56}\cos\theta\sin\phi\cos\beta$$

$$f_r(x,\delta) = k_{61}p^2 + k_{62}q^2 + k_{63}r^2 + k_{64}pq + k_{65}pr + k_{66}qr + k_{67}p + k_{68}q +$$

$$+ k_{69}r + k_{6a}a_3 + k_{6b}a_2 + k_{6c}a_1 + k_{6d}\alpha + k_{6e}\beta + k_{6f}\delta_p + k_{6g}\delta_q + k_{6h}\delta_r$$

$$a_1 = (k_{71}\alpha + k_{72}q + k_{73}\delta_q)\cos\alpha\sec\beta$$

$$a_2 = (\cos\alpha\cos\phi\cos\theta + \sin\alpha\sin\theta)\sec\beta$$

$$a_3 = \tan\beta(p\cos\alpha - r\sin\alpha)$$

The exogenous states of yaw and pitch angle are given by

$$\dot{\psi} = \sec\theta(q\sin\phi + r\cos\phi)$$

$$\dot{\theta} = q\cos\phi - r\sin\phi$$

Additionally, each input is effected through an actuator modeled by

$$\delta_x = \frac{1}{\tau s + 1}\delta_{xc}, \text{ with } \tau = .0064.$$

PBTT commands consist of two primary maneuvers. The first is a bank angle change, and the second is to track a desired angle of attack. This separation has led to separate autopilot designs. One achieves bank angle tracking while regulating pitch and yaw. The other regulates the roll and yaw while effecting a pitching maneuver. We will design a trajectory tracking autopilot which can effectively handle both. Indeed, as mentioned earlier, it will realize any maneuver that falls within the capability of the missile. This design has the inherent benefit in that only one complete design is required to achieve both objectives.

In implementing this design, a few simplifying assumptions have been made. First, the derivative of Φ is assumed to be p. This is a reasonable assumption as most flight is nearly level and yawing is to be kept small, which means that term $r(t)\sin\theta$ is nearly zero. Second, the actuator dynamics are assumed to be sufficiently fast to be ignored in the design. Third, k_{73}, k_{54}, and k_{55} are assumed to be zero. This assumption in effect ignores the zero dynamics in the yaw and pitch channels of the plant. In this case the zero dynamics are fast enough to be ignored. This assumption is common in autopilot design, particularly in inversion designs such as feedback linearization. This is a form of output redefinition that is useful in handling nonminimum phase systems.

With these assumptions and the outputs chosen as $[\alpha \quad \Phi \quad \beta]^T$ the model used for the design is given by

$$\dot{\xi} = f_m(\xi, \delta) = f(\xi) + g(\xi)\delta$$

$$y = \begin{bmatrix} \alpha \\ \Phi \\ \beta \end{bmatrix} = \begin{bmatrix} h_1(\xi) \\ h_2(\xi) \\ h_3(\xi) \end{bmatrix}$$

The first derivative of α with respect to t is

$$\frac{d\alpha}{dt} = L_f h_1 + L_g h_1$$

$$= q - \tan\beta(p\cos\alpha - r\sin\alpha) + k_{11}(\cos\alpha\cos\phi\cos\theta + \sin\alpha\sin\theta)\sec\beta +$$

$$+ k_{12}(k_{71}\alpha + k_{72}q)\cos\alpha\sec\beta$$

which is not a function of the input. Taking a second derivative with respect to time gives

$$\frac{d^2\alpha}{dt} = L_f^2 h_1 + L_g L_f h_1$$

$$= L_f^2 h_1 + k_{2f}\delta_p + k_{2g}\delta_q + k_{2h}\delta_r$$

which is a function of the inputs. Thus the pitch channel is of relative degree 2. Similarly, the other two channels are also of relative degree two

$$\ddot{\Phi} = L_f^2 h_2 + L_g L_f h_2$$

$$\ddot{\beta} = L_f^2 h_3 + L_g L_f h_3$$

and the vector relative degree of the system is $[2 \quad 2 \quad 2]^T$. The input-output relation is given by

$$\begin{bmatrix} \ddot{\alpha} \\ \ddot{\Phi} \\ \ddot{\beta} \end{bmatrix} = \begin{bmatrix} L_f^2 h_1 \\ L_f^2 h_2 \\ L_f^2 h_3 \end{bmatrix} + \begin{bmatrix} k_{2q} & k_{2f} & k_{2h} \\ k_{4g} & k_{4f} & k_{4h} \\ k_{6g} & k_{6f} & k_{6h} \end{bmatrix} \begin{bmatrix} \delta_q \\ \delta_p \\ \delta_r \end{bmatrix}$$

In order to generate an inverse $y \rightarrow \delta$ derivatives up to the second order of the three outputs are required. As such information is not assumed available from the guidance, an

estimate is necessary. Three filters are used to give a bandwidth limited approximation of the command. The filter is of the form

$$G_i(s) = \frac{a_{i1}}{s^3 + a_{i3}s^2 + a_{i2}s + a_{i1}}$$

with the filter constants a_{ij} chosen to stabilize the filter and fast enough to track signals that fall within the performance requirements of the plant. The filtered output and the first two derivatives can be generated from a realization in the same form as figure 5.18.

Four of the nominal states are determined by the commanded outputs.

$$\begin{bmatrix} \bar{\xi}_1 \\ \bar{\xi}_3 \\ \bar{\xi}_4 \\ \bar{\xi}_5 \end{bmatrix} = \begin{bmatrix} \widehat{\alpha} \\ \widehat{\Phi} \\ \dot{\widehat{\Phi}} \\ \widehat{\beta} \end{bmatrix}$$

These nominal states can be used to solve for approximations of the other two. However, this can be rather tedious and in this case adequate results are achieved by using the other two true states. With these 6 nominal states the pseudo-inverse that generates the nominal control $\bar{\delta}$ can be realized with

$$y \longrightarrow \delta : \bar{\delta} = \begin{bmatrix} k_{2q} & k_{2f} & k_{2h} \\ k_{4g} & k_{4f} & k_{4h} \\ k_{6g} & k_{6f} & k_{6h} \end{bmatrix}^{-1} \left(\begin{bmatrix} \widehat{y}_1^{(2)} \\ \widehat{y}_2^{(2)} \\ \widehat{y}_3^{(2)} \end{bmatrix} - \begin{bmatrix} L_f^2 h_1(\bar{\xi}) \\ L_f^2 h_2(\bar{\xi}) \\ L_f^2 h_3(\bar{\xi}) \end{bmatrix} \right)$$

The input matrix is invertible and thus this pseudo-inversion is valid for all command trajectories.

With the pseudo-inversion, a nominal control that approximately generates the desired trajectory has been developed. What is required now is a trajectory stabilizing controller which can minimize the errors inherent in the approximate nature of this pseudo-inverse and force the plant output to follow the desired trajectory. The first step

is to linearize the error dynamics about the nominal trajectory. The linearized error dynamics are given by

$$\dot{\boldsymbol{x}} = \boldsymbol{A}(t)\boldsymbol{x} + \boldsymbol{B}(t)\boldsymbol{u}$$

$$\boldsymbol{z} = \boldsymbol{C}\boldsymbol{x}$$

where

$$\boldsymbol{A}(t) = \frac{\partial}{\partial \boldsymbol{\xi}} f_m(\overline{\boldsymbol{\xi}}, \overline{\boldsymbol{\delta}}),\ \boldsymbol{B}(t) = \frac{\partial}{\partial \boldsymbol{\delta}} f_m(\overline{\boldsymbol{\xi}}, \overline{\boldsymbol{\delta}}),\ \text{and}\ \boldsymbol{C}(t) = \frac{\partial}{\partial \boldsymbol{\xi}} h(\overline{\boldsymbol{\xi}})$$

A unique transformation to phase variable canonical form exists. The linearized output errors are all of relative degree 2, and the output matrix is constant. With these facts, the derivatives of the ith output w.r.t. t are

$$z_i = c_i \boldsymbol{x}(t)$$

$$\dot{z}_i = c_i \boldsymbol{A}(t)\boldsymbol{x}(t)$$

$$\ddot{z}_i = c_i(\dot{\boldsymbol{A}}(t) + \boldsymbol{A}^2(t))\boldsymbol{x}(t) + c_i \boldsymbol{A}(t)\boldsymbol{B}(t)\boldsymbol{u}$$

The second derivatives of the output can be written as

$$\ddot{\boldsymbol{z}} = \boldsymbol{C}(\dot{\boldsymbol{A}}(t) + \boldsymbol{A}^2(t))\boldsymbol{x}(t) + \boldsymbol{C}\boldsymbol{A}(t)\boldsymbol{B}(t)\boldsymbol{u} \tag{5.11}$$

We now define a time varying matrix $\boldsymbol{M}(t)$ that relates the outputs and first derivatives with the error states where

$$\begin{bmatrix} z_1 \\ \dot{z}_1 \\ z_2 \\ \dot{z}_2 \\ z_3 \\ \dot{z}_3 \end{bmatrix} = \boldsymbol{M}(t)\boldsymbol{x}(t) = \begin{bmatrix} c_1 \\ c_1\boldsymbol{A}(t) \\ c_2 \\ c_2\boldsymbol{A}(t) \\ c_3 \\ c_3\boldsymbol{A}(t) \end{bmatrix} \boldsymbol{x}(t)$$

It is important to note that $\boldsymbol{M}(t)$ is a square row wise rearrangement of the first two elements of the output matrix. $\boldsymbol{M}(t)$ is a function of the nominal state trajectories. It is determined to be bounded, invertible, and have a bounded derivative for all commanded

trajectories. This means that $\boldsymbol{M}(t)$ is a Lyapunov transformation that preserves the stability and thus a feedback that uniformly exponentially stabilizes the realization of the transformed system by PD-spectrum assignment will uniformly exponentially stabilize the LTV error dynamics of the original realization and thus will achieve exponential tracking of the desired trajectory. Using the relation between the states and the outputs equation 5.11 can be rewritten as

$$\ddot{\boldsymbol{z}} = \boldsymbol{C}(\dot{\boldsymbol{A}}(t) + \boldsymbol{A}^2(t))\boldsymbol{M}(t)^{-1} \begin{bmatrix} z_1 \\ \dot{z}_1 \\ z_2 \\ \dot{z}_2 \\ z_3 \\ \dot{z}_3 \end{bmatrix} + \boldsymbol{C}\boldsymbol{A}(t)\boldsymbol{B}(t)\boldsymbol{u}(t)$$

$$= \boldsymbol{P}(t) \begin{bmatrix} z_1 \\ \dot{z}_1 \\ z_2 \\ \dot{z}_2 \\ z_3 \\ \dot{z}_3 \end{bmatrix} + \boldsymbol{Q}(t)\boldsymbol{u}(t)$$

Then the system matrix is in phase variable form. Next, since $\boldsymbol{C}\boldsymbol{A}(t)\boldsymbol{B}(t)$ is invertible for any nominal trajectory where $\alpha_c < 90°$ it is possible to make an input transformation

$$v(t) = (\boldsymbol{C}\boldsymbol{A}(t)\boldsymbol{B}(t))^{-1}\boldsymbol{u}(t)$$

so that 5.11 can be represented by

$$\ddot{\boldsymbol{z}} = \boldsymbol{C}(\dot{\boldsymbol{A}}(t) + \boldsymbol{A}^2(t))\boldsymbol{M}(t)^{-1} \begin{bmatrix} z_1 \\ \dot{z}_1 \\ z_2 \\ \dot{z}_2 \\ z_3 \\ \dot{z}_3 \end{bmatrix} + \boldsymbol{I}_3\boldsymbol{v}(t)$$

Defining the new states as the outputs and their first derivatives of the above equations according to the relation

$$\begin{bmatrix} w_1 \\ w_2 \\ w_3 \\ w_4 \\ w_5 \\ w_6 \end{bmatrix} := \begin{bmatrix} z_1 \\ \dot{z}_1 \\ z_2 \\ \dot{z}_2 \\ z_3 \\ \dot{z}_3 \end{bmatrix} = \boldsymbol{M}(t)\boldsymbol{x}(t)$$

gives a system in the desired input decoupled MVPV canonical form

$$\dot{\boldsymbol{w}} = \begin{bmatrix} 0 & 1 & 0 & 0 & 0 & 0 \\ p_{11}(t) & p_{12}(t) & p_{13}(t) & p_{14}(t) & p_{15}(t) & p_{16}(t) \\ 0 & 0 & 0 & 1 & 0 & 0 \\ p_{21}(t) & p_{22}(t) & p_{23}(t) & p_{24}(t) & p_{25}(t) & p_{26}(t) \\ 0 & 0 & 0 & 0 & 0 & 1 \\ p_{31}(t) & p_{32}(t) & p_{33}(t) & p_{34}(t) & p_{35}(t) & p_{36}(t) \end{bmatrix} \boldsymbol{w} + \begin{bmatrix} 0 & 0 & 0 \\ 1 & 0 & 0 \\ 0 & 0 & 0 \\ 0 & 1 & 0 \\ 0 & 0 & 0 \\ 0 & 0 & 1 \end{bmatrix} v$$

The three diagonal blocks in the MVPV system matrix are of size 2×2 and thus 6 PD-eigenvalues must be assigned with two associated with each output error block. That is, there are two PD-eigenvalues associated with the pitch channel, two associated with the roll channel, and two associated with the yaw channel. The PD-synthesis equation for each block with 2 PD-eigenvalues $\rho_{i1,2}$ is given by

$$a_{i1} = \frac{\rho_{i1}\dot{\rho}_{i2} - \rho_{i1}\rho_{i2}^2 + \rho_{i2}\dot{\rho}_{i1} + \rho_{i2}\rho_{i1}^2}{\rho_{i1} - \rho_{i2}}$$

$$a_{i2} = \frac{\dot{\rho}_{i1} + \rho_{i1}^2 - \dot{\rho}_{i2} - \rho_{i2}^2}{\rho_{i2} - \rho_{i1}}$$

By using the error feedback

$$v = \begin{bmatrix} a_{11} - p_{11} & a_{12} - p_{12} & -p_{13} & -p_{14} & -p_{15} & -p_{16} \\ -p_{21} & -p_{22} & a_{21} - p_{23} & a_{12} - p_{24} & -p_{25} & -p_{26} \\ -p_{31} & -p_{32} & -p_{33} & -p_{34} & a_{31} - p_{35} & a_{32} - p_{36} \end{bmatrix} \boldsymbol{w}$$

$$= \mathbf{K}(t)\boldsymbol{w}$$

the closed loop error dynamics are given by

$$\dot{w} = \begin{bmatrix} 0 & 1 & 0 & 0 & 0 & 0 \\ a_{11}(t) & a_{12}(t) & 0 & 0 & 0 & 0 \\ 0 & 0 & 0 & 1 & 0 & 0 \\ 0 & 0 & a_{21}(t) & a_{22}(t) & 0 & 0 \\ 0 & 0 & 0 & 0 & 0 & 1 \\ 0 & 0 & 0 & 0 & a_{31}(t) & a_{32}(t) \end{bmatrix} w$$

Thus the PD-eigenvalues of each block form the PD-eigenvalues of the 6×6 full system matrix. Finally, this form clearly illustrates a useful property of this method of assigning PD-eigenvalues to the error dynamics. Each error channel is output decoupled by making the states coincide with the output. This means that nothing more is needed to achieve output decoupling.

The trajectory linearizaiton design will be compared to two other common nonlinear design methods. The first is a dynamic inversion method developed by Snell [103]. His design was a flight control problem for a Super maneuverable aircraft. He compared the performance of his design with a typical Gain Scheduled design and achieved considerable performance improvement. This method has been modified to create a PBTT Autopilot. The second design is by feedback linearization, *cf.* [101].

The same assumptions used in the trajectory linearization design will be made in the dynamic inversion design. The nominal nonlinear model is

$$\dot{\xi} = f(\xi) + g(\xi)\delta$$

Following Snell's design we divide the plant into fast and slow dynamics. Angle of attack, roll angle, and sideslip angle are the so called slow states which are also the outputs. Pitch rate, roll rate, and yaw rate are the fast states which will be used to drive the slow rates to the desired values. We will rewrite the nonlinear equation in terms of the fast and slow subsystems.

$$\dot{\xi} = f_s(\xi) + f_f(\xi) + g(\xi)\delta$$

$$= \begin{bmatrix} f_\alpha(\xi) \\ 0 \\ f_\Phi(\xi) \\ 0 \\ f_\beta(\xi) \\ 0 \end{bmatrix} + \begin{bmatrix} 0 \\ f_q(\xi) \\ 0 \\ f_p(\xi) \\ 0 \\ f_r(\xi) \end{bmatrix} + g(\xi)\delta$$

With the fast and slow dynamics so defined, the tracking problem will be reduced to an inner loop and an outer loop. The outer loop uses the fast states as inputs to the slow dynamics to cause the slow states to achieve the desired outputs. The purpose of the inner loop is to cause the fast states to achieve the desired trajectories as required by the outer loop. This design can be considered as a singular perturbation design, and thus the rates must be sufficiently separated.

First we will consider the outer loop design. The slow dynamics are given by

$$\begin{bmatrix} \dot{\alpha} \\ \dot{\Phi} \\ \dot{\beta} \end{bmatrix} = \begin{bmatrix} f_\alpha(\xi) \\ f_\Phi(\xi) \\ f_\beta(\xi) \end{bmatrix}$$

For many airframe problems including this one the nonlinear equations can be separated into

$$\begin{bmatrix} \dot{\alpha} \\ \dot{\Phi} \\ \dot{\beta} \end{bmatrix} = \begin{bmatrix} f_{\alpha s}(\xi_s) \\ f_{\Phi s}(\xi_s) \\ f_{\beta s}(\xi_s) \end{bmatrix} + g_{s1}(\xi_s) \begin{bmatrix} p \\ q \\ r \end{bmatrix} + g_{s2}(\xi)\delta$$

where the subscript s is used to designate that the object in question is solely a function of the slow states. Our assumptions already have $g_{s2}(\xi) = [0 \quad 0 \quad 0]^T$. Snell also makes this assumption and claims such assumptions are common in airframe design. Now the guidance system generates the output commands α_c, Φ_c, and β_c. The desired outputs are given by the closed outer loop dynamics

$$\dot{\alpha}_d = \omega_\alpha(\alpha_c - \alpha)$$

$$\dot{\Phi}_d = \omega_\Phi(\Phi_c - \Phi)$$

$$\dot{\beta}_d = \omega_\beta(\beta_c - \beta)$$

where ω_x is the outer loop bandwidth of the x channel. This outer loop is slightly different as an aircraft requires that the airframe tracks a roll rate and the missile autopilot must track a desired bank angle. The fast states are used as inputs to drive the slower states. The slow input gain $g_{s1}$is defined by the kinematics and is thus the same for any airframe. This matrix is invertible for any sideslip except where $\cos\beta = 0$. Thus we can find the command values for the fast states by

$$\begin{bmatrix} q_c \\ p_c \\ r_c \end{bmatrix} = g_{s1}^{-1}(\xi_s)\left\{\begin{bmatrix} \dot{\alpha}_d \\ \dot{\Phi}_d \\ \dot{\beta}_d \end{bmatrix} - f_s(\xi_s)\right\}$$

The inner loop tracks the desired fast states. The desired fast dynamics are given by

$$\dot{q}_d = \omega_q(q_c - q)$$

$$\dot{p}_d = \omega_p(p_c - p)$$

$$\dot{r}_d = \omega_r(r_c - r)$$

where ω_y is the inner bandwidth of the y fast state. The inner bandwidth must be chosen to allow for good performance without exceeding the actuator limits and to avoid exciting unmodeled modes. The outer bandwidth must be chosen to achieve the output performance objectives and sufficiently below the bandwidth of the inner loop to avoid coupling between the inner and outer loop dynamics. The fast state dynamics are given by

$$\begin{bmatrix} \dot{q} \\ \dot{p} \\ \dot{r} \end{bmatrix} = \begin{bmatrix} f_q(\xi) \\ f_p(\xi) \\ f_r(\xi) \end{bmatrix} + g_f(\xi)\delta$$

The fast states input matrix $g_f(\xi)$ is invertible, so the inputs to achieve the desired fast states are given by

$$\delta = g_f^{-1}(\xi)\left\{\begin{bmatrix}\dot{q}_d\\ \dot{p}_d\\ \dot{r}_d\end{bmatrix} - \begin{bmatrix}f_q(\xi)\\ f_p(\xi)\\ f_r(\xi)\end{bmatrix}\right\}$$

The above design is equivalent to the design method presented by Snell. It was designed, implemented, and then simulated in *Simulink* on the complete nonlinear plant. The autopilot tracked the desired trajectories but exhibited undesirable transients in the angle of attack during large roll maneuvers. Simulation and testing led to a modification of the design which achieved much improved performance. The tail fin perturbation to angle of attack was found to lead to undesirable transient behavior. Explicit compensation of this disturbance term is used. In effect, an additional nonlinear cancellation is required in the pitch channel. To avoid an algebraic loop, a low pass filter approximation of the actuator output is given by

$$\delta_{qe} = \frac{k}{s+k}\delta_{qc}$$

Where δ_{qc} is the commanded pitch fin deflection. The actual fin deflection is determined by the actuator performance. This deflection estimate is then treated as a known disturbance and is explicitly canceled in the outer loop. The modified outer loop is

$$\begin{bmatrix}q_c\\ p_c\\ r_c\end{bmatrix} = g_{s1}^{-1}(\xi_s)\left\{\begin{bmatrix}\dot{\alpha}_d\\ \dot{\Phi}_d\\ \dot{\beta}_d\end{bmatrix} - g_{s2}\begin{bmatrix}\delta_{qe}\\ 0\\ 0\end{bmatrix} f_s(\xi_s)\right\}$$

Which results in excellent performance for the nominal plant.

The following plots show the results of the closed loop system for the nonlinear plants with three different design methods. All simulations include the actuator dynamics. The first simulation is based on the trajectory linearization method. The second simulation is based on the standard input-output feedback linearization design as outlined in Slotine [101]. The desired closed loop poles for each subsystem are the same for both the Feedback linearization and DAST designs. Each subsystem has two real

poles, one at -10 and one at -11. These poles were chosen to make a direct comparison of the inherent robustness in each design. The third simulation is based on the dynamic inversion design method.

Each simulation shows a four second profile in which the missile is commanded to roll to 180° at 0 seconds. At 1 second, the missile is to pitch to 20° of angle of attack and then to pitch down to 0° of angle of attack. At 3 seconds, the missile is to roll back to 0° of bank angle. The sideslip is to be kept below 5° at all times. Additionally, the roll rate and all three actuator rates should be kept below 500° per second. Each design was able to meet the design requirements for the nominal case. To test the inherent robustness of each design, the aerodynamic coefficient $C_{m\alpha}$ is perturbed by first $+20\%$, and then -20%. The aerodynamic coefficients are time varying parameters that are assumed to be within $\pm 20\%$ of the constant nominal value used in the design. Experiments determined that the closed loop system was more sensitive to perturbations in this coefficient for this maneuver and thus it was used for the test case. In fact perturbations of some of the other coefficients on the order of 1000% were found to have minimal effect on the performance in all three designs.

Figures 5.45-47 show the results of simulation 1. This simulation is an implementation of the DAST control strategy applied to the nonlinear missile. Figure 5.45 shows the AOA performance. The output for the perturbed plant is within 3.2° of the desired value. Figure 5.46 shows the bank angle performance. The performance does not show perceptible degradation for either perturbation. Figure 5.47 shows the sideslip is below .05° which is well within the 5° limit.

Figures 5.48-50 display the results of simulation 2. This simulation implements a feedback linearization with poles placed in the same location as in the first simulation. Figure 5.48 shows the AOA tracking capability in the perturbed cases. When the perturbation is -20%, the AOA reaches nearly 35°. This trajectory has probably exceeded the stall angle and would cause the missile to plummet and to possibly loose

stability. The bank angle is similar to case 1. While the sideslip angle is acceptable, it is an order of magnitude larger than that of case 1.

The third simulation is in figures 5.51-53. This simulation is based on Snell's nonlinear inversion and implements the design detailed above. The inner loop bandwidth for the fast states has been set to 20 rad/sec, and the outer bandwidth for the slow states has been set to 5 rad/sec. Simulation results have shown that these bandwidths keep the roll and actuator rates and magnitudes within the limits. The design objective is to increase the bandwidth sufficiently to achieve the specified performance, but not made so large that the actuator limits are exceeded or the roll rate exceeds the 500° per second that insures that the flexibility modes are not excited. Additionally, the bandwidth of the outer loop must be sufficiently distanced from the inner loop bandwidth to insure the validity of the assumption about the slowness of the inner with respect to the outer. Figure 5.51 shows that this design also has some problems. Namely, with a -20% perturbation on $C_{m\alpha}$ the AOA exceeds 30° for a command of 20. This design would also probably exceed the stall angle. Similarly, the bank angle performance is acceptable, while the sideslip shows a marked increase, but still falls well below the limits.

The dynamic inversion design is easy to implement and achieved good performance for the nominal case after one modification. This design was the only one in which the simplifying assumptions about the zero dynamics were found to cause unacceptable transient performance. Early simulations indicated that these assumptions were causing a large disturbance in the angle-of-attack during role maneuvers. Thus the design had to be modified to account for the pitching effect caused during rolling. After the modifications, the design was found to be satisfactory for the nominal system. Unfortunately, it is very difficult to predict the behavior of the closed loop perturbed nonlinear system or to design for greater robustness.

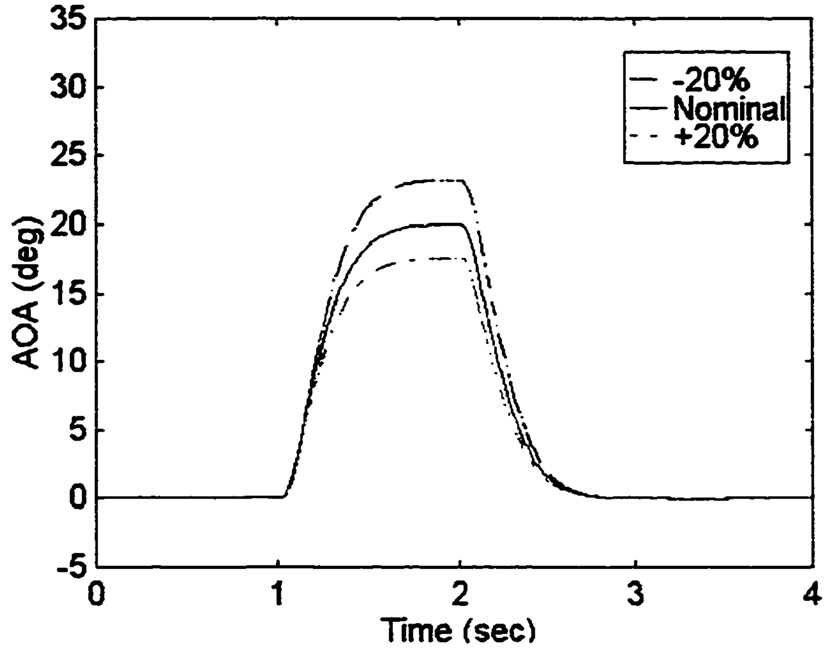

Figure 5.45 AOA Tracking with DAST Stabilization

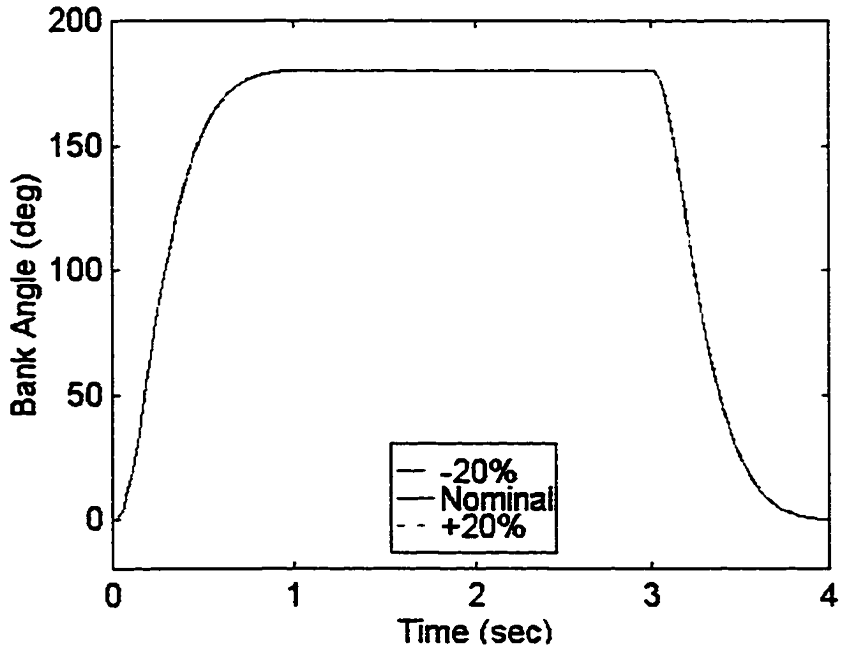

Figure 5.46 Bank Angle Tracking with DAST Stabilization

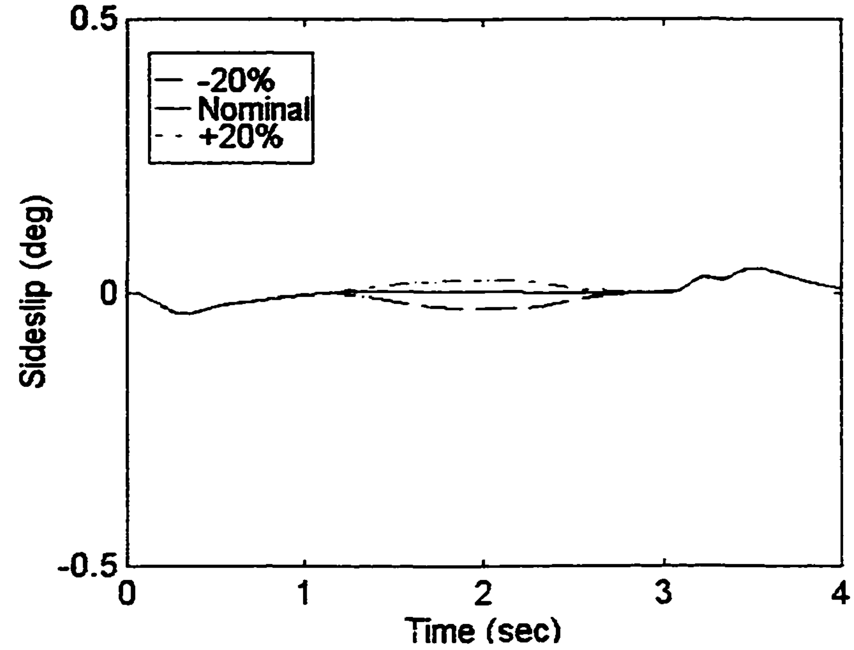

Figure 5.47 Sideslip with DAST Stabilization

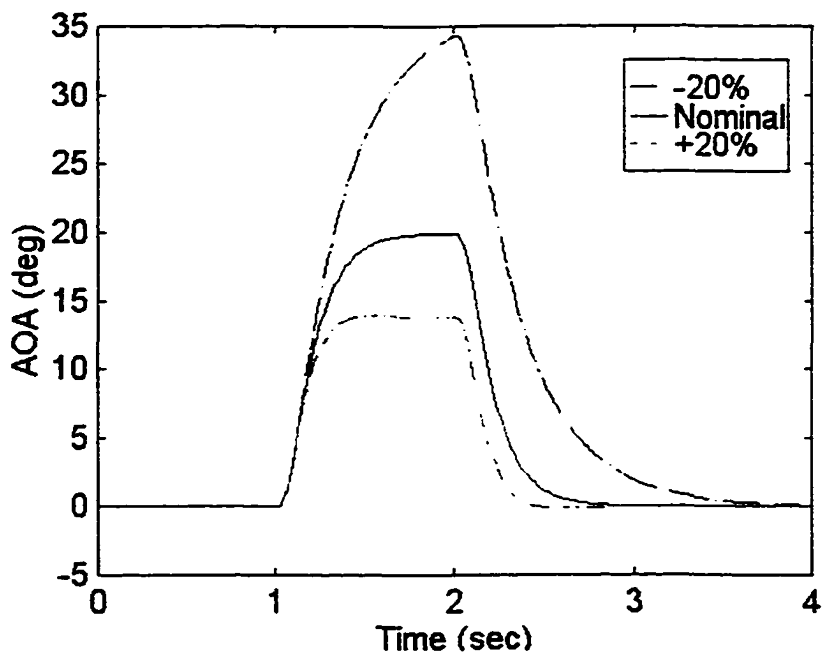

Figure 5.48 AOA Tracking with Feedback Linearization

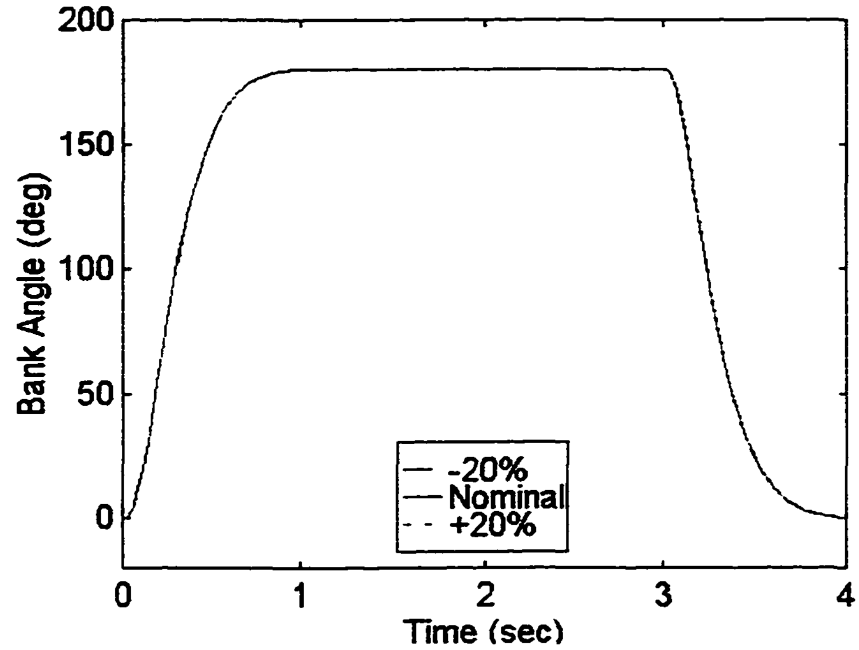

Figure 5.49 Bank Angle Tracking with Feedback Linearization

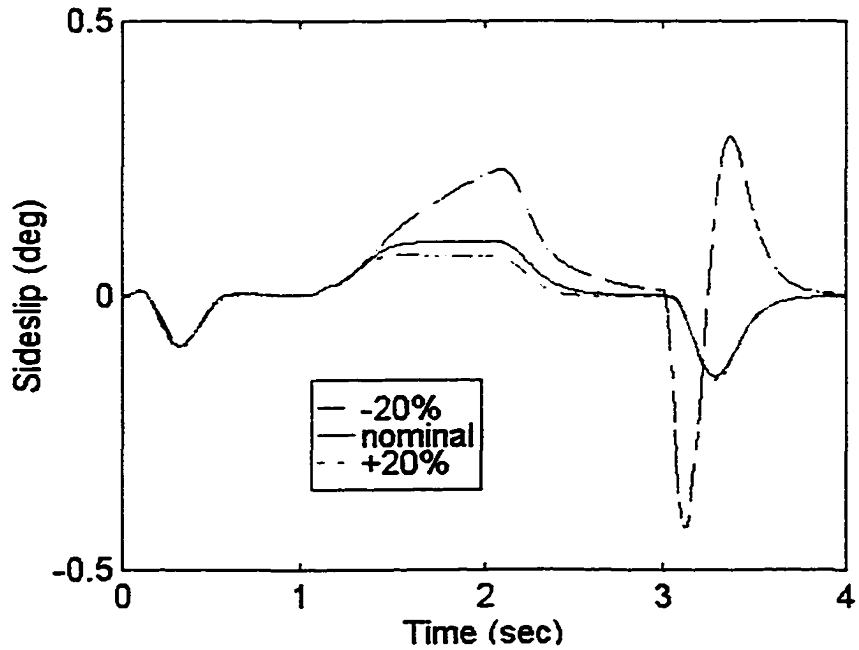

Figure 5.50 Sideslip with Feedback Linearization

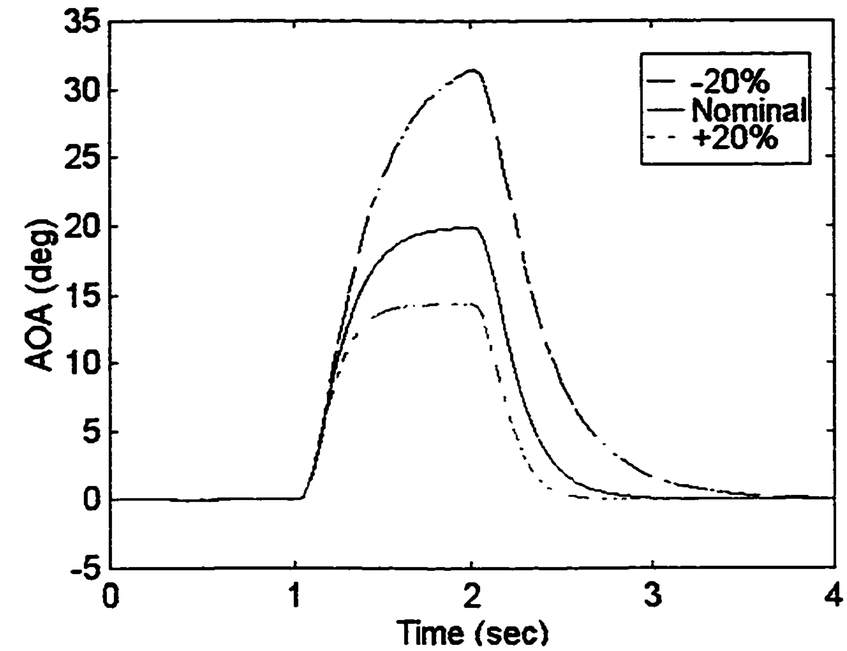

Figure 5.51 AOA Tracking with Nonlinear Inversion

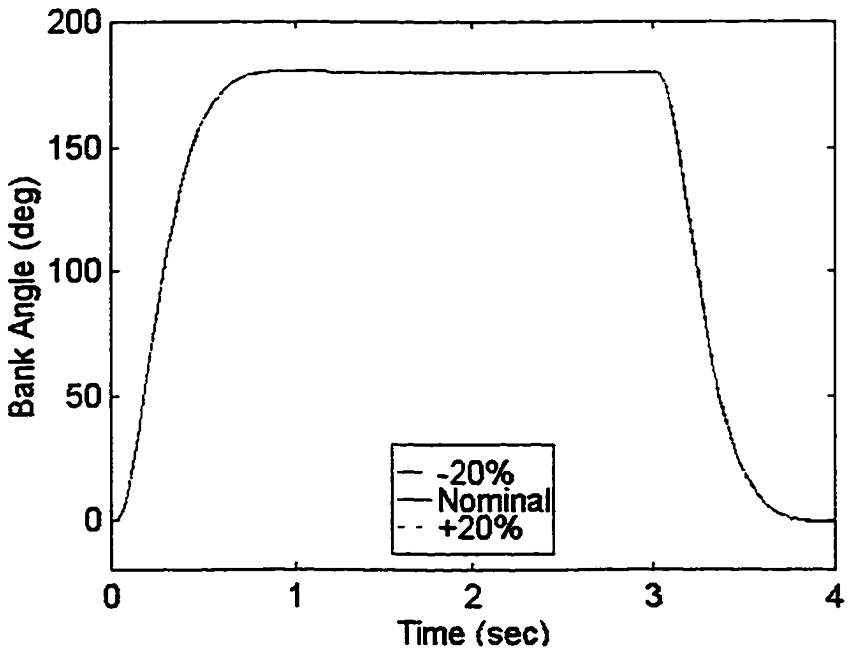

Figure 5.52 Bank Angle Tracking with Nonlinear Inversion

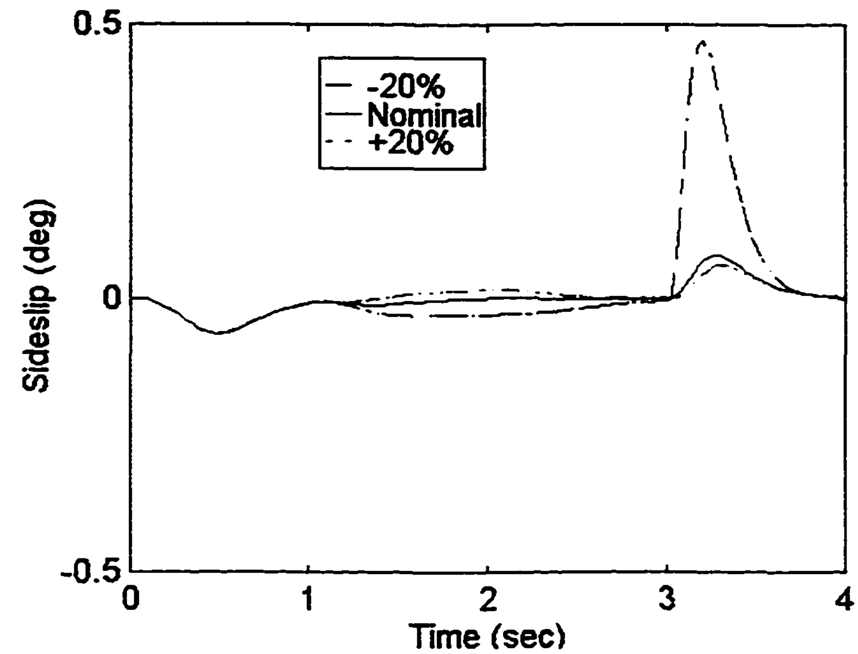

Figure 5.53 Sideslip with Nonlinear Inversion

Due to the non-axisymmetric configuration, the coupling from sideslip to roll of the EMRAAT missile is very large. Such coupling can lead to large sensitivity to wind gusts which could destabilize the system for relatively small disturbances. Also, this coupling could lead to decreased performance in the end game resulting in a clean miss of the target as the missile guidance system commands the most demanding trajectories to compensate for the pilots attempts at evasion. Thus, it is particularly important to verify that the sideslip is strongly decoupled from the roll channel. The next simulations are based on a similar test for an optimal eigenstructure decoupling controller of a LTI approximation of a BTT missile and are adapted from [116]. This test was designed to assess the decoupling between the sideslip and the roll channel. Good performance on this test is a strong indication of adequate decoupling. An initial sideslip of 1° is set in the simulation. Figures 5.54-57 show the system response. The Bank Angle shown in figure 5.55 indicates a small coupling which is tolerable.

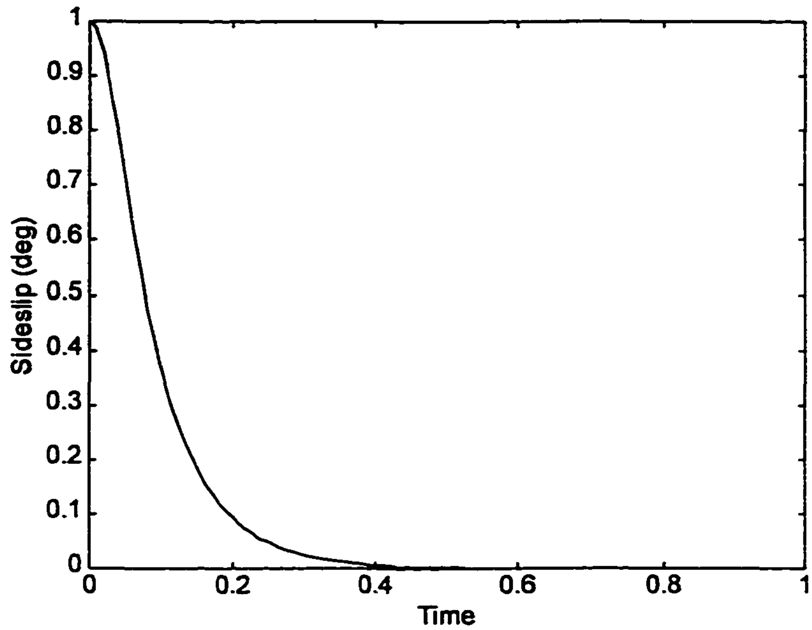

Figure 5.54 Sideslip Behavior With Initial Error

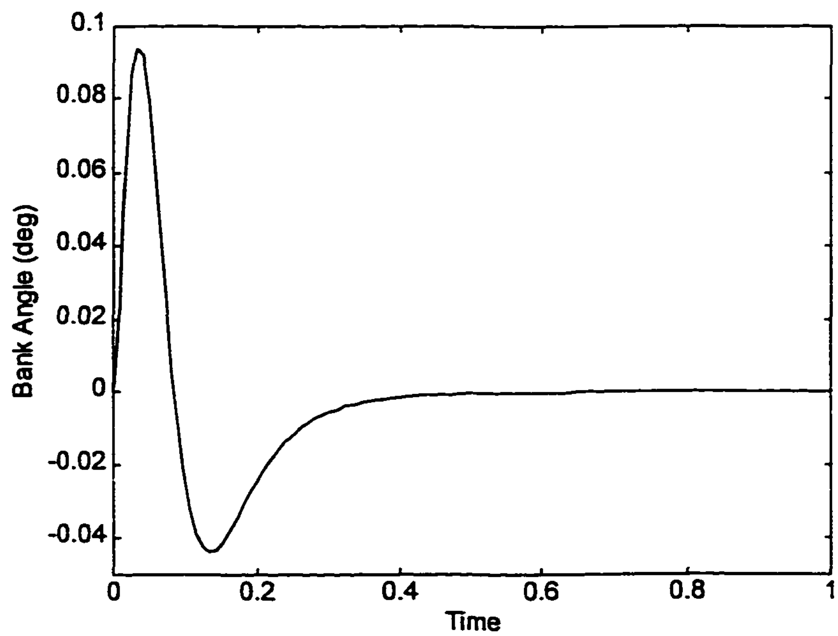

Figure 5.55 Bank Angle Disturbance

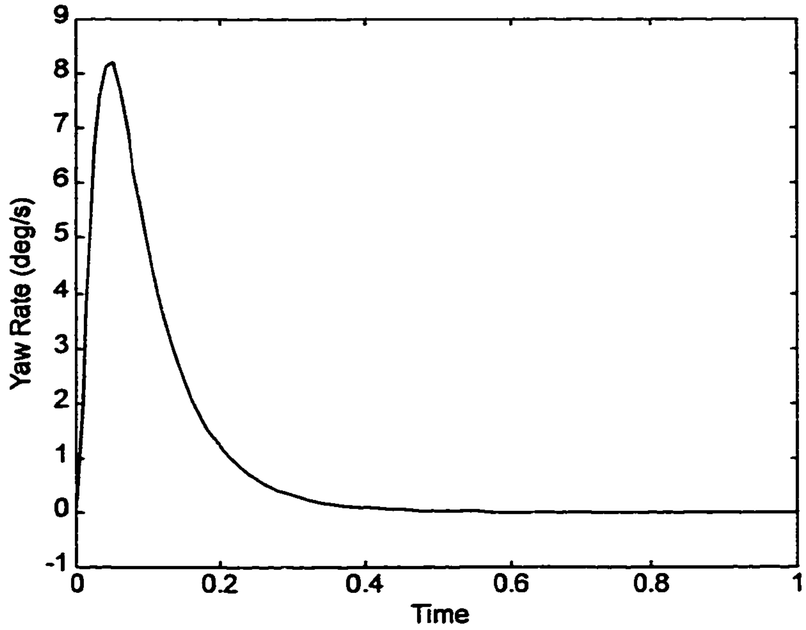

Figure 5.56 Yaw Rate Performance

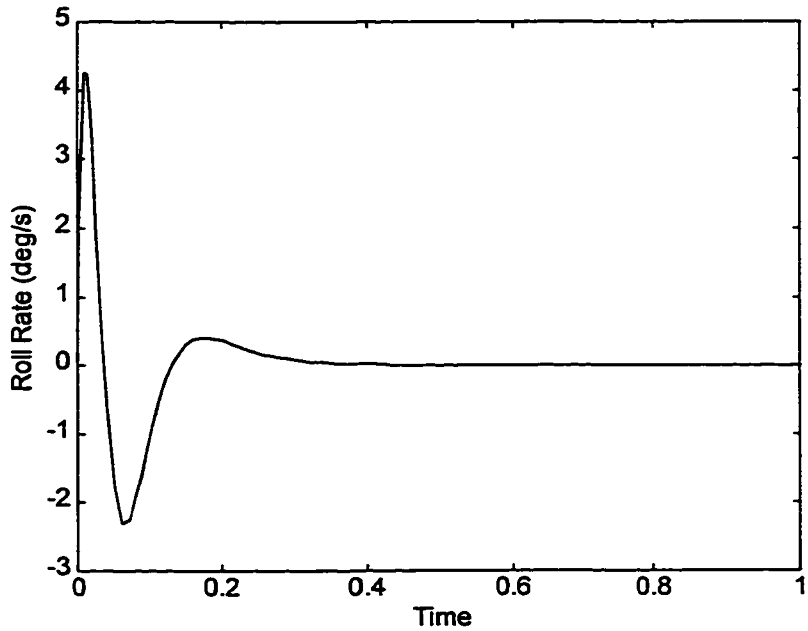

Figure 5.57 Roll Rate Performance

The simulation results in Figure 5.45 show that the AOA tracking of the trajectory linearization design achieves steady state errors on the order of 3° for a 20 percent perturbation in the aerodynamic coefficients $C_{m\alpha}$, which is significantly better than the other designs. However, it is desirable to further reduce these errors. To this end, the integral tracking error regulator design used for the robotic arm in Section 5.2 is applied to the AOA tracking subsystem. The AOA error subsystem is augmented with an integral term resulting in the augmented LTV error system

$$\dot{\boldsymbol{w}} = \begin{bmatrix} 0 & 1 & 0 & 0 & 0 & 0 & 0 \\ 0 & 0 & 1 & 0 & 0 & 0 & 0 \\ 0 & p_{11} & p_{12} & p_{13} & p_{14} & p_{15} & p_{16} \\ 0 & 0 & 0 & 0 & 1 & 0 & 0 \\ 0 & p_{21} & p_{22} & p_{23} & p_{24} & p_{25} & p_{26} \\ 0 & 0 & 0 & 0 & 0 & 0 & 1 \\ 0 & p_{31} & p_{32} & p_{33} & p_{34} & p_{35} & p_{36} \end{bmatrix} \boldsymbol{w} + \begin{bmatrix} 0 & 0 & 0 \\ 0 & 0 & 0 \\ 1 & 0 & 0 \\ 0 & 0 & 0 \\ 0 & 1 & 0 \\ 0 & 0 & 0 \\ 0 & 0 & 1 \end{bmatrix} \boldsymbol{v}$$

Seven PD-eigenvalues need to be assigned, three for the AOA subsystem, two for the roll subsystem, and two for the yaw subsystem. The PD-eigenvalues are at -10, -11 for the roll and yaw subsytems, and at $-16.5 \pm j0.5737$, -15.5 for the pitch subsystem. We then use state feedback to achieve PD-spectral synthesis for each subsystem and state decoupling to achieve the desired augmented error dynamics

$$\dot{\boldsymbol{w}} = \begin{bmatrix} 0 & 1 & 0 & 0 & 0 & 0 & 0 \\ 0 & 0 & 1 & 0 & 0 & 0 & 0 \\ \beta_{11} & \beta_{12} & \beta_{13} & 0 & 0 & 0 & 0 \\ 0 & 0 & 0 & 0 & 1 & 0 & 0 \\ 0 & 0 & 0 & \beta_{21} & \beta_{22} & 0 & 0 \\ 0 & 0 & 0 & 0 & 0 & 0 & 1 \\ 0 & 0 & 0 & 0 & 0 & \beta_{31} & \beta_{32} \end{bmatrix} \boldsymbol{w}$$

The modified trajectory linearization was then designed and simulated for the nonlinear system for the same perturbations of $\pm 20\%$ in the aerodynamic coefficient $C_{m\alpha}$. As shown in Figures 5.58-60, significant improvement on AOA errors was

achieved, while the Bank Angle tracking and sideslip regulating errors remain small as before.

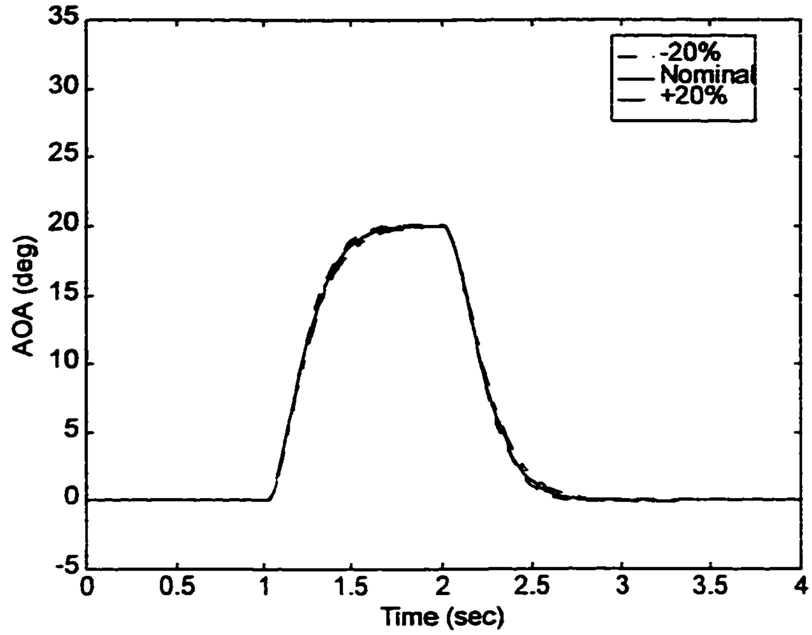

Figure 5.58 Angle of Attack Tracking with Modified Controller

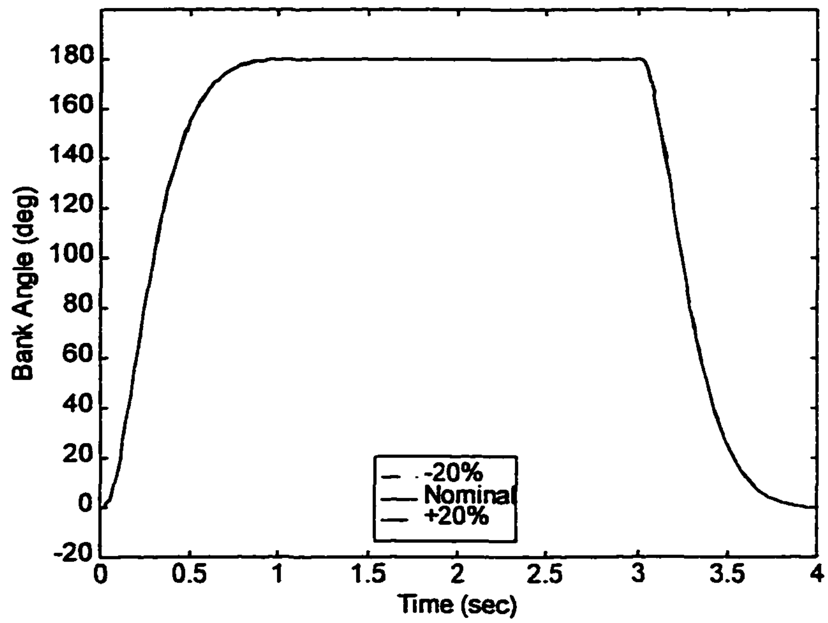

Figure 5.59 Bank Angle Tracking with Modified Controller

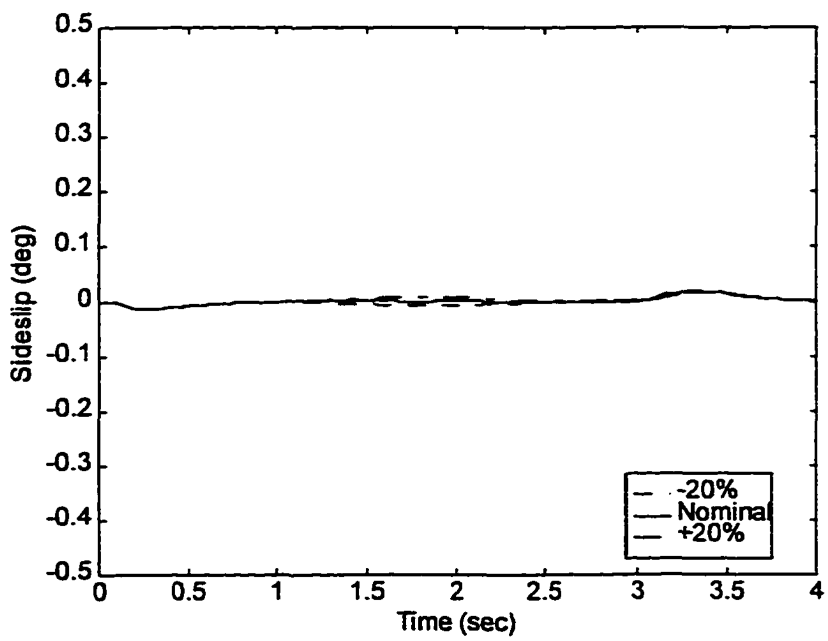

Figure 5.60 Sideslip with Modified Controller

CHAPTER 6

SUMMARY AND CONCLUSIONS

In this chapter we will first present a brief summary of the main contributions presented in this dissertation, and then outline some areas in which further research is needed and may provide some useful insight and results.

6.1 - Summary of Main Results

In this dissertation, the control design technique for nonlinear trajectory tracking known as trajectory linearization is presented. The main challenges to trajectory linearization design has been the problem of nonlinear inversion, and the lack of LTV control techniques. These two challenges have been addressed. The main contributions presented herein include: developing robustness measures based on PD-spectra; combining state-of-the-art NL control techniques to accomplish causal, stable nonlinear pseudo-inversion; designing and implementing in simulation LTV stabilizing controllers and observers based on PD-spectral assignment; making practical application of LTV transformations to achieve state feedback stabilization and realizing time varying system matrices; and applying these techniques to the design of demanding control problems.

The trajectory linearization design presented herein relies on PD-spectral assignment of the LTV error dynamics and does not suffer from the same limitations as even the most sophisticated gain scheduling designs. Early simulations of trajectory linearization designs seemed to indicate a large amount of inherent robustness. This dissertation has

sought to give some justification to this robustness and present some insight on how to design nonlinear controllers which can track a given trajectory for plants in which there is some uncertainty. This insight was then used in the design and simulation of several nonlinear control problems.

Chapter 4 develops the inherent robustness of trajectory linearization. First, perturbation bounds for LTV systems in phase variable canonical form are presented based on the PD-spectrum. This bound on the system perturbation matrix proves BIBO stability and then the exponential stability of the perturbed system. Next, the robustness of nonlinear tracking using trajectory linearization is considered in terms of the PD-spectrum. Finally, conditions on the system are given to guarantee the exponential stability of observer based control where only the outputs are available for feedback control.

Chapter 5 presents the results of the trajectory linearization design method applied to several nonlinear systems. First, an academic problem first considered by Khalil is examined. The performance of the trajectory linearization is compared with two gain scheduled designs, and a LTI design. Significant performance enhancements are shown to be possible using the trajectory linearization design. Second, this new method is used to design a trajectory tracking controller for a two link robot manipulator. The robustness of this method is illustrated by considering the movement of a poorly known load by the manipulator. The third nonlinear problem is a pitch axis missile model. The trajectory linearization design technique is used to create an Angle of Attack tracking controller. The fourth was the design of an autopilot for a 4DOF missile autopilot. The final design was a nonlinear autopilot for a 6DOF BTT missile. The trajectory linearization design was compared to two other designs with similar pole assignments. The results indicate superior performance of the trajectory linearization design for identical perturbations of the comparable designs.

6.2 - Suggestions for Further Studies

This dissertation presents original analysis of the robustness of trajectory linearization based on the PD-spectrum. Additionally, simulation results are offered for several nonlinear systems which indicate the capability of the trajectory linearization method for some problems. However, there are still several avenues of research that are needed to improve the capabilities of this method.

One important area that requires further research is in the area of pseudo-inversion of nonlinear systems. There has been significant research into the invertibility of certain classes of autonomous nonlinear systems. In order to make this method applicable to a greater variety of systems, these results must be extended to non-autonomous nonlinear systems. More systematic methods must be developed to handle non-minimum phase systems for both SISO and MIMO plants. Additionally, optimization results that balance tracking error and control effort would be useful for handling stable causal inversion of nonminimum phase plants.

A second important area of further research is the problem of PD-spectrum assignment. Currently this procedure is implemented by using state feedback based on the phase-variable canonical form. The Silverman-Wolovich transformation realizes this canonical form and can be implemented using a symbolic manipulator. However, it can often lead to very complicated coefficients which limits the applicability to practical problems. One practical solution is to limit the number of terms used in the implementation based on heuristic knowledge of the particular plant and required command trajectories. Research to consider the effects and limits of such designs are required. Another useful direction for research into this problem is to consider other means of synthesizing a desired PD-spectrum. The TV Pole Placement control method of Tsakalis and Ioannou [109] has been tried as an alternative synthesis method in nonlinear control without success.

Overall the method has had sufficient success in certain nonlinear problems to justify further research into this control method. Certain nonlinear problems such as the n-link nonlinear robot manipulator trajectory tracking controller problem naturally lends itself naturally to the technique of trajectory linearization. Also, the similarity of many airframe control problems lends support to the statement that trajectory linearization is a useful method for generating controllers for these plants.

BIBLIOGRAPHY

[1] Anderson, B. D. O. and John B. Moore, *Optimal Control Linear Quadratic methods*, Prentice-Hall, Englewood Cliffs, NJ, 1990.

[2] Antsaklis, Panos J. and Anthony N. Michel, *Linear Systems*, McGraw-Hill, New York, NY, 1997.

[3] Balas, G. , W. Garrard, and J. Reiner, "Robust Dynamic inversion conrol laws for aircraft control," *Proc. of the AIAA Guidance, Navigation, and Control Conference 1992.*, 192-205.

[4] Benedetto, M. D. Di and P. Lucibello, "Inversion of Nonlinear Time-Varying Systems," *IEEE Trans. on Automatic Control*, vol. 38, no. 8, 1259-1264, August 1993.

[5] Bugajski, D. , D. Enns, and M. Elgersma, "A Dynamic inversion based control law with Application to the High Angle-of-Attack Vehicle," *Proc. of the AIAA Guidance, Navigation, and Control Conference 1990.*, 826-839.

[6] Byrnes, Christopher, Biswa N. Datta, Clyde F. Martin, and David S. Gilliam, *Systems and Control in the Twenty-First Century*, Birkhäuser,Boston, MA, 1996.

[7] Byrnes, Christopher I., Francesco Delli Priscoli, and Alberto Isidori, *Output Regulation of Uncertain Nonlinear Systems*, Birkhäuser,Boston , MA, 1997.

[8] Carter, L. H., "Gain-Scheduled Bank-to-Turn Missile Autopilot Design Using Linear Parameter Varying Transformations," *Final Reports for the 1994 AFOSR Graduate Student Research Program*, pp.5-1 to 5-20, Sept. 1994.

[9] Chen, Chi-Tsong, *Linear System Theory and Design*, Harcourt Brace College Publishers, Austin, Tx, 1984.

[10] Chen, Degang, "Output Tracking Control of Nonlinear Nonminimum Phase Systems," *Proceedings of the 33rd Conference on Decision and Control*, Lake Buena Vista, FL, December, 1994.

[11] Cloutier, James R., Johnny Evers, and Joseph J. Freely, "Assessment of Air-to-Air Missile Guidance and Control Technology," *IEEE Control Systems Magazine*, 27-34, October 1989.

[12] Colonius, Fritz, and Wolfgang Kliemann, "The Lyapunov Spectrum of Families of Time-Varying Matrices," *Transactions of the American Mathematical Society*, vol. 318, no. 11, 4389-4408, November 1996.

[13] Colonius, Fritz, and Wolfgang Kliemann, "Lyapunov Exponents of Control Flows,".

[14] D'Angelo, Henry , *Linear Time-Varying Systems: Analysis and Synthesis*, Allyn and Bacon, Boston, MA, 1970.

[15] Devasia, S. and B. Paden,"Exact Output Tracking for Nonlinear Time-Varying Systems," *Proceedings of the 33rd Conference on Decision and Control*, Lake Buena Vista, FL, December 1994.

[16] Devasia, S. D. , D. Chen, and B. Paden, "Nonlinear inversion based output tracking," *IEEE Trans. on Automatic Control*, vol. AC-41, 930-942, 1996.

[17] D'Souza, Christopher N. and Curtis P. Mracek,"Derivation of the Full Nonlinear Equations of Motion for a Rigid Airframe," Technical note, U.S. Air Force Armament Directorate, 1994.

[18] Elanayar, Sunil V.T., and Yung C. Shin, "Radial Basis Function Neural Network for Approximation and Estimation of Nonlinear Stochastic Dynamic Systems," *IEEE Trans. on Neural Networks*, vol. 5, no. 4, 594-603, July 1994.

[19] Enns D., "Robustness of Dynamic Inversion vs. μ Synthesis: Lateral Directional Flight Control Example," *Proc. of the AIAA Guidance, Navigation, and Control Conference 1992.*, 210-222.

[20] Floquet, G., *Sur les Equations Differentielles Lineaires a Coefficients Periodiques*, Ann. Sci. École Norm. Sup. (4), 12, pp.47-82, 1883.

[21] Floquet, M. Gaston, *Sur La Theorie des Equations Differentielles Lineaires*, Annales Scientifiques de l'École Normale Supérieure, Deuxiéme Série, Supplément au Tome VIII, 1879.

[22] Floquet, G., Annales Scientifiques de l'École Normale Supérieure, (2) 13, p.47, 1883.

[23] Gantmacher, F. R., *The Theory of Matrices*, Chelsea Publishing, New York, NY, 1993.

[24] Georgiou, T. T. and M. C. Smith, "Robustness analysis of Nonlinear Feedback Systems: an input output approach," *IEEE Trans. on Automatic Control*, vol. AC-42, no. 9, 1200-1221, 1997.

[25] Gopalswamy, S. and Hedrick, J. K., "Control of a high performance aircraft with unacceptable zerodynamics," *Proc. 1992 American Control Conference*, Chicago, IL, American Automatic Control Council, June, 1992, pp. 1834-1838.

[26] Gorinevsky, Dmitry, "On the Persistency of Excitation in Radial Basis Function Network Identification of Nonlinear Systems," *IEEE Trans. on Neural Networks*, vol. 6, no. 5, 1237-1244, September 1995.

[27] Graham, D.,"Retrospective Essay on Nonlinearities in Aircraft Flight Control," *AIAA Journal of Guidance, Control and Dynamics*, vol. 14 no. 6, pp.1089-1099, Nov-Dec 1991.

[28] Greenwood, Donald T., *Principles of Dynamics 2nd ed.*, Prentice-Hall, Englewood Cliffs, NJ, 1988.

[29] Gu, G., J.R. Cloutier and G. Kim, "Gain Scheduled Missile Autopilot Design Using Observer-Based $\mathcal{H}_\infty$ Control," *Proceedings of the American Control Conference*, Seattle, Washington, June 1995.

[30] Guggenheimer, Heinrich W., *Differential Geometry*, Dover Publications, New York, NY, 1977.

[31] Hale, Jack K., *Ordinary Differential Equations*, John Wiley & Sons, New York, NY, 1969.

[32] Hess, R. A., C. Gao, and S. H. Wang, "Generalized Technique for Inverse Simulation Applied to Aircraft Maneuvers," *AIAA Journal of Guidance and Control*, vol. 14, no. 5, 920-926, September-October 1991.

[33] Hirschorn, Ronald M., "Invertibility of Multivariable Nonlinear Control Systems," *IEEE Trans. on Automatic Control*, vol. AC-24, no. 2, 855-865, December 1979.

[34] Hirschorn, Ronald M., "Invertibility of Nonlinear Control Systems," *Siam J. Control and Optimization*, vol. 17, no. 2, 289-297, March 1979.

[35] Hirschorn, Ronald M., "Invertibility of Control Systems on Lie Groups," *Siam J. Control and Optimization*, vol. 15, no. 6, 1034-1049, November 1977.

[36] Horn, Roger A. and Charles R. Johnson, *Matrix Analysis*, Cambridge University Press, New York, NY, 1985.

[37] Huang, J., C.F. Lin, J.R. Cloutier, J.H. Evers and C. D'Souza, "Robust Feedback Linearization Approach to Autopilot Design," *1992 IEEE Conference on Control Applications*, vol. 1, pp.220-225, Dayton, Ohio, September 1992.

[38] Huang, J., C.F. Lin, J.R. Cloutier, and J.H. Evers, "Robust Full-Envelope missile autopilot design," *1992 IEEE Conference on Control Applications*, vol. 1, pp.231-236, Dayton, Ohio, September 1992.

[39] Hunt, L. R. and G. Meyer, "Stable inversion for nonlinear systems," *Automatica*, to appear, 1997.

[40] Ince, E. L., *Ordinary Differential Equations*, Dover, New York, NY, 1956.

[41] Isidori, A. , *Nonlinear Control Systems: An Introduction, 2nd edition*, Springer-Verlag, New York, NY, 1989.

[42] Isidori, A. , *Nonlinear Control Systems: An Introduction*, Springer-Verlag, New York, NY, 1985.

[43] Jones, Richard D. and Joseph A. Bossi,"Development and Application of A Nonlinear Fin Mixer," *American Control Conference*, 1327-1331, Chicago, IL, June 1992.

[44] Juang, J.C., C.F. Lin, J.R. Cloutier, and J.H. Evers, "Robust Full-Envelope Missile Autopilot Design," *1992 IEEE Conference on Control Applications*, vol. 1, pp.231-236, Dayton, Ohio, September 1992.

[45] Kamen, E. W., "The poles and zeros of a linear time varying system," *Linear Algebra and Its Applications*, vol. 98, 263-289, 1988.

[46] Kailath, Thomas, *Linear Systems*, Prentice-Hall, Englewood Cliffs, NJ, 1980.

[47] Keel, L. H. and S. P. Bhattacharyya, "Robust, Fragile, or Optimal," *IEEE Trans. on Automatic Control*, vol. AC-42, no. 8, 1098-1105, 1997.

[48] Khalil, Hassan K., *Nonlinear Systems 2nd ed.*, Prentice-Hall, Upper Saddle River, NJ, 1996.

[49] Kokotovic, Petar, Hassan K. Khalil, John O'Reilly, *Singular Perturbation Methods in Control: Analysis and Design*, Academic Press, Boston, MA, 1986.

[50] Krener, Arthur J. and Witold Respondek,"Nonlinear Observers with Linearizable Error Dynamics," *SIAM Journal of Control and Optimization*, vol. 23, no. 2, 197-216, March 1985.

[51] Kreyszig, Erwin, *Introductory Functional Analysis with Applications*, John Wiley & Sons, New York, NY, 1978.

[52] Krstic, I. Kannellakopoulos and P. Kokotovic, *Nonlinear and Adaptive Control Design*, John Wiley & Sons, New York, NY, 1995.

[53] Lawrence, D. A. and Rugh, W. J., "Gain scheduling dynamic linear controllers for a nonlinear plant," *Proc. the 32nd IEEE Conference on Decision and Control*, San Antonio, TX, IEEE Control System Society, Dec. 1993, pp. 1024-1029.

[54] Lawrence, Douglas A., and Wilson J. Rugh,"Input-Output Pseudolinearization for Nonlinear Systems," *IEEE Trans. on Automatic Control*, vol. AC-39, no. 11, 757-761, November 1994.

[55] Lee, K.L. and M.A. Langehough, "Modern Control Bank-to-Turn Autopilot for Have Dash II Missile," *1992 IEEE Conference on Control Applications*, vol. 1, pp.214-219, Dayton, Ohio, September 1992.

[56] Lewis, F. L., C. T. Abdallah, and D. M. Dawson, *Control of Robot Manipulators*, MacMillan, New York, NY, 1993.

[57] Lin, C.F. and J. Huang,"Sliding Mode Control of HAVE DASH II Missile Systems," *Proceedings of 1993 American Control Conference*, vol. 1, pp.183-187.

[58] Lin, Ching-Fang, "Advanced Controller Design for Robot Arms," *IEEE Trans. on Automatic Control*, vol. AC-29, no. 4, 350-353, April 1984.

[59] Lin, C.F., J.R. Cloutier and J.H. Evers,"High Performance, Robust, Bank to Turn Missile Autopilot Design," *AIAA Journal of Guidance, Control and Dynamics*, vol. 18 no. 1, pp.46-53, Jan-Feb 1995.

[60] Luenberger, David G., "Canonical Forms for Linear Multivariable Systems," *IEEE Trans. on Automatic Control*, pp. 290-293, June 1967.

[61] Lyapunov, A. M. , *The General Problem of the Stability of Motion*, Translated to French by É. Davaux in 1907, Translated from French to English by A.T. Fuller, Taylor&Francis, Washington, DC, 1992.

[62] Mickle, M. Chris and J. Jim Zhu, "A Nonlinear Roll-Yaw Missile Autopilot Based on Plant Inversion and PD-Spectral Assignment," *Proceedings, 37th IEEE Conference on Decsion and Control*, to appear, 1998.

[63] Mickle, M. C. and J. Zhu, "Nonlinear missile planar autopilot design based on PD-spectrum assignment," *Proceedings, 36th IEEE Conference on Decision and Control*, San Diego, CA, 3914-3919, Dec. 1997.

[64] Mickle, M. Chris and J. Jim Zhu, "Simulation Results for Missile Autopilot Design Based on Extended Mean Assignment," *Proceedings, 28th IEEE Southeastern Symposium on Systems Theory*, 120-124, Baton Rouge, LA, April 1996.

[65] Mickle, M. C., "Missile autopilot design based on a unified spectral theory for linear time-varying systems," *Final Reports for the 1995 AFOSR Summer Graduate Research Program*, pp. 22-1 to 22-20, July, 1995.

[66] Morton, Blaise ,"A Dynamic Inversion Control Approach for High-Mach Trajectory Tracking," *American Control Conference*, 1332-1336, Chicago, IL, June 1992.

[67] Narendra, K. S., *Neural Networks for Identification and Control*, Yale University, 1994.

[68] Nemytskii, V. V. and V. V. Stepanov, *Qualitative Theory of Differential Eqautions*, Dover, New York, NY, 1989.

[69] Nguyen, Charles C., "Arbitrary Eigenvalue Assignments for Linear Time-Varying Multivariable Control Systems," *International Journal of Control*, vol. 45, no. 3, 1051-1057, 1987.

[70] Nguyen, Charles C., "Canonical Transformation for a Class of Time-Varying Multivariable Systems," *International Journal of Control*, vol. 43, no. 4, 1061-1074, 1986.

[71] Nichols, R. A., Reichert, R. T. Rugh W. J., "Gain scheduling for H-infinity controllers: a flight control example," *IEEE Trans. on Ctrl. Systems Tech*, Vol. 1, No. 2, 1993, pp. 69-79.

[72] O'Brien, Richard, and Pablo A. Iglesias, "Poles and Zeroes for Time Varying Systems," *Proc. of the American Control Conference*, 1997.

[73] Ochi, Y. and K. Kanai,"Design of Restructurable Flight Control Systems using Feedback linearization," *AIAA Journal of Guidance, Control and Dynamics*, vol. 14 no. 5, pp.903-911, Sept-Oct 1991.

[74] Packard, Andy *et. al.*, "Theory and Application of Linear Parameter Varying Control Techniques," *A workshop presented at the 1997 ACC*, Albuquerque, NM, 1997.

[75] Pallet, E. H. J. , *Automatic Flight Control 2nd ed.*, Granada, New York, NY, 1983.

[76] Pierre, Donald A., *Optimization Theory with Applications*, Dover, New York, NY, 1986.

[77] Rebhuhn, Deborah, "Invertibility of C^∞ Multivariable Input-Output Systems," *IEEE Trans. on Automatic Control*, vol. AC-25, no. 2, 207-212, April 1980.

[78] Recker, D. A., and P. V. Kokotovic,"Approximate Decoupling of Regularly Perturbed Nonlinear Systems," *American Control Conference*, 522-527, Boston, MA, June 1991.

[79] Reichert, R.T., "Dynamic Scheduling of Modern-Robust-Control Autopilot Designs for Missiles," *IEEE Control systems*, pp.35-42, October 1992.

[80] Reiner, J. G. Balas, and W. Garrard, "Robust Dynamice Inversion for control of highly maneuverable Aircraft," *AIAA Journal of Guidance, Control, and Navigation.*, 18(1) 1995.

[81] Rugh,W.J., "Analytical Framework for Gain Scheduling," *IEEE Control Systems*, p. 79, 1991.

[82] Rugh, Wilson J., *Linear System Theory*, Prentice-Hall, Englewood Cliffs, NJ, 1993.

[83] Rugh, Wilson J., "An Extended Linearization Approach to Nonlinear System Inversion," *IEEE Trans. on Automatic Control*, vol. AC-31, no. 8, 725-733, August 1986.

[84] Sacker, Robert J. , and George R. Sell, "A Spectral Theory for Linear Differential Systems," *Journal of Differential Equations*, vol. 27, pp. 320-358, 1978.

[85] Sain, Michael K. and James L. Massey,"Invertibility of Linear Time-Invariant Dyamical Systems," *IEEE Trans. on Automatic Control*, vol. AC-14, no. 2, 141-149, April 1969.

[86] Schumacher, D. A. , *Tactical Missile Autopilot Design Using Nonlinear Control*, Dissertation for Doctor of Philosophy in Aerospace Engineering, The University of Michigan, 1994.

[87] Seal, C. E. and A. R. Stubberud,"Canonical forms for multi-input time-variable systems," *IEEE Trans. on Automatic Control*, vol. AC-14, 704-707, December 1969.

[88] Shafai, B. and R. L. Carrol,"Minimal Order Observer Design for Linear Time Varying Multivariable Systems," *IEEE Trans. on Automatic Control*, vol. AC-31, no. 8, 757-761, August 1986.

[89] Shamma, J.S. and J.R. Cloutier,"Gain Scheduled Autopilot Design Using Linear Parameter Varying Transformations," *AIAA Journal of Guidance, Control and Dynamics*, vol. 16 no. 2, pp.256-263, March-April 1993.

[90] Shamma, Jeff S., James R. Cloutier,"A Linear Parameter Varying Approach to Gain Scheduled Missile Autopilot Design," *American Control Conference*, 1317-1321, Chicago, IL, June 1992.

[91] Shamma, J.S. and M. Athens, "Gain Scheduling: potential hazards and possible remedies ,"*IEEE Control Systems*, p. 101, 1992.

[92] Shamma, J.S. and J.R. Cloutier, "Trajectory Scheduled Missile Autopilot Design," *1992 IEEE Conference on Control Applications*, vol. 1, pp.237-242, Dayton, Ohio, September 1992.

[93] Shokoohi, Shahriar, Leonard M. Silverman, and Paul M. Van Dooren ,"Linear Time-Variable Systems: Balancing and Model Reduction," *IEEE Trans. on Automatic Control*, vol. AC-28, no. 8, pp.810-817, August 1983.

[94] Shtessel, Yuri, Christian Tournes, and Don Krupp,"Reusable Launch Vehicle control in Sliding Modes," *AIAA Journal of Guidance, Control and Dynamics*.

[95] Shtessel, Y. B. ,"Nonlinear Tracking in conventional and dynamic sliding manifolds," *IEEE Trans. on Automatic Control*, vol. 42, no. 9, 1282-1286, 1997.

[96] Shtessel, Yuri, and Christian Tournes,"Nonminimum Phase Output Tracking in Dynamic Sliding Manifolds with Application to Aircraft Control," *Proceedings of the 35th Conference on Decision and Control*, Kobe, Japan, December 1995.

[97] Silverman, Leonard M., "Transformation of Time-Variable Systems to Canonical (Phase-Variable) Form," *IEEE Trans. on Automatic Control*, 300-303, April 1966.

[98] Silverman, Leonard M., "Inversion of Multivariable Linear Systems," *IEEE Trans. on Automatic Control*, vol. AC-14, no. 3, 270-276, June 1969.

[99] Silverman, L. M., and H. E. Meadows, "Controllability and Observability in Time Variable Linear Systems," *SIAM Journal of Control*, vol. 5, no. 1, 64-73, 1967.

[100] Singh, Sahjendra N., "A Modified Algorithm for Invertibility in Nonlinear Systems," *IEEE Trans. on Automatic Control*, vol. AC-26, no. 2, 595-598, April 1981.

[101] Slotine, Jean-Jacques E., Weiping Li, *Applied Nonlinear Control*, Prentice-Hall, Englewood Cliffs, NJ, 1991.

[102] Snell, S. Anthony, Dale F. Ennis, and William L. Garrard Jr., "Nonlinear Inversion Flight Control for a Supermaneuverable Aircraft", *Journal of Guidance, Control, and Dynamics*. Vol. 15, No. 4, pp. 976-984, July-August 1992.

[103] Snell, S. , D. Ennis, and W. Garrard, "Nonlinear Inversion Flight Control for a Supermaneuverable Aircraft", *Proc. of the AIAA Guidance, Navigation, and Control Conference 1990*. 808-825.

[104] Sobel, K. and J.R. Cioutier,"Eigenstructure Assignment for the Extended Medium Range Air-to-Air Missile," *AIAA Journal of Guidance, Control and Dynamics*, vol. 15 no. 2, pp.529-531, March-April 1992.

[105] Sontag, E.D. , *Mathematical Control Theory: Deterministic Finite Dimensional Systems*, Springer-Verlag, New York, 1990.

[106] Spong, Mark W. and M. Vidyasagar, *Robot Dynamics and Control*, John Wiley & Sons, New York, NY, 1989.

[107] Stengel, Robert F., *Optimal Control and Estimation*, Dover, New York, NY, 1994.

[108] Sun, X-D, and T. Clarke,"A New Formulation of Nonlinear Inverse Dynamics for Aircraft Control," *IEEE Conference on Control Applications*, Glasgow, Scotland, 89-94, August 1994.

[109] Tsakalis, S. K. and P. A. Ioanou, *Linear time-varying systems, control and adaptation*, Prentice Hall, 1993.

[110] Vidyasagar, M. , *Nonlinear Systems Analysis*, Prentice-Hall, Englewood Cliffs, NJ, 1993.

[111] Vincent, Thomas L. and Walter J. Grantham, *Nonlinear and Optimal Control*, John Wiley & Sons, New York, NY, 1997.

[112] Wang, J. and N. Sundararajan, "Control of a High performance Fighter Aircraft using Scheduled Local Nonlinear Control Laws," *1994 IEEE Conference on Control Applications*, vol. 1, pp.101-106, Glasgow, Scotland, August 1994.

[113] Warner, Frank W., *Foundations of Differentiable Manifolds and Lie Groups*, Scott, Foresman and Company, Glenview, IL, 1971.

[114] White, D. P., Wozniak, J. G. and Lawrence, D. A., "Missile autopilot design using a gain scheduling technique," *Proc., 26th IEEE Southeastern Symposium on Systems Theory*, Baton Rouge, LA, IEEE Computer Society Press, Los Alamitos, CA, March, 1994, pp. 606-610.

[115] White, David Paul ,"Missile Autopilot Design Using A Gain Scheduling Technique," Master's Thesis in ECE.

[116] Wilson, Robert F., James R. Cloutier, and R. K. Yedavalli, "Control Design for Robust Eigenstructure Assignment in Linear Uncertain Systems," *IEEE Control Systems*, October 1992.

[117] Wise, K. A.,"Comparison of Six Robustness Tests Evaluating Missile Autopilot Robustness to Uncertain Aerodynamics," *AIAA Journal of Guidance, Control and Dynamics,* vol. 15 no. 4, pp.861-870, July-Aug 1992.

[118] Wise, K. A.,"Singular Value Robustness tests for Missile Autopilot Uncertainties," *AIAA Journal of Guidance, Control and Dynamics,* vol. 14 no. 3, pp.597-606, May-June 1991.

[119] Wise, Kevin A.,"Nonlinear Aircraft Flight Control Using Dynamic Inversion," *American Control Conference,* 1322-1326, Chicago, IL, June 1992.

[120] Wise, Kevin A.and Tam Nguyen,"Optimal Disturbance Rejection in Missile Autopilot Design Using Projective Controls," *IEEE Control Systems,* pp.43-49, October 1992.

[121] Wolovich, William A. , "On The Stabilization of Controllable Systems," *IEEE Trans. on Automatic Control,* October 1968.

[122] Zadeh, Lotfi A. and Charles A. Desoer, *Linear System Theory: The State Space Approach,* Robert E. Krieger Publishing Co., Huntington, NY, 1979.

[123] Zames, G., "On The Input-Output Stability of Time-Varying Nonlinear Feedback Systems Part I: Conditions Derived Using Concepts of Loop Gain, Conicity, and Positivity," *IEEE Trans. on Automatic Control,* vol. AC-11, no. 2, 228-238, April 1968.

[124] Zhao, H. and D. Chen, "A Finite Energy Property of Stable Inversion to Nonminimum Phase Nonlinear Systems," *IEEE Trans. on Automatic Control,* vol. AC-43, no. 8, 1170-1174, August, 1998.

[125] Zhou, Kemin with John C. Doyle and Keith Glover, *Robust and Optimal Control,* Prentice-Hall, Upper Saddle River, NJ, 1996.

[126] Zhu, J. and M. C. Mickle, "Synthesis of time-varying bandwidth filters based on all-pole LTI prototypes," *Proceedings, American Control Conference,* Philadelphia, PA, , June, 1998.

[127] Zhu, J. and M. C. Mickle, "Missile autopilot design using a new linear time-varying control technique," *AIAA Journal on Guidance, Control and Dynamics,* vol. 20, no. 1, 1-8, Jan. 1997.

[128] Zhu, J. "A necessary and sufficient stability criterion for linear time-varying systems," *Proceedings, 28th IEEE Southeastern Symposium on Systems Theory,* Baton Rouge, LA, IEEE Computer Society Press, Los Alamitos, CA, April 1996, pp. 115-119.

[129] Zhu, J., "PD-eigenstructure assignment control for multivariable nonlinear tracking and decoupling," *Final Report for the 1995 AFOSR Summer Research Extension Program*, Dec., 1996.

[130] Zhu, J. and M. C. Mickle, "Missile autopilot design based on a unified spectral theory for linear time-varying systems," *Proceedings, 13th World Congress of the International Federation of Automatic Control*, San Francisco, CA, vol. P, 231-236, July, 1996.

[131] Zhu, J.,"A necessary and sufficient stability criterion for linear time-varying systems," *Proceedings, 28th IEEE Southeastern Symposium on Systems Theory*, 115-119, Baton Rouge, LA, April 1996.

[132] Zhu, J.,"A unified spectral theory for linear time-varying systems—progress and challenges," *Proceedings, 34th IEEE Conference on Decision and Control*, New Orleans, LA, IEEE Control System Society, Dec. 1995. pp. 2540-2546.

[133] Zhu, J. (with M. C. Mickle), "Missile autopilot design based on a unified spectral theory for linear time-varying systems," *Final Reports for the 1995 AFOSR Summer Faculty Research Program*, pp. 64-1 to 64-20, July, 1995.

[134] Zhu, J. and M. C. Mickle, "Missile autopilot design using the extended-mean assignment control, part I: stabilization," *Proceedings, 27th IEEE Southeastern Symposium on System Theory*, Starkville, MS, 247-251, March 1995.

[135] Zhu, J. and Xiao, W., "Intelligent control of time-varying dynamical systems using CMAC artificial neural network," *Mathematical and Computer Modeling*, Special Issue on Neural Networks, Vol. 21, No. 1/2, 1995, pp. 89-107.

[136] Zhu, J. "Well defined series and parallel D-spectra for linear time-varying systems," *Proceedings, American Control Conference*, Baltimore, MD, 734-738, June, 1994.

[137] Zhu, J. "Parallel D-eigenvalues and parallel D-eigenvectors for linear time-varying systems," *Proceedings, 26th IEEE Southeastern Symposium on System Theory*, Athens, OH, 297-301, March 1994.

[138] Zhu, J., "A note on the extension of the eigenvalue concept," *IEEE Control Systems Magazine*, p.101, 1992.

[139] Zhu, J. and C. H. Morales, "On linear ordinary differential equations with functionally commutative coefficient matrices," *Linear Algebra and Its Applications*, vol. 170, 81-105, June 1992.

[140] Zhu, J. and Johnson, C. D. "Unified canonical forms for matrices over a differential ring," *Linear Algebra and Its Applications*, vol. 147, March 1991, pp. 201-248.

[141] Zhu, J. and C. H. Morales, "Spatial decomposition of functionally commutative matrices," *Linear Algebra and Its Applications*, vol. 131, 71-92, April 1990.

[142] Zhu, J.,*A Unified Eigenvalue Theory for Linear Dynamical Systems*, Ph. D. Dissertation, Electrical and Computer Engineering Department, University of Alabama in Huntsville, May 1989.

[143] Zhu, J. and C. D. Johnson, "New results on the reduction of linear time-varying dynamical systems," *SIAM J. on Control and Optimization*, vol. 27, no. 3, 476-494, May 1989.

APPENDIX A

NONLINEAR PITCH MISSILE MODEL

- Pitch Airframe

$$\dot{\alpha}(t) = K_\alpha M(t) C_n[\alpha(t), \delta(t), M(t)] \cos(\alpha(t)) + q(t)$$

$$\dot{q}(t) = K_q M^2(t) C_m[\alpha(t), \delta(t), M(t)] + K_q q_m M^2(t) q(t)$$

$$\eta_z(t) = K_z M^2(t) C_n[\alpha(t),\ \delta(t), M(t)]$$

  - Use $q_m \neq 0$ to make model more realistic

- Aerodynamic Coefficients

$$C_n[\alpha, \delta, M] = a_n \alpha^3 + b_n \alpha|\alpha| + c_n(2 - M/3)\alpha + d_n \delta$$

$$C_m[\alpha, \delta, M] = a_m \alpha^3 + b_m \alpha|\alpha| + c_m(-7 + 8M/3)\alpha + q_m q + d_m \delta$$

- Actuator Dynamics

$$\frac{\mathrm{d}}{\mathrm{d}t}\begin{bmatrix}\delta(t)\\ \dot{\delta}(t)\end{bmatrix} = \begin{bmatrix}0 & 1\\ -\omega_a^2 & -2\zeta\omega_a\end{bmatrix}\begin{bmatrix}\delta(t)\\ \dot{\delta}(t)\end{bmatrix} + \begin{bmatrix}0\\ \omega_a^2\end{bmatrix}\delta_c(t)$$

Glossary of Terms

$K_\alpha = \frac{.7P_0S}{mv_s}$

$K_q = \frac{.7P_0Sd}{I_y}$

$K_z = \frac{.7P_0S}{m}$

$P_0 = 973.3\,\frac{\text{lbs}}{\text{ft}^2}$	static pressure at 20,000 ft
$S = 0.44\,\text{ft}^2$	surface area
$m = 13.98\,\text{slugs}$	mass
$v_s = 1036.4\,\frac{\text{ft}}{\text{s}}$	speed of sound at 20,000 ft
$d = 0.75\,\text{ft}$	missile diameter
$I_y = 182.5\,\text{slug}\cdot\text{ft}^2$	pitch moment of inertia
$\zeta = 0.7$	actuator damping ratio
$\omega_\alpha = 150\,\frac{\text{rad}}{\text{s}}$	actuator natural frequency

$a_n = 0.000103\,\text{deg}^{-3}$

$b_n = -0.00945\,\text{deg}^{-2}$

$c_n = -0.1696\,\text{deg}^{-1}$

$d_n = -0.034\,\text{deg}^{-1}$

$a_m = 0.000215\,\text{deg}^{-3}$

$b_m = -0.0195\,\text{deg}^{-2}$

$c_m = -0.051\,\text{deg}^{-1}$

$d_m = -0.206\,\text{deg}^{-1}$

$\lambda_1(t), \lambda_2(t)$	= open loop SD-eigenvalues
$k_1(t), k_2(t)$	= time varying feedback gains
$\gamma_1(t), \gamma_2(t)$	= closed loop SD-eigenvalues
$\alpha(t)$	= angle of attack, deg
$q(t)$	= pitch rate, deg/sec
$M(t)$	= Mach number
$\delta_c(t)$	= commanded tail fin deflection, deg
$\delta(t)$	= actual tail fin deflection, deg
$\eta_c(t)$	= commanded normal acceleration, g
$\eta_z(t)$	= actual normal acceleration in g's
$C_n[\alpha, \delta, M]$	= aerodynamic lift coefficient
$C_m[\alpha, \delta, M]$	= pitch moment coefficient
ξ_1, ξ_2	= state variables for α, q
$\bar{\xi}, \bar{\delta}$	= nominal state trajectory, and nominal control input respectively
$x(t)$	= state tracking error
$y(t)$	= normal acceleration tracking error, g

$z(t)$	= angle of attack tracking error, deg
$v(t)$	= tracking error control input

APPENDIX B

NONLINEAR BTT MISSILE MODEL

State Equations for the EMRAAT Missile

$$\dot{\alpha} = q - \tan(\beta)[p(\cos(\alpha) - r\sin(\alpha)] + \frac{g}{V\cos(\beta)}(\cos(\alpha)\cos(\phi)\cos(\theta) + \sin(\alpha)\sin(\theta))$$
$$+ \frac{gQS}{WV\cos(\beta)}(C_{N_\alpha}\alpha + C_{N_{\dot{\alpha}}}\dot{\alpha} + C_{N_q}q + C_{N_{\delta_q}}\delta_q)\cos(\alpha)$$

$$\dot{\beta} = p\sin(\alpha) - r\cos(\alpha) + \frac{gQS}{WV}(C_{Y_\beta}\beta + C_{Y_p}p + C_{Y_r}r + C_{Y_{\delta_p}}\delta_p + C_{Y_{\delta_r}}\delta_r)\cos(\beta)$$
$$+ \frac{g}{V}\cos(\theta)\sin(\phi)\cos(\beta)$$

$$
\begin{aligned}
\dot{p} = [&(-I_{xy}I_{xz}I_{zz} - I_{xz}^2 I_{yz} + I_{xy}^2 I_{yz} + I_{xy}I_{xz}I_{yy})p^2 + \\
&+ (I_{yy}I_{yz}I_{zz} - I_{yz}^3 - I_{xy}^2 I_{yz} - I_{xy}I_{xz}I_{yy})q^2 + \\
&+ (-I_{yy}I_{yz}I_{zz} + I_{xy}I_{xz}I_{zz} + I_{yz}^3 + I_{xz}^2 I_{yz})r^2 + \\
&+ (-I_{xy}I_{yz}I_{zz} + I_{xz}I_{yy}I_{zz} - 2I_{yz}^2 I_{xz} - I_{xy}I_{yy}I_{yz} + I_{xx}I_{xy}I_{yz} - I_{xz}I_{yy}^2 + I_{xx}I_{xz}I_{yy})pq + \\
&+ (I_{xy}I_{zz}^2 + I_{xz}I_{yz}I_{zz} - I_{xy}I_{yy}I_{zz} - I_{xx}I_{xy}I_{zz} + 2I_{xy}I_{yz}^2 + I_{xz}I_{yy}I_{yz} - I_{xx}I_{xz}I_{yz})pr + \\
&+ (-I_{yy}I_{zz}^2 + I_{yz}^2 I_{zz} + I_{yy}^2 I_{zz} - I_{yy}I_{yz}^2 - I_{xz}^2 I_{yy})qr + \\
&+ QSd(C_{l_p}(I_{yy}I_{zz} - I_{yz}^2) + C_{n_p}(I_{xy}I_{yz} + I_{xz}I_{yy}))p + \\
&+ QSd(C_{m_q}(I_{xy}I_{zz} + I_{xz}I_{yz}))q + \\
&+ QSd(C_{l_r}(I_{yy}I_{zz} - I_{yz}^2) + C_{n_r}(I_{xy}I_{yz} + I_{xz}I_{yy}))r + \\
&+ QSd(C_{m_\alpha}(I_{xy}I_{zz} + I_{xz}I_{yz}))\dot{\alpha} + \\
&+ QSd(C_{m_\alpha}(I_{xy}I_{zz} + I_{xz}I_{yz}))\alpha + \\
&+ QSd(C_{l_\beta}(I_{yy}I_{zz} - I_{yz}^2) + C_{n_\beta}(I_{xy}I_{yz} + I_{xz}I_{yy}))\beta + \\
&+ QSd(C_{l_{\delta_p}}(I_{yy}I_{zz} - I_{yz}^2) + C_{n_{\delta_p}}(I_{xy}I_{yz} + I_{xz}I_{yy}))\delta_p + \\
&+ QSd(C_{m_{\delta_q}}(I_{xy}I_{zz} + I_{xz}I_{yz}))\delta_q + \\
&+ QSd(C_{l_{\delta_r}}(I_{yy}I_{zz} - I_{yz}^2) + C_{n_{\delta_r}}(I_{xy}I_{yz} + I_{xz}I_{yy}))\delta_r] \\
&(I_{xx}I_{yy}I_{zz} - I_{xy}^2 I_{zz} - I_{xx}I_{yz}^2 - 2I_{xy}I_{xz}I_{yz} - I_{xz}^2 I_{yy})^{-1}
\end{aligned}
$$

$$
\begin{aligned}
\dot{q} = [&(-I_{xx}I_{xz}I_{zz} + I_{xx}I_{xy}I_{yz} + I_{xy}^3 + I_{xy}^2 I_{xz})p^2 + \\
&+ (I_{xy}I_{yz}I_{zz} + I_{yz}^2 I_{xz} - I_{xx}I_{xy}I_{yz} - I_{xy}^2 I_{xz})q^2 + \\
&+ (-I_{xy}I_{yz}I_{zz} + I_{xx}I_{xz}I_{zz} - I_{xz}I_{yz}^2 - I_{xz}^3)r^2 + \\
&+ (-I_{xx}I_{yz}I_{zz} + I_{xy}I_{xx}I_{zz} + 2I_{xz}^2 I_{yz} - I_{xx}I_{yy}I_{yz} - I_{xy}I_{xz}I_{yy} + I_{yz}I_{xx}^2 + I_{xx}I_{xy}I_{xz})pq + \\
&+ (I_{xx}I_{zz}^2 - I_{xz}^2 I_{zz} - I_{xy}^2 I_{zz} - I_{xx}^2 I_{zz} + I_{xx}I_{yz}^2 + I_{xz}^2 I_{xx})pr + \\
&+ (-I_{xy}I_{zz}^2 - I_{xz}I_{yz}I_{zz} + I_{xy}I_{yy}I_{zz} + I_{xx}I_{xy}I_{zz} + I_{xz}I_{yy}I_{yz} - I_{xz}I_{xx}I_{yz} - 2I_{xz}^2 I_{xy})qr + \\
&+ QSd(C_{l_p}(I_{xy}I_{zz} - I_{xz}I_{yz}) + C_{n_p}(I_{xx}I_{yz} + I_{xy}I_{xz}))p + \\
&+ QSd(C_{m_q}(I_{xx}I_{zz} - I_{xz}^2))q + \\
&+ QSd(C_{l_r}(I_{xy}I_{zz} + I_{xz}I_{yz}) + C_{n_r}(I_{xx}I_{yz} + I_{xy}I_{xz}))r + \\
&+ QSd(C_{m_\alpha}(I_{xx}I_{zz} - I_{xz}^2))\dot{\alpha} + \\
&+ QSd(C_{m_\alpha}(I_{xx}I_{zz} - I_{xz}^2))\alpha + \\
&+ QSd(C_{l_\beta}(I_{xy}I_{zz} + I_{xz}I_{yz}) + C_{n_\beta}(I_{xx}I_{yz} + I_{xz}I_{xy}))\beta + \\
&+ QSd(C_{l_{\delta_p}}(I_{xy}I_{zz} + I_{xz}I_{yz}) + C_{n_{\delta_p}}(I_{xx}I_{yz} + I_{xz}I_{xy}))\delta_p + \\
&+ QSd(C_{m_{\delta_q}}(I_{xx}I_{zz} - I_{xz}^2))\delta_q + \\
&+ QSd(C_{l_{\delta_r}}(I_{xy}I_{zz} + I_{xz}I_{yz}) + C_{n_{\delta_r}}(I_{xx}I_{yz} + I_{xz}I_{xy}))\delta_r] \\
&(I_{xx}I_{yy}I_{zz} - I_{xy}^2 I_{zz} - I_{xx}I_{yz}^2 - 2I_{xy}I_{xz}I_{yz} - I_{xz}^2 I_{yy})^{-1}
\end{aligned}
$$

$$
\begin{aligned}
\dot{r} = [&(-I_{xx}I_{xz}I_{yz} + I_{xx}I_{xy}I_{yy} - I_{xy}^3 - I_{xz}^2 I_{xy})p^2 + \\
&+ (I_{xz}I_{yy}I_{yz} + I_{yz}^2 I_{xy} - I_{xx}I_{xy}I_{yy} + I_{xy}^3)q^2 + \\
&+ (-I_{xy}I_{yz}^2 - I_{xz}I_{yy}I_{yz} + I_{xx}I_{xz}I_{yz} + I_{xy}I_{xz}^2)r^2 + \\
&+ (-I_{xx}I_{yz}^2 - I_{yy}^2 I_{xx} + I_{xz}^2 I_{yy} + I_{xy}^2 I_{yy} + I_{yy}I_{xx}^2 - I_{xy}^2 I_{xx})pq + \\
&+ (I_{xx}I_{yx}I_{zz} + I_{xy}I_{xz}I_{zz} + I_{xx}I_{yy}I_{yz} - 2I_{xy}^2 I_{yz} - I_{yz}I_{xx}^2 - I_{xy}I_{xz}I_{yy} - I_{xx}I_{xy}I_{xz})pr + \\
&+ (-I_{xy}I_{yz}I_{zz} - I_{xz}I_{yy}I_{zz} + I_{xy}I_{yy}I_{yz} + I_{xx}I_{xy}I_{yz} + I_{xz}I_{yy}^2 - I_{xx}I_{xz}I_{yy} + 2I_{xy}^2 I_{xz})qr + \\
&+ QSd(C_{l_p}(I_{xy}I_{yz} - I_{xz}I_{yy}) + C_{n_p}(I_{xx}I_{yy} - I_{xy}^2))p + \\
&+ QSd(C_{m_q}(I_{xx}I_{yz} + I_{xy}I_{xz}))q + \\
&+ QSd(C_{l_r}(I_{xy}I_{yz} + I_{xz}I_{yy}) + C_{n_r}(I_{xx}I_{yy} - I_{xy}^2))r + \\
&+ QSd(C_{m_{\dot{\alpha}}}(I_{xx}I_{yz} - I_{xy}I_{xz}))\dot{\alpha} + \\
&+ QSd(C_{m_\alpha}(I_{xx}I_{yz} - I_{xy}I_{xz}))\alpha + \\
&+ QSd(C_{l_\beta}(I_{xy}I_{yz} + I_{xz}I_{yy}) + C_{n_\beta}(I_{xx}I_{yy} - I_{xy}^2))\beta + \\
&+ QSd(C_{l_{\delta_p}}(I_{xy}I_{yz} + I_{xz}I_{yy}) + C_{n_{\delta_p}}(I_{xx}I_{yy} - I_{xy}^2))\delta_p + \\
&+ QSd(C_{m_{\delta_q}}(I_{xx}I_{yz} - I_{xy}I_{xz}))\delta_q + \\
&+ QSd(C_{l_{\delta_r}}(I_{xy}I_{yz} + I_{xz}I_{yy}) + C_{n_{\delta_r}}(I_{xx}I_{yy} - I_{xy}^2))\delta_r] \\
&(I_{xx}I_{yy}I_{zz} - I_{xy}^2 I_{zz} - I_{xx}I_{yz}^2 - 2I_{xy}I_{xz}I_{yz} - I_{xz}^2 I_{yy})^{-1}
\end{aligned}
$$

Glossary of Terms

α — Angle of attack
β — Angle of sideslip
p — Roll rate
q — Pitch rate
r — Yaw rate
Q — Dynamic Pressure
S — Reference area
d — Reference length/diameter
V — Missile velocity
W — Missile weight
g — Acceleration due to gravity
ψ — Yaw angle
θ — Pitch angle
ψ — Roll angle
δp — Roll control input (surface deflection)
δq — Pitch control input (surface deflection)
δr — Yaw control input (surface deflection)
$\widetilde{Q}$ — (gQS/WV)
N — Normal force
Y — Side force
C_{a_b}— Aerodynamic Coefficient- a due to b
l — Aerodynamic moment about x-axis
m — Aerodynamic moment about y-axis
n — Aerodynamic moment about z-axis
I_{i_j} — Moment or product of inertia

EMRAAT Physical Properties

$g = 32.2$ ft/s^2
$d = 0.625$ ft.
$S = 0.3067$ ft^2
$W = 227$ lbs.
$V = 1936.16$ ft/s
$M = 2.0$
$Q = 1100.75$ lb./ft^2

$I_{xx} = 1.08\,\text{slug*ft}^2$
$I_{yy} = 70.13\,\text{slug*ft}^2$
$I_{zz} = 70.66\,\text{slug*ft}^2$
$I_{xy} = 0.274\,\text{slug*ft}^2$
$I_{xz} = -0.704\,\text{slug*ft}^2$
$I_{yz} = 0.017\,\text{slug*ft}^2$
Air Density $= 5.87 \times 10^{-4}\,\text{slug/ft}^3$
Altitude $= 30,000$ ft.

Aerodynamic coefficients (Mach = 2.0)

$C_{N_\alpha} = 36.6$
$C_{n_{\dot\alpha}} = 0.0274$
$C_{N_q} = 0.0145$
$C_{N_{\delta_q}} = 6.0165$
$C_{Y\beta} = -14.9$
$C_{Y_p} = -0.00073$
$C_{Y_r} = 0.0161$
$C_{Y_{\delta_p}} = -0.01$
$C_{Y_{\delta_r}} = 0.08$
$C_{l_\beta} = 5.44$
$C_{l_p} = -0.011$
$C_{l_r} = 0.0021$
$C_{l_{\delta_p}} = -6.30$
$C_{l_{\delta_r}} = -5.16$
$C_{m_\alpha} = -82$
$C_{m_{\dot\alpha}} = -0.014$
$C_{m_q} = -0.202$
$C_{m_{\delta_q}} = -40.7$
$C_{n_\beta} = 35.52$
$C_{n_p} = 0.006$
$C_{n_r} = -0.2$
$C_{n_{\delta_p}} = 1.72$
$C_{n_{\delta_r}} = -28.65$

VITA

Michael Christopher Mickle received the bachelor of science degree in Electrical Engineering with the highest honor of Summa Cum Laude from Lamar University in 1993, and the master of science degree in Electrical Engineering from Louisiana State University in 1995. He is currently a doctoral candidate in the Electrical and Computer Engineering Department of L.S.U. He received a fellowship from the Louisiana Board of Regents for the period of August 1993 to August 1998.

From January 1990 to August 1992, he was a Co-op student at Gulf States Utilities in Production Support. While in this group he worked on steam turbine controllers for large generators, generator maintenance, motor testing, among other tasks. In the Summer of 1995, Mr. Mickle was selected by the AFOSR as a Summer Graduate Associate at Eglin AFB to participate in exploratory research on missile autopilot design using the DAST led by Dr. J. Jim Zhu. Mr. Mickle is a student member of the IEEE. He is also a member of the engineering and academic honor societies Eta Kappa Nu, Tau Beta Pi and Phi Kappa Phi.

DOCTORAL EXAMINATION AND DISSERTATION REPORT

Candidate: Michael Christopher Mickle

Major Field: Electrical Engineering

Title of Dissertation: NONLINEAR TRACKING CONTROL USING A ROBUST DIFFERENTIAL-ALGEBRAIC APPROACH

Approved:

Major Professor and Chairman

Dean of the Graduate School

EXAMINING COMMITTEE:

Date of Examination:

10-22-1998

IMAGE EVALUATION TEST TARGET (QA-3)

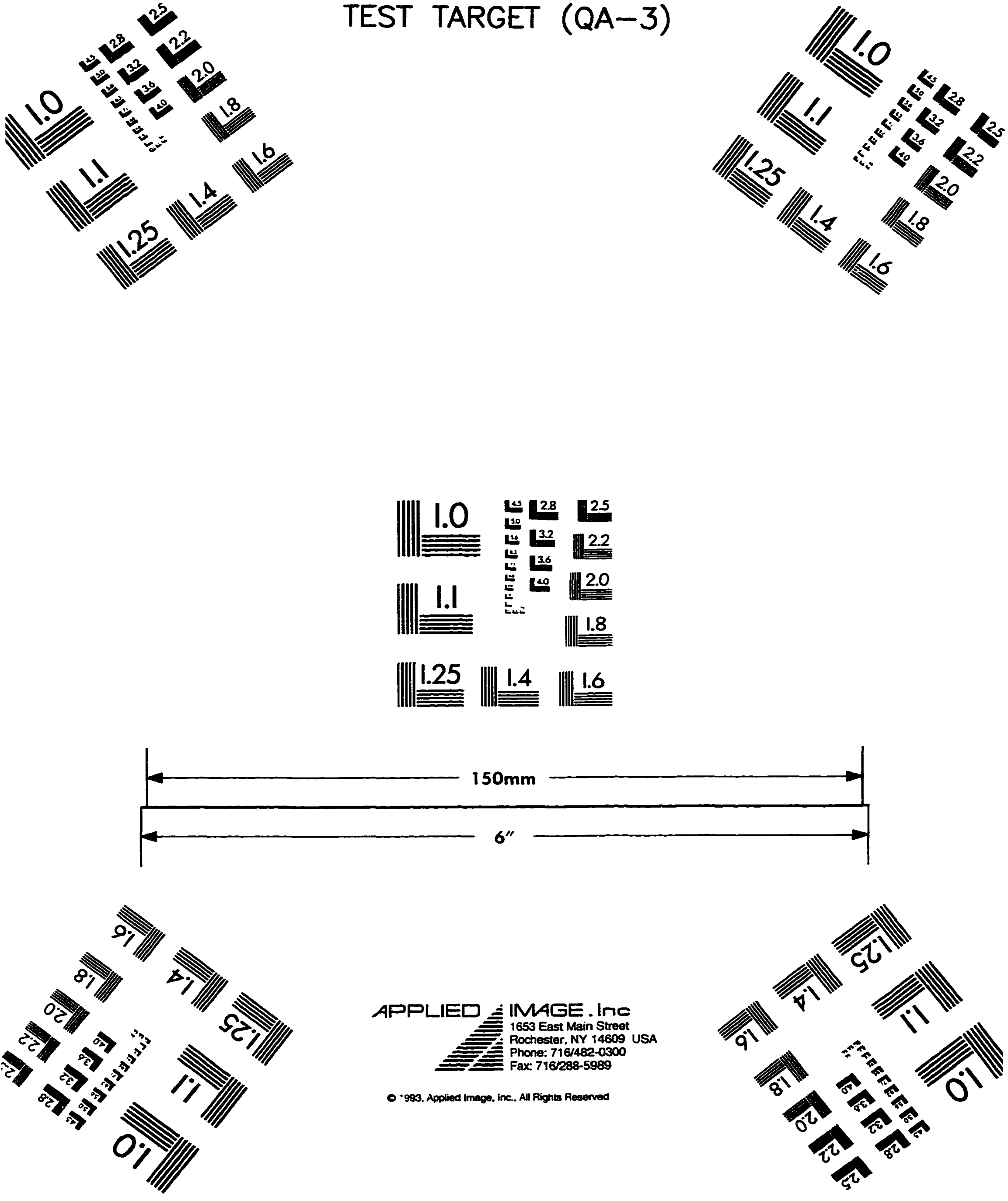

APPLIED IMAGE . Inc
1653 East Main Street
Rochester, NY 14609 USA
Phone: 716/482-0300
Fax: 716/288-5989